

Technische Universität Dresden

**Coordinated Multi-Point under a Constrained Backhaul and
Imperfect Channel Knowledge**

Patrick Marsch

der Fakultät Elektrotechnik und Informationstechnik
der Technischen Universität Dresden

zur Erlangung des akademischen Grades eines

Doktoringenieurs

(Dr.-Ing.)

genehmigte Dissertation

Vorsitzender: Prof. Dr.-Ing. habil. Rüdiger Hoffmann

Gutachter: Prof. Dr.-Ing. Gerhard Fettweis

Prof. Dr. rer. nat. Rudolf Mathar

Tag der Einreichung: 7. Dezember 2009

Tag der Verteidigung: 1. März 2010

Dresden, 20. Mai 2010

Abstract

Mobile communication has become an essential part of today's information society. Especially the demand for ubiquitous mobile Internet access has significantly increased in the past years, creating a severe challenge for mobile operators to respond to the demand for mobile data rates, while at the same time strongly reducing cost per bit. This challenge can only be successfully addressed if the spectral efficiency and fairness of mobile communications are continuously increased. In today's cellular systems, both aspects are more and more limited through the interference between cells, especially in dense urban deployments.

From theory it is known that this inter-cell-interference can be canceled or even exploited if base stations cooperatively process signals connected to multiple terminals, a concept commonly referred to as *Coordinated Multi-Point* (CoMP). As these schemes promise significant improvements of spectral efficiency and a more homogeneous throughput distribution, they are seen as a key technology of future mobile systems. Beside many implementation challenges, such as the synchronization of the cooperating entities and an accurate estimation of the involved wireless links, a main issue connected to CoMP is the additional infrastructure required for data exchange between cooperating base stations, usually referred to as *backhaul*.

This work provides an information theoretical analysis of the trade-off between capacity gains and required backhaul achievable with various CoMP concepts, also taking into consideration the major impact of imperfect channel knowledge at base station and terminal side. A key finding is that the relative benefit of CoMP in fact increases in certain scenarios under less accurate channel knowledge. Also, major throughput gains are already possible through flexible user assignment and decoding concepts, without requiring any backhaul. For the cellular uplink, two cooperation strategies are identified that should ideally be used adaptively, depending on the current interference situation. One can be used for a very backhaul-efficient, low complexity, decentralized cancelation of weak interference, where the base stations exchange decoded data. In the other, centralized, scheme, the base stations exchange received signals, providing larger gains under stronger interference conditions, but requiring more backhaul. For the downlink, a flexible scheme of moderate complexity is identified that provides a good throughput/backhaul trade-off for most channel conditions. Iterative cooperation concepts are shown to be of minor value, despite several publications in this field.

Beside the analysis of small CoMP scenarios, the work also provides a concept for the backhaul-efficient usage of CoMP in large cellular systems. This concept exploits the fact that co-located base stations can cooperate without requiring backhaul, while smart clustering and resource partitioning concepts can provide further gain at minimal backhaul. This yields a system with strong fairness and capacity gains over a conventional system, while requiring an additional backhaul infrastructure with a capacity less than twice the system capacity.

Zusammenfassung

Die mobile Kommunikation hat einen enormen Stellenwert in der heutigen Gesellschaft eingenommen. Insbesondere die steigende Nachfrage nach allgegenwärtigem, mobilem Internetzugang stellt Netzbetreiber zunehmend vor die Herausforderung, flächendeckend höhere Datenraten anzubieten, bei gleichzeitig verringerten Kosten pro Bit. Hierzu muß die spektrale Effizienz und Fairness von Mobilfunksystemen konsequent verbessert werden, die in heutigen Systemen primär durch die Interferenz zwischen benachbarten Zellen beschränkt ist.

Aus der Theorie ist bekannt, dass Inter-Zellen-Interferenz reduziert oder sogar ausgenutzt werden kann, wenn Basisstationen kooperativ die Signale mehrerer Endgeräte verarbeiten. Diese so genannten *Coordinated Multi-Point* (CoMP) Verfahren versprechen erhebliche Steigerungen und eine homogenere Verteilung von Datenraten und gelten als Schlüsseltechnologien des Mobilfunks der Zukunft. Neben diversen Herausforderungen bei der Implementierung, z.B. der zellübergreifenden Synchronisation und Kanalschätzung, besteht ein Hauptproblem bei CoMP jedoch darin, dass eine zusätzliche Kommunikationsinfrastruktur zwischen kooperierenden Basisstationen benötigt wird - so genannter *Backhaul*.

Die vorliegende Arbeit führt eine informationstheoretische Analyse des Verhältnisses aus Datenrate und benötigtem Backhaul von verschiedenen Kooperationsstrategien durch, wobei auch der Einfluss fehlerhafter Kanalkennntnis berücksichtigt wird. Eine wesentliche Beobachtung ist, dass der relative Gewinn durch CoMP in bestimmten Szenarien zunimmt, je schlechter die Kanalkennntnis ist. Ferner können innovative Nutzerzuordnungs- und Dekodierkonzepte Kapazitätssteigerungen erzielen, ohne dass Backhaul benötigt wird. Für die zellulare Aufwärtsstrecke werden zwei Kooperationsverfahren identifiziert, zwischen denen ein System idealerweise je nach Interferenzsituation umschaltet. Das erste, dezentralisierte Verfahren erlaubt eine Backhaul-effiziente Reduktion von schwacher Interferenz bei geringer Komplexität. Hierbei werden zwischen den Basisstationen dekodierte Nutzdaten ausgetauscht. Ein zweites, zentralisiertes Verfahren, basierend auf dem Austausch quantisierter Empfangssignale, ist vorteilhaft in Szenarien starker Interferenz, benötigt jedoch mehr Backhaul. In der Abwärtsstrecke wird ein flexibles Verfahren mittlerer Komplexität vorgestellt, das ein gutes Verhältnis aus Datenraten und benötigtem Backhaul für eine Vielzahl von Kanälen ermöglicht. Auch iterative Kooperationsverfahren werden untersucht, erweisen sich jedoch als wenig attraktiv.

Neben der Betrachtung kleiner CoMP Szenarien stellt die Arbeit ein Gesamtkonzept für Backhaul-effizientes CoMP in großen zellularen Systemen vor. Dieses nutzt die Tatsache aus, dass am gleichen Ort befindliche Basisstationen ohne Backhaulbedarf kooperieren können, und verwendet Gruppierungs- und Ressourcenpartitionierungskonzepte, um weitere Kapazitätsgewinne bei geringem Backhaulbedarf zu erzielen. Zudem sind deutliche Fairnessverbesserungen gegenüber herkömmlichen Mobilfunksystemen zu verzeichnen, obwohl auf dem Backhaul lediglich ein der doppelten Systemkapazität entsprechender Datenaustausch erforderlich ist.

Acknowledgement

This thesis is the result of my work at the Vodafone Chair Mobile Communications Systems at Technische Universität Dresden. I would particularly like to thank Prof. Gerhard Fettweis, who not only convinced me to do a Ph.D. in his team and hence made the work possible, but who also gave me a large number of opportunities and interesting challenges in the past four years that enabled me to improve both academic and personal skills. For example, he gave me the chance to be strongly involved in one of the most renowned research projects connected to next generation mobile communications systems, namely the project EASY-C, partially funded by the German Federal Ministry of Education and Research (BMBF). It was highly interesting and challenging to design a CoMP experimentation platform at a point in time when 3GPP was just only starting the discussion on this topic, and I am of course happy to see that recent field trial results do in fact support many of the statements made in this thesis. I would like to thank Steffen Watzek for the great collaboration, and all EASY-C team members for their continuous enthusiasm, stamina and humor, in particular during the last-minute preparation of several live demonstrations.

Since April 2009, I also had the chance to setup a new research group within the Vodafone Chair, observing system-level aspects of CoMP and heterogeneous cellular deployments, and venturing into the novel viewpoint of energy-efficient communications. I would like to thank the group members for the many fruitful discussions and the great ideas brought up, and I am looking forward to continuing joint work in the upcoming months.

The thesis wouldn't be what it is without the great support of Peter Rost, Michael Grieger, Fabian Diehm and Albrecht Fehske, who rigorously proof-read the document and/or with whom I had many discussions that helped shape the work. Thanks also to Prof. Rudolf Mathar, who provided the second advisory opinion on the thesis and gave me important hints for the defense presentation. I finally want to thank Shahid Khattak and André Fonseca dos Santos for the enlightening time we had when working or traveling together, and Ernesto Zimmermann, who originally motivated me to join the Vodafone Chair.

Last but surely not least, I am deeply grateful to my family and friends for their continuous encouragement and support, and to my dear Ines, whose patience and understanding even in the longest nights of writing up this work was amazing.

Contents

Abstract / Zusammenfassung	vii
Acknowledgement	ix
Contents	xi
List of Figures	xiv
List of Tables	xv
Abbreviations	xvii
Symbols	xix
1 Introduction	1
1.1 Motivation	1
1.2 Contribution of this Work	2
1.3 Related Work	3
1.4 Structure of this Thesis	4
1.5 Notation	5
2 Information-Theoretic Basics	7
2.1 General Concepts	7
2.2 Uplink	8
2.2.1 Transmission Model	8
2.2.2 Modeling of Imperfect Channel Knowledge	10
2.2.3 Capacity Region Under Infinite BS Cooperation	11
2.2.4 Capacity Region without BS Cooperation	13
2.2.5 Basic Base Station Cooperation Schemes	17
2.3 Downlink	29
2.3.1 Transmission Model	29
2.3.2 Modeling of Imperfect Channel Knowledge	30
2.3.3 Capacity Region Under Infinite BS Cooperation	32
2.3.4 Capacity Region without BS Cooperation	37
2.3.5 Basic Base Station Cooperation Schemes	40
2.4 Performance and Backhaul-Constrained Capacity Regions	44
2.5 Summary	48

3	Information-Theoretic Analysis	49
3.1	Scenarios, Channels and Metrics Considered	49
3.1.1	Uplink	50
3.1.2	Downlink	52
3.1.3	Channel Matrices	53
3.1.4	Sum Rate and Common Rate	53
3.2	Cut-Set Bound	54
3.3	Uplink Analysis	55
3.3.1	Capacity Gains through CoMP in the Uplink	55
3.3.2	Performance of Uplink CoMP Schemes for Specific Channels	59
3.3.3	Benefit of Source Coding and Superposition Coding	67
3.3.4	Benefit of Iterative BS Cooperation Schemes	68
3.3.5	Choice of Best Coop. Scheme and Cooperation Direction	74
3.3.6	Sensitivity of Schemes to Channel Orthogonality and SNR	76
3.3.7	Performance of Uplink CoMP Schemes in Scenarios with $M = K = 3$	78
3.3.8	Summary	81
3.4	Downlink Analysis	82
3.4.1	Capacity Gains through CoMP in the Downlink	82
3.4.2	Performance of Downlink CoMP Schemes for Specific Channels	88
3.4.3	Benefit of Superposition Coding in the Downlink	93
3.4.4	Performance of Downlink CoMP Schemes for Arbitrary Channels	94
3.4.5	Choice of Best Cooperation Scheme	95
3.4.6	Sensitivity of Schemes to Channel Orthogonality and SNR	97
3.4.7	Performance of Downlink CoMP Schemes in Scenarios with $M = K = 3$	98
3.4.8	Summary	100
4	System Level Simulation	101
4.1	Simulation Setup	101
4.1.1	Channel Model	101
4.1.2	Simulation Flow	102
4.2	Clustering and Resource Partitioning	105
4.2.1	The Benefit of Resource Partitioning	109
4.3	Uplink Simulation Results	110
4.4	Downlink Simulation Results	113
4.5	Summary	114
5	Implications on Practical Systems	117
5.1	General Implications of our Work	117
5.1.1	Fundamental Trade-Offs in the Context of CoMP	117
5.1.2	Mobile Network Organization	117
5.1.3	Backhaul Topology	118
5.1.4	On the Value of Iterative BS Cooperation Schemes	118
5.2	Practical Considerations	120
5.2.1	Practical Implementation of BS Cooperation Schemes	120
5.2.2	CSI Exchange, ARQ and Complexity Issues	121
5.2.3	Scheduling for CoMP	125
5.2.4	Ad-hoc BS Cooperation after Transmission	126

5.3	Extension of the Work to other Scenarios	127
5.3.1	Intra-cell CoMP in the Uplink	127
5.3.2	Terminals with more Receive Antennas in the Downlink	127
5.4	Summary	128
6	Conclusions	131
6.1	Contribution of this Work	131
6.2	Main Conclusions	131
6.3	Future Outlook	133
A	Literature Overview on CoMP	135
B	Proofs connected to Imperfect Channel Knowledge	137
B.1	Modified Transmission Equation for UL under Imp. CSI	137
B.2	Modified Transmission Equation for DL under Imp. CSI	139
B.3	Downlink SINRs under Imperfect CSI	141
C	Proofs connected to Uplink-Downlink Duality	143
C.1	DL SCO Problem with Per-Antenna Power Constraints	143
C.2	Equivalence of UL and DL Capacity Region under Per-Ant. Power Constr.	147
D	Proofs connected to Capacity Regions	149
D.1	Uplink Capacity Region under Infinite BS cooperation	149
D.2	UL Capacity Region with DIS/CIF/DAS BS Cooperation	150
D.3	Downlink Capacity Region Calculation	157
D.4	Downlink Capacity Region with Common Messages	160
E	Motivation of Simulation Parameters	163
F	Proofs connected to Specific BS Cooperation Schemes	169
F.1	Proofs Connected to Iterative DIS (I-DIS)	169
F.2	Benefit of Iterative DAS (I-DAS)	171
F.3	UL DAS with Source Coding Approaching Cut-set Bound	172
F.4	Best Cooperation Direction for Uplink DAS	174
F.5	Superiority of DIS over CIF	176
	Bibliography	179
	Publication List	197
	Curriculum Vitae	200

List of Figures

2.1	Model of the uplink transmission considered in this work.	9
2.2	Model of the uplink transmission assuming infinite BS cooperation.	12
2.3	Uplink capacity region under no or infinite BS cooperation.	17
2.4	Admissible rate region of Slepian-Wolf source coding [SW73].	18
2.5	Illustration of a combined DIS/CIF/DAS base station cooperation strategy. .	22
2.6	Illustration of the downlink transmission considered in this work.	30
2.7	Downlink capacity region under no or infinite BS cooperation.	40
2.8	Uplink performance region for different CoMP schemes.	45
2.9	Backhaul-constrained uplink capacity region for different CoMP schemes. . .	47
2.10	Backhaul-constrained downlink capacity region for different CoMP schemes. .	47
3.1	Scenarios considered in the uplink and downlink analysis in this chapter. . . .	50
3.2	Uplink transmit power and path gain as a function of UE location.	51
3.3	Illustration of the cut-set bound.	54
3.4	CoMP gain in uplink scenarios with $M = K = 2$ of average orthogonality. . .	56
3.5	CoMP gain in uplink scenarios with $M = K = 3$ of average orthogonality. . .	58
3.6	Impact of imperfect CSIR and pathloss exponent on uplink CoMP.	59
3.7	Non-iterative uplink CoMP schemes for $M = K = 2$ analyzed in this chapter.	62
3.8	Sum rate vs. backhaul for uplink CoMP schemes and specific channels.	66
3.9	Gain through source coding or superposition coding in uplink CoMP.	68
3.10	Iterative uplink CoMP schemes for $M = K = 2$ analyzed in this chapter. . . .	72
3.11	Benefit of iterative uplink CoMP schemes for $M = K = 2$	73
3.12	Best choice of BS cooperation scheme in uplink CoMP.	75
3.13	Impact of channel orthogonality and SNR on uplink CoMP schemes.	77
3.14	Monte Carlo simulation results for $M = K = 3$ in the uplink.	80
3.15	CoMP gain in downlink scenarios with $M = K = 2$ of average orthogonality.	84
3.16	CoMP gain in downlink scenarios with $M = K = 3$ of average orthogonality.	86
3.17	Impact of imperfect CSIT and CSIR on downlink CoMP.	87
3.18	Downlink CoMP schemes for $M = K = 2$ analyzed in this chapter.	90
3.19	Sum rate vs. backhaul for downlink CoMP schemes and specific channels. . .	92
3.20	Monte Carlo simulation results for $M = K = 2$ in the downlink.	94
3.21	The best choice of BS cooperation scheme in downlink CoMP.	96
3.22	Impact of channel orthogonality and SNR on downlink CoMP schemes. . . .	98
3.23	Monte Carlo simulation results for $M = K = 3$ in the downlink.	99
4.1	Cellular setup considered for system level simulations.	102

4.2	Example of a highly asymmetric uplink interference scenario.	105
4.3	Clustering concepts compared through system level simulations.	107
4.4	Uplink SINRs obtainable through clustering and interference cancellation. . .	108
4.5	Downlink SINRs obtainable through clustering and interference cancellation.	109
4.6	User throughput distribution and average user throughput vs. backhaul for different cooperation sizes and strategies (uplink).	112
4.7	User throughput distribution and average user throughput vs. backhaul for different cooperation sizes and strategies (downlink).	113
5.1	Benefit of backhaul-aware CoMP scheduling in a scenario with $M = K = 2$. .	125
E.1	Channel estimation and CSI feedback process.	164
E.2	Pilot structure in each PRB from the LTE downlink assumed in this appendix.	165
F.1	Illustration of adding one iteration to a DIS cooperation and decoding process.	170

List of Tables

3.1	Relation between BS-UE assignment \mathbf{m} and Ψ for non-coop. DL transmission.	83
4.1	Parameters used for system level simulations.	103
4.2	Summary on Monte-Carlo simulation results for scenarios with $M = K = 3$. .	116
4.3	Summary on system level simulation results.	116
5.1	Comparison of uplink BS cooperation schemes, considering practical aspects.	122
5.2	Comparison of downlink BS cooperation schemes, considering practical aspects.	123

Abbreviations

3GPP	Third Generation Partnership Project
ARQ	Automatic Repeat Request
BC	Broadcast channel
bh.	backhaul
bpcu	bits per channel use
BS(s)	Base Station(s)
CDMA	Code Division Multiple Access
CEO	<i>here</i> : Chief Estimation Officer
CIF	Compressed Interference Forwarding
CoMP	Coordinated Multi-Point
CQI	Channel Quality Indicator
CSI	Channel State Information (or: <i>channel knowledge</i>)
CSIR	Channel State Information at the receiver side
CSIT	Channel State Information at the transmitter side
Ctr.	Centralized
DAS	Distributed Antenna System (<i>uplink or downlink BS coop. scheme</i>)
Dec.	Decentralized
DIS	Distributed Interference Subtraction (<i>uplink BS cooperation scheme</i>)
DPC	Dirty Paper Coding
DL	Downlink
FDD	Frequency Division Duplex
FDM	Frequency Division Multiplex
FFT	Fast Fourier Transform
GPS	Global Positioning System
HK	Han-Kobayashi scheme (<i>here referring to a channel coding concept</i>)
IAP	Interference-Aware Precoding
IC	Interference Channel
ICI	Inter-Carrier Interference
I-DAS	Iterative DAS scheme (<i>uplink BS cooperation scheme</i>)
I-DIS	Iterative DIS scheme (<i>uplink BS cooperation scheme</i>)
i.i.d.	independently and identically distributed
IRC	Interference Rejection Combining
ISD	Inter-Site Distance
ISI	Inter-Symbol Interference
LTE	Long Term Evolution (<i>evolution of mobile standards after UMTS</i>)

MAC	Multiple Access Channel
MAP	Maximum A posteriori Probability
mcp.c.	multi-cell power control
MIMO	Multiple Input Multiple Output
MISO	Multiple Input Single Output
MMSE	Minimum Mean Square Error
MRC	Maximum Ratio Combining
MRT	Maximum Ratio Transmission
N-DAS	Network DAS (<i>DAS scheme with decoding at a central network entity</i>)
OFDM	Orthogonal Frequency Division Multiplex
p.a. pwr.	per-antenna power constraint
pf. / ip. CSI	perfect / imperfect channel knowledge
PRB	Physical Resource Block (<i>resource unit in LTE</i>)
QSC	Quantized Sequence based Cooperation (<i>downlink BS coop. scheme</i>)
RRH	Remote Radio Head
SCER	Signal-to-Channel-Estimation-Error Ratio
SCM	Spatial Channel Model
SCO	SINR Constrained Optimization
SIC	Successive Interference Cancellation
SINR	Signal-to-Interference-and-Noise Ratio
SISO	Single Input Single Output
SNR	Signal-to-Noise Ratio
SOCP	Second Order Cone Program
SON	Self-Organizing Network
sum pwr.	sum power constraint
TDM	Time Division Multiplex
THP	Tomlinson Harashima Precoding
TS	Time-share (<i>between no and infinite BS cooperation in downlink</i>)
TTI	Transmit Time Interval (<i>corresponds to 1 ms in an LTE system</i>)
UE(s)	User Equipment or terminal(s)
UL	Uplink
UMC	Unquantized Message based Cooperation (<i>downlink BS coop. scheme</i>)
UMTS	Universal Mobile Telecommunications System
ZF	Zero Forcing
WSSUS	Wide-Sense Stationary Uncorrelated Scattering

Symbols

Setup

M, K	Number of BSs and UEs, respectively
\mathcal{M}, \mathcal{K}	Sets of all involved BSs and UEs, respectively
$N_{\text{bs}}, N_{\text{mt}}$	Number of receive/transmit antennas per BS and UE, respectively
$N_{\text{BS}}, N_{\text{MT}}$	Overall no. receive/transmit ant. at BS and UE side, respectively
$\mathbf{d} = [d_1 \dots d_K]^T$	Normalized distance of UEs to their BSs
$\theta, \lambda_{m,k}$	Path loss exponent and path gain between BS m and UE k
$\varphi_{AB}, \varphi_{Ab}, \dots$	Angles representing channel orthonogonality \rightarrow see Section 3.1.3

Transmission Model

$\mathbf{H} = [\mathbf{h}_1, \mathbf{h}_2, \dots, \mathbf{h}_K]$	Channel matrix
$\hat{\mathbf{H}}, \hat{\mathbf{H}}^{\text{UE}}, \hat{\mathbf{H}}^{\text{BS}}$	Estimated channel in UL and DL (UE and BS side), respectively
$\hat{\mathbf{E}}, \hat{\mathbf{E}}^{\text{UE}}, \hat{\mathbf{E}}^{\text{BS}}$	Channel estim. error in UL and DL (UE and BS side), respectively
\mathbf{H}^e	Power-reduced, effective channel due to imperfect CSI
$\mathbf{E}^e, \mathbf{E}^{e,\text{UE}}, \mathbf{E}^{e,\text{BS}}$	Effective channel estimation error in uplink and downlink (UE and BS side), respectively, uncorrelated from the estimated channel
\mathbf{W}	Precoding matrix employed in the downlink
Ψ	Diagonal scaling matrix connected to antenna selection and quantization in the downlink
$\mathbf{m} = [m_1 \dots m_K]^T$	Assignment of UEs to BSs
Π_{ant}	Assignment of antennas to BSs
σ^2, σ_E^2	Background noise variance and channel estimation noise variance
N_p, N_d	Number of pilots per transmission block used in uplink and downlink, and number of quantization bits per channel coefficient used for CSI feedback
t	Symbol index (typically omitted in this work for brevity)
$\mathbf{s}^{[t]}$	Transmitted signals in channel access t
$\mathbf{y}^{[t]}, \mathbf{n}^{[t]}$	Received signals and noise in channel access t
$\mathbf{v}^{[t]}, \mathbf{v}^{\text{UE}}[t], \mathbf{v}^{\text{BS}}[t]$	Noise term in channel access t caused by imperfect CSI in UL and DL (UE and BS-side), respectively
S_k, Y_m, \bar{Y}_m	Overall signal sequence transmitted by UE k , and overall signal sequence (over all antennas) received by BS m , before and after signal processing (only relevant in the uplink)
$N_{m,a}, N_k$	Noise sequence received at antenna a of BS m (uplink), and received by user k (downlink)
$\mathbf{P} = \text{diag}(\mathbf{p})$	Uplink transmit power (or uplink transmit covariance)

$\mathbf{P}(\mathcal{F})$	Uplink transmit power connected to all messages in set \mathcal{F}
$\hat{\mathbf{P}}^{\max} = \text{diag}(\hat{\mathbf{p}}^{\max})$	Maximum transmit power (per user) in the uplink
$\check{\mathbf{P}}^{\max} = \text{diag}(\check{\mathbf{p}}^{\max})$	Maximum transmit power (per antenna, if applicable) in the uplink
$\hat{\mathbf{B}}^{\max}, \check{\mathbf{B}}^{\max}$	Total backhaul available in uplink and downlink, respectively
$\hat{\mathbf{B}}^{\text{dis}}, \hat{\mathbf{B}}^{\text{cif}}, \hat{\mathbf{B}}^{\text{das}}, \hat{\mathbf{B}}^{\text{net}}$	Extent of backhaul infrastructure invested into DIS, CIF and DAS schemes and network forwarding in the uplink, respectively
\mathbf{C}	Auxiliary variable used in the downlink, denoting the number of quantization bits used when providing messages to certain BSs
$\check{\mathbf{B}}(\mathbf{C})$	Backhaul infrastructure required in the downlink for a certain choice of auxiliary variable \mathbf{C}
β	Additional backhaul needed as compared to a non-cooperative system
$\beta(\mathbf{r}, \mathbf{B})$	Function returning the sum backhaul needed in addition to a non-cooperative system, given a rate tuple \mathbf{r} and backhaul matrix \mathbf{B}

Covariances and Quantization Noise

Φ^{ss}	Downlink transmit covariance
Φ^{hh}	Noise covariance connected to channel estimation errors
$\Phi_m^{\text{yy}}, \bar{\Phi}_m^{\text{yy}}$	Receive signal covariance at BS m <i>before</i> and <i>after</i> signal processing
$\Phi_{k,m}^{\text{yy}}, \Phi_{k,m m'}^{\text{yy}}$	Receive signal covariance at BS m connected to UE k , and the same covariance <i>conditioned</i> on the receive signals at BS m'
$\bar{\Phi}_{m m'}^{\text{yy}}, \bar{\Phi}_{m m',\mathcal{M}'}^{\text{yy}}$	Receive signal covariance at BS m after signal proc., conditioned on the receive signals at BS m' , or conditioned on the receive signals at BS m' and signals provided by BSs in \mathcal{M}' to BS m'
$\Phi_{m \rightarrow m'}^{\text{qq}}$	Covariance of quantization noise introduced when forwarding receive signals from BS m to BS m'

Messages, Sequences and Functions

N_{sym}	Number of symbols transmitted successively in one block
F, X	Message (data bits) and sequence (of N_{sym} symbols, assumed to be a Gaussian process), respectively
$\hat{\mathcal{F}}_{\text{all}}, \check{\mathcal{F}}_{\text{all}}$	Sets of all messages involved in UL or DL transmission, respectively
$\hat{\mathcal{F}}_{\text{all}^*}$	Set of all uplink messages <i>not</i> decoded by a central network entity
$\hat{\mathcal{F}}_k, \check{\mathcal{F}}_k$	Sets of all messages connected to UE k , in UL or DL, respectively
$\hat{F}_k^{\mathcal{M}'}$	Uplink message originating from UE k and decoded individually by all BSs in \mathcal{M}'
$\hat{F}_k^{\mathcal{M}', m \rightarrow \mathcal{M}''}$	Uplink message originating from UE k , decoded individually by all BSs in \mathcal{M}' , and DIS-forwarded by BS $m \in \mathcal{M}'$ to all BSs in \mathcal{M}''
$\hat{F}_k^{\mathcal{M}', m \nrightarrow \mathcal{M}''}$	Uplink message originating from UE k , decoded individually by all BSs in \mathcal{M}' , and CIF-forwarded by BS $m \in \mathcal{M}'$ to all BSs in \mathcal{M}''
$\mathcal{F}^{[m]}, \check{\mathcal{F}}^{[m]}$	Set of messages decoded by BS m , and set of messages neither decoded by BS m nor provided to BS m by any other BS through DIS or CIF concepts
$\check{\mathcal{F}}^{[m]}, \mathcal{F}^{\nrightarrow [m]}$	Sets of messages provided to a BS m through the DIS or CIF concept, respectively

$e(\cdot), d(\cdot)$	Encoding function, mapping a message F to a sequence $X = e(F)$, and corresponding decoding function
$\mathbf{g}(\cdot)$	Encoding function used for DPC in the downlink
$q(\cdot), s(\cdot)$	Quantization and Slepian-Wolf source coding function, respectively

Terms connected to Uplink-Downlink Duality

$\hat{\Phi}_{\text{nn}}$	Noise covariance in the dual uplink
$\hat{\mathbf{P}} = \text{diag}(\hat{\mathbf{p}})$	Transmit powers in the dual uplink
$\mathcal{J}_1(k), \mathcal{J}_2(k)$	Sets of UEs causing interference or CSIT related noise in the DL
$\mathcal{J}_1^*(k), \mathcal{J}_2^*(k)$	Sets of UEs causing interference or CSIT related noise in the dual uplink (dual sets to $\mathcal{J}_1(k), \mathcal{J}_2(k)$)

Rates, Capacity Regions and Performance Regions

ν_F	Rate connected to a message F
$\mathbf{r} = [r_1 \dots r_K]^T$	Rates connected to UEs
$\hat{\mathcal{R}}_\infty, \hat{\mathcal{R}}_0, \hat{\mathcal{R}}_0^{\text{fdm}}, \hat{\mathcal{R}}_0^{\text{hk}}$	Lower bounds on UL capacity regions for infinite BS coop. ($\hat{\mathcal{R}}_\infty$), or no BS cooperation, assuming only one message per UE ($\hat{\mathcal{R}}_0$), FDM ($\hat{\mathcal{R}}_0^{\text{fdm}}$) or Han-Kobayashi concepts ($\hat{\mathcal{R}}_0^{\text{hk}}$)
$\check{\mathcal{R}}_\infty, \check{\mathcal{R}}_0, \check{\mathcal{R}}_0^{\text{hk}}$	Lower bounds on downlink capacity regions for infinite BS cooperation ($\check{\mathcal{R}}_\infty$), or no BS cooperation, assuming only one message per UE ($\check{\mathcal{R}}_0$), or Han-Kobayashi concepts ($\check{\mathcal{R}}_0^{\text{hk}}$)
$\hat{\mathcal{R}}^{\text{das,fdm}}(\hat{\mathbf{B}}^{\text{das}}, \hat{\mathbf{B}}^{\text{net}})$	Lower bound on the capacity region of DAS-enhanced FDM, using extents of backhaul $\hat{\mathbf{B}}^{\text{das}}$ and $\hat{\mathbf{B}}^{\text{net}}$
$\hat{\mathcal{R}}^{\text{coop}}(\hat{\mathbf{B}}^{\text{dis}}, \hat{\mathbf{B}}^{\text{cif}}, \hat{\mathbf{B}}^{\text{das}}, \hat{\mathbf{B}}^{\text{net}})$	Lower bound on cap. region of DIS/CIF/DAS schemes in UL
$\check{\mathcal{R}}_{\text{coop}}(\check{\mathbf{B}}^{\text{max}})$	Lower bound on cap. region for DAS/UMC/QSC schemes in DL
$\hat{\mathcal{Z}}^{\text{dis}}, \hat{\mathcal{Z}}^{\text{cif}}, \hat{\mathcal{Z}}^{\text{dasd}}, \hat{\mathcal{Z}}^{\text{dasc}}$	Performance regions connected to various schemes in the uplink, capturing both achievable rates as also the sum backhaul required in addition to a non-cooperative system
$\check{\mathcal{Z}}^{\text{das}}, \check{\mathcal{Z}}^{\text{ts}}, \check{\mathcal{Z}}^{\text{umc}}, \check{\mathcal{Z}}^{\text{qsc}}$	Performance regions connected to various schemes in the downlink
$\mathcal{R}_\beta^{\text{xy}}$	Constrained capacity region of scheme xy , given sum-backhaul β
$f_s(\cdot), f_c(\cdot)$	Functions returning the maximum sum-rate of a capacity region, if the sum-rate itself or the common rate is maximized, respectively
α_k	Weight applied to UE k when performing weighted sum-rate maximization

Chapter 1

Introduction

1.1 Motivation

Mobile communication has gained significant importance in today's society. Just recently, the number of mobile phone users worldwide has surpassed 4 billion [WTI08], while the global annual mobile revenue is expected to top \$1 trillion in 2013 [TM08]. Beside conventional voice services, novel mobile applications such as location-based services, video conferencing or mobile gaming [Com09], and the demand for ubiquitous Internet connectivity have triggered an unprecedented growth of mobile data traffic. But though analysts predict this traffic to double annually in the next years [For09], mobile data revenues are merely expected to increase two-fold until 2013 [TM08], creating a severe challenge for mobile operators to respond to the demand for ubiquitous mobile bandwidth, while significantly reducing cost per bit.

These requirements can only be met if the *spectral efficiency* of mobile networks, i.e. the throughput achievable per bandwidth, is strongly increased. The denser, however, a network operator reuses licensed spectrum, the more the system performance becomes limited through inter-cell interference [GK00]. The recently finalized standard LTE Release 8 [Sch09, Erg09] partially addresses this problem by foreseeing multiple antennas at base station and terminal side [McC07], rendering so-called *multiple input - multiple output* (MIMO) techniques possible [FG98, Tel99, Tay04]. These enable spatial multiplexing (e.g. multiple data streams per communication link), array gain (as multiple antennas can coherently pick up or emit signal power), and interference mitigation (making use of the *spatial signature* of interference). As the number of deployable antennas is limited, e.g. through regulatory issues at the base station side, or form factor issues at the terminal side, other means are necessary to further increase spectral efficiency in the presence of inter-cell interference.

Coordinated Multi-Point for Inter-Cell Interference Exploitation

From information theory it is known that inter-cell interference can be seen as an opportunity, rather than a curse, if base stations *cooperatively* process signals [SSZ04]. Such techniques are often referred to as *virtual MIMO*, *network MIMO*, or, more recently, *Coordinated Multi-Point* (CoMP), and they are seen as a key technology of *LTE Advanced* [PDF⁺08, PA09]. Briefly, such schemes allow *interference exploitation* in the uplink through the joint detection of multiple terminals by cooperating base stations, or *interference avoidance* in the downlink, through the joint and coherent transmission from multiple base stations to multiple terminals. CoMP

schemes are also known to provide more *fairness*, i.e. a more homogeneous distribution of throughput over the area, an aspect so far insufficiently addressed in LTE Release 8. Whether CoMP can furthermore improve the *energy* or *cost* efficiency of cellular networks is a topic still under investigation. On one hand, such schemes reduce the transmit power required per transmitted bit, but increased complexity and other overhead might compensate for these efficiency gains. A comprehensive literature overview on CoMP is given in Appendix A.

The Backhaul Bottleneck

Beside many challenges, one major issue connected to CoMP is the large network infrastructure required between cooperating base stations, typically referred to as *backhaul*. Even in current systems, the backhaul infrastructure tends to become the system bottleneck [Buc08, Chu08]. Consequently, the revenues of backhaul solution providers are expected to double in the next four years [Res09]. Introducing cooperation between base stations can easily lead to yet another n-fold increase of backhaul infrastructure [MF07b, MF07c] unless smart and backhaul-efficient cooperation techniques are employed. The focus of this work is hence on

- identifying scenarios in which CoMP is most beneficial, also taking into account the major impact of imperfect channel knowledge at base station and terminal side.
- analyzing a variety of CoMP concepts w.r.t. the achievable throughput/backhaul trade-off, and proposing general backhaul-efficient CoMP strategies for cellular systems.

CoMP vs. Soft Handoff

Please note that CoMP is often wrongly equated with *soft handoff* concepts [VVGZ94, WL97] used in CDMA systems [Ass93]. Here, a cell-edge terminal is served by two or more base stations, such that it is instantaneously detected by the best base station in the uplink, yielding so-called *macro diversity*. In the downlink, the terminal receives individual transmissions from all involved base stations and can jointly exploit them through *maximum ratio combining* (MRC) [MLG99]. In both cases, multiple resources have to be reserved for this terminal, leading to an effective loss of spectral efficiency. Furthermore, soft handoff does *not* aim at exploiting spatial multiplexing gain or combating inter-cell interference, but is solely targeted towards improving the performance of handoff processes between cells.

1.2 Contribution of this Work

Information-theoretic Analysis of the Throughput/Backhaul Trade-Off

In this work, the throughput/backhaul trade-off of various CoMP strategies is investigated, also taking into account the detrimental impact of imperfect channel knowledge. The topic is observed from an information-theoretic point of view, where existing work has not sufficiently captured the many degrees of freedom of backhaul-efficient CoMP or provided conclusive answers yet. The research in this work is initially based on reasonably dimensioned and detailed CoMP scenarios that are still analytically tractable, while yielding a more meaningful insight into the topic than the models of other authors. The results are then complemented with a system-level perspective on backhaul-efficient CoMP, as well as a discussion on practical issues connected to the considered schemes.

Major Conceptual and Theoretical Contributions

Besides delivering a comprehensive overview on the issue of backhaul-aware CoMP, this thesis also provides new methodology for the characterization of the downlink capacity region under no, infinite or partial base station cooperation, and under imperfect channel knowledge at base station and terminal side. A major theoretical contribution is the generalization of uplink/downlink duality to these aspects [MF09a], as well as the introduction of the concept of *performance regions* [MF08e]. The latter enable to capture both the achievable rates of terminals under certain cooperation schemes, as well as the required backhaul.

1.3 Related Work

To the best of our knowledge, there are only few research groups beside the Vodafone Chair that have worked on the topic of backhaul-efficient CoMP from an information-theoretic point of view:

Amichai Sanderovich, Oren Somekh, Osvaldo Simeone, Shlomo Shamai (Shitz), Benjamin M. Zaidel and Vincent Poor have written a multitude of publications connected to backhaul-constrained CoMP in uplink and downlink. Their research is mainly based on simplified cellular scenarios, such as one- or two-dimensional Wyner models [Wyn94], where intra- and inter-cell signal propagation is characterized through very few parameters. This facilitates the derivation of analytical expressions, through which for example asymptotic throughput/backhaul trade-offs for an infinite transmit power, number of cells etc. can be investigated. The key findings of the stated authors are summarized as follows:

The authors initially investigated uplink CoMP in [SSSK05, SSSP06, SSS09], observing a two-antenna transmitter and two receiving base stations, which independently quantize and forward their received signals to a central processing unit in the network. The authors point out that large gains in the throughput/backhaul trade-off can be obtained if quantization schemes are used that exploit the signal correlation between different base stations. Observations were extended to an arbitrary number of base stations with symmetric inter-cell interference in [SSS07a, SSS⁺07b, SSS⁺08a, SSS⁺08b]. It was shown that the throughput/backhaul trade-off can be further improved if partial decoding already takes place at the base stations, hence prior to cooperation. For a slightly modified setup with asymmetric interference links, the authors have introduced a set of base station cooperation concepts in [SSPS08b, SSPSO9b]. These include the possibility that base stations decode the transmission of an assigned terminal and then forward the decoded bits (or any representation thereof) to another base station for interference cancellation, similar to concepts discussed in [KF07, MF08e, KF08].

Regarding the cellular downlink, the authors have also considered a circular Wyner model with simplified, asymmetrical interference in [SSPS07, SSS⁺07b, SSSP08, SSS⁺08a, SSS⁺08b, SSPSO8a, SSPSO9a]. The authors compare cooperation strategies where each base station either performs local encoding (possibly with knowledge on the encoding function of a set of adjacent base stations), where a central network entity performs the encoding for the transmissions targeted to all terminals and forwards quantized signals to the base stations, or a combination of both. They conclude that local encoding approaches are only superior under strongly constrained backhaul and large SINR, and otherwise inferior to centralized approaches, while mixed strategies are not beneficial at all.

Aitor del Coso and **Sebastian Simoens** have worked on distributed compression of received signals for cooperation in a cellular uplink [dCS08,dS08]. Their model foresees decoding to take place both at a centralized network entity, or by one of the base stations involved. Basically, their work is a generalization of distributed compression and source coding schemes introduced in [SSSK05,SSSP06] to scenarios with an arbitrary number of antennas per base station, which is essential for observing achievable throughput/backhaul trade-offs for MIMO channels under fast fading realizations. The cited work hence provides a fundamental mathematical basis for the models derived in this thesis.

Recently, **I-Hsiang Wang** and **David Tse** have started investigating interfering transmissions under partial receiver-side cooperation [WT09], but have focused on the observation of strong interference cases and regimes of asymptotically large signal-to-noise ratio, which is probably of minor value for the practical usage of CoMP.

Note that some authors consider base station cooperation to take place over the same wireless resource as the communication between terminals and base stations [HM06,PV09], which, however, is an entirely different scenario than the one considered in this thesis.

1.4 Structure of this Thesis

The thesis is organized as follows:

In Chapter 2, the transmission models considered for uplink and downlink CoMP are introduced, and inner bounds on *capacity regions* for a non-cooperative, partially cooperative (i.e. backhaul-constrained), or fully cooperative system under imperfect channel knowledge at the transmitter and receiver side are derived. Furthermore, the before mentioned concept of *performance regions* is introduced.

In Chapter 3, the general models stated before are used for the observation of small cooperation scenarios that are still analytically and numerically tractable, while yielding a valuable insight into the degrees of freedom of CoMP. General gains expectable through CoMP in uplink and downlink are observed, and the throughput/backhaul trade-off achievable with the introduced cooperation concepts is evaluated for various scenarios.

Observations are extended to large cellular systems in Chapter 4, where *clustering* and *resource partitioning* concepts are introduced in order to break down such systems into the cooperation scenarios treated before. It is shown that the typical structure of cellular systems allows large portions of CoMP gains to be obtained at a reasonable investment into backhaul.

After a comprehensive discussion on the implications of the models and key findings of this work on practical cellular systems in Chapter 5, the work is concluded in Chapter 6.

1.5 Notation

The following notation is used throughout the work:

- Capital, italic letters (e.g. X, Y) refer to *sequences* of transmitted or received symbols.
- Capital, bold letters (e.g. \mathbf{H}^e, \mathbf{C}) denote matrices (superscripts distinguish different matrices), where single column vectors are denoted through the corresponding lower-case letter and the column index, e.g. $\mathbf{h}_k^e, \mathbf{c}_k$. A single element in the i th row and j th column of the matrix is addressed as $h_{i,j}^e, c_{i,j}$, respectively. A notation such as $\mathbf{h}_{m,k}^e$ or Φ_m^{nn} can refer to a sub-part of a matrix, which will be explained explicitly where necessary. Operator $\text{vec}(\cdot)$ stacks all columns of a matrix into one long column vector.
- $\mathbf{A} \succeq 0$ denotes positive semidefiniteness, $\mathbf{A} \succeq \mathbf{B}$ states that $\mathbf{A} - \mathbf{B}$ is positive semidefinite, and $\mathbf{A} > \mathbf{B}$ denotes element-wise inequality.
- Calligraphic letters (e.g. \mathcal{M}, \mathcal{F}) refer to sets, \emptyset refers to the empty set, and e.g. $|\mathcal{M}|$ denotes the size, or cardinality, of a set.
- The sets of real, complex and integer numbers are denoted as \mathbb{R}, \mathbb{C} , and \mathbb{N} , respectively.
- Operator $\Delta(\cdot)$ is used on symmetric matrices and sets all off-diagonal values to zero, while operator $\mathbf{M} = \text{diag}(\mathbf{m}), \mathbf{m} = \text{diag}(\mathbf{M})$ returns a symmetric matrix \mathbf{M} with diagonal elements taken from vector \mathbf{m} , or extracts the diagonal \mathbf{m} from a given matrix \mathbf{M} , depending on the operand, as known from MATLAB.
- Operators $H(\cdot)$ and $h(\cdot)$ denote entropy and differential entropy, respectively, and $I(X; Y)$ denotes the mutual information between X and Y .
- Expressions $(\cdot)^T$ and $(\cdot)^H$ denote matrix and Hermitian transpose, respectively.
- Various variables are used with an accent (i.e. \hat{X}, \check{X}) to indicate their connection to the uplink or downlink, respectively.
- The operator \cup denotes a convex hull operation, and $E_{xy}\{\cdot\}$ denotes the expectation value of the term in parentheses over many realizations of xy .
- \mathbf{I} denotes the identity matrix, and $\mathbf{0}_{[i \times j]}, \mathbf{1}_{[i \times j]}$ denote matrices of size $i \times j$, filled with zeros or ones, respectively.
- The notation $\mathbf{x} \sim \mathcal{N}_{\mathbb{C}}(\mathbf{m}, \Phi)$ states that \mathbf{x} is a vector of complex Gaussian random variables with mean $E\{\mathbf{x}\} = \mathbf{m}$ and covariance $E\{\mathbf{x}\mathbf{x}^H\} = \Phi$.
- $\text{tr}\{\mathbf{A}\}$ and $|\mathbf{A}|$ denote matrix trace and determinant, respectively.

Chapter 2

Information-Theoretic Basics

In this chapter, the information theoretical concepts are introduced which form the basis of all further analysis in this thesis. A novel framework is described, which allows to determine inner bounds on the capacity regions for uplink and downlink CoMP with no, backhaul-constrained or infinite base station cooperation, while incorporating the impact of imperfect channel knowledge at both base station and terminal side. A key aspect is that the downlink model captures various degrees of freedom of base station cooperation in arbitrarily large setups, while being able to exploit uplink/downlink duality for rate region computation at reasonable complexity. Further, the novel concepts of performance regions and backhaul-constrained capacity regions are introduced, which capture the trade-off between achievable rates and required backhaul.

The chapter is structured as follows. We first clarify some essential wording used in this thesis, and explain general concepts connected to all considered transmission schemes in Section 2.1. We then introduce our uplink and downlink models in Sections 2.2 and 2.3, respectively. Both sections are structured in the same way that we first state the transmission model, then model the impact of imperfect channel knowledge, after which rate regions are derived first for the extreme cases of infinite or no cooperation, and then for various backhaul-limited base station cooperation schemes. The concepts of performance regions and backhaul-constrained rate regions are then introduced in Section 2.4.

2.1 General Concepts

Nomenclature

In this work, the terms *CoMP* or *base station cooperation* refer to schemes where base stations exchange received signals or information connected to the data bits of certain terminals for the purpose of interference mitigation. Schemes that merely make use of *coordination* between base stations, e.g. joint scheduling or interference-aware precoding, are considered *non-cooperative*, which might deviate from the nomenclature in other work. For these reasons, schemes denoted as *non-cooperative* may already be superior to those used in current mobile communication systems. Schemes denoted as *cooperative* are generally based on *multi-cell joint signal processing* and require an *additional* exchange of signals between base stations as compared to a *non-cooperative* system. In this respect, *backhaul infrastructure* refers to the overall connectivity of base stations and the network, while any *backhaul* quantity always refers to the backhaul capacity required *in addition* to that of a non-cooperative system.

Messages and Sequences

A *message* is a set of discrete information (i.e. a block of data bits) that is supposed to be conveyed from base station (BS) side to terminal (UE) side, or vice versa. Messages are generally denoted as \hat{F}_{yz} or \check{F}_{yz} , where yz can be any arbitrary subscript. Throughout this work, the accent helps to distinguish between variables used in the uplink or downlink, respectively. The transmitter side employs an encoding function $e(\cdot)$ to map messages onto *sequences* of $N_{\text{sym}} \in \mathbb{N}^+$ transmit symbols, which are then denoted as \hat{X}_{yz} or \check{X}_{yz} . Each sequence $X_{yz} = (x_{yz}^{[1]}, x_{yz}^{[2]}, \dots, x_{yz}^{[N_{\text{sym}}]})$ is assumed to be a complex Gaussian random process, where each symbol is drawn randomly and independently from a Gaussian distribution with zero mean and unit variance¹, i.e. $E_t\{x_{yz}^{[t]}(x_{yz}^{[t]})^H\} = 1$. N_{sym} is assumed large, such that all random processes are ergodic and fully characterized through their mean and variance. Typically, the transmitter side will perform precoding on a set of sequences, or compute a superposition of these, before they are transmitted symbol-wise over the channel in N_{sym} successive channel accesses. After various kinds of signal processing, the receiver side will finally map sequences onto estimates of the transmitted messages, using a *decoding function* $d(\cdot)$.

Setup and Wireless Channel

In both uplink and downlink, we denote the number of BSs as M , and the number of UEs as K . We assume that each BS employs N_{bs} antennas, and each UE employs N_{mt} antennas, such that the overall number of antennas at BS and UE side is given as $N_{\text{BS}} = M \cdot N_{\text{bs}}$ and $N_{\text{MT}} = K \cdot N_{\text{mt}}$, respectively. We further introduce $\mathcal{M} = \{1, 2, \dots, M\}$ and $\mathcal{K} = \{1, 2, \dots, K\}$ as sets containing all BSs and UEs, respectively. We generally assume that all BSs and UEs are perfectly synchronized in time and frequency, and that transmission takes place over a frequency-flat channel, such that it is free of inter-symbol interference. This could e.g. be realized by transmitting symbols in one or multiple sub-carriers of an *orthogonal division multiplex* (OFDM) system.

2.2 Uplink

2.2.1 Transmission Model

We consider an uplink transmission from K UEs to M BSs, as depicted in Figure 2.1, where each UE has $N_{\text{mt}} = 1$ transmit antenna, as this is the configuration in the recently finalized mobile communications standard LTE Release 8 [McC07]. The BSs, however, can be equipped with any arbitrary number N_{bs} of receive antennas each. Each UE $k \in \mathcal{K}$ has a set $\hat{\mathcal{F}}_k$ of messages it intends to transmit over the channel. It maps these onto a set $\hat{\mathcal{X}}_k$ of sequences, using the encoding function $e(\cdot)$ introduced in Section 2.1 separately for each message. We capture all messages transmitted by all UEs in a set $\hat{\mathcal{F}}_{\text{all}} = \hat{\mathcal{F}}_1 \cup \hat{\mathcal{F}}_2 \cup \dots \cup \hat{\mathcal{F}}_K$, and all sequences consequently in a set $\hat{\mathcal{X}}_{\text{all}} = \hat{\mathcal{X}}_1 \cup \hat{\mathcal{X}}_2 \cup \dots \cup \hat{\mathcal{X}}_K$. The overall transmission from all UEs to the BSs in one single channel access $1 \leq t \leq N_{\text{sym}}$ can be stated as

$$\mathbf{y}^{[t]} = \mathbf{H}\mathbf{s}^{[t]} + \mathbf{n}^{[t]}, \quad (2.1)$$

¹Note that using Gaussian signals is not necessary optimal, especially under imperfect channel knowledge considered later [Med00, LS02], but this strongly simplifies information-theoretic derivations.

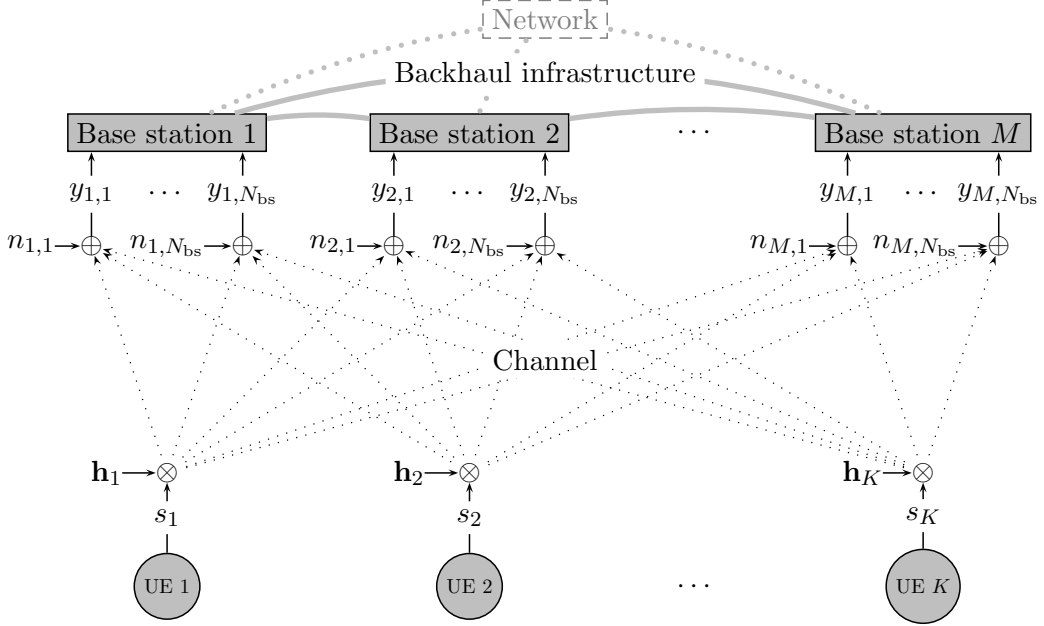


Figure 2.1: Model of the uplink transmission considered in this work.

where $\mathbf{y}^{[t]} = [y_{1,1}^{[t]} \dots y_{1,N_{bs}}^{[t]}, y_{2,1}^{[t]} \dots y_{2,N_{bs}}^{[t]}, \dots, y_{M,1}^{[t]} \dots y_{M,N_{bs}}^{[t]}]^T \in \mathbb{C}^{[N_{BS} \times 1]}$ are the signals received at the BSs, and $\mathbf{H} = [\mathbf{h}_1 \mathbf{h}_2 \dots \mathbf{h}_K] \in \mathbb{C}^{[N_{BS} \times K]}$ is the channel matrix, where each column \mathbf{h}_k is connected to UE k . The channel is modeled as a random variable where each element is taken from an independent, zero-mean Gaussian distribution $h_{i,j} \sim \mathcal{N}_{\mathbb{C}}(0, E\{|h_{i,j}|^2\})$, known as *Rayleigh fading* [Rap96]. Besides considering a fading process at this point, we assume the channel to remain constant throughout a block of N_{sym} channel accesses, typically referred to as a *block fading model* [MH99]. In this thesis, we usually observe the properties of a transmission under a fixed channel matrix \mathbf{H} , but the channel's statistical properties are needed for derivations in later sections. $\mathbf{s}^{[t]} \in \mathbb{C}^{[K \times 1]}$ are the symbols transmitted from the UEs, which are given as

$$\forall k \in \mathcal{K} : s_k^{[t]} = \sum_{\forall F \in \hat{\mathcal{F}}_k} \sqrt{\rho_F} [e(F)]^{[t]}, \quad (2.2)$$

where $\rho_F \in \mathbb{R}_0^+$ is the transmit power assigned to message F . We use $\mathcal{P} = \{\rho_F : F \in \hat{\mathcal{F}}_{\text{all}}\}$ to denote the set of all transmit powers of all messages, i.e. the overall uplink power allocation. According to (2.2), each UE k transmits a superposition of sequences in set $\hat{\mathcal{X}}_k$, each weighted with a different transmit power. $\mathbf{n}^{[t]} = [n_{1,1}^{[t]} \dots n_{1,N_{bs}}^{[t]}, n_{2,1}^{[t]} \dots n_{2,N_{bs}}^{[t]}, \dots, n_{M,1}^{[t]} \dots n_{M,N_{bs}}^{[t]}]^T \in \mathbb{C}^{[N_{BS} \times 1]}$ is additive noise at the receiver side, which we assume to consist of uncorrelated, zero-mean Gaussian random processes with diagonal covariance matrix $E_t\{\mathbf{n}^{[t]}(\mathbf{n}^{[t]})^H\} = \sigma^2 \mathbf{I}$. We state the covariance of the transmitted signals as $E_t\{\mathbf{s}^{[t]}(\mathbf{s}^{[t]})^H\} = \mathbf{P} = \text{diag}(\mathbf{p})$ with $\mathbf{p} \in \mathbb{R}_0^{+[K \times 1]}$, where each element p_k corresponds to the overall transmit power (over all transmitted sequences) of UE k , and assume that the transmit powers are subject to the power constraint $\mathbf{P} \preceq \hat{\mathbf{P}}^{\text{max}}$. Hence, each UE has an individual power constraint defined by the entries of the diagonal matrix $\hat{\mathbf{P}}^{\text{max}} = \text{diag}(\hat{\mathbf{p}}^{\text{max}})$ with $\hat{\mathbf{p}}^{\text{max}} \in \mathbb{R}_0^{+[K \times 1]}$. Later, we will need the transmit

covariance connected to only a subset of messages $\mathcal{F} \subseteq \hat{\mathcal{F}}_{\text{all}}$, which we denote as $\mathbf{P}(\mathcal{F})$, where the diagonal elements are given as

$$[\mathbf{P}(\mathcal{F})]_{k,k} = \sum_{\forall F \in \{\hat{\mathcal{F}}_k \cap \mathcal{F}\}} \rho_F. \quad (2.3)$$

In later sections, we will also use the expressions $\forall k \in \mathcal{K} : S_k = \sum_{F \in \hat{\mathcal{F}}_k} \rho_F \cdot e(F)$ as the superposition of all sequences transmitted by UE k , $\forall m \in \mathcal{M} : Y_m$ as the sequence of all symbols received at all antennas of BS m , and $\forall m \in \mathcal{M}, 1 \leq a \leq N_{\text{bs}} : N_{m,a}$ as the noise sequence received by BS m at antenna a . As indicated in Figure 2.1, the BSs are assumed to be connected through a mesh of error-free backhaul links of finite capacity $\hat{\mathbf{B}}^{\text{max}} \in \mathbb{R}_0^{[M+1 \times M]}$. Here, each entry $\forall i, j \in \mathcal{M} : \hat{b}_{i,j}^{\text{max}}$ denotes the one-directional backhaul link capacity from BS j to BS i , and $\forall j \in \mathcal{K} : \hat{b}_{M+1,j}^{\text{max}}$ denotes a backhaul link from BS j to the network. In the remainder of this work, we will omit the symbol index t for notational brevity.

2.2.2 Modeling of Imperfect Channel Knowledge

We now want to incorporate the impact of imperfect *channel state information* (CSI) into our transmission model. Clearly, as each UE k is equipped with only one antenna, it can simply map the symbols s_k directly to this one antenna, and the performance is independent of whether the UE has channel knowledge or not². In this section, we will thus focus on the (significant) impact of imperfect CSI at the base station or *receiver* side, abbreviated as CSIR. For this, let us assume that all BSs have knowledge of the same overall channel estimate

$$\hat{\mathbf{H}} = \mathbf{H} + \hat{\mathbf{E}}, \quad (2.4)$$

with $\hat{\mathbf{H}} \in \mathbb{C}^{[N_{\text{BS}} \times K]}$, and where the channel estimation error $\hat{\mathbf{E}} \in \mathbb{C}^{[N_{\text{BS}} \times K]}$ is modeled as a matrix of i.i.d. Gaussian random variables with covariance

$$E \left\{ \text{vec}(\hat{\mathbf{E}}) \text{vec}(\hat{\mathbf{E}})^H \right\} = \frac{\sigma_{\text{pilots}}^2}{N_p \cdot p_{\text{pilots}}} \cdot \mathbf{I} = \sigma_E^2 \cdot \mathbf{I}. \quad (2.5)$$

Same as the channel matrix \mathbf{H} , the estimated channel $\hat{\mathbf{H}}$ and its estimation error $\hat{\mathbf{E}}$ are assumed to be constant over one transmission block. Equation (2.5) is based on the Kramer-Rao lower bound [Kay93], yielding the absolute estimation error variance, given that an optimal channel estimation has been performed based on the transmission of N_p pilots of power p_{pilots} each, and has been subject to Gaussian noise with variance σ_{pilots}^2 . Note that the latter noise variance can differ from the noise variance σ^2 experienced by the actual data transmission in (2.1) if multi-sector (quasi-)orthogonal pilot sequences are employed, as in LTE Release 8 [McC07]. For the remainder of this work, we will assume unit-power pilots ($p_{\text{pilots}} = 1$), and choose an *effective* number of pilots $N_p = 2$ that is motivated through the observation of a specific channel estimation scheme in a frequency-selective *orthogonal frequency division multiple access* (OFDMA) system in Appendix E. Hence, we can draw

²The notion of capacity regions, however, which we will introduce later, implies that the transmitters operate at specific rates and employ specific transmit powers. This means that the receiver side has to inform the transmitters about which rates and power levels to use, which can be seen as a minimal extent of channel information made available to the transmitters.

conclusions from a simple transmission model based on a flat channel, while choosing N_p such that it represents a complex, practical system. We can now rewrite (2.1) with (2.4) as

$$\mathbf{y} = \left(\hat{\mathbf{H}} - \mathbf{E} \right) \mathbf{s} + \mathbf{n}, \quad (2.6)$$

which we can interpret as a transmission over a channel $\hat{\mathbf{H}}$ subject to noise $-\mathbf{E}\mathbf{s} + \mathbf{n}$. As the terms $\hat{\mathbf{H}}$ and \mathbf{E} , however, are correlated due to the definition in (2.4), we ideally want to reformulate (2.6) such that we have a transmission over an *effective* channel subject to additional and *uncorrelated* channel estimation noise. This is done in the following theorem:

Theorem 2.2.1 (Modified uplink transmission equation under imperfect CSIR). *An inner bound for the capacity region of the uplink transmission in (2.1) under imperfect receiver-side channel knowledge (and for any arbitrary BS cooperation scheme observed later) can be found by observing the capacity region connected to the transmission*

$$\mathbf{y} = \mathbf{H}^e \mathbf{s} + \mathbf{v} + \mathbf{n}, \quad (2.7)$$

which involves a power-reduced effective channel $\mathbf{H}^e \in \mathbb{C}^{[N_{\text{BS}} \times K]}$ with elements

$$\forall i, j : h_{i,j}^e = \frac{h_{i,j}}{\sqrt{1 + \sigma_E^2 / E \{ |h_{i,j}|^2 \}}} \quad (2.8)$$

and is subject to an additional Gaussian noise term $\mathbf{v} \in \mathbb{C}^{[N_{\text{BS}} \times 1]}$ with diagonal covariance

$$E \{ \mathbf{v}\mathbf{v}^H \} = \mathbf{\Phi}^{\text{hh}} = \Delta \left(\bar{\mathbf{E}}^e \mathbf{P} \left(\hat{\mathcal{F}}_{\text{all}} \right) \left(\bar{\mathbf{E}}^e \right)^H \right), \quad \text{where } \forall i, j : \bar{e}_{i,j}^e = \sqrt{\frac{E \{ |h_{i,j}|^2 \} \cdot \sigma_E^2}{E \{ |h_{i,j}|^2 \} + \sigma_E^2}}. \quad (2.9)$$

Proof. Briefly, the theorem is based on the fact that (2.7) overestimates the detrimental impact of imperfect CSIR by assuming \mathbf{v} to be a Gaussian random variable with a different realization in each channel use. Note that 2.8 denotes an instantaneous effective channel which is interesting for later observing the capacity connected to an instantaneous channel realization. The proof is stated in Appendix B.1. \square

Note that the model in general implies that the extent of channel estimation error, hence σ_E^2 , as well as the average power of all links $E \{ |h_{i,j}|^2 \}$, are known to the receiver side.

2.2.3 Capacity Region Under Infinite BS Cooperation

If we assume that an infinite backhaul infrastructure enables full cooperation between all BSs, we can regard the transmission from (2.1) as a transmission from K UEs to *one* virtual super receiver with N_{BS} receive antennas, as depicted in Figure 2.2. This corresponds to a *multiple access channel* (MAC), which was originally introduced by [Ahl71], and where a simple single-letter expression describes the *capacity region* [Ahl71, Lia72]. The latter contains all tuples of rates at which the K UEs can transmit, such that the virtual receiver can decode all UEs with a probability of error that decreases exponentially in the block length N_{sym} [CT06]. It is easy to see that all points on the boundary of the capacity region can be achieved

by *successive interference cancellation* (SIC), i.e. the successive decoding and subtraction of the signals from the UEs, in combination with time-sharing, i.e. a weighted combination of different transmission and decoding strategies over time [CT06]. This means that in theory, i.e. under large N_{sym} , optimal codes, optimal rate adaptation to the channel, capacity can be achieved with a simple linear post-processing at the BS side prior to the application of SIC. Recent work has been on the computation of the capacity region for a large number of UEs with multiple antennas per UE, which is in principle a convex optimization problem, but can be computationally complex [VBW98, VTA01, YRBC04].

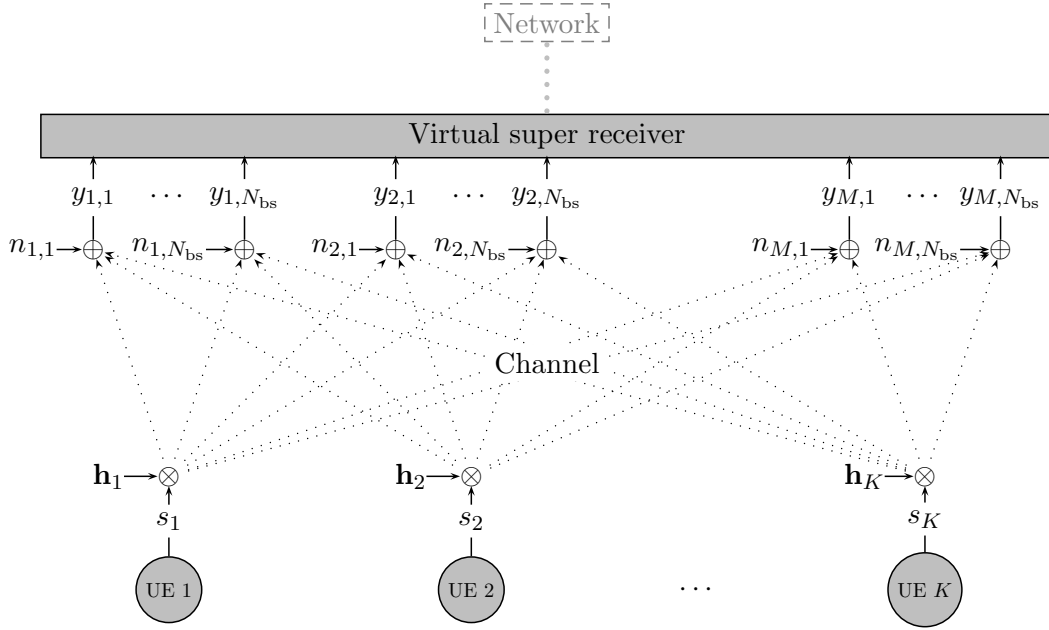


Figure 2.2: Model of the uplink transmission assuming infinite BS cooperation.

In [MF09b], the capacity region for the modified transmission equation in (2.7) has been derived, incorporating the impact of imperfect channel knowledge. In the context of a MAC, there is no benefit of letting UEs transmit superimposed messages [CT06], hence one sole message per UE is sufficient. We therefore constrain the employed messages to

$$\forall k \in \mathcal{K} : \hat{\mathcal{F}}_k := \{\hat{F}_k\}, \hat{\mathcal{F}}_{\text{all}} := \{\hat{F}_1, \hat{F}_2, \dots, \hat{F}_K\} \text{ and } \mathcal{P} := \{\rho_{\hat{F}_1}, \rho_{\hat{F}_2}, \dots, \rho_{\hat{F}_K}\} \quad (2.10)$$

and state the following theorem:

Theorem 2.2.2 (Uplink capacity region under infinite BS cooperation). *An inner bound for the capacity region of the uplink transmission in (2.1) assuming infinite BS coop. is given as*

$$\hat{\mathcal{R}}_{\infty} = \bigcup_{\mathcal{P} : \mathbf{P}(\hat{\mathcal{F}}_{\text{all}}) \preceq \hat{\mathbf{P}}^{\text{max}}} \hat{\mathcal{R}}_{\infty}(\mathcal{P}) \quad (2.11)$$

where \bigcup denotes a convex hull operation. Expression $\hat{\mathcal{R}}_{\infty}(\mathcal{P})$ denotes an inner bound on the achievable rate region for a given power allocation \mathcal{P} , for which all rate tuples $\mathbf{r} \in \hat{\mathcal{R}}_{\infty}(\mathcal{P})$

fulfill $\forall k \in \mathcal{K} : 0 \leq r_k \leq \nu_{\hat{F}_k}$ and $\forall \mathcal{F} \subseteq \hat{\mathcal{F}}_{\text{all}}$:

$$\sum_{F \in \mathcal{F}} \nu_F \leq \log_2 \left| \mathbf{I} + \left(\sigma^2 \mathbf{I} + \Delta \left(\bar{\mathbf{E}}^e \mathbf{P} \left(\hat{\mathcal{F}}_{\text{all}} \right) \left(\bar{\mathbf{E}}^e \right)^H \right) \right)^{-1} \mathbf{H}^e \mathbf{P} \left(\mathcal{F} \right) \left(\mathbf{H}^e \right)^H \right|, \quad (2.12)$$

where ν_F is the rate connected to message F .

Proof. The proof is based on the modified transmission equation from (2.7) and given in Appendix D.1. \square

Equation (2.12) basically states that the sum rate of any subset of UEs is limited by the sum capacity of the channel, assuming that all other UEs have already been decoded and their signals subtracted from the system. In the case of perfect channel knowledge at the BS side, their signals can be removed completely after decoding, whereas under imperfect CSIR, a certain extent of noise covariance $\Delta(\bar{\mathbf{E}}^e \mathbf{P}(\hat{\mathcal{F}}_{\text{all}})(\bar{\mathbf{E}}^e)^H)$ remains. Clearly, this noise term has a detrimental impact on the transmission in general, regardless of which signal processing strategy will be employed later. If the sum rate is to be maximized and all links have unit power on average ($\forall i, j : E\{|h_{i,j}|^2\} = 1$), (2.12) simplifies to

$$\sum_{k=1}^K r_k \leq \log_2 \left| \mathbf{I} + \left(\sigma^2 + \sigma_{E'}^2 \text{tr} \left\{ \mathbf{P} \left(\hat{\mathcal{F}}_{\text{all}} \right) \right\} \right)^{-1} \mathbf{H}^e \mathbf{P} \left(\hat{\mathcal{F}}_{\text{all}} \right) \left(\mathbf{H}^e \right)^H \right|, \quad (2.13)$$

with $\sigma_{E'}^2 = \sigma_E^2 / (1 + \sigma_E^2)$, which corresponds to the expression derived for *classical MIMO transmission* under imperfect channel estimation in [YG06]³. We can see from (2.12) and (2.13) that the impact of channel estimation error grows with increasing transmit power, and hence the resulting capacity region differs from that of the MAC under perfect channel knowledge. More precisely, increasing one UE's transmit power will in most cases lead to a degradation of the rates of all other UEs, as this will increase the extent of signal power connected to channel estimation error that has to be accepted as background noise. This will be illustrated for an example channel in Section 2.2.5. As the transmission in (2.7) overestimates the impact of channel estimation error, the capacity region in Theorem 2.2.2 is an inner bound on the capacity region of our original uplink transmission in (2.1) under imperfect CSIR.

Capacity Region Computation

Under perfect CSIR, capacity region computation is easily possible by observing the sum-rate of any subset of UEs, knowing that capacity is achieved if all UEs transmit at maximum power. As this is not the case under imperfect CSIR, we generally compute such rate regions through a brute-force search over all possible power allocations \mathcal{P} at reasonable granularity.

2.2.4 Capacity Region without BS Cooperation

In the case where no cooperation is possible between BSs, our scenario is similar to a Gaussian *interference channel* (IC), which was originally introduced by [Ahl74] and has since been widely investigated. The classical IC is defined as an arbitrary number of independent transmitter-receiver pairs that communicate on the same time/frequency resource, such that

³Note that the cited authors base their capacity expression on an instantaneous channel estimate, whereas we use an effective channel. This is discussed in Appendix B.1.

the transmissions are subject to mutual interference. Unfortunately, the capacity region of the Gaussian IC is only known for certain interference conditions, for example the case of *very strong interference*, where the interference links are much stronger than the actual communication links between the transmitters and their dedicated receivers. In this case, the achievable rates of the UEs are the same as if there were no interference between the communication links at all [Car75]. On the other hand, it has been shown in [SKC07] that the best (capacity achieving) strategy is to treat all interference as noise, if the interference links are weaker than a certain threshold. In the intermediate regime of moderate interference, the best known transmission strategy is the *Han-Kobayashi* (HK) scheme [HK81], being an extension of previous work by [Car78]. Here, each UE splits its transmit power into the transmission of a *private message*, which is decoded only at the dedicated BS, and (in the usually observed case of $M = K = 2$) a *common message*, which is decoded by both BSs individually. The benefit is that both BSs can decode a portion of the other UE's transmission and thus reduce the effective level of interference. As the optimality of the Han-Kobayashi scheme could not yet be proved (i.e. it can only be considered as an inner capacity bound), various authors have suggested outer bounds on the capacity region of the interference channel [Sat78, Car83, Kra04], typically based on the assumption of Genie information made available to the receivers. As the computation of the optimal power allocation for the Han-Kobayashi scheme is complex, a simplified, yet equivalent framework has been introduced by [CMGE06], and a further simplified, suboptimal scheme has been proposed by [ETW08], proved to be within one bit of sum capacity. Recent work has been on the IC with multiple antennas per receiver [WT08], with partial cooperation between receivers [WT09, PV09], or observing the topic from the point of view of *interference alignment* [MAMK08]. Note that our scenario differs from the classical IC in the way that it does not matter at which BS parts of the UE's transmissions are decoded, hence in the regime of *strong* or *very strong* interference (according to the definition in [ETW08]), we have the extra degree of freedom of letting one BS decode multiple UEs, or simply swap the assignment of BSs to UEs.

To determine the capacity region without BS cooperation, we generalize the Han-Kobayashi scheme to any arbitrary number of UEs and BSs, and incorporate the possibility of arbitrary BS-UE assignments. For this, we define the set of messages transmitted by UE $k \in \mathcal{K}$ as

$$\hat{\mathcal{F}}_k := \left\{ \hat{F}_k^{\mathcal{M}'} : \mathcal{M}' \subseteq \mathcal{M} \right\}, \quad (2.14)$$

where $\hat{F}_k^{\mathcal{M}'}$ denotes the message originating from UE k and decoded individually by all BSs in set \mathcal{M}' . Note that the sets stated through (2.14) capture any decoding of a UE transmission by any possible subset of BSs, allowing us to model arbitrary configurations of the Han-Kobayashi scheme in conjunction with arbitrary BS-UE assignments. The challenge is to find the optimal power allocation strategy \mathcal{P} for all messages. Let us define for each BS $m \in \mathcal{M}$:

$$\mathcal{F}^{[m]} := \left\{ F_j^{\mathcal{M}'} \in \hat{\mathcal{F}}_{\text{all}} : m \in \mathcal{M}' \right\} \quad (2.15)$$

$$\bar{\mathcal{F}}^{[m]} := \left\{ F_j^{\mathcal{M}'} \in \hat{\mathcal{F}}_{\text{all}} : m \notin \mathcal{M}' \right\} \quad (2.16)$$

as the sets of messages *decoded* or *not decoded* by this BS, respectively. We can now state an inner bound on the capacity region as follows:

Theorem 2.2.3 (Uplink capacity region without BS cooperation). *An inner bound of the capacity region of the uplink transmission in (2.1) without BS cooperation is given as*

$$\hat{\mathcal{R}}_0^{\text{hk}} = \bigcup_{\mathcal{P} : \mathbf{P}(\hat{\mathcal{F}}_{\text{all}}) \preceq \hat{\mathbf{P}}^{\text{max}}} \hat{\mathcal{R}}_0^{\text{hk}}(\mathcal{P}), \quad (2.17)$$

where $\hat{\mathcal{R}}_0^{\text{hk}}(\mathcal{P})$ is an inner bound on the achievable rate region for a given power allocation \mathcal{P} , for which all rate tuples $\mathbf{r} \in \hat{\mathcal{R}}_0^{\text{hk}}(\mathcal{P})$ fulfill $\forall k \in \mathcal{K} : 0 \leq r_k \leq \sum_{F \in \hat{\mathcal{F}}_k} \nu_F$ and $\forall m \in \mathcal{M} :$

$$\forall \mathcal{F}' \subseteq \mathcal{F}^{[m]} : \sum_{F \in \mathcal{F}'} \nu_F \leq \log_2 \left| \mathbf{I} + (\Phi_m^{\text{ii}})^{-1} \mathbf{H}_m^e \mathbf{P}(\mathcal{F}') (\mathbf{H}_m^e)^H \right|$$

$$\text{with } \Phi_m^{\text{ii}} = \sigma^2 \mathbf{I} + \underbrace{\Delta \left(\bar{\mathbf{E}}_m^e \mathbf{P}(\hat{\mathcal{F}}_{\text{all}}) (\bar{\mathbf{E}}_m^e)^H \right)}_{\text{Channel estimation impact}} + \underbrace{\mathbf{H}_m^e \mathbf{P}(\hat{\mathcal{F}}^{[m]}) (\mathbf{H}_m^e)^H}_{\text{Interference}}, \quad (2.18)$$

where ν_F is again the rate connected to message F , \mathbf{H}_m^e is the effective channel connected to BS m , and $\bar{\mathbf{E}}_m^e$ is the part of matrix $\bar{\mathbf{E}}^e$ from (2.9) connected to BS m .

Proof. The theorem is a straightforward extension of the work in [HK81] to the transmission in (2.7) with an arbitrary number of communication paths and employed messages. \square

Unfortunately, it is tedious to determine the capacity region $\hat{\mathcal{R}}_0^{\text{hk}}$ for any setup with more than 2 BSs and 2 UEs. From a practical point of view, any scheme that requires the UE to perform superposition coding would introduce a significant increase in complexity to both the UE and BS side. Furthermore, it is known from [Kra04] that gains over a transmission where each UE invests its transmit power into a single message only exist in certain, limited regimes of interference and scenarios of reasonably high *signal-to-noise ratio* (SNR). Hence, we will also observe non-cooperative capacity regions where the set of messages is constrained to

$$\hat{\mathcal{F}}_{\text{all}} := \{F_1^{m_1}, F_2^{m_2}, \dots, F_K^{m_K}\}, \quad (2.19)$$

where $\mathbf{m} \in \{1..M\}^{[K \times 1]}$ denotes the single BS where each UE is decoded at. A lower bound on the corresponding capacity region, denoted as $\hat{\mathcal{R}}_0$, can then again be derived from (2.17).

Frequency Division Multiplex

As the capacity regions $\hat{\mathcal{R}}_0$ and $\hat{\mathcal{R}}_0^{\text{hk}}$ are based on a convex hull operation, they inherently incorporate *time-sharing*, hence the option of using a weighted mixture of different transmission and decoding strategies, assuming that the power constraint $\mathbf{P} \preceq \hat{\mathbf{P}}^{\text{max}}$ is fulfilled *instantaneously* for each employed strategy. This is often referred to as *naive time division multiplex (TDM)*. Alternatively, we could assume that $\hat{\mathbf{P}}^{\text{max}}$ refers to the *average* transmit power of each UE. In this case, it would be possible for a UE to e.g. transmit only 50% of the time, but then use twice the allowed instantaneous transmit power, consequently referred to as *non-naive TDM*. As the latter also corresponds to the case where UEs focus their transmit power on only a portion of the system bandwidth, it is often also called *frequency division multiplex (FDM)*. The original proposal of the Han-Kobayashi scheme in [HK81] also considers FDM, but this makes the capacity region computation even more complex. In addition to the capacity region given through Theorem 2.2.3, we hence only observe the capacity region of

pure FDM schemes, where all UEs invest their transmit power into strictly orthogonal parts of the spectrum. As orthogonal transmission is free of interference, the best strategy is to let each UE k transmit at maximum transmit power \hat{p}_k^{\max} . We introduce the spectrum allocation parameter $\mathbf{\Lambda} = \text{diag}(\lambda_1, \lambda_2, \dots, \lambda_K)$ with $\mathbf{\Lambda} \succeq 0$ and $\text{tr}\{\mathbf{\Lambda}\} = 1$, and can state the transmission of each UE $k \in \mathcal{K}$ separately as

$$\mathbf{y}^{[k,t]} = \mathbf{h}_k^e \sqrt{\frac{\hat{p}_k^{\max}}{\lambda_k}} s_k^{[t]} + \mathbf{v}^{[k,t]} + \mathbf{n}^{[k,t]} \quad \text{with} \quad E_t \left\{ \mathbf{v}^{[k,t]} (\mathbf{v}^{[k,t]})^H \right\} = \frac{\hat{p}_k^{\max}}{\lambda_k} \Delta \left(\bar{\mathbf{e}}_k^e (\bar{\mathbf{e}}_k^e)^H \right), \quad (2.20)$$

where $\forall k \in \mathcal{K} : \mathbf{y}^{[k,t]} \in \mathbb{C}^{[N_{\text{BS}} \times 1]}$ is the signal received at all BSs and connected to the resources of UE k , and \mathbf{h}_k^e is the effective, power reduced channel connected to UE k from Theorem 2.2.1. Further, $\forall k \in \mathcal{K} : E_t \{ \mathbf{n}^{[k,t]} (\mathbf{n}^{[k,t]})^H \} = \sigma^2 \mathbf{I}$. The capacity region is then inner-bounded as follows:

Theorem 2.2.4 (Uplink capacity region without BS cooperation, employing FDM). *The capacity region of the uplink transmission from (2.20) without BS cooperation and based on FDM can be inner-bounded as*

$$\hat{\mathcal{R}}_0^{\text{fdm}} = \bigcup_{\mathbf{\Lambda}: \mathbf{\Lambda} \succeq 0 \wedge \text{tr}\{\mathbf{\Lambda}\}=1} \hat{\mathcal{R}}_0^{\text{fdm}}(\mathbf{\Lambda}), \quad (2.21)$$

where $\hat{\mathcal{R}}_0^{\text{fdm}}(\mathbf{\Lambda})$ is the achievable rate region for a given spectrum allocation $\mathbf{\Lambda}$, where all rate tuples $\mathbf{r} \in \hat{\mathcal{R}}_0^{\text{fdm}}(\mathbf{\Lambda})$ fulfill $\forall k \in \mathcal{K} :$

$$0 \leq r_k \leq \lambda_k \cdot \max_{m \in \mathcal{M}} \log_2 \left| \mathbf{I} + \left(\sigma^2 \mathbf{I} + \frac{\hat{p}_k^{\max}}{\lambda_k} \Delta \left(\bar{\mathbf{e}}_{m,k}^e (\bar{\mathbf{e}}_{m,k}^e)^H \right) \right)^{-1} \frac{\hat{p}_k^{\max}}{\lambda_k} \mathbf{h}_{m,k}^e (\mathbf{h}_{m,k}^e)^H \right|. \quad (2.22)$$

Proof. The proof is given through a straightforward application of Theorem 2.2.2 to the transmission in (2.20). \square

In (2.22), the *max* statement assures that each UE is decoded at the best possible BS according to the channel realization.

Capacity Region Computation

The computation of $\hat{\mathcal{R}}_0^{\text{hk}}$ is tedious even for small numbers of communicating entities M and K . For a given overall power allocation \mathcal{P} , (2.18) states a linear optimization problem with a large number of linear constraints, which is convex and can be solved efficiently [BV04]. For the special case of $M = K = 2$, a closed-form expression of the rate region for a given power allocation was stated in [HK81]. However, the rate optimization over all possible \mathcal{P} is non-convex in the single power parameters, and we hence use an exhaustive search.

The computation of the FDM-based capacity region $\hat{\mathcal{R}}_0^{\text{fdm}}$ can be performed via a weighted sum-rate maximization with varying weights, which for a given set of weights is convex in the spectrum allocation parameter $\mathbf{\Lambda}$ and hence solvable with standard techniques [BV04]. This can be seen as tracing the capacity region with a tangent plane at different angles. At the same complexity, however, it is also possible to perform a brute force search over $\mathbf{\Lambda}$.

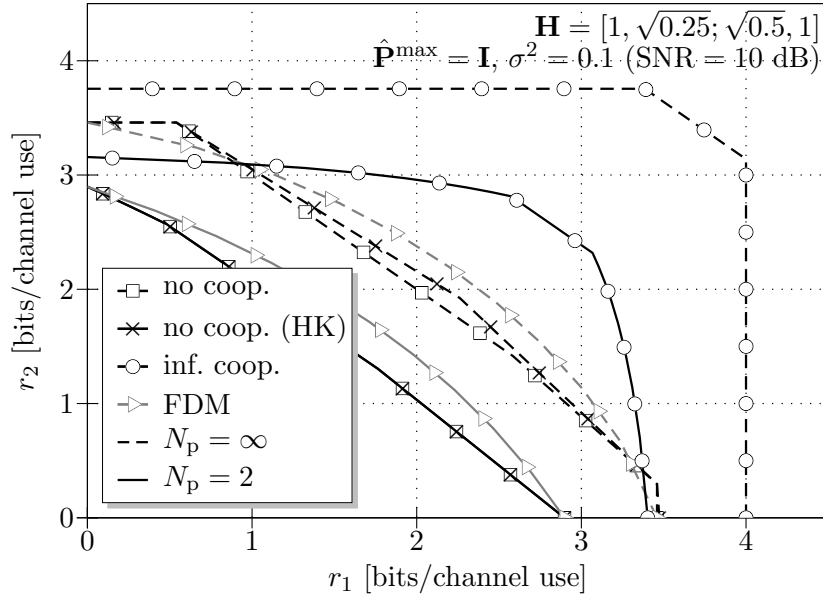


Figure 2.3: Uplink capacity region under no or infinite BS cooperation.

Capacity Region Illustration

The capacity regions $\hat{\mathcal{R}}_\infty$, $\hat{\mathcal{R}}_0$, $\hat{\mathcal{R}}_0^{\text{hk}}$ and $\hat{\mathcal{R}}_0^{\text{fdm}}$, corresponding to infinite or no BS cooperation, are illustrated in Figure 2.3 for an example channel with $M = K = 2$ and $N_{\text{bs}} = 1$. The channel matrix is set to $\mathbf{H} = [1, \sqrt{0.25}; \sqrt{0.5}, 1]$, $\hat{\mathbf{P}}^{\text{max}} = \mathbf{I}$ and $\sigma^2 = 0.1$, hence we have a SISO SNR on the main (unit gain) links of 10 dB. The capacity regions are plotted for perfect ($N_p = \infty$) and imperfect ($N_p = 2$) receiver-side channel knowledge, where the latter choice, as mentioned before, is based on a detailed analysis of the channel estimation performance in an LTE Release 8 system [McC07] under urban channel conditions in Appendix E. In the case of infinite BS cooperation and perfect channel knowledge, the capacity region has the well-known pentagon shape [CT06], and is fully characterized through the cases where both UEs transmit at maximum power and SIC is employed. Under imperfect CSIR, we can see a significant drop in performance, and also the fact that reducing one UE's transmit power can increase the rate of the other UE. In the case of no cooperation, common message concepts, i.e. Han-Kobayashi schemes, are slightly beneficial under perfect CSIR, but the gain diminishes under imperfect CSIR. This is intuitive, as in the latter case, the noise connected to channel estimation increases the overall noise level, such that partial decoding of interference becomes less beneficial. For this particular channel, FDM is attractive if no BS cooperation is possible, but we will see later that FDM schemes become strongly inferior to other schemes if a moderate extent of backhaul is available.

2.2.5 Basic Base Station Cooperation Schemes

We now consider the case where a finite extent of backhaul infrastructure $\hat{\mathbf{B}}^{\text{max}}$ is available that allows a limited cooperation between BSs. In principle, two kinds of information exchange over the backhaul are thinkable: BSs can *decode and forward* received signals such that other BSs can subtract known interference, or they can *compress and forward* received signals such

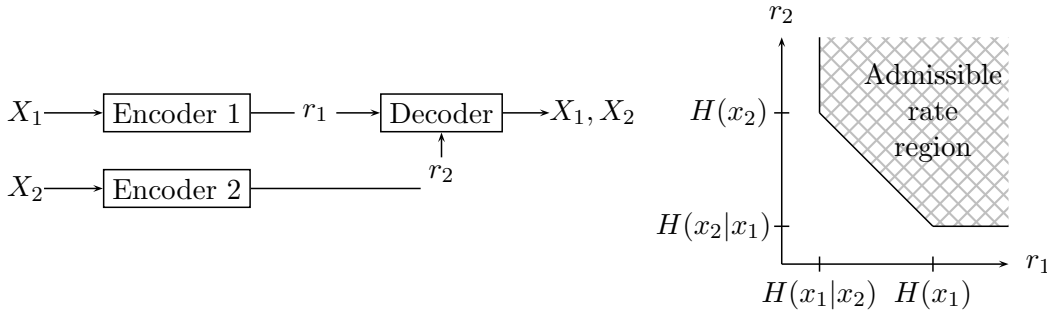


Figure 2.4: Admissible rate region of Slepian-Wolf source coding [SW73].

that improved decoding takes place at a remote BS. As our wording suggests, both strategies are similar to well-known concepts from relaying [CG79], but are used in a very different setup. The most important difference is that the BSs communicate over finite-rate, but lossless links that do not interfere with the actual air interface. In both schemes, we have the situation that information is being provided to other BSs which may already be partially known to the other side, as all BSs receive more or less strongly correlated signals from the UEs. In order to explore the information theoretical limits, we hence have to review some basic concepts of lossless and lossy source coding.

Slepian-Wolf Source Coding for Discrete Sources

Slepian and Wolf [SW73] initially observed the scenario where two *discrete*, correlated random sequences are to be separately encoded and relayed to a remote joint decoder, as depicted in Figure 2.4. They derived an *admissible rate region* of all possible tuples of rates with which the two encoders can communicate with the decoder, such that the decoder can perfectly reconstruct both random sequences. One conclusion is that if, for example, encoder 1 relays sequence X_1 just as it is, requiring a rate corresponding to the average entropy $H(x_1)$ of each symbol, then it suffices if encoder 2 forwards at a rate corresponding to the average *conditional* entropy $H(x_2|x_1)$ of each symbol, given that x_1 is already known that the decoder. Hence, encoder 2 can exploit the fact that the decoder has side information on X_2 available, only by knowing the joint statistics of sequences X_1 and X_2 . The achievability of the above result is usually proved through *random binning* arguments [Ber78]: In our case, assuming that X_1 and X_2 are sequences of length N_{sym} , encoder 2 would group all $2^{N_{\text{sym}} \cdot H(x_2)}$ possible realizations of X_2 into $2^{N_{\text{sym}} \cdot H(x_2|x_1)}$ randomly generated bins, and forward only the bin indices at rate $H(x_2|x_1)$ to the decoder. The latter then searches for the realization of sequence X_2 that is *jointly typical* with the received bin indices and the information provided by encoder 1. The probability of error in reconstructing X_2 at the decoder then decreases exponentially in the block length N_{sym} . The admissible rate region shown in Figure 2.4 can be achieved by alternating the roles of the encoders and applying timesharing, or by schemes where both encoders apply random binning simultaneously [CT06].

Wyner-Ziv Source Coding for Continuous Sources

Wyner and Ziv [WZ76] extended the above scenario to the case where a certain extent of *distortion* is allowed at the decoder output, for the special case where one random source is exactly known to the decoder, while the other is relayed after lossy compression. They established the rate/distortion trade-off for lossy compression of a single *discrete* source with side-information at the receiver, and extended the work to the case of a *continuous* source in [Wyn78]. For Gaussian sources and a quadratic distortion metric, it was shown that the rate/distortion trade-off is the same as if the side-information were known to the compressing encoder (which is not the case for arbitrary sources or other metrics, where a rate loss was shown and upper bounded in [Zam96]). The case where both encoders perform compression and hence two distortion measures are involved is often referred to as *multi-terminal source coding*, and was initially observed for discrete sources by [Ber78, Tun78]. The obtained rate/distortion trade-off in this work, however, could not yet be proved optimal. An upper bound was derived in [BHO⁺79], which was shown in [Ooh97] to partially coincide with the lower bound mentioned before, and where previous work was also extended to the case of Gaussian random variables. The setup of two compressed random sources and additional side information at the decoder was observed in [Gas04] and extended to an arbitrary number of encoders in [Gas03]. Note that in our case, the BSs perform the source coding on the received signals, and not the UEs, such that the term "multi-terminal source coding" might appear confusing to the reader in this context.

A special case of multi-terminal source coding is when all random sources are in fact noisy observations of the same single random source, which is often referred to as the *CEO problem*, introduced in [BZV96] and extended to the Gaussian case in [VB97]. The main difference to previously discussed schemes is that the decoder, i.e. the *central estimation officer* or CEO, is only interested in reconstructing the original source, but not the noisy observations of the agents. This corresponds to our considered scenario: Cooperating BSs make correlated observations of the same UE transmissions, and aim at jointly achieving a certain minimum distortion of the UE transmission under a constrained backhaul. The standard CEO problem is an example of multi-terminal source coding for which the optimum rate-distortion function has been established [Ooh98, PTR04]. The key observation is that a certain extent of backhaul is always wasted for the compression of observation noise, hence it is not beneficial to increase the number of agents without similarly increasing the sum backhaul. The authors in [dCS08, dS08] have combined aspects of multi-terminal source coding and the CEO problem to the case of multiple random sources and an arbitrary channel, which provides an essential basis for our model described in the sequel. They use a scheme referred to as *distributed Wyner-Ziv compression* based on [Gas04, Gas03], noting that the optimality of the scheme is still uncertain, as stated in the paragraph before.

Distributed Interference Subtraction (DIS)

Let us first model a decode-and-forward concept where a message is decoded by one or multiple BSs individually and then forwarded to another BS for interference subtraction, which we refer to as *distributed interference subtraction* (DIS) [KF07, MF08e]. For this, we extend the set of

messages each UE k can invest its transmit power into from (2.14) to

$$\hat{\mathcal{F}}_k := \left\{ \hat{F}_k^{\mathcal{M}'} : \mathcal{M}' \subseteq \mathcal{M} \right\} \cup \left\{ \hat{F}_k^{\mathcal{M}', m \rightarrow \mathcal{M}''} : \mathcal{M}', \mathcal{M}'' \subseteq \mathcal{M} \wedge m \in \mathcal{M}' \wedge (\mathcal{M}' \cap \mathcal{M}'' = \emptyset) \right\}, \quad (2.23)$$

where $\hat{F}_k^{\mathcal{M}', m \rightarrow \mathcal{M}''}$ denotes a message that originates from UE k , is decoded by all BSs in set \mathcal{M}' individually (i.e. enabling HK concepts as in the last section), after which one BS $m \in \mathcal{M}'$ forwards the decoded message to all BSs in set \mathcal{M}'' . The required backhaul can be reduced if Slepian-Wolf source coding is applied, hence if BS m makes use of possible side-information contained in the signals received by BSs in set \mathcal{M}'' . In this case, each DIS-receiving BS is provided only with a source-encoded version $s(\hat{F}_k^{\mathcal{M}', m \rightarrow \mathcal{M}''})$ carrying enough information such that the BS can successfully decode message $\hat{F}_k^{\mathcal{M}', m \rightarrow \mathcal{M}''}$ itself. As one might consider such source coding concepts unfeasible for practical systems (an aspect discussed in Chapter 5), we will generally observe the rate/backhaul trade-off for DIS-schemes that exploit inter-BS signal correlation, as well as those that simply forward complete decoded messages. Regardless of the assumption on source coding, the result is that all BSs in \mathcal{M}'' can decode various other messages free of the interference from message $\hat{F}_k^{\mathcal{M}', m \rightarrow \mathcal{M}''}$, provided that decoding takes place *after* the data has been received from BS m . Hence, DIS enables a certain extent of interference cancellation in the network, but offers no additional array gain, as only information on interference is exchanged, but not on signals to be exploited. If set \mathcal{M}' only consists of BS m , we abbreviate $\hat{F}_k^{\mathcal{M}', m \rightarrow \mathcal{M}''}$ by writing $\hat{F}_k^{m \rightarrow \mathcal{M}''}$. In the sequel, we assume that a portion of backhaul $\hat{\mathbf{B}}^{\text{dis}} \in \mathbb{R}_0^{+[M+1 \times M]}$ is made available to DIS cooperation concepts, where each element $\hat{b}_{i,j}^{\text{dis}}$ states the backhaul from BS j to BS i , or to the network if $i = M + 1$.

Compressed Interference Forwarding (CIF)

A BS cooperation scheme similar to DIS was observed in [SSPS08b,SSPS09b,Gri09,GMFC09], where a message $\hat{F}_k^{\mathcal{M}', m \rightleftharpoons \mathcal{M}''}$ is decoded by the BSs in set \mathcal{M}' , after which BS m re-modulates the originally transmitted sequence $X_k^{\mathcal{M}', m \rightleftharpoons \mathcal{M}''}$ and forwards a *quantized* version $q(X_k^{\mathcal{M}', m \rightleftharpoons \mathcal{M}''})$ to all BSs in set \mathcal{M}'' , again possibly employing Slepian-Wolf source coding to exploit potential side information. In this case, $s(q(X_k^{\mathcal{M}', m \rightleftharpoons \mathcal{M}''}))$ is exchanged. The receiving BSs then use this information to reconstruct $q(X_k^{\mathcal{M}', m \rightleftharpoons \mathcal{M}''})$ and *approximately* subtract the interference caused by message $\hat{F}_k^{\mathcal{M}', m \rightleftharpoons \mathcal{M}''}$. We refer to this scheme as *compressed interference forwarding* (CIF). In general, the properties of CIF are similar to DIS. The scheme enables a certain extent of interference cancellation, while offering no array gain, but introduces quantization noise into the interference subtraction process. However, we will see later that CIF is an interesting option from an implementation point of view, and for this reason also considered in our model. We will assume in the sequel that a certain extent of backhaul $\hat{\mathbf{B}}^{\text{cif}} \in \mathbb{R}^{[M+1 \times M]}$ is made available to CIF cooperation concepts. Please note the subtle difference in our notation for messages that are used for DIS-cooperation (e.g. $\hat{F}_k^{\mathcal{M}', m \rightarrow \mathcal{M}''}$), and those used for CIF (e.g. $\hat{F}_k^{\mathcal{M}', m \rightleftharpoons \mathcal{M}''}$).

Distributed Antenna Systems (DAS)

We now add to our model compress-and-forward concepts that enable BSs to exchange quantized received signals to benefit from spatial diversity as well as array gain. If a BS does not perform any decoding itself, but just quantizes and forwards all received signals to another BS or to a central network entity, it is basically degraded to a *remote radio head* (RRH), such that these schemes are often referred to as *distributed antenna systems* (DAS). In the sequel,

we will assume that a portion

$$\hat{\mathbf{B}}^{\text{das}} \in \mathbb{R}_0^{+[M+1 \times M]}, \quad \text{for example } \hat{\mathbf{B}}^{\text{das}} = \begin{bmatrix} 0 & 0 & 0 \\ 0 & 0 & 0 \\ 8 & 8 & 0 \\ 0 & 0 & 0 \end{bmatrix} \quad (2.24)$$

of the available backhaul is invested into DAS concepts, where each non-zero element $\hat{b}_{m',m}^{\text{das}}$ denotes that BS m employs a certain number of bits per symbol to quantize and forward the received signals to BS m' if $m' \leq M$, or to a central network entity otherwise. In the above example, BSs 1 and 2 both employ 8 bits per symbol to forward signals to BS 3. Clearly, DAS can also be performed such that the signal correlation between BSs is exploited. As we are only considering Gaussian signaling, we can model without loss of optimality the Wyner-Ziv source coding performed by a BS m as a quantization of receive signals Y_m yielding $q(Y_m)$, succeeded by Slepian-Wolf source coding, so that finally $s(q(Y_m))$ is exchanged [WZ76]. A DAS-receiving BS then uses its own received signals in conjunction with $s(q(Y_m))$ to reconstruct $q(Y_m)$, which can then be used to decode other messages. As one might consider such source coding techniques and the exploitation of side-information to be questionable in practical systems, we will always also observe schemes where each BS m simply quantizes and forwards $q(Y_m)$ directly, as well as schemes based on a practical quantizer to be defined later.

In the remainder of this work, we assume for simplicity that each BS operates according to the following procedure:

1. (Possibly) receive compressed signals (DAS) from other BSs
2. (Possibly) receive and forward compressed messages (CIF) from other BSs
3. (Possibly) receive and decode partially forwarded messages (DIS) from other BSs
4. Decode messages that are to be decoded locally
5. (Possibly) forward decoded messages (DIS or CIF) and/or compress and forward the remaining signals (DAS) to other BSs

This particular order is mainly interesting in the context of BS cooperation exploiting side-information. If, for example, DIS concepts are used with Slepian-Wolf source coding, the DIS-receiving BS can also exploit as side-information the receive signals provided by other BSs through the DAS concept. The above mentioned order facilitates the analytical derivation of achievable rates and appears beneficial in a wide range of scenarios, but must not necessarily be optimal in all cases. We further assume that the set of messages $\hat{\mathcal{F}}_{\text{all}}$ and the backhaul available for DAS $\hat{\mathbf{B}}^{\text{das}}$ is chosen such that there is a non-cyclic flow of information between the BSs. This means that any joint DIS/CIF/DAS cooperation concept can be illustrated as a (possibly disconnected) directed graph, which is shown in Figure 2.5 for an example setup with $M = K = 4$. Here, the following cooperation concepts are used (note that the UEs are not displayed in the figure), assuming in this example that source coding is *not* employed:

- UE 1 transmits $\hat{F}_1^{\{1,2\}}$, which is decoded by BSs 1 and 2 individually, and $\hat{F}_1^{1 \rightarrow \{2,3\}}$, being decoded by BS 1 and forwarded to BSs 2 and 3 according to the DIS-concept
- UE 2 transmits message $\hat{F}_2^{2 \rightarrow 3}$, which is decoded by BS 2, re-encoded to $\hat{X}_2^{2 \rightarrow 3}$, quantized to $q(\hat{X}_2^{2 \rightarrow 3})$ and forwarded to BS 3 according to the CIF concept
- UEs 3 and 4 transmit messages \hat{F}_3^3 and \hat{F}_4^3 , respectively, both decoded only by BS 3

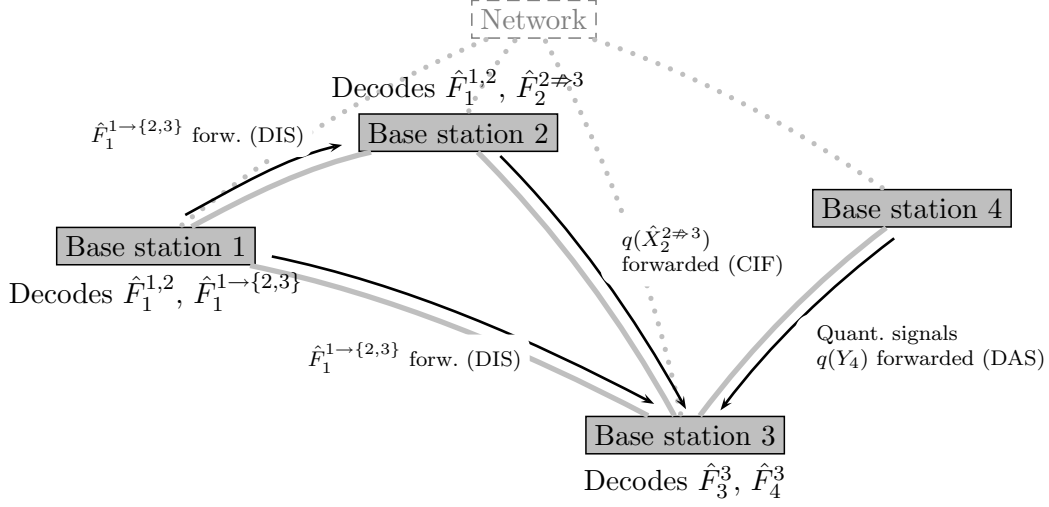


Figure 2.5: Illustration of a combined DIS/CIF/DAS base station cooperation strategy.

- All decoding processes at BS 3 can make use of the received and quantized signals $q(Y_4)$ provided by BS 4 according to the DAS concept

Clearly, the information flow determines the order of BS activation and introduces latency into the decoding process, which we will discuss in Section 5.2. Let us now update our notation of messages decoded or not decoded by a particular BS m from (2.15) to $\forall m \in \mathcal{M}$:

$$\mathcal{F}^{[m]} := \left\{ F_j^{\mathcal{M}'}, F_j^{\mathcal{M}', m' \rightarrow \mathcal{M}''}, F_j^{\mathcal{M}', m' \not\rightarrow \mathcal{M}''} \in \hat{\mathcal{F}}_{\text{all}} : m \in \mathcal{M}' \right\} \quad (2.25)$$

$$\bar{\mathcal{F}}^{[m]} := \left\{ F_j^{\mathcal{M}'}, F_j^{\mathcal{M}', m' \rightarrow \mathcal{M}''}, F_j^{\mathcal{M}', m' \not\rightarrow \mathcal{M}''} \in \hat{\mathcal{F}}_{\text{all}} : m \notin \mathcal{M}' \wedge m \notin \mathcal{M}'' \right\} \quad (2.26)$$

$$\bar{\mathcal{F}}^{[m]} := \left\{ F_j^{\mathcal{L}, l \rightarrow \mathcal{L}'} \in \hat{\mathcal{F}}_{\text{all}} : m \in \mathcal{L}' \right\} \quad (2.27)$$

$$\bar{\mathcal{F}}^{[m]} := \left\{ F_j^{\mathcal{L}, l \not\rightarrow \mathcal{L}'} \in \hat{\mathcal{F}}_{\text{all}} : m \in \mathcal{L}' \right\}, \quad (2.28)$$

where $\mathcal{F}^{[m]}$ denotes all messages decoded by BS m , as before, while $\bar{\mathcal{F}}^{[m]}$ now denotes all messages neither decoded by BS m itself, nor forwarded from any other BS to BS m according to the DIS or CIF concept. Set $\bar{\mathcal{F}}^{[m]}$ denotes all messages provided through the DIS-concept to BS m , while set $\bar{\mathcal{F}}^{[m]}$ denotes all messages forwarded to BS m according to the CIF-concept. We further denote all messages that are *not* decoded by a central network entity as

$$\hat{\mathcal{F}}_{\text{all}^*} = \left\{ F_j^{\mathcal{L}}, F_j^{\mathcal{L}, l \rightarrow \mathcal{L}'}, F_j^{\mathcal{L}, l \not\rightarrow \mathcal{L}'} \in \hat{\mathcal{F}}_{\text{all}} : M+1 \notin \mathcal{L} \right\}. \quad (2.29)$$

In the sequel, we will use another backhaul-related variable $\hat{\mathbf{B}}^{\text{net}} \in \mathbb{R}_0^{+[M+1, M]}$ denoting backhaul capacity that is invested into forwarding decoded messages to the network. This is required to ensure a fair comparison between cooperation schemes where decoding takes

place at a central network entity, or those where decoding takes place at the BSs themselves. An inner bound in the capacity of a transmission with arbitrary DIS, CIF and/or DAS information exchange between BSs is stated in the following theorem:

Theorem 2.2.5 (Uplink capacity region with DIS/CIF/DAS-based BS cooperation). *An inner bound on the capacity region of transmission (2.1) with DIS/CIF/DAS-based BS cooperation under a backhaul usage stated through $\hat{\mathbf{B}}^{\text{dis}}$, $\hat{\mathbf{B}}^{\text{cif}}$, $\hat{\mathbf{B}}^{\text{das}}$ and $\hat{\mathbf{B}}^{\text{net}}$ is given as*

$$\hat{\mathcal{R}}^{\text{coop}}\left(\hat{\mathbf{B}}^{\text{dis}}, \hat{\mathbf{B}}^{\text{cif}}, \hat{\mathbf{B}}^{\text{das}}, \hat{\mathbf{B}}^{\text{net}}\right) = \bigcup_{\hat{\mathcal{F}}_{\text{all}}, \mathcal{P}: \mathbf{P}(\hat{\mathcal{F}}_{\text{all}}) \preceq \hat{\mathbf{P}}^{\text{max}}} \hat{\mathcal{R}}^{\text{coop}}(\hat{\mathcal{F}}_{\text{all}}, \mathcal{P}, \hat{\mathbf{B}}^{\text{dis}}, \hat{\mathbf{B}}^{\text{cif}}, \hat{\mathbf{B}}^{\text{das}}, \hat{\mathbf{B}}^{\text{net}}), \quad (2.30)$$

where a lower bound on the rate region for a given set $\hat{\mathcal{F}}_{\text{all}}$, power allocation \mathcal{P} and backhaul $\hat{\mathbf{B}}^{\text{dis}}, \hat{\mathbf{B}}^{\text{cif}}, \hat{\mathbf{B}}^{\text{das}}, \hat{\mathbf{B}}^{\text{net}}$ is stated as $\hat{\mathcal{R}}^{\text{coop}}(\hat{\mathcal{F}}_{\text{all}}, \mathcal{P}, \hat{\mathbf{B}}^{\text{dis}}, \hat{\mathbf{B}}^{\text{cif}}, \hat{\mathbf{B}}^{\text{das}}, \hat{\mathbf{B}}^{\text{net}})$. Here, each rate tuple $\mathbf{r} \in \hat{\mathcal{R}}^{\text{coop}}(\hat{\mathcal{F}}_{\text{all}}, \mathcal{P}, \hat{\mathbf{B}}^{\text{dis}}, \hat{\mathbf{B}}^{\text{cif}}, \hat{\mathbf{B}}^{\text{das}}, \hat{\mathbf{B}}^{\text{net}})$ fulfills $\forall k \in \mathcal{K}: 0 \leq r_k \leq \sum_{F \in \hat{\mathcal{F}}_k} \nu_F$ and $\forall m \in \mathcal{M}$:

$$\forall \mathcal{F} \subseteq \mathcal{F}^{[m]}: \sum_{\forall F \in \mathcal{F}} \nu_F \leq \log_2 \left| \mathbf{I} + \mathbf{P}(\mathcal{F}) \left(\sum_{m'=1}^M (\mathbf{H}_{m'}^e)^H (\Phi_{m' \rightarrow m}^{\text{ii}})^{-1} \mathbf{H}_{m'}^e \right) \right|, \quad (2.31)$$

with the interference term

$$\Phi_{m' \rightarrow m}^{\text{ii}} = \underbrace{\sigma^2 \mathbf{I}}_{\text{Noise}} + \underbrace{\Phi_{m'}^{\text{hh}}}_{\text{Chn. est.}} + \underbrace{\mathbf{H}_{m'}^e \mathbf{P}(\bar{\mathcal{F}}^{[m]} \cap \bar{\mathcal{F}}^{[m']}) (\mathbf{H}_{m'}^e)^H}_{\text{Intfr. from msgs. neither decoded by nor provided to BSs } m \text{ or } m'} + \underbrace{\Phi_{m'}^{\text{cc}}}_{\text{Residual intfr. rel. to CIF}} + \underbrace{\Phi_{m' \rightarrow m}^{\text{qq}}}_{\text{Quant. noise rel. to DAS}}, \quad (2.32)$$

where $\forall m \in \mathcal{M}: \Phi_m^{\text{hh}} = \Delta(\bar{\mathbf{E}}_m^e \mathbf{P}(\hat{\mathcal{F}}_{\text{all}}) (\bar{\mathbf{E}}_m^e)^H)$ is a channel estimation related noise term connected to BS m as in Theorem 2.2.3. $\forall m \in \mathcal{M}: \Phi_m^{\text{cc}}$ is the residual quantization noise after CIF-based partial interference cancellation stated in Appendix D.2, and $\Phi_{m' \rightarrow m}^{\text{qq}}$ is the quantization noise introduced for the signals compressed and forwarded from BS m' to BS m according to the DAS concept. This quantization noise is constrained by the backhaul infrastructure $\hat{\mathbf{B}}^{\text{das}}$ invested into DAS concepts as $\forall m \in \mathcal{M}: \Phi_{m \rightarrow m}^{\text{qq}} = \mathbf{0}$ and

$$\forall \mathcal{M}' \subseteq \{\mathcal{M} \setminus m\}: \log_2 \left| \mathbf{I} + (\Phi_{\mathcal{M}' \rightarrow m}^{\text{qq}})^{-1} \bar{\Phi}_{\mathcal{M}'|m, \mathcal{M} \setminus \mathcal{M}'}^{\text{yy}*} \right| \leq \sum_{m' \in \mathcal{M}'} \hat{b}_{m, m'}^{\text{das}}, \quad (2.33)$$

where

$$\Phi_{\mathcal{M}' \rightarrow m}^{\text{qq}} = \text{diag} \left(\Phi_{m'_1 \rightarrow m}^{\text{qq}}, \Phi_{m'_2 \rightarrow m}^{\text{qq}}, \dots, \Phi_{m'_{|\mathcal{M}'|} \rightarrow m}^{\text{qq}} \right) \text{ for } \mathcal{M}' = \{m'_1, \dots, m'_{|\mathcal{M}'|}\} \quad (2.34)$$

is the quantization noise due to DAS concepts at BSs \mathcal{M}' . Term $\bar{\Phi}_{\mathcal{M}'|m, \mathcal{M} \setminus \mathcal{M}'}^{\text{yy}*}$ is the signal covariance at DAS-forwarding BSs after local decoding of messages and (possibly) interference cancellation through DIS and CIF, conditioned on the received signals at BS m and quantized signals provided to BS m by BSs in set $\mathcal{M} \setminus \mathcal{M}'$. The latter term is derived and explained in

detail in Appendix D.2. We further have the CIF-related backhaul constraint $\forall m \in \mathcal{M}$:

$$\begin{aligned} \forall \mathcal{F} \subseteq \hat{\mathcal{F}}^{\neq[m]}, \quad \mathcal{M}' = \underbrace{\left\{ m' \in \mathcal{M} : F_j^{\mathcal{L}, l \neq \mathcal{L}'} \in \mathcal{F} \wedge m' = l \right\}}_{\text{Set of BSs that CIF-forward messages in } \mathcal{F} \text{ to BS } m} : \\ \sum_{\forall F \in \mathcal{F}} \log_2 \left(\frac{\rho_F}{\xi_{F \neq m}} \right) - \underbrace{\log_2 \left| \mathbf{I} + \bar{\Psi}_m(\mathcal{F}) \left(\sum_{m'=1}^M (\mathbf{H}_{m'}^e)^H \left(\Phi_{m' \rightarrow m}^{\text{ii, cif}} \right)^{-1} \mathbf{H}_{m'}^e \right) \right|}_{\text{Portion of quantized sequences } q(e(\mathcal{F})) \text{ decodable by BS } m \text{ by itself}} \leq \sum_{m' \in \mathcal{M}'} \hat{b}_{m, m'}^{\text{cif}}, \end{aligned} \quad (2.35)$$

where $\xi_{F \neq m}$ is the quantization noise introduced when message F is CIF-forwarded to BS m , $\bar{\Psi}_m(\mathcal{F})$ is a diagonal matrix containing the effective powers of the messages in \mathcal{F} , with

$$\forall k \in \mathcal{K} : [\bar{\Psi}_m(\mathcal{F})]_{k, k} = \sum_{F \in \{\hat{\mathcal{F}}_k \cap \mathcal{F}\}} \rho_F - \xi_{F \neq m}, \quad (2.36)$$

and the interference and noise terms $\Phi_{m \rightarrow m}^{\text{ii, cif}}$ and $\Phi_{m' \rightarrow m}^{\text{ii, cif}}$ in (2.35) are given as

$$\Phi_{m \rightarrow m}^{\text{ii, cif}} = \mathbf{H}_m^e \mathbf{P} \left(\hat{\mathcal{F}}_{\text{all}} \setminus \hat{\mathcal{F}}^{\neq[m]} \right) (\mathbf{H}_m^e)^H + \Phi_m^{\text{cc}} + \Phi_m^{\text{hh}} + \sigma^2 \mathbf{I} \quad \text{and} \quad (2.37)$$

$$\Phi_{m' \rightarrow m}^{\text{ii, cif}} = \mathbf{H}_{m'}^e \mathbf{P} \left(\hat{\mathcal{F}}^{[m']} \setminus \hat{\mathcal{F}}^{\neq[m]} \right) (\mathbf{H}_{m'}^e)^H + \Phi_{m'}^{\text{cc}} + \Phi_{m'}^{\text{hh}} + \sigma^2 \mathbf{I} + \Phi_{m' \rightarrow m}^{\text{qq}}. \quad (2.38)$$

Terms $\forall m \in \mathcal{M} : \Phi_m^{\text{cc}}$ state the residual interference after a BS has exploited CIF-signals, as given in Appendix D.2. We also have the DIS-related backhaul constraint $\forall m \in \mathcal{M}$:

$$\begin{aligned} \forall \mathcal{F} \subseteq \vec{\mathcal{F}}^{[m]}, \quad \mathcal{M}' = \underbrace{\left\{ m' \in \mathcal{M} : F_j^{\mathcal{L}, l \rightarrow \mathcal{L}'} \in \mathcal{F} \wedge m' = l \right\}}_{\text{Set of BSs that forward messages in } \mathcal{F} \text{ to BS } m} : \\ \sum_{F \in \mathcal{F}} \nu_F - \log_2 \left| \mathbf{I} + \mathbf{P}(\mathcal{F}) \left(\sum_{m'=1}^M (\mathbf{H}_{m'}^e)^H \left(\Phi_{m' \rightarrow m}^{\text{ii, dis}} \right)^{-1} \mathbf{H}_{m'}^e \right) \right| \leq \sum_{m' \in \mathcal{M}'} \hat{b}_{m, m'}^{\text{dis}}, \end{aligned} \quad (2.39)$$

Portion of messages \mathcal{F} already decodable by BS m by itself

where the interference and noise terms $\Phi_{m \rightarrow m}^{\text{ii, dis}}$ and $\Phi_{m' \rightarrow m}^{\text{ii, dis}}$ are given as

$$\Phi_{m \rightarrow m}^{\text{ii, dis}} = \mathbf{H}_m^e \mathbf{P} \left(\hat{\mathcal{F}}_{\text{all}} \setminus \left\{ \hat{\mathcal{F}}^{[m]} \cup \hat{\mathcal{F}}^{\neq[m]} \right\} \right) (\mathbf{H}_m^e)^H + \Phi_m^{\text{cc}} + \Phi_m^{\text{hh}} + \sigma^2 \mathbf{I} \quad (2.40)$$

$$\Phi_{m' \rightarrow m}^{\text{ii, dis}} = \mathbf{H}_{m'}^e \mathbf{P} \left(\hat{\mathcal{F}}^{[m']} \setminus \hat{\mathcal{F}}^{[m]} \right) (\mathbf{H}_{m'}^e)^H + \Phi_{m'}^{\text{cc}} + \Phi_{m'}^{\text{hh}} + \sigma^2 \mathbf{I} + \Phi_{m' \rightarrow m}^{\text{qq}}. \quad (2.41)$$

Finally, we have backhaul constraints due to the fact that messages decoded by BSs, rather than by a central network entity, have to be forwarded to the network, i.e. $\forall \mathcal{F} \subseteq \hat{\mathcal{F}}_{\text{all}}^*$ and

$$\mathcal{M}' = \underbrace{\left\{ m' \in \mathcal{M} : \exists F_j^{\mathcal{L}}, F_j^{\mathcal{L}, l \rightarrow \mathcal{L}'}, F_j^{\mathcal{L}, l \neq \mathcal{L}'} \in \mathcal{F} : m' \in \mathcal{L} \right\}}_{\text{Set of all BSs that decode messages in } \mathcal{F}} : \sum_{F \in \mathcal{F}} \nu_F \leq \sum_{m \in \mathcal{M}'} \hat{b}_{M+1, m}^{\text{net}}. \quad (2.42)$$

Proof. The proof and a detailed explanation of all terms are given in Appendix D.2. \square

Equation (2.31) is basically the same as (2.18) which was used in the context of non-cooperative decoding. In this case, however, each decoding BS m can also make use of the quantized signals provided by other BSs (DAS concept), where messages that are either provided to BS m itself or to one of the DAS-supporting BSs (through the DIS or CIF concept) are not counted as interference. Corresponding quantization noise matrices are then constrained by the backhaul infrastructure invested into DAS concepts (see (2.33)). Equation (2.35) states backhaul constraints connected to CIF schemes, where the key aspect is that a BS need only forward the delta in information that the CIF-receiving BS requires to decode a quantized representation of an interfering sequence by itself, if Slepian-Wolf source coding concepts are applied. The situation is similar for DIS concepts, where corresponding backhaul constraints are stated in (2.39). Here, the second line can be interpreted in such a way that the sum rate of any subset of messages being DIS-forwarded to BS m minus the portion of the message subset that BS m can already decode without help must be less than the available sum backhaul on the involved links. As the DIS backhaul constraint poses additional linear constraints on the rate region, it is clear that if the available backhaul is increased beyond a certain threshold, these constraints become inactive, and those in (2.31) become the limiting factor. Hence, increasing the backhaul for DIS concepts beyond a certain point will not lead to a further rate increase. A detailed explanation of Equations (2.30)-(2.42) is given in Appendix D.2.

Practical Cooperation Schemes

The lower capacity region bound for BS cooperation under a constrained backhaul as stated before is based on many information-theoretical concepts, where the usage in practical mobile communications systems is questionable. Equation (2.33), for example, is based on the assumption that distributed Wyner-Ziv is employed, where not only the signal correlation between a DAS-forwarding and the DAS-receiving BS is exploited, but also the correlation between all DAS-forwarding BSs that are jointly supporting another BS. As these schemes appear rather questionable for the implementation in practical systems (a discussion will follow in Section 5.2.1), we also observe rate/backhaul trade-offs based on the rate-distortion bound without the exploitation of inter-BS signal correlation. In this case, (2.33) can be modified to a single constraint for each individual quantization noise term $\Phi_{m' \rightarrow m}^{\text{qq}}$, i.e. $\forall m \in \mathcal{M}$:

$$\forall m' \in \{\mathcal{M} \setminus m\} : \log_2 \left| \mathbf{I} + (\Phi_{m' \rightarrow m}^{\text{qq}})^{-1} \bar{\Phi}_{m'}^{\text{yy}} \right| \leq \hat{b}_{m,m'}^{\text{das}}, \quad (2.43)$$

where $\bar{\Phi}_{m'}^{\text{yy}}$ is the unconditioned receive signal covariance after local message decoding and possibly interference cancellation at BS m' . Equation (2.43), however, still assumes that the signal correlation between the N_{bs} antennas at the quantizing BS is exploited, and that joint processing of large blocks of received symbols is performed, which would be computationally intractable in a practical system. As a third level of realism of DAS schemes, we hence also observe the performance of a system based on a concrete quantizer design proposed in [LBG80]. Modeled in a simplified way, we here assume that the backhaul is invested equally into each real signal dimension to be quantized, and one bit is lost per real dimension. Under these considerations, (2.33) is finally changed to

$$\forall m' \neq m : \Phi_{m' \rightarrow m}^{\text{qq}} = \left(2^{\max\left(\frac{\hat{b}_{m,m'}^{\text{das}}}{N_{\text{bs}}} - 2, 0\right)} - 1 \right)^{-1} \Delta(\bar{\Phi}_{m'}^{\text{yy}}). \quad (2.44)$$

Similarly, CIF performance in (2.35) is based on the assumption that side information present at a CIF-receiving DIS can be used to reduce the extent of backhaul needed for the exchange of quantized interference sequences. If we consider this to be practically questionable, we change the second line in (2.35) to

$$\sum_{F \in \mathcal{F}} \log_2 \left(\frac{\rho_F}{\xi_{F \neq m}} \right) \leq \sum_{m' \in \mathcal{M}'} \hat{b}_{m,m'}^{\text{cif}}, \quad (2.45)$$

or, assuming the same practical quantization scheme as in (2.44), the second line in (2.35) is changed to

$$\sum_{F \in \mathcal{F}} \left(\log_2 \left(\frac{\rho_F}{\xi_{F \neq m}} \right) + 2 \right) \leq \sum_{m' \in \mathcal{M}'} \hat{b}_{m,m'}^{\text{cif}}. \quad (2.46)$$

Last but not least, we also consider a more practical implementation of DIS schemes, where decoded messages are forwarded as a whole, without exploiting potential side-information at the receiver side. In this case, the second line in (2.39) simply changes to

$$\sum_{F \in \mathcal{F}} \nu_F \leq \sum_{m' \in \mathcal{M}'} \hat{b}_{m,m'}^{\text{dis}}. \quad (2.47)$$

As DIS concepts do not involve signal quantization, we do not consider a third performance bound here. A major advantage of DIS concepts is that the rate/backhaul trade-off is highly predictable, while implementation is straightforward. In this work, we will hence always present simulation results where the rate/backhaul trade-off of BS cooperation schemes is displayed not as a line, but as an area, where we compare

- **DIS schemes:**

- Best known scheme in information theory (based on Slepian-Wolf source coding)
- Practical scheme (exchange of a complete decoded messages over the backhaul)

- **CIF and DAS schemes:**

- Best known scheme in information theory (based on Wyner-Ziv source coding)
- Scheme operating on the rate-distortion bound
- Practical scheme, assuming a concrete quantizer implementation

DAS-enhanced FDM

The frequency division multiplex (FDM) scheme explained in the context of schemes without BS cooperation in Section 2.2.4 can also be assisted through exchanging quantized signals between BSs. In the simplified FDM case we observe in this work, all UEs are placed onto orthogonal resources, such that the usage of DIS/CIF concepts or common messages is not beneficial. If backhaul is provided, each UE can be decoded jointly by multiple BSs, where inter-BS correlation can be exploited. As there is no benefit of employing superimposed messages, it again suffices if each UE k transmits exactly one message \hat{F}_k at maximum transmit power $\forall k \in \mathcal{K} : \rho_{\hat{F}_k} = \hat{p}_k^{\text{max}}$. The transmission equation remains the same as in (2.20), and the capacity region can be lower-bounded by the following theorem:

Theorem 2.2.6 (Uplink capacity region with DAS-enhanced FDM). *A lower bound on the capacity region of transmission (2.20) with FDM and DAS-based BS cooperation constrained by a backhaul infrastructure $\hat{\mathbf{B}}^{\text{das}}$ and $\hat{\mathbf{B}}^{\text{net}}$ is given as*

$$\hat{\mathcal{R}}^{\text{das,fdm}}(\hat{\mathbf{B}}^{\text{das}}, \hat{\mathbf{B}}^{\text{net}}) = \bigcup_{\mathbf{\Lambda}: \mathbf{\Lambda} \succeq \mathbf{0} \wedge \text{tr}\{\mathbf{\Lambda}\}=1} \hat{\mathcal{R}}^{\text{das,fdm}}(\mathbf{\Lambda}, \hat{\mathbf{B}}^{\text{das}}, \hat{\mathbf{B}}^{\text{net}}), \quad (2.48)$$

where a lower bound on the rate region for a given spectrum allocation $\mathbf{\Lambda}$ and backhaul $\hat{\mathbf{B}}^{\text{das}}$, $\hat{\mathbf{B}}^{\text{net}}$ can be stated as all rate tuples $\mathbf{r} \in \hat{\mathcal{R}}^{\text{das,fdm}}(\mathbf{\Lambda}, \hat{\mathbf{B}}^{\text{das}}, \hat{\mathbf{B}}^{\text{net}})$, where $\forall k \in \mathcal{K}$:

$$0 \leq r_k \leq \max_{1 \leq m \leq M+1} \lambda_k \log_2 \left(1 + \frac{\hat{p}_k^{\max}}{\lambda_k} \left(\sum_{m'=1}^M (\mathbf{h}_{m',k}^e)^H (\mathbf{\Phi}_{k,m' \rightarrow m}^{\text{ii}})^{-1} \mathbf{h}_{m',k}^e \right) \right) \\ \text{with } \mathbf{\Phi}_{k,m' \rightarrow m}^{\text{ii}} = \underbrace{\sigma^2 \mathbf{I}}_{\text{Noise}} + \underbrace{\frac{\hat{p}_k^{\max}}{\lambda_k} \Delta (\bar{\mathbf{e}}_{m',k}^e (\bar{\mathbf{e}}_{m',k}^e)^H)}_{\text{Channel estimation impact}} + \underbrace{\mathbf{\Phi}_{k,m' \rightarrow m}^{\text{qq}}}_{\text{Quant. noise}}, \quad (2.49)$$

where $\mathbf{\Phi}_{k,m' \rightarrow m}^{\text{qq}}$ is the quantization noise involved in the compression of signals from BS m' to BS m (or the central network entity) on the spectrum connected to UE k , and we have the DAS-related backhaul constraint

$$\forall k \in \mathcal{K}, \forall m \in \mathcal{M} : \mathbf{\Phi}_{k,m \rightarrow m}^{\text{qq}} = \mathbf{0}_{[N_{\text{bs}} \times N_{\text{bs}}]} \text{ and } \forall m \in \{1..M+1\}, \forall \mathcal{M}' \subseteq \{\mathcal{M} \setminus m\} : \\ \sum_{k \in \mathcal{K}: m_k=m} \lambda_k \log_2 \left| \mathbf{I} + \left(\mathbf{\Phi}_{k,\mathcal{M}' \rightarrow m}^{\text{qq}} \right)^{-1} \mathbf{\Phi}_{k,\mathcal{M}'|m,\mathcal{M} \setminus \mathcal{M}'}^{\text{yy}} \right| \leq \sum_{m' \in \mathcal{M}'} \hat{b}_{m,m'}^{\text{das}}, \quad (2.50)$$

where $\mathbf{m} \in \{1, 2, \dots, M+1\}^{[K \times 1]}$ denotes the BSs at which the UEs are decoded, according to the maximization operation performed for each UE in (2.49). Further, $\mathbf{\Phi}_{k,\mathcal{M}'|m,\mathcal{M} \setminus \mathcal{M}'}^{\text{yy}}$ is the joint signal covariance at all BSs in \mathcal{M}' connected to the resources allocated by UE k and conditioned on the receive signal covariance connected to the same resources at BS m and the information provided by all BSs in set $\mathcal{M} \setminus \mathcal{M}'$ to BS m . $\mathbf{\Phi}_{k,\mathcal{M}' \rightarrow m}^{\text{qq}}$ is a block-diagonal matrix containing the quantization covariances introduced at all BSs in \mathcal{M}' and connected to the reception of UE k . Note that (2.49) also includes the case where a UE is decoded by a central network entity. As the central network entity itself does not receive any signals, we can state $\mathbf{\Phi}_{k,\mathcal{M}'|M+1,\mathcal{M} \setminus \mathcal{M}'}^{\text{yy}} = \mathbf{\Phi}_{k,\mathcal{M}'|\mathcal{M} \setminus \mathcal{M}'}^{\text{yy}}$. Finally, we have the network-related backhaul constraint

$$\forall m \in \mathcal{M} : \sum_{k \in \mathcal{K}: m_k=m} r_k \leq \hat{b}_{M+1,m}^{\text{net}}. \quad (2.51)$$

This final constraint assures that backhaul links are available over which user data can be forwarded to the network, if decoding takes place by a BS, and not by the network entity itself.

Proof. The theorem is a direct application of Theorem 2.2.5 to (2.20). Briefly, (2.50) states that the joint information flow from multiple BSs to those BSs that actually decode one or multiple UEs must be less or equal to the backhaul links involved. Equation (2.51) assures that backhaul links are also available for forwarding decoded messages to the network. \square

Similarly to the non-cooperative FDM scheme in Section 2.2.4, the maximization operation in (2.49) assures that each UE is decoded at the best possible BS (or at a central network

entity), depending on both the channel realization and the available backhaul infrastructure. Note that (2.50) implies an additional degree of freedom, namely the possibility to assign different extents of backhaul to different UEs, if these are decoded by the same entity, and hence the same backhaul links are involved. The backhaul constraint in (2.50) is based on the assumption of Wyner-Ziv source coding, but we again also consider the case where we operate on the rate-distortion bound, but do not exploit inter-BS receive signal correlation, where (2.50) is then restated as

$$\forall k \in \mathcal{K}, \forall m \in \{1..M+1\}, m' \in \{\mathcal{M} \setminus m\} : \sum_{k \in \mathcal{K}: m_k=m} \lambda_k \log_2 \left| \mathbf{I} + \left(\Phi_{k,m' \rightarrow m}^{\text{qq}} \right)^{-1} \Phi_{k,m'}^{\text{yy}} \right| \leq \hat{b}_{m,m'}^{\text{das}}, \quad (2.52)$$

where $\Phi_{k,m'}^{\text{yy}}$ is the covariance of the signals connected to UE k received by BS m' . Finally, a practical quantization scheme is considered, as introduced in Section 2.2.5, where the received signal at each BS antenna is quantized individually and one bit is lost per real dimension towards the rate-distortion bound, and (2.50) changes to

$$\forall k \in \mathcal{K}, \forall m \in \{1..M+1\}, m' \in \{\mathcal{M} \setminus m\} : \sum_{k \in \mathcal{K}: m_k=m} \lambda_k \left(\log_2 \left| \mathbf{I} + \left(\Phi_{k,m' \rightarrow m}^{\text{qq}} \right)^{-1} \Delta \left(\Phi_{k,m'}^{\text{yy}} \right) \right| + 2N_{\text{bs}} \right) \leq \hat{b}_{m,m'}^{\text{das}}. \quad (2.53)$$

In this case it is clear from (2.53) that $\Phi_{k,m' \rightarrow m}^{\text{qq}}$ should be a diagonal matrix containing the number of bits used for quantization of the signal at each different BS antenna.

Calculation of Capacity Regions

Due to the many degrees of freedom in the parameters connected to DIS, CIF and DAS, it is difficult to state a general procedure for the computation of $\hat{\mathcal{R}}^{\text{coop}}$. If for example a weighted sum-rate maximization is to be performed on the capacity region, the optimization problem is generally non-convex in power parameter \mathcal{P} , which renders a brute force search necessary. For a fixed power allocation and a focus on pure DAS schemes, the calculation of optimal DAS quantization covariance matrices that fulfill (2.33) can be performed according to a scheme in [dCS08]. Here, for each compressing BS, an Eigenvalue decomposition of the (possibly conditioned) signal covariance is performed, known as a Karhonen-Loeve transformation [GDV02], and then the available backhaul is invested into the different Eigenmodes of the signal covariance through waterfilling. If multiple BSs forward signals to the same target applying distributed Wyner-Ziv compression, their quantization strategies have to be updated iteratively to ensure a non-redundant flow of information to the target BS. Though the authors in [dCS08, dS08] cannot prove convergence analytically, an implementation of the algorithm has shown convergence in all cases. In the remainder of this work, the scenarios and cooperation schemes we observe are limited enough to enable a brute force search through the parameter space, in conjunction with the algorithm from [dCS08].

For the computation of $\hat{\mathcal{R}}^{\text{das,fdm}}$, we perform a brute force search over the spectrum allocation parameter $\mathbf{\Lambda}$, and again use the scheme from [dCS08] to compute optimal DAS quantization noise covariances.

An illustration of the lower bounds on capacity regions for limited BS cooperation will be provided in Section 2.4.

2.3 Downlink

2.3.1 Transmission Model

We consider a downlink transmission from M BSs to K UEs, as depicted in Figure 2.6. We assume that each BS has an arbitrary number of N_{bs} antennas, while the UEs only have $N_{\text{mt}} = 1$ receive antenna. This setup is different from that typically assumed for LTE Release 8 [McC07], which considers multiple antennas per UE, but strongly simplifies our models and analysis in this work. Further, the results can still be extended to the case of $N_{\text{mt}} > 1$, as discussed in Section 5.3.2. We assume that the BSs map a set of messages $\check{\mathcal{F}}_{\text{all}}$ onto a set of sequences $\check{\mathcal{X}}_{\text{all}}$, which are precoded and transmitted symbol-wise over the channel. The transmission in each single channel access at time $1 \leq t \leq N_{\text{sym}}$ can be stated as

$$\mathbf{y}^{[t]} = \mathbf{H}^H \mathbf{s}^{[t]} = \mathbf{H}^H \mathbf{W} \mathbf{x}^{[t]} + \mathbf{n}^{[t]} = \mathbf{H}^H \mathbf{W} \mathbf{g}^{[t]}(\check{\mathcal{X}}_{\text{all}}) + \mathbf{n}^{[t]}, \quad (2.54)$$

where $\mathbf{y}^{[t]} = [y_1^{[t]}, y_2^{[t]}, \dots, y_K^{[t]}]^T \in \mathbb{C}^{[K \times 1]}$ are the signals received at the UEs. Matrix $\mathbf{H}^H = [\mathbf{h}_{1,1} \dots \mathbf{h}_{1,N_{\text{bs}}}, \mathbf{h}_{2,1} \dots \mathbf{h}_{2,N_{\text{bs}}}, \dots, \mathbf{h}_{M,1} \dots \mathbf{h}_{M,N_{\text{bs}}}]^H \in \mathbb{C}^{[K \times N_{\text{BS}}]}$ denotes the channel, which is used in Hermitian notation due to a duality to the uplink transmission from Section 2.2.1 that we will exploit later. We again assume that the channel is subject to block fading, while having the statistical properties of a zero-mean Gaussian distribution $h_{i,j} \sim \mathcal{N}_{\mathbb{C}}(0, E\{|h_{i,j}|^2\})$. $\mathbf{s}^{[t]} = [s_{1,1}^{[t]} \dots s_{1,N_{\text{bs}}}^{[t]}, s_{2,1}^{[t]} \dots s_{2,N_{\text{bs}}}^{[t]}, \dots, s_{M,1}^{[t]} \dots s_{M,N_{\text{bs}}}^{[t]}]^T \in \mathbb{C}^{[N_{\text{BS}} \times 1]}$ are the signals transmitted from the N_{BS} BS antennas. $\mathbf{s}^{[t]}$ is the result of linear precoding, and has a positive semidefinite covariance $E_t\{\mathbf{s}^{[t]} \mathbf{s}^{[t]H}\} = E_t\{\mathbf{W} \mathbf{x}^{[t]} \mathbf{x}^{[t]H} \mathbf{W}^H\} = \mathbf{\Phi}^{\text{ss}} \succeq 0$. Matrix $\mathbf{W} \in \mathbb{C}^{[N_{\text{BS}} \times |\check{\mathcal{F}}_{\text{all}}|]}$ is the employed linear precoding matrix, which is also assumed to remain constant throughout a block of N_{sym} consecutive channel accesses, and where each column constitutes the precoding vector connected to one particular message $F \in \check{\mathcal{F}}_{\text{all}}$, which we will also denote as \mathbf{w}_F . Term $\mathbf{x}^{[t]} = \mathbf{g}^{[t]}(\check{\mathcal{X}}_{\text{all}}) \in \mathbb{C}^{[|\check{\mathcal{X}}_{\text{all}}| \times 1]}$ are the symbols connected to the messages to be transmitted in channel access t . Here, $\mathbf{g}(\cdot)$ can be non-linear in the context of *dirty paper coding*, which we will consider later, or a simple identity projection with $\mathbf{g}^{[t]}(\check{\mathcal{X}}_{\text{all}}) = [x_1^{[t]}, x_2^{[t]}, \dots, x_{|\check{\mathcal{X}}_{\text{all}}|}^{[t]}]^T$ in the case of *pure linear precoding*. In both cases, the projection $\mathbf{g}^{[t]}(\check{\mathcal{X}}_{\text{all}})$ yields zero-mean Gaussian vectors with covariance $E_t\{\mathbf{x}^{[t]} \mathbf{x}^{[t]H}\} = \mathbf{I}$. $\mathbf{n}^{[t]} = [n_1^{[t]}, n_2^{[t]}, \dots, n_K^{[t]}]^T \in \mathbb{C}^{[K \times 1]}$ is additive noise at the receiver side, also assumed to be zero-mean Gaussian with $E_t\{\mathbf{n}^{[t]} \mathbf{n}^{[t]H}\} = \sigma^2 \mathbf{I}$. Again we will drop the symbol index t for notational brevity. Throughout this chapter, we will either assume that the transmission is subject to

- a *per-antenna* power (p.a. pwr) constraint, i.e. $\forall 1 \leq i \leq N_{\text{BS}} : [\mathbf{\Phi}^{\text{ss}}]_{i,i} \leq \check{p}_i^{\text{max}}$
- or a *sum* power constraint with $\text{tr}\{\mathbf{\Phi}^{\text{ss}}\} \leq \check{P}^{\text{max}}$.

In the first case, $\check{\mathbf{P}}^{\text{max}} = \Delta(\check{p}_1^{\text{max}}, \check{p}_2^{\text{max}}, \dots, \check{p}_{N_{\text{BS}}}^{\text{max}})$ contains the per-antenna power constraints, which can be motivated through the fact that in a mobile communications system each BS transmit antenna is typically equipped with an own power amplifier, where the linear region is constrained. On the other hand, assuming a sum power constraint \check{P}^{max} significantly simplifies the derivation and computation of rate regions, as we will see later. It is also possible to observe *per-base-station* power constraints, i.e. constraints on the sum power of groups of antennas, which is not further pursued in this work, but briefly discussed in Appendix C. The BSs are connected through a backhaul mesh of finite capacity $\check{\mathbf{B}}^{\text{max}} \in \mathbb{R}_0^{+[M \times M+1]}$, where $\forall 1 \leq i, j \leq M$ each entry $\check{b}_{i,j}^{\text{max}}$ denotes the one-directional backhaul link capacity from BS j to BS i , and $\forall 1 \leq i \leq M$ each entry $\check{b}_{i,M+1}^{\text{max}}$ denotes the one-directional backhaul capacity from a central network entity to BS i .

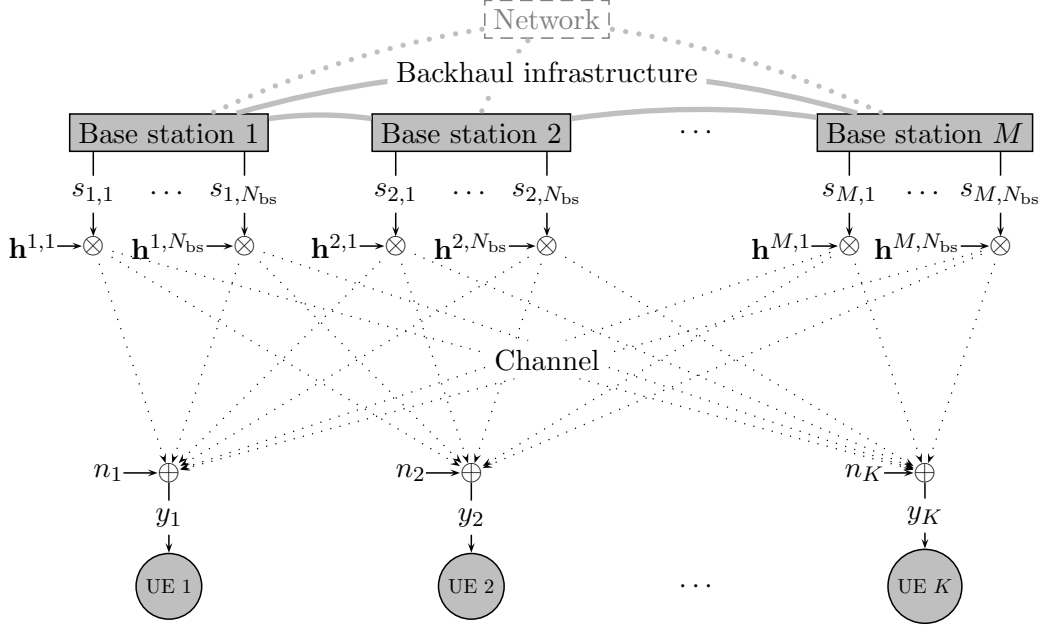


Figure 2.6: Illustration of the downlink transmission considered in this work.

2.3.2 Modeling of Imperfect Channel Knowledge

In the downlink transmission considered in our work, achievable rates depend strongly on the extent of channel knowledge available at the transmitter side [CS03]. Hence, practical systems that cannot exploit channel reciprocity must somehow feedback channel information from the receiver to the transmitter side. As in the uplink, a further performance degradation occurs if the channel knowledge at the UE side is limited. In our model, we assume that the UEs have an erroneous channel estimate, which they then quantize and feed back to the BSs. This implies that the *transmitter-sided channel state information* (CSIT) is strictly less accurate than that at the receiver side (CSIR)⁴. More specifically, we assume that

$$\hat{\mathbf{H}}^{\text{UE}} = \mathbf{H} + \hat{\mathbf{E}}^{\text{UE}} \quad (2.55)$$

$$\text{and } \hat{\mathbf{H}}^{\text{BS}} = \underbrace{\sqrt{1 - 2^{-N_b}}}_{\text{Scaling factor}} \hat{\mathbf{H}}^{\text{UE}} + \hat{\mathbf{E}}^{\text{BS}} \quad (2.56)$$

are the channel estimates known to the UEs and the BSs, respectively. $\hat{\mathbf{E}}^{\text{UE}} \in \mathbb{C}^{[N_{BS} \times K]}$ and $\hat{\mathbf{E}}^{\text{BS}} \in \mathbb{C}^{[N_{BS} \times K]}$ are channel estimation errors at the UE and BS side, respectively, that will be explained in the sequel. We here assume that each UE only has a channel estimate for the partial channel matrix connected to itself, while the BSs share the same global estimate of the complete channel $\hat{\mathbf{H}}^{\text{BS}}$, a requirement we will discuss in Section 5.2.2. As in the uplink, we model the elements of the channel estimation error $\hat{\mathbf{E}}^{\text{UE}}$ as i.i.d. Gaussian random variables with covariance $E \{ \text{vec}(\hat{\mathbf{E}}^{\text{UE}}) \text{vec}(\hat{\mathbf{E}}^{\text{UE}})^H \} = \sigma_E^2 \cdot \mathbf{I}$, where σ_E^2 depends on the number of pilots N_p

⁴In practical systems, a major aspect is also the feedback delay, leading to an inevitable degradation of CSIT if the channel coherence time is short. We model this implicitly in our later choice of N_b .

per codeword as stated in (2.5). We then model the CSI feedback process as if each channel coefficient in $\hat{\mathbf{H}}^{\text{UE}}$ was quantized individually with $N_b \in \mathbb{R}^+$ quantization bits and provided instantaneously to the BS side. Both parameters N_p and N_b are chosen based on a detailed analysis of a concrete channel prediction and CSI feedback scheme for an OFDMA system and a fading channel in Appendix E, which inherently models the aspect of unavoidable feedback delay. This leads to the fact that we can observe a fairly simple transmission model based on the assumption of a flat channel, while choosing parameters N_p and N_b such that our results reflect the performance of practical signal processing schemes under realistic channel conditions. The channel estimation error terms at the BS side in our model are given through rate-distortion theory [CT06] as $E\{|\hat{e}_{i,j}^{\text{BS}}|^2\} = 2^{-N_b} \cdot (E\{|h_{i,j}|^2\} + \sigma_E^2)$. The scaling factor in (2.56) is used to assure that the mean power of the quantizer output, including quantization noise, corresponds to the mean power of the quantizer input [CT06, Bus52]. The transmission in (2.54) can now be rewritten with (2.55) and (2.56) as

$$\mathbf{y} = \left((1 - 2^{-N_b})^{-\frac{1}{2}} \left(\hat{\mathbf{H}}^{\text{BS}} - \hat{\mathbf{E}}^{\text{BS}} \right) - \hat{\mathbf{E}}^{\text{UE}} \right) \mathbf{W}\mathbf{x} + \mathbf{n}. \quad (2.57)$$

Similar as in the uplink, we state a transmission equation that underestimates the performance of (2.54), but is significantly easier to handle, in the following theorem:

Theorem 2.3.1 (Modified downlink transmission equation under imperfect CSI). *The capacity region connected to a downlink transmission as in (2.54) can be inner-bounded by observing the capacity region of the following transmission:*

$$\mathbf{y} = \underbrace{\mathbf{H}^e \mathbf{W}\mathbf{x}}_{\text{Controllable term}} + \underbrace{\mathbf{v}^{\text{BS}}}_{\text{Add. impact of imp. CSI at BS}} + \underbrace{\mathbf{v}^{\text{UE}}}_{\text{Impact of imp. CSI at BS and UE}} + \mathbf{n} \quad (2.58)$$

$$\text{with } \forall i, j: h_{i,j}^e = h_{i,j} \cdot \sqrt{\frac{E\{|h_{i,j}|^2\}(1-2^{-N_b})}{E\{|h_{i,j}|^2\} + \sigma_E^2}} \quad (2.59)$$

$$\text{and } \mathbf{v}^{\text{BS}} \sim \mathcal{N}_{\mathbb{C}} \left(\mathbf{0}, \Delta \left(\bar{\mathbf{E}}^{e,\text{BS}} \Phi^{\text{ss}} (\bar{\mathbf{E}}^{e,\text{BS}})^H \right) \right), \quad \mathbf{v}^{\text{UE}} \sim \mathcal{N}_{\mathbb{C}} \left(\mathbf{0}, \Delta \left(\bar{\mathbf{E}}^{e,\text{UE}} \Phi^{\text{ss}} (\bar{\mathbf{E}}^{e,\text{UE}})^H \right) \right)$$

$$\text{where } \forall 1 \leq i \leq N_{\text{BS}}, 1 \leq j \leq K: \bar{e}_{i,j}^{\text{BS}} = \sqrt{2^{-N_b} \frac{(E\{|h_{i,j}|^2\})^2}{E\{|h_{i,j}|^2\} + \sigma_E^2}} \quad \text{and} \quad \bar{e}_{i,j}^{\text{UE}} = \sqrt{\frac{E\{|h_{i,j}|^2\} \sigma_E^2}{E\{|h_{i,j}|^2\} + \sigma_E^2}}$$

where $\mathbf{v}^{\text{UE}} \in \mathbb{C}^{[N_{\text{BS}} \times 1]}$ and $\mathbf{v}^{\text{BS}} \in \mathbb{C}^{[N_{\text{BS}} \times 1]}$ are additive, Gaussian, element-wise independent noise terms connected to the imperfect channel knowledge at both BS and UE, and the additional imperfectness of CSIT, respectively.

Proof. The proof is given in Appendix B.2. □

Briefly, Theorem 2.3.1 follows from the same argumentation as in Theorem 2.2.1. Hence, the error terms $\hat{\mathbf{E}}^{\text{BS}}$ and $\hat{\mathbf{E}}^{\text{UE}}$ are re-written into terms $\mathbf{E}^{e,\text{BS}}$ and $\mathbf{E}^{e,\text{UE}}$, respectively, which are uncorrelated with each other and with the estimated channel [PSS04]. Assuming that the products $\mathbf{E}^{e,\text{UE}} \mathbf{W}\mathbf{x}$ and $\mathbf{E}^{e,\text{BS}} \mathbf{W}\mathbf{x}$ are Gaussian variables with a different realization in each channel access poses an overestimation of their impact. As long as these statistical terms are never actually exploited as useful signal energy, we hence underestimate the performance of the original downlink transmission (2.54) by observing (2.58).

We can see from (2.58) that the impact of imperfect channel knowledge is in fact a function of the chosen transmit covariance Φ^{ss} . Hence, the BSs can transmit in such a way that

the negative impact of imperfect CSIT is minimized, provided the BSs know the extent of channel knowledge imperfectness (i.e. the variance of the error terms stated above). This appears intuitive, as a BS would for example not invest much transmit power into a link that is only badly known. Analogue to the uplink, the model implies that σ_E^2 , N_b and the statistics of the channel $\forall i, j : E\{|h_{i,j}|^2\}$ are known to both BS and UE side, such that all entities can calculate $\bar{\mathbf{E}}^{e,BS}$ and $\bar{\mathbf{E}}^{e,UE}$. The model provides a fairly tight bound for moderate N_b , but underestimates performance in the regime of very small N_b . This is due to the fact that according to Theorem 2.3.1, the effective, usable channel becomes zero for $N_b \rightarrow 0$, meaning that capacity will also tend to zero. In reality, however, non-zero rates would be achievable even if the BSs had no channel knowledge at all. In this case, the best transmission strategy under a sum power constraint would be to transmit from one antenna to each UE successively, or to compute precoding vectors based on the average properties of the channel under a per-antenna power constraint. Then, the powers of signals transmitted from multiple antennas to a user would sum up on average, leading to a moderately good mean capacity. The outage capacity, however, would be bad, as instantaneous channel realizations would lead to a destructive overlap of signals. In the remainder of this work, however, we will use a value of $N_b = 6$ that on one hand represents the performance of a practical CSI feedback concept as motivated in Appendix E, while letting us operate in a regime of N_b where a large extent of the possible CoMP gain is obtained, as we will see in Section 3.4.1.

As in the uplink, it is clear that the channel estimation related noise terms in (2.58) constitute an additional background noise that cannot be canceled. All downlink BS cooperation schemes to be observed in this work will hence be equally subject to this impairment, but the fact that this narrows down the regime in which CoMP is generally attractive, as we will see later, renders certain BS cooperation schemes less valuable than others.

2.3.3 Capacity Region Under Infinite BS Cooperation

Under infinite BS cooperation, the downlink transmission (2.54) corresponds to the setup of a Gaussian MIMO *broadcast channel* (BC). This was initially introduced by D. Blackwell in 1963, and has since been widely investigated. The capacity region of the *general* BC (hence with arbitrary joint probabilities of input and output signals) still remains unknown, though upper bounds have been stated by [Cov72], [Sat78] and [Mar79]. A bound derived in the latter work is known to be tight for all special BC cases for which the capacity region has so far been established. One of these cases is the *degraded* BC, where the channel inputs and outputs form a Markov chain [CT06], i.e. where the signals received by one UE are simply a noisier, degraded version of the signals received by another UE. This is for example the case when the BSs have only $N_{BS} = 1$ antenna in total [Sat78], where it has been shown that capacity is achieved through a superposition coding strategy [Ber74]. For the *Gaussian* MIMO BC, which is of interest in our work, Caire and Shamai [CS03] showed for $K = 2$ that the sum rate is maximized by applying *dirty-paper coding* (DPC) [Cos83] at the BS side. This means that the BSs transmit to one terminal in such a way that the interference caused by another, superimposed transmission to the other UE is canceled. Considering our transmission equation from (2.54), DPC can be seen as a non-linear operation performed on the set of sequences \check{X}_{all} before applying the linear precoding matrix \mathbf{W} . This scheme is basically a particular application of the more general concept of transmission under a random channel state known only to the transmitter [GP80]. The proof of optimality of DPC for the BC was extended to the sum rate under an arbitrary number of UEs by [VJG03, VT03,

YC04], and finally to the complete capacity region in [WSS04, WSS06]. Recent research has primarily focused on two major problems connected to the BC: First, the fact that DPC is complex to be implemented in practical systems has led to the proposal of sub-optimal schemes such as *Tomlinson-Harashima precoding* (THP) [Tom71, HM72, Et05]. Second, the fact that it is computationally complex to calculate the optimal precoding matrix \mathbf{W} for capacity-approaching transmission has resulted in a large extent of work on simplified, sub-optimal schemes such as *zero-forcing* (ZF) [SSH04], *channel inversion* [PHS05, HPS05] or *zero-forcing dirty-paper coding* (ZF-DPC) [CS03, KFVY06], all of which achieve capacity in the asymptotic high SNR regime.

While the previously referenced work was based on the assumption that both BSs and UEs have perfect channel knowledge, it was pointed out in [CS03] that BCs are significantly more sensitive to imperfect CSIT than point-to-point MIMO links. As pointed out before, without any CSIT, the best strategy is to transmit to each UE successively. Various publications have appeared e.g. on the asymptotic capacity of the MIMO BC in high SNR regimes. It has for example been shown that if arbitrarily approximate, yet imperfect CSIT is available, the asymptotic multiplexing gain in an $N_{\text{BS}} = K = 2$ and $N_{\text{mt}} = 1$ setup for $\text{SNR} \rightarrow \infty$ is limited to $4/3$ [LSW05]. Achieving the maximum asymptotic multiplexing gain of 2 requires that the CSI feedback is increased proportionally to the (logarithmic) SNR [Jin06b, SCJ07]. A variety of concrete CSI feedback and precoding schemes have been proposed, e.g. where the UEs feed back the indices of precoding vectors that maximize their SINR [SH05], possibly using only one precoding vector with which only the best UE can be served [VTL02], or where a specific kind of channel information is available at the BSs [DLZ07]. Other authors have assumed the same model of Gaussian channel estimation error as in Section 2.3.2, for example observing the sum rate achievable with zero-forcing [PSS04] or ZF-DPC [DLZ05], or the complete capacity region [DSH06]. All these authors, however, assume that CSIR is equal to CSIT, and to our knowledge, the first model considering different extents of CSI at receiver and transmitter side has been introduced in [MF09a].

The computation of the capacity region in the downlink is significantly more complex than in the uplink, but can be made mathematically more amenable by the notion of *uplink-downlink duality*, which was observed by, e.g. [JVG04]. It is known that the capacity region of a downlink transmission under a sum power constraint over all BS antennas is equivalent to that of an uplink transmission through the same (reciprocal) channel under the same sum power constraint [BS02a]. It has further been shown that duality also holds for a downlink transmission under a *per-antenna*-(group) power constraint [YL07], which corresponds to an uplink subject to a particular, least favorable noise covariance matrix. In this work, we extend the concepts from [YL07] by also incorporating different extents of CSIT and CSIR, and the impact of different BS cooperation schemes, as we will investigate later.

In this section, we consider the capacity regions achievable under linear or non-linear precoding (based on DPC), knowing that a practical system with reasonable complexity could then achieve a performance in between these two bounds. In the case where CSIT equals CSIR (i.e. $N_{\text{b}} = \infty$), it is clear from (2.58) that the imperfect channel knowledge leads to an error term \mathbf{v}^{UE} that neither BSs nor UEs can combat. In this case, it is straightforward to calculate *signal-to-interference-and-noise ratios* (SINRs) for both the linear and non-linear precoding case [DSH06], based on the modified transmission equation in (2.58). For the more realistic case of better CSIR than CSIT, i.e. finite N_{b} , deriving tight lower bounds on SINRs is difficult. In the linear precoding case, it appears intuitive that the receiver side can exploit

the additional channel knowledge. A simple example is the case where the channel gain is in fact stronger than according to the channel estimate at the BS side, and where the UE can simply make use of the improved gain through its more accurate own channel estimate. However, it is difficult to formulate this in a closed-form SINR expression, as then a statistical term connected to the channel estimation error at the BS side would appear in the nominator of the SINR expression, conflicting with Jensen's inequality. In this work, we hence use a lower bound of the SINR, where the corresponding error term appears neither as a useful signal term, nor as a noise term, which we prove to be a valid lower bound in Appendix B.3. In the case of DPC, it becomes strongly questionable whether a UE can exploit better CSI than at the BS side. This is due to the fact that DPC, as it has originally been formulated from an information theory point of view [Cos83], requires the UE to decode information contained in the *superposition* of the desired signal and the interference known to the BS. For this reason, we assume that the performance is limited due to the BS-side knowledge on this superposition, regardless of CSIR. As a consequence, we use a lower SINR bound in the context of DPC that assumes that the better CSI at the receiver side cannot be exploited at all. Note that this leads to the fact that in our simulations, linear precoding techniques can outperform DPC techniques for certain channels and a large difference between CSIT and CSIR. This is unintuitive in the way that DPC always includes linear precoding as a subset and should hence perform at least as good. However, the SINR expressions and corresponding capacity regions reveal a good insight into whether a system would actually invest complexity at the BS side into DPC-approaching schemes, or rather fall back to pure linear precoding schemes. Find more discussion on this aspect in Appendix B.3.

In a BC with one receive antenna per UE, there is no benefit of using more than one message per UE. Hence, we here constrain ourselves to the case where

$$\check{\mathcal{F}}_{\text{all}} := \{\check{F}_1, \check{F}_2, \dots, \check{F}_K\}. \quad (2.60)$$

We denote as \mathbf{w}_k the precoding vector connected to the (single) message \check{F}_k to be decoded by UE k and state the following lemma:

Lemma 2.3.2 (Downlink SINR under imperfect CSI and infinite BS cooperation). *Under infinite BS cooperation, imperfect CSIT and CSIR and linear and/or non-linear precoding (where in the non-linear case we assume without loss of generality that the streams directed to the UEs are encoded in the order $K..1$, such that lower indices profit most from DPC), the achievable downlink SINR at each UE $k \in \mathcal{K}$ can be lower-bounded as*

$$\text{SINR}_k^{\text{inf}} \geq \frac{\overbrace{\left| (\mathbf{h}_k^e)^H \mathbf{w}_k \right|^2}^{\text{Desired signal}}}{\underbrace{\sum_{j \in \mathcal{J}_1(k)} \left| (\mathbf{h}_k^e)^H \mathbf{w}_j \right|^2}_{\text{Inter-user interference}} + \underbrace{\sum_{j \in \mathcal{J}_2(k)} \sum_{a=1}^{N_{\text{BS}}} \left| \bar{e}_{a,k}^{\text{BS}} w_{a,j} \right|^2}_{\text{Add. impact of imp. CSI at BS}} + \underbrace{\sum_{j=1}^K \sum_{a=1}^{N_{\text{BS}}} \left| \bar{e}_{a,k}^{\text{UE}} w_{a,j} \right|^2}_{\text{Imp. CSI at BS and UE}} + \sigma^2}. \quad (2.61)$$

Here, $\mathcal{J}_1(k) = \mathcal{J}_2(k) = \mathcal{K} \setminus k$ for the case of linear precoding, and $\mathcal{J}_1(k) = \{1..k-1\}$, $\mathcal{J}_2(K) = \{1..K-1\}$ and $\forall k < K : \mathcal{J}_2(k) = \mathcal{K}$ for non-linear precoding.

Proof. The proof is stated in Appendix B.3. □

Briefly, sets \mathcal{J}_1 and \mathcal{J}_2 reflect that

- in the linear precoding case, each transmission is interfered by each other transmission (hence $\mathcal{J}_1(k) = \mathcal{K} \setminus k$), but each UE is *not* negatively impacted by the lesser degree of CSIT (hence also $\mathcal{J}_2(k) = \mathcal{K} \setminus k$), as discussed before.
- in the non-linear precoding case, UEs are only interfered by the transmissions that are encoded subsequently (hence $\mathcal{J}_1(k) = \{1..k-1\}$), and all UEs $k < K$ that benefit from DPC suffer from the lesser degree of CSIT (hence $\forall k < K : \mathcal{J}_2(k) = \mathcal{K}$). Only for UE K , which is encoded first and does not benefit from DPC, the lesser degree of BS-side CSIT does not pose additional interference, so that $\mathcal{J}_2(K) = \{1..K-1\}$.

Despite having stated simple SINR expressions in (2.61), it is difficult to calculate the capacity region directly from (2.61), as the SINRs of the UEs are crosscoupled through the choice of precoding matrix \mathbf{W} [BS02b]. However, it is possible to exploit uplink-downlink duality and show that the downlink capacity region is equivalent to a that of a dual uplink transmission, which we do in the following theorem:

Theorem 2.3.3 (Downlink capacity region under imperfect CSI and infinite BS cooperation). *The capacity region of a downlink transmission from M fully cooperative BSs with N_{bs} antennas each to K non-cooperative UEs with 1 antenna each, as in (2.54), with imperfect CSI and a per-antenna or sum power constraint can be inner-bounded through the capacity region of a dual uplink transmission from K non-cooperative UEs with 1 antennas each to M fully cooperative BSs with N_{bs} antennas each, subject to a sum power constraint, imperfect CSIR at the BSs and a least favorable noise covariance. More precisely, the capacity region is inner-bounded by all rate tuples $\mathbf{r} \in \tilde{\mathcal{R}}_\infty$ that fulfill $\forall k \in \mathcal{K} : r_k \geq 0$ and (assuming without loss of generality the encoding order $K..1$) $\forall \alpha_1 \geq \alpha_2 \geq \dots \geq \alpha_K \geq 0$ with $\sum_k \alpha_k = 1$:*

$$\sum_{k=1}^K \alpha_k r_k \leq \min_{\hat{\Phi}_{\text{nn}}} \max_{\hat{\mathbf{P}}} \sum_{k=1}^K \alpha_k \cdot \log_2 \left| \mathbf{I} + \frac{\hat{p}_k \mathbf{h}_k^e (\mathbf{h}_k^e)^H}{\sum_{j \in \mathcal{J}_1^*(k)} \hat{p}_j \mathbf{h}_j^e (\mathbf{h}_j^e)^H + \sum_{j \in \mathcal{J}_2^*(k)} \hat{p}_j \Delta \left(\bar{\mathbf{e}}_j^{\text{e,BS}} (\bar{\mathbf{e}}_j^{\text{e,BS}})^H \right) + \sum_{j=1}^K \hat{p}_j \Delta \left(\bar{\mathbf{e}}_j^{\text{e,UE}} (\bar{\mathbf{e}}_j^{\text{e,UE}})^H \right) + \hat{\Phi}_{\text{nn}}} \right|$$

s.t. $\text{tr}\{\hat{\mathbf{P}}\} \leq \text{tr}\{\check{\mathbf{P}}^{\text{max}}\}$, $\text{tr}\{\hat{\Phi}_{\text{nn}} \check{\mathbf{P}}^{\text{max}}\} \leq \sigma^2 \text{tr}\{\check{\mathbf{P}}^{\text{max}}\}$ and $\hat{\Phi}_{\text{nn}} \succeq 0$, (2.62)

where $\mathcal{J}_1^*(k)$ and $\mathcal{J}_2^*(k)$ are dual sets of $\mathcal{J}_1(k)$ and $\mathcal{J}_2(k)$, respectively, with $\mathcal{J}_1^*(k) = \{j \in \mathcal{K} : k \in \mathcal{J}_1(j)\}$ and $\mathcal{J}_2^*(k) = \{j \in \mathcal{K} : k \in \mathcal{J}_2(j)\}$. $\hat{\mathbf{P}} = \text{diag}(\hat{\mathbf{p}})$ with $\hat{\mathbf{p}} \in \mathbb{R}_0^{+[K \times 1]}$ denotes the transmit powers in the dual uplink transmission, and $\hat{\Phi}_{\text{nn}}$ is the uplink noise covariance which is connected to the per-antenna power constraints. Under a sum power constraint in the downlink, $\hat{\Phi}_{\text{nn}}$ is fixed, i.e. the last line in (2.62) simplifies to

$$\text{s.t. } \text{tr}\{\hat{\mathbf{P}}\} \leq \text{tr}\{\mathbf{P}^{\text{max}}\} \text{ and } \hat{\Phi}_{\text{nn}} = \sigma^2 \mathbf{I}. \quad (2.63)$$

Proof. The proof is given in Appendix C. □

Briefly, the weights $\alpha_1.. \alpha_K$ reflect a *weighted* sum rate maximization, hence different choices of these weights (and swapping UE indices for generality) allow to trace the complete capacity region, which will be illustrated later. Note that the stated order of weights must reflect the downlink *encoding* order $K..1$ (i.e. the strongest weighted UE 1 must be the one that profits most from DPC) [VVH03]. However, the *decoding* order in the dual uplink is exactly the opposite (benefiting users with larger indices). This interesting aspect is due to the dual sets $\mathcal{J}_1^*(k)$ and $\mathcal{J}_2^*(k)$ in (2.62) and has been discussed in detail in [VJG03].

Capacity Region Calculation

Being able to observe downlink capacity regions through uplink-downlink duality, such that an explicit calculation of precoding vectors \mathbf{w}_k is not necessary, does not mean that the calculation of the capacity region itself becomes trivial. In fact, to the author's knowledge, only for the case of perfect CSIT and CSIR and a DPC strategy there exists a gradient-based approach for capacity region computation at reasonable complexity. In this case, assuming without loss of generality that $\alpha_1 \geq \alpha_2 \geq \dots \geq \alpha_K \geq 0$, (2.62) simplifies to

$$\sum_{k=1}^K \alpha_k r_k \leq \min_{\hat{\Phi}_{\text{nn}}} \max_{\hat{\mathbf{P}}} \sum_{k=1}^K \alpha_k \log_2 \left| \mathbf{I} + \frac{\hat{p}_k \mathbf{h}_k \mathbf{h}_k^H}{\sum_{j < k} \hat{p}_j \mathbf{h}_j \mathbf{h}_j^H + \hat{\Phi}_{\text{nn}}} \right|$$

s.t. $\text{tr}\{\hat{\mathbf{P}}\} \leq \text{tr}\{\check{\mathbf{P}}^{\text{max}}\}$, $\text{tr}\{\hat{\Phi}_{\text{nn}} \check{\mathbf{P}}^{\text{max}}\} \leq \sigma^2 \text{tr}\{\check{\mathbf{P}}^{\text{max}}\}$ and $\hat{\Phi}_{\text{nn}} \succeq 0$. (2.64)

This can be re-stated as [VVH03]

$$\sum_{k=1}^K \alpha_k r_k \leq \min_{\hat{\Phi}_{\text{nn}}} \max_{\hat{\mathbf{P}}} \alpha_K \log_2 \left| \sum_{j=1}^K \hat{p}_j \mathbf{h}_j \mathbf{h}_j^H + \hat{\Phi}_{\text{nn}} \right|$$

$$+ \sum_{k=1}^{K-1} (\alpha_k - \alpha_{k+1}) \log_2 \left| \sum_{j=1}^k \hat{p}_j \mathbf{h}_j \mathbf{h}_j^H + \hat{\Phi}_{\text{nn}} \right| - \alpha_1 \log_2 \left| \hat{\Phi}_{\text{nn}} \right|$$

s.t. $\text{tr}\{\hat{\mathbf{P}}\} \leq \text{tr}\{\check{\mathbf{P}}^{\text{max}}\}$, $\text{tr}\{\hat{\Phi}_{\text{nn}} \check{\mathbf{P}}^{\text{max}}\} \leq \sigma^2 \text{tr}\{\check{\mathbf{P}}^{\text{max}}\}$ and $\hat{\Phi}_{\text{nn}} \succeq 0$, (2.65)

which is clearly concave in $\hat{\mathbf{P}}$ (as $\forall k = 1..K-1 : \alpha_k - \alpha_{k+1} \geq 0$) and convex in $\hat{\Phi}_{\text{nn}}$. It can thus be solved through interior point methods or gradient-based approaches [BV04], where the latter has been proposed for the case of a sum power constraint in the downlink in [VVH03], and for the case of per-antenna-(group) power constraints in [YL07].

For linear precoding techniques and/or under the impact of imperfect channel estimation, however, the optimization problem in (2.65) is no longer concave in $\hat{\mathbf{P}}$. In this work, we calculate downlink rate regions by performing a brute force search over different dual uplink power allocations $\hat{\mathbf{P}}$, for which we iteratively

- update the weights $\alpha_1.. \alpha_K$ to ensure that these correspond to the gradient of the rate region in the desired point, and
- update the uplink noise covariance $\hat{\Phi}_{\text{nn}}$ via a gradient technique, such that it remains within the polyhedron defined by $\text{tr}\{\hat{\Phi}_{\text{nn}} \check{\mathbf{P}}^{\text{max}}\} \leq \sigma^2 \text{tr}\{\check{\mathbf{P}}^{\text{max}}\}$ and $\hat{\Phi}_{\text{nn}} \succeq 0$.

The algorithm is stated in detail in Appendix D.3.

2.3.4 Capacity Region without BS Cooperation

If no cooperation is possible between BSs, each transmission to a UE may only originate from one BS, i.e. all elements of the involved precoding vector are constrained to zero except for those connected to exactly this BS [MF07c]. If multiple BSs were involved in the transmission to a single UE k , the corresponding message \check{F}_k would have to be provided to the BSs by the network, or exchanged among BSs, requiring additional backhaul traffic. However, we have the possibility that two or more UEs can be served by the same BS, such that DPC techniques can be applied locally, which would correspond to local successive interference cancellation in the dual uplink. In this case, other BSs might simply be turned off, though this situation is rarer if per-antenna power constraints are considered than in the uplink, as turning off BSs of course means giving up potential transmit power.

We initially establish an inner bound on the capacity region assuming that the transmission to a UE $k \in \mathcal{K}$ is treated as interference by all other UEs, unless DPC techniques are used such that this interference does not affect certain other UEs. Then, we extend the capacity region through the concept of common messages that are decoded by multiple UEs for interference reduction. For both cases, we make use of variable $\mathbf{m} \in \{1..M\}^{[K \times 1]}$, where each element m_k denotes the BS index that is serving UE k , and state the following theorem:

Lemma 2.3.4 (Downlink SINR under imperfect CSI and without BS cooperation). *Without BS cooperation, under imperfect CSI and using linear precoding and/or DPC techniques (where in the latter case we assume without loss of generality that streams are encoded in the order $K..1$ whenever these are transmitted from the same BS), the achievable downlink SINR at each UE $k \in \mathcal{K}$ can be lower-bounded as*

$$\check{\text{SINR}}_k^{\text{zero}} \geq \frac{\overbrace{\left| (\mathbf{h}_k^e)^H \boldsymbol{\Psi}_{m_k} \mathbf{w}_k \right|^2}^{\text{Desired signal}}}{\underbrace{\sum_{j \in \mathcal{J}_1(k)} \left| (\mathbf{h}_k^e)^H \boldsymbol{\Psi}_{m_j} \mathbf{w}_j \right|^2}_{\text{Inter-user interference}} + \underbrace{\sum_{j \in \mathcal{J}_2(k)} \sum_{a=1}^{N_{\text{BS}}} \left| \bar{e}_{a,k}^{\text{BS}} w_{a,j} \right|^2}_{\text{Add. imp. of BS CSI}} + \underbrace{\sum_{j=1}^K \sum_{a=1}^{N_{\text{BS}}} \left| \bar{e}_{a,k}^{\text{BS}} w_{a,j} \right|^2}_{\text{Imp. of BS and UE CSI}} + \sigma^2}. \quad (2.66)$$

Here, $\boldsymbol{\Psi}_m = \Delta([\mathbf{\Pi}_{\text{ant}}]_m)$ is a diagonal matrix with ones only in the diagonal elements connected to the indices of the antennas of BS m , and $\mathbf{\Pi}_{\text{ant}} \in \{0, 1\}^{[N_{\text{BS}} \times M]}$ denotes the connection between antenna indices and BS indices. We have $\mathcal{J}_1(k) = \mathcal{J}_2(k) = \mathcal{K} \setminus k$ for linear precoding and $\mathcal{J}_1(k) = \{j \in \mathcal{K} : j < k \vee m_j \neq m_k\}$ and $\mathcal{J}_2(k) = \{j \in \mathcal{K} : j \neq k \vee (\exists j' \geq k : m_{j'} = m_k)\}$ if DPC techniques can be exploited.

Proof. The proof is a straightforward extension of Lemma 2.3.2 to the fact that only certain BS antennas can be used to transmit to particular users, and that only groups of UEs served by the same BS can benefit from DPC. \square

The same uplink-downlink duality concept as in the last section can be applied, such that an inner bound on the capacity region can be stated as in the following theorem:

Theorem 2.3.5 (Downlink capacity region under imperfect CSI and without BS cooperation). *The capacity region of a downlink transmission from M non-cooperative BSs with N_{bs} antennas each to K non-cooperative UEs with 1 antenna each, according to (2.54),*

with imperfect CSI and per-antenna or sum power constraints, can be inner-bounded through the capacity region given through all rate tuples $\mathbf{r} \in \check{\mathcal{R}}_0$ that fulfill $\forall k \in \mathcal{K} : r_k \geq 0$ and $\forall \alpha_1 \geq \alpha_2 \geq \dots \geq \alpha_K \geq 0$ with $\sum_k \alpha_k = 1$

$$\sum_{k=1}^K \alpha_k r_k \leq \max_{\mathbf{m}} \min_{\hat{\Phi}_{\text{nn}}} \max_{\hat{\mathbf{P}}} \sum_{k=1}^K \alpha_k \cdot \log_2 \left| \mathbf{I} + \frac{\hat{p}_k \Psi_{m_k} \mathbf{h}_k^e (\mathbf{h}_k^e)^H \Psi_{m_k}}{\sum_{j \in \mathcal{J}_1^*(k)} \hat{p}_j \left(\mathbf{h}_j^e (\mathbf{h}_j^e)^H \right) + \sum_{j \in \mathcal{J}_2^*(k)} \Delta \left(\bar{\mathbf{e}}_j^{\text{e,BS}} (\bar{\mathbf{e}}_j^{\text{e,BS}})^H \right) + \sum_{j=1}^K \hat{p}_j \Delta \left(\bar{\mathbf{e}}_j^{\text{e,UE}} (\bar{\mathbf{e}}_j^{\text{e,UE}})^H \right) + \hat{\Phi}_{\text{nn}}} \right|$$

s.t. $\text{tr}\{\hat{\mathbf{P}}\} \leq \text{tr}\{\check{\mathbf{P}}^{\text{max}}\}$, $\underbrace{\text{tr}\{\hat{\Phi}_{\text{nn}} \check{\mathbf{P}}^{\text{max}}\} \leq \sigma^2 \text{tr}\{\check{\mathbf{P}}^{\text{max}}\}}_{\text{Per-antenna power constraint}}$ or $\underbrace{\hat{\Phi}_{\text{nn}} = \sigma^2 \mathbf{I}}_{\text{Sum power}}$. (2.67)

As before, $\Psi_m = \Delta([\mathbf{\Pi}_{\text{ant}}]_m)$ and $\mathcal{J}_1^*(k)$ and $\mathcal{J}_2^*(k)$ are again the dual sets to $\mathcal{J}_1(k)$ and $\mathcal{J}_2(k)$, respectively, as defined before. The last line in (2.67) reduces to (2.63) under a sum power constraint.

Proof. The proof is a straightforward extension of Theorem 2.3.3 to the SINR statement in Lemma 2.3.4. Following the lines of Theorem 2.3.3, it can be shown that the term Ψ introduced in (2.66), which is directly coupled to the employed precoding vectors in the downlink, is coupled to the receive filters in the dual uplink. Note that the order of the minimization and maximization operations in (2.67) is important. In particular, the rates must be *minimized* over all possible uplink covariance matrices $\hat{\Phi}_{\text{nn}}$ for a given uplink power allocation $\hat{\mathbf{P}}$ (see Appendix C), but are finally *maximized* over all possible BS-UE assignments \mathbf{m} . \square

Common Message Concepts

The capacity region stated through Theorem 2.3.5 can be extended if common message concepts are used as in the uplink in Section 2.2.4. In this case, the UEs can decode and remove parts of the interference from transmissions targeted to other UEs. As observed in the uplink, however, such techniques are only beneficial in regimes of fairly strong interference [Kra04]⁵. As we are typically considering downlink scenarios with multiple antennas at each BS ($N_{\text{bs}} > 1$), the cases where even after local (non-cooperative) beamforming the interference is strong are quite rare, and hence the benefit of common message concepts is marginal. To our knowledge, only few publications exist on multiple-antenna (MISO or MIMO) ICs, where the capacity region is only given for few channel examples [JF07, HSU09] or the IC is observed from a game theory point of view [SSB⁺09]. The interested reader is referred to Appendix D.4, where an inner bound $\check{\mathcal{R}}_0^{\text{hk}} \supseteq \check{\mathcal{R}}_0$ on the rate region achievable without BS cooperation, but with common message concepts and for arbitrary N_{bs} , is stated.

Frequency Division Multiplex

As in the uplink, we can also consider FDM, i.e. the possibility of splitting the spectrum such that multiple transmissions can focus their transmit power on orthogonal resources and

⁵Note that the word 'strong' here does *not* refer to the classification of ICs in, e.g. [Kra04]

are free of inter-user interference. While FDM schemes have shown to be beneficial in the uplink under strongly limited backhaul, the usage of such schemes is rather questionable in the downlink, due to the following reasons:

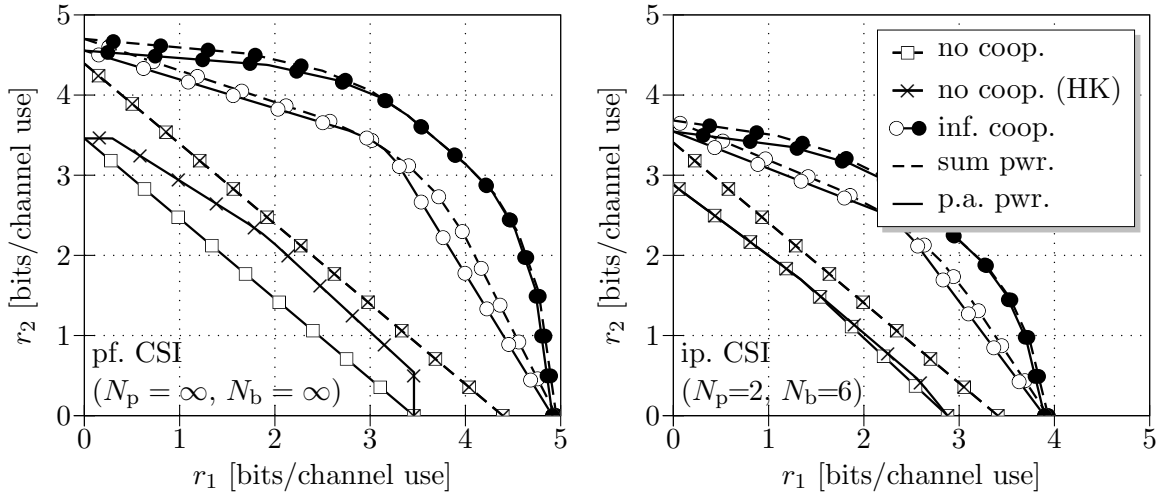
- The main advantage of FDM as opposed to TDM is to mitigate instantaneous transmit power constraints, by transmitting at a higher spectral density on only a portion of the system bandwidth. Clearly, there is no benefit at all of doing so in a downlink with a *sum power constraint*, as then the rates achieved from FDM can never exceed those achieved through a simple time-share between investing all transmit power into transmitting to certain UEs.
- If backhaul enables a certain extent of BS cooperation, BS antennas are used for the transmission to multiple UEs simultaneously. Also in this case, there is little benefit of using FDM. Furthermore, FDM will usually be strongly inferior to any other scheme, as it cannot exploit the spatial degrees of freedom the channel offers.

Hence, FDM is only interesting under *per-antenna* or *per-base-station* power constraints, and only in regimes of no or minimal BS cooperation. Furthermore, its performance can simply be upper-bounded through TDM under a sum power constraint, and we will see later that the difference between a sum power and per-antenna power constraint is rather marginal for most observed channels. For these reasons, we do not further observe FDM in the downlink.

Capacity Region Illustration

Figure 2.7 illustrates the previously derived inner bounds on capacity regions $\check{\mathcal{R}}_0$, $\check{\mathcal{R}}_0^{\text{hk}}$ and $\check{\mathcal{R}}_\infty$ for an example channel with $M = K = 2$, $N_{\text{bs}} = 1$ and $\mathbf{H} = [1, \sqrt{0.25}; \sqrt{0.5}, 1]$ and $\sigma^2 = 0.1$, hence a SISO SNR of 10 dB. We observe these regions under perfect CSIT and CSIR in Plot 2.7(a) ($N_{\text{p}} = N_{\text{b}} = \infty$), and for limited CSI in the right plot 2.7(b) ($N_{\text{p}} = 2$ and $N_{\text{b}} = 6$). The latter choice of parameters is motivated in Appendix E. In both cases, we consider either a sum power constraint with $\check{P}^{\text{max}} = 2$, or per-antenna power constraints with $\check{\mathbf{P}}^{\text{max}} = \mathbf{I}$, such that the sum power in both cases is the same. For infinite BS cooperation, we distinguish between schemes based on DPC (filled markers) and those based on linear precoding (hollow markers), a notation we will use for the downlink in the remainder of this thesis. In principle, local precoding to multiple UEs at one BS, making use of DPC, can be an interesting option, but not for this particular channel example with $N_{\text{bs}} = 1$.

We can see that the impact of per-antenna power constraints is rather minimal, and mainly affects the sides of the capacity regions, but not so much the point where the UE sum-rate would be maximized. Furthermore, we can see that DPC can partially mitigate the detrimental effects of per-antenna power constraints. In this example, the introduction of imperfect CSI leads to a significant decrease of rates, but this effects all schemes almost equally. We can, however, see that the gain of DPC over pure linear precoding techniques is slightly reduced, an aspect we will observe in detail in Section 3.4.1. One main effect of imperfect CSI is that now, the gain of common message concepts (HK) in the non-cooperative regime is strongly reduced. This is due to the fact that the decoding of interference is less beneficial, as imperfect CSI has significantly increased the level of background noise. For this reason, and the before mentioned aspect that such Han-Kobayashi schemes are computationally complex to optimize, we will not consider these further in the remainder of this work.



(a) Perfect CSIT and CSIR.

(b) Imperfect CSIT and CSIR.

Hollow \circ and filled \bullet markers denote linear precoding and DPC, respectively.

Figure 2.7: Downlink capacity region under no or infinite BS cooperation.

2.3.5 Basic Base Station Cooperation Schemes

We now observe the case of a downlink transmission under a limited backhaul infrastructure \mathbf{B}^{\max} . We must first of all mention a major difference of the downlink as compared to the uplink, namely the fact that in the downlink the performance of infinite BS cooperation can already be achieved with a finite amount of backhaul. More precisely, if e.g. all M BSs are involved in the joint transmission to all K UEs, then the maximum extent of cooperation is possible if all messages to be transmitted to all UEs are provided to each single BS⁶. In this case, the sum capacity of backhaul infrastructure required is simply M times the sum rate of all UEs, as opposed to *once* the sum rate of all UEs in a conventional system. This means that the required backhaul grows quadratically in the number of cooperating cells, assuming one BS and one UE on each resource per cooperating cell. As the number of BSs jointly transmitting to UEs is limited through various other aspects, such as synchronization [KF10], multi-cell channel estimation and signaling, one might conclude that the backhaul required in the downlink is in fact a minor issue. However, we will now state cooperation schemes that were introduced in [MF08c] and allow for a further, in some cases significant improvement of the rate/backhaul trade-off.

- **Unquantized Message based Cooperation (UMC).** A rather intuitive approach is to let each BS be provided only with the messages connected to the terminals to which it has a link strong enough to have a reasonable beamforming contribution. This scheme has the benefit of a fairly limited number of degrees of freedom, as each BS is either provided with a particular message or not.
- **Quantized Sequence based Cooperation (QSC).** The rate/backhaul trade-off can be further improved by allowing BSs to be provided with *quantized* versions $q(X)$ of the sequences to be transmitted to particular UEs. This is beneficial if the link from a BS

⁶In addition, the cooperating BSs will also need to exchange channel knowledge, as discussed later.

to a certain UE is rather weak, and where the additional backhaul invested into this link should somehow reflect the importance of the beamforming contribution of the BS to the UE. We can see immediately that in the context of QSC, source coding concepts such as Slepian-Wolf or Wyner-Ziv are not applicable, as there is no side-information the BSs could exploit when receiving quantized sequences from the network. Clearly, it does not make sense to invest more bits into the quantization of a sequence than the rate of the corresponding message itself. We assume in this work that the unquantized message is provided to the BS if enough backhaul is available, such that QSC schemes are always superior to UMC schemes.

- **Distributed Antenna Systems (DAS).** As in the uplink, it is also possible that BSs are used as *remote radio heads*, i.e. that some BSs perform all required linear or non-linear precoding, and then quantize and forward the calculated signals to other BSs for transmission. We assume for simplicity that quantization is performed separately for each transmit antenna, i.e. the BSs exchange $q(S_{m,a})$. While this approach is clearly suboptimal, it facilitates the usage of uplink/downlink duality, as we will see later.

The different BS cooperation schemes will be illustrated for small scenarios in Section 3.4.2. In the sequel, we describe a framework introduced in [MF09a] that allows to inner-bound the capacity regions of all three cooperation schemes. All schemes have in common that a certain extent of quantization noise is introduced at certain BSs when transmitting certain sequences⁷. We can model this aspect through the auxiliary variable

$$\mathbf{C} \in \mathbb{R}_0^{+[M \times K]}, \quad (2.68)$$

where each element $\forall m \in \mathcal{M}, k \in \mathcal{K} : c_{m,k}$ denotes the number of quantization bits per symbol the transmission contribution from BS m to UE k is subject to. Depending on the BS cooperation scheme observed, variable \mathbf{C} will then have different properties:

- If we generally only allow **Unquantized Message based Cooperation (UMC)**, \mathbf{C} is constrained to $\mathbf{C} \in \{0, \infty\}^{[M \times K]}$, hence a transmission from a BS m to a UE k is either subject to $c_{m,k} = 0$ or $c_{m,k} = \infty$ quantization bits. In the first case, the BS has *no* knowledge on the message \check{F}_k at all, and participating in beamforming to UE k would mean dissipating pure noise. In the second case, the BS has *perfect* knowledge on \check{F}_k and can have a beamforming contribution to UE k free of any quantization noise.
- For **Quantized Sequence based Cooperation (QSC)**, \mathbf{C} can take on any arbitrary value $\mathbf{C} \in \mathbb{R}_0^{+[M \times K]}$.
- For **Distributed Antenna Systems (DAS)**, matrix \mathbf{C} will have a certain structure, e.g. for $M = K = 3$: $\mathbf{C} = [\infty, \infty, \infty; \gamma_2, \gamma_2, \gamma_2; \gamma_3, \gamma_3, \gamma_3]$. In this example, BS 1 knows all messages $\check{F}_1 \cdots \check{F}_K$ and can transmit to all UEs free of quantization noise. It then performs the precoding for BSs 2 and 3, and forwards the precoded signals with γ_2 and γ_3 quantization bits, respectively, to the other BSs. In this case, we assume for simplification that the signals are quantized individually for each BS antenna such that all 3 streams are equally subject to quantization. A better rate/distortion trade-off could be achieved if the correlation of the transmit signals would be exploited, but this would render an application of uplink/downlink duality difficult.

⁷We can see UMC as an approach where we either apply zero or infinite quantization bits to sequences provided to BSs, as we will see later.

Let us state the SINRs achievable by the UEs as in the following lemma:

Lemma 2.3.6 (Downlink SINR under imperfect CSI and limited BS cooperation). *Under backhaul-constrained BS cooperation with UMC, QSC or DAS concepts, imperfect CSI and linear and/or non-linear precoding, the achievable downlink SINR of each UE $k \in \mathcal{K}$ can be lower-bounded as*

$$\begin{aligned} \check{\text{SINR}}_k^{\text{coop}} &\geq \frac{\overbrace{\left| (\mathbf{h}_k^e)^H \sqrt{\Psi_k} \mathbf{w}_k \right|^2}^{\text{Desired signal}}}{\underbrace{\sum_{j \in \mathcal{J}_1(k)} \left| (\mathbf{h}_k^e)^H \sqrt{\Psi_j} \mathbf{w}_j \right|^2}_{\text{Inter-sequence interference}} + \underbrace{\sigma_{\text{Q}}^2}_{\text{Quant. noise}} + \underbrace{\sigma_{\text{CSI}}^2}_{\text{Chn. est. noise}} + \sigma^2} \quad \text{where} \quad (2.69) \\ \sigma_{\text{Q}}^2 &= \underbrace{\sum_{j \in \mathcal{K}} \sum_{m=1}^M \left| (\mathbf{h}_{m,k}^e)^H \sqrt{\mathbf{I} - \Psi_j^m} \mathbf{w}_j^m \right|^2}_{\text{Quantization noise when using UMC or QSC}} \quad \text{or} \quad \sigma_{\text{Q}}^2 = \underbrace{\sum_{j \in \mathcal{K}} \sum_{a=1}^{N_{\text{BS}}} \left| h_{a,k}^e \sqrt{1 - \Psi_j^a} w_j^a \right|^2}_{\text{Quantization noise when using DAS}} \\ \sigma_{\text{CSI}}^2 &= \underbrace{\sum_{j \in \mathcal{J}_2(k)} \sum_{a=1}^{N_{\text{BS}}} \left| \bar{e}_{a,k}^{\text{BS}} w_j^a \right|^2 + \sum_{j \in \mathcal{K}} \sum_{a=1}^{N_{\text{BS}}} \left| \bar{e}_{a,k}^{\text{UE}} w_j^a \right|^2}_{\text{Channel estimation related noise}}, \end{aligned}$$

where $\mathcal{J}_1(k) = \mathcal{J}_2(k) = \mathcal{K} \setminus k$ if only pure linear precoding techniques are used. In the case of non-linear precoding, stating terms $\mathcal{J}_1(k)$ and $\mathcal{J}_2(k)$ becomes rather tedious, and we will hence do this only for specific, small scenarios in Section 3.4.2. Terms $\forall k \in \mathcal{K} : \Psi_k$ are now used to model the impact of quantization noise, and are given as

$$\forall k \in \mathcal{K} : \Psi_k = \Delta \left(\begin{array}{c} \mathbf{\Pi}_{\text{ant}} \begin{bmatrix} 1 - 2^{-c_{1,k}} \\ 1 - 2^{-c_{2,k}} \\ \vdots \\ 1 - 2^{-c_{M,k}} \end{bmatrix} \end{array} \right). \quad (2.70)$$

Proof. The SINR expressions derived here are simply based on rate-distortion theory. Regardless of whether quantization is applied to sequences (as for QSC, and virtually also for UMC), or to signals transmitted from certain antennas (DAS), the useful signal terms emitted by each BS antenna and connected to a certain UE are scaled down, and an antenna- and UE-specific quantization noise term is introduced. \square

The scaling factors in (2.70) are based on rate distortion theory [CT06] and ensure that the overall power emitted from the BS antennas does not change through the fact that precoding has been performed based on quantized message knowledge. Hence, when a BS has less knowledge on a certain UE message \hat{F} , the signal transmitted to this UE from any antennas of the BS will consist of a larger portion of quantization noise, while the useful signal contribution scales down in power. Note that the main difference between quantization noise in UMC/QSC contexts or in DAS is that in the latter case all interference terms connected to all channel coefficients are uncorrelated, and hence their powers simply sum up. For the former cooperation schemes UMC or QSC, we assume that sequences are provided to BSs in

a quantized form, and precoding is applied by the BS itself, such that the quantization noise emitted from the different antennas of the same BS and connected to a certain sequence is correlated. As opposed to the uplink, we here only observe performance based on the rate-distortion bound. This is motivated through the fact that quantization is performed knowing the original, discrete messages, where we assume that quantization codebooks can be used that are optimized in advance. Based on Lemma 2.3.6, we can now state an inner-bound on the capacity region through the following theorem:

Theorem 2.3.7 (Downlink capacity region under imperfect CSI and limited BS cooperation). *The capacity region of a downlink transmission from M BSs with N_{bs} antennas each to K UEs with 1 antenna each, according to (2.54), where BS cooperation is constrained by a backhaul infrastructure $\check{\mathbf{B}}^{\text{max}}$, with imperfect CSI and per-antenna or sum power constraints can be inner-bounded through the capacity region given through all rate tuples $\mathbf{r} \in \check{\mathcal{R}}_{\text{coop}}(\check{\mathbf{B}}^{\text{max}})$ that fulfill $\forall k \in \mathcal{K} : r_k \geq 0$ and $\forall \alpha_1 \geq \alpha_2 \geq \dots \geq \alpha_K \geq 0$ with $\sum_k \alpha_k = 1$*

$$\begin{aligned}
\sum_{k=1}^K \alpha_k r_k &\leq \max_{\mathbf{C}: \check{\mathbf{B}}^{\text{req}}(\mathbf{C}) \preceq \check{\mathbf{B}}^{\text{max}}} \min_{\hat{\Phi}_{\text{nn}}} \max_{\hat{\mathbf{P}}} \sum_{k \in \mathcal{K}} \alpha_k \cdot \log_2 \left| \mathbf{I} + \frac{\hat{p}_k \sqrt{\Psi_k} \mathbf{h}_k^e (\mathbf{h}_k^e)^H \sqrt{\Psi_k}}{\Phi^{\text{ii}}(k) + \Phi^{\text{qq}}(k) + \Phi^{\text{CSI}}(k) + \hat{\Phi}_{\text{nn}}} \right| \\
\text{s.t. } &\underbrace{\text{tr}\{\hat{\mathbf{P}}\} \leq \text{tr}\{\check{\mathbf{P}}^{\text{max}}\}}_{\text{Dual uplink power constraint}}, \quad \underbrace{\text{tr}\{\hat{\Phi}_{\text{nn}} \check{\mathbf{P}}^{\text{max}}\} \leq \sigma^2 \text{tr}\{\check{\mathbf{P}}^{\text{max}}\}}_{\text{DL per-antenna power constraint}} \quad \text{or} \quad \underbrace{\hat{\Phi}_{\text{nn}} = \sigma^2 \mathbf{I}}_{\text{DL sum power constraint}} \\
&\text{where } \underbrace{\Phi^{\text{ii}}(k) = \sum_{j \in \mathcal{J}_1^*(k)} \hat{p}_j \sqrt{\Psi_k} \mathbf{h}_j^e (\mathbf{h}_j^e)^H \sqrt{\Psi_k}}_{\text{Interference}} \quad \text{and} \\
&\underbrace{\forall m \in \mathcal{M} : \Phi_m^{\text{qq}}(k) = \sum_{j \in \mathcal{K}} \hat{p}_j \sqrt{\mathbf{I} - \Psi_k^m} \mathbf{h}_{m,j}^e (\mathbf{h}_{m,j}^e)^H \sqrt{\mathbf{I} - \Psi_k^m}}_{\text{Quantization noise when using UMC or QSC}} \\
&\quad \text{or } \underbrace{\Phi^{\text{qq}}(k) = \sum_{j \in \mathcal{K}} \hat{p}_j \Delta \left(\sqrt{\mathbf{I} - \Psi_k} \mathbf{h}_j^e (\mathbf{h}_j^e)^H \sqrt{\mathbf{I} - \Psi_k} \right)}_{\text{Quantization noise when using DAS}} \\
&\Phi^{\text{CSI}}(k) = \sum_{j \in \mathcal{J}_2^*(k)} \hat{p}_j \Delta \left(\bar{\mathbf{e}}_j^{\text{e,BS}} \left(\bar{\mathbf{e}}_j^{\text{e,BS}} \right)^H \right) + \sum_{j \in \mathcal{K}} \hat{p}_j \Delta \left(\bar{\mathbf{e}}_j^{\text{e,UE}} \left(\bar{\mathbf{e}}_j^{\text{e,UE}} \right)^H \right), \quad (2.71)
\end{aligned}$$

where $\hat{\mathbf{P}}$ is again a diagonal matrix containing the dual uplink powers of the UEs, and $\Phi^{\text{qq}}(k) = \Delta(\Phi_1^{\text{qq}}(k), \Phi_2^{\text{qq}}(k), \dots, \Phi_M^{\text{qq}}(k))$ is a block-diagonal matrix. As before, $\mathcal{J}_1^*(k)$ and $\mathcal{J}_2^*(k)$ are the dual sets to $\mathcal{J}_1(k)$ and $\mathcal{J}_2(k)$, respectively, with $\mathcal{J}_i^*(k) = \{j \in \mathcal{K} : k \in \mathcal{J}_i(j)\}$. $\check{\mathbf{B}}^{\text{req}}(\mathbf{C})$ is a function that states the required backhaul for a given message knowledge configuration \mathbf{C} . This is rather difficult to state in general, as it depends on the concrete cooperation concept observed, and will hence be stated only for particular scenarios in this work.

Proof. The proof is a straightforward application of Theorem 2.3.3 to (2.69). Similarly as in the proof of Theorem 2.3.5, scaling factors Ψ now connected to the impact of quantization noise that are directly connected to precoding vectors in the downlink are connected to receive filters in the dual uplink. The quantization in the downlink can hence be modeled by a UE-specific receiver-side quantization in the dual uplink. Similarly, the quantization noise introduced in the downlink can be seen as individual noise terms at each receive antenna

impairing different UEs in the dual uplink. Note that as in Theorem 2.3.5, the order of maximization and minimization in (2.71) is important, hence the rates are *minimized* over all possible uplink covariance matrices $\hat{\Phi}_{\text{nn}}$ for a fixed power allocation $\hat{\mathbf{P}}$, and finally *maximized* over all possible BS cooperation strategies described through \mathbf{C} . \square

When DAS is applied, we assume as stated before that signal quantization is performed *per BS antenna*, i.e. $\Phi^{\text{qq}}(k)$ has only non-zero values on the diagonal. For UMC or QSC, it has a block-diagonal structure, as then quantization is performed *per UE and per BS*, and the signal correlation between antennas of the same BS remains unaffected by quantization.

2.4 Performance and Backhaul-Constrained Capacity Regions

In the past sections, we have observed lower bounds on capacity regions for fixed extents of backhaul invested into different BS cooperation schemes. Ultimately, we are interested in the overall rate/backhaul trade-off achievable for different extents of backhaul infrastructure. In [MF08e], the concept of *performance regions* was introduced, which capture both achievable UE rates and the backhaul required to achieve these. We define a performance point Z as a tuple of achievable rates and required backhaul, i.e.

$$Z = \langle \mathbf{r}, \mathbf{B} \rangle, \quad (2.72)$$

and define a *performance region* connected to an arbitrary BS cooperation scheme yz as

$$\mathcal{Z}^{yz*} = \bigcup \{ \langle \mathbf{r}, \mathbf{B} \rangle : \exists \mathcal{W} : \mathbf{B}^{\text{req}}(\mathcal{W}) \leq \mathbf{B} \wedge \mathbf{r} \in \mathcal{R}^{yz}(\mathcal{W}) \}, \quad (2.73)$$

where \mathcal{W} is any kind of set of parameters, depending on which scheme is observed. Matrix $\mathbf{B}^{\text{req}}(\mathcal{W})$ is the backhaul required under a set of parameters, and $\mathcal{R}^{yz}(\mathcal{W})$ is an achievable rate region of the involved UEs under this set of parameters. Equation (2.73) basically defines a performance region as all tuples of rates and backhaul such that the rates can be achieved with the corresponding backhaul. The convex hull operation denoted through \bigcup assures that any weighted combination of cooperation strategies can also be performed using time-sharing. It can for example be beneficial to perform a time-share between non-cooperative decoding and a DAS strategy with a reasonable extent of backhaul, rather than using DAS with little backhaul, due to the concavity of the rate-backhaul function. As an example, we can state the performance region of combined DIS, CIF and DAS approaches in the uplink as

$$\hat{\mathcal{Z}}^{\text{coop}*} = \bigcup \left\{ \langle \mathbf{r}, \mathbf{B} \rangle : \exists \hat{\mathbf{B}}^{\text{dis}}, \hat{\mathbf{B}}^{\text{cif}}, \hat{\mathbf{B}}^{\text{das}}, \hat{\mathbf{B}}^{\text{net}} : \right. \\ \left. \hat{\mathbf{B}}^{\text{dis}} + \hat{\mathbf{B}}^{\text{cif}} + \hat{\mathbf{B}}^{\text{das}} + \hat{\mathbf{B}}^{\text{net}} \leq \mathbf{B} \wedge \mathbf{r} \in \hat{\mathcal{R}}^{\text{coop}} \left(\hat{\mathbf{B}}^{\text{dis}}, \hat{\mathbf{B}}^{\text{cif}}, \hat{\mathbf{B}}^{\text{das}}, \hat{\mathbf{B}}^{\text{net}} \right) \right\} \quad (2.74)$$

Even for a setup with few BSs, the number of involved backhaul links described in \mathbf{B} becomes large, and corresponding performance regions are of high dimensionality. In this work, we hence draw our attention to the *sum* backhaul required by various BS cooperation schemes *in addition* to a non-cooperative system. As our models in both uplink and downlink also allow encoding, precoding or decoding to take place at a central network entity, we have to consider for a fair comparison of cooperative and non-cooperative concepts that in such

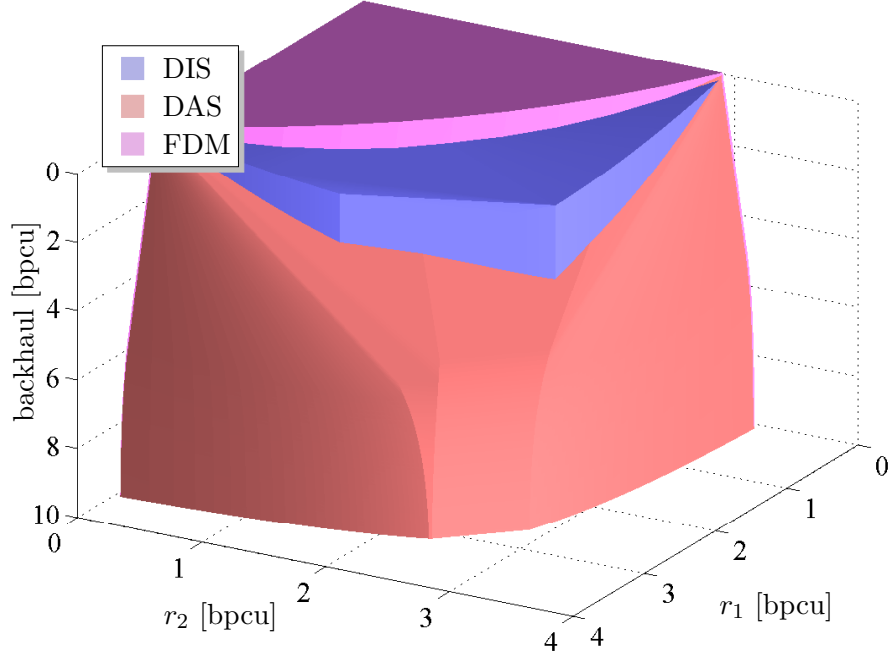


Figure 2.8: Uplink performance region for different CoMP schemes.

case the data bits need not be forwarded to or from the network any more. We compute this extent of additional sum backhaul as

$$\beta = \beta(\mathbf{r}, \mathbf{B}) = \mathbf{1}^T \mathbf{B} \mathbf{1} - \mathbf{1}^T \mathbf{r}, \quad (2.75)$$

which is simply the sum backhaul required on all links (between BSs as well as between BSs and the network) *minus* the backhaul which would be required in a non-cooperative system, which is nothing else than the sum rate of all UEs. This lets us now define a performance region with only $K + 1$ dimensions for any arbitrary cooperation scheme yz as

$$\mathcal{Z}^{yz} = \bigcup \{ \langle \mathbf{r}, \beta \rangle : \exists \mathcal{W} : \beta(\mathbf{r}, \mathbf{B}^{\text{req}}(\mathcal{W})) \leq \beta \wedge \mathbf{r} \in \mathcal{R}^{yz}(\mathcal{W}) \}, \quad (2.76)$$

or again, for the example of any arbitrary DIS/CIF/DAS combination in the uplink,

$$\hat{\mathcal{Z}}^{\text{coop}} = \bigcup \left\{ \langle \mathbf{r}, \beta \rangle : \exists \hat{\mathbf{B}}^{\text{dis}}, \hat{\mathbf{B}}^{\text{cif}}, \hat{\mathbf{B}}^{\text{das}}, \hat{\mathbf{B}}^{\text{net}} : \right. \\ \left. \beta(\mathbf{r}, \hat{\mathbf{B}}^{\text{dis}} + \hat{\mathbf{B}}^{\text{cif}} + \hat{\mathbf{B}}^{\text{das}} + \hat{\mathbf{B}}^{\text{net}}) \leq \beta \wedge \mathbf{r} \in \hat{\mathcal{R}}^{\text{coop}}(\hat{\mathbf{B}}^{\text{dis}}, \hat{\mathbf{B}}^{\text{cif}}, \hat{\mathbf{B}}^{\text{das}}, \hat{\mathbf{B}}^{\text{net}}) \right\}. \quad (2.77)$$

Finally, the notion of *backhaul-constrained capacity regions* was introduced in [MF08e]. These capacity regions are connected to a particular sum backhaul constraint, but implicitly allow time-sharing along the backhaul dimension. For any arbitrary cooperation scheme yz , we define the constrained rate region w.r.t. a sum backhaul of β as

$$\mathcal{R}_\beta^{yz} = \{ \mathbf{r} : \langle \mathbf{r}, \beta' \rangle \in \mathcal{Z}^{yz} \wedge \beta' \leq \beta \}. \quad (2.78)$$

Illustrations

Let us now show performance regions and constrained rate regions for exemplary uplink and downlink cooperation schemes. Figure 2.8 shows the performance region of DIS, CIF, FDM

or DAS-based cooperation in an uplink setup with $M = K = 2$ and $N_{\text{bs}} = 1$, again for the previous example channel $\mathbf{H} = [1, \sqrt{0.25}; \sqrt{0.5}, 1]$, $\sigma^2 = 0.1$ (hence SISO SNR = 10 dB) and $N_{\text{p}} = 2$. The specific cooperation schemes observed are

1. **DIS**, where either **a)** UE 1 is decoded by BS 1 and the bits then forwarded to BS 2 (meaning that power is only invested into messages $\hat{\mathcal{F}}_1 := \{\hat{F}_1^{1 \rightarrow 2}\}$ and $\hat{\mathcal{F}}_2 = \{\hat{F}_2^2\}$), or **b)** UE 2 is decoded by BS 2 and the bits then forwarded to BS 1 (using messages $\hat{\mathcal{F}}_1 = \{\hat{F}_1^1\}$ and $\hat{\mathcal{F}}_2 = \{\hat{F}_2^{2 \rightarrow 1}\}$).
2. **CIF**, where either **a)** UE 1 is decoded by BS 1 and the corresponding transmit sequence \hat{X}_1 then quantized and forwarded to BS 2 (employing messages $\hat{\mathcal{F}}_1 := \{\hat{F}_1^{1 \rightarrow 2}\}$ and $\hat{\mathcal{F}}_2 = \{\hat{F}_2^2\}$), or **b)** UE 2 is decoded by BS 2 and the corresponding transmit sequences then forwarded to BS 1 (with messages $\hat{\mathcal{F}}_1 = \{\hat{F}_1^1\}$ and $\hat{\mathcal{F}}_2 = \{\hat{F}_2^{2 \rightarrow 1}\}$).
3. **DAS**, where either **a)** BS 1 compresses and forwards all received signals to BS 2, where both UEs are decoded (employing $\hat{\mathcal{F}}_1 = \{\hat{F}_1^2\}$ and $\hat{\mathcal{F}}_2 = \{\hat{F}_2^2\}$), or **b)** BS 2 compresses and forwards all received signals to BS 1 (employing $\hat{\mathcal{F}}_1 = \{\hat{F}_1^1\}$ and $\hat{\mathcal{F}}_2 = \{\hat{F}_2^1\}$).
4. **DAS-enhanced FDM** scheme, where the two UEs transmit on orthogonal resources.

In this two-user-setup, we plot the rates of the UEs on the x- and y-axis, respectively, while we plot the required backhaul on the z-axis, where lower points mean more backhaul. The top surface of the performance region hence illustrates the capacity region of the UEs without BS cooperation, while the intersection of the performance region with the x-y plane approximates the capacity region for infinite BS cooperation. Note that we have here only considered BS cooperation schemes under practical considerations, hence without source coding concepts, and CIF and DAS concepts are based on the assumption of a practical quantizer. We can see that for the example channel, FDM schemes are beneficial in the regime of no or hardly any backhaul (as already suggested through Figure 2.3 in Section 2.2.4), DIS concepts are interesting for low backhaul, whereas DAS is the only scheme that provides spatial multiplexing gain and approaches the MAC region for a large extent of available backhaul. CIF is not visible at all, as it is always inferior to the other schemes in any parts of the performance region for this particular channel example.

For the same uplink cooperation schemes, Figure 2.9 now illustrates constrained capacity regions for a sum backhaul extent of $\beta = 2$. We compare these capacity regions to those for no ($\hat{\mathcal{R}}_0$) or infinite BS cooperation ($\hat{\mathcal{R}}_\infty$), as derived in Section 2.2.5. All four cooperation schemes are shown as areas, where the difference between the inner and outer bounds of the area emphasizes the difference between practical schemes and information theoretic limits. For DAS concepts, for instance, the outer bound of the area denotes the performance of the best known information theoretic scheme using source coding to exploit inter-BS signal correlation. The thick line within the area denotes operation on the rate/distortion bound, but without source coding, whereas the inner bound of the area corresponds to the performance of a practical quantizer, as introduced in Section 2.2.5. The same holds for all other compared approaches, except that for DIS, practical quantization is not applicable, and for this particular channel realization there is no benefit of source coding, as we will see later in Section 3.3.2.

For the downlink schemes introduced in Section 2.3.5, we show exemplary constrained rate regions in Figure 2.10, for the same channel matrix as before, imperfect CSI with $N_{\text{p}} = 2$, $N_{\text{b}} = 6$, and per-antenna power constraints with $\hat{\mathbf{P}}^{\text{max}} = \mathbf{I}$. We observe the following BS cooperation schemes, as before for a sum backhaul constraint of $\beta = 2$ bits/channel use:

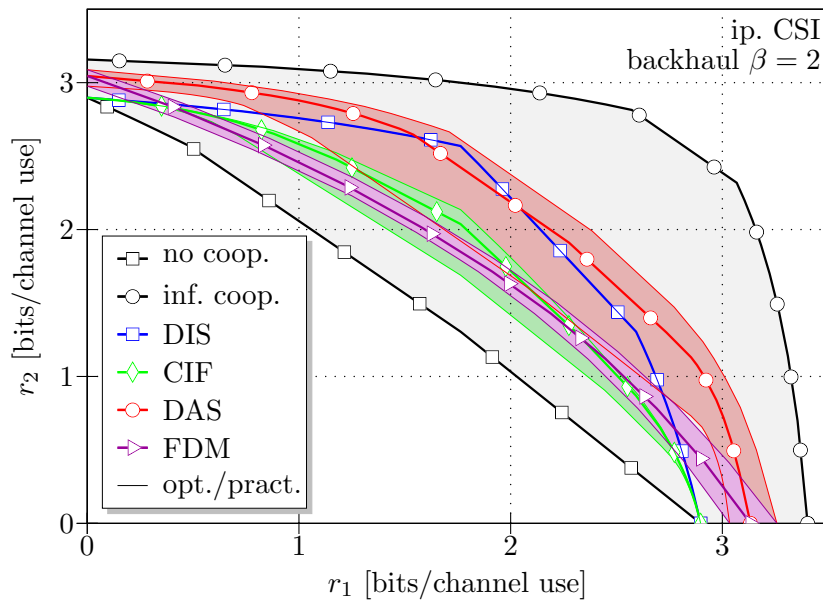
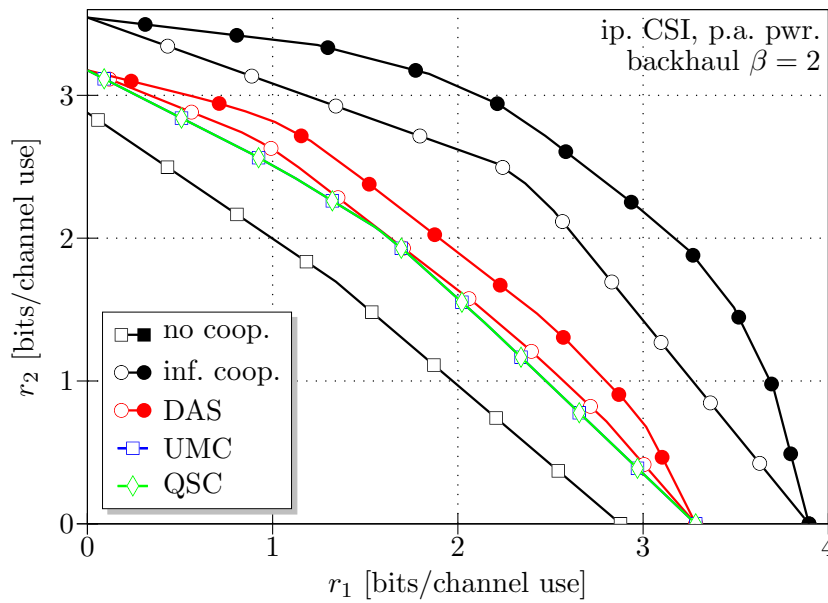


Figure 2.9: Backhaul-constrained uplink capacity region for different CoMP schemes.



Hollow \circ and filled \bullet markers denote linear precoding and DPC, respectively.

Figure 2.10: Backhaul-constrained downlink capacity region for different CoMP schemes.

1. **UMC**, where variable \mathbf{C} can take on values $\mathbf{C} \in \{[\infty, 0; 0, \infty], [\infty, \infty; 0, \infty], [\infty, 0; \infty, \infty], [\infty, \infty; \infty, \infty]\}$. Hence, we assume that each BS m is always supplied with the message connected to the UE with the same index $k = m$, and optionally with knowledge on the message targeted to the other UE.
2. **QSC**, where the intermediate variable \mathbf{C} can take on values $\mathbf{C} \in \{[\infty, \gamma; \delta, \infty]$, where $\gamma, \delta \in \mathbb{R}_0^+$ can take on arbitrary values. Hence, we assume that each BS m is always supplied with the message connected to the UE with the same index $k = m$, and optionally with quantized knowledge on the sequences targeted to the other UE.
3. **DAS**, where either BS 1 is supplied with the messages targeted to both UEs, performs DPC, and then forwards precoded and quantized signals to the other BS (hence $\mathbf{C} \in \{[\infty, \infty; \gamma, \gamma]\}$, where $\gamma \in \mathbb{R}_0^+$ can take on arbitrary values), or vice versa (with $\mathbf{C} \in \{[\gamma, \gamma; \infty, \infty]\}$).

For the considered UMC and QSC schemes, the required sum backhaul can be stated as $\beta(\mathbf{r}, \mathbf{B}^{\text{req}}(\mathbf{C})) = \min(c_{1,1}, c_{2,1}, r_1) + \min(c_{1,2}, c_{2,2}, r_2)$, from which we can see that the required backhaul (beyond that of a conventional, non-cooperative system) is at most $r_1 + r_2$, corresponding to our discussion before. For DAS, the required sum backhaul is given as $\beta(\mathbf{r}, \mathbf{B}^{\text{req}}(\mathbf{C})) = \min(c_{1,1}, c_{2,1}, c_{1,2}, c_{2,2})$. Note that for UMC and QSC schemes, we only consider linear precoding, as the performance of DPC would depend on the exact message knowledge at the different BSs, requiring the consideration of many more sub-cases, as done in [MF09a]. As this becomes highly tedious even for moderately sized scenarios, we will generally constrain ourselves to UMC and QSC schemes under linear precoding in this work.

In this example, it appears that DAS schemes are superior to UMC or QSC, but we will see in Section 3.4.2 that this is in fact rarely the case for $N_{\text{bs}} > 1$, as then DAS-based quantization becomes inefficient. UMC and QSC here perform equally, though we will see in Section 3.4.2 that QSC can gain ground over UMC schemes in regimes of very weak interference.

2.5 Summary

In this chapter, information theoretical models were derived to observe inner bounds on capacity regions under no, backhaul-constrained or infinite BS cooperation. The models take into consideration the detrimental impact of imperfect channel knowledge at base station and terminal side. A multitude of BS cooperation schemes was considered, and the concept of performance regions was introduced, which facilitate a comprehensive analysis of the rate/backhaul trade-offs achievable with these schemes.

One key finding in this chapter is that in both uplink and downlink, the impact of imperfect channel knowledge can be modeled as an additional noise term, which is the same for any employed BS cooperation scheme. We will see in the next chapter, however, that this narrows down the scenarios in which CoMP is attractive, hence rendering certain BS cooperation schemes more relevant than others.

A major contribution of this chapter was the statement of a general model for a large variety of downlink BS cooperation schemes that strongly facilitates achievable rate computation through the notion of uplink/downlink duality.

Chapter 3

Information-Theoretic Analysis

In this chapter, we investigate the performance of the CoMP schemes in uplink and downlink that were introduced in the last chapter through analytical and numerical analysis. We observe small and simplified scenarios, for which we derive basic, qualitative rules of how base stations should cooperate in order to optimize the rate/backhaul trade-off. The results reveal the potential gains of CoMP in uplink and downlink, the extent of backhaul required to obtain major portions of these gains, and the potential of improving the rate/backhaul trade-off by adaptively switching between different cooperation schemes according to the channel realization.

We will first define some general concepts in Sections 3.1 and 3.2, before analyzing the uplink and downlink in Sections 3.3 and 3.4, respectively. Both sections are concluded with a summary on the key findings.

3.1 Scenarios, Channels and Metrics Considered

We consider scenarios of either $M = K = 2$ or $M = K = 3$ BSs and UEs, which are reasonably easy to analyze, while the latter case already yields results that are also valuable for a system level observation of CoMP (see Chapter 4). The stated scenarios are illustrated in Figure 3.1, where we can see that for each UE $k \in \mathcal{K}$ a normalized BS-UE distance $0 \leq d_k \leq 1$ states whether the UE is closer to the BS with the same index $m = k$ (small value of d_k), at the cell edge between all involved BSs ($d_k = 0.5$), or even closer to other BSs than to BS $m = k$ ($d_k > 0.5$). We will later show plots where the performance of CoMP schemes is given as a function of these distance metrics, where we either observe

- symmetrical cases, where $d_1 = d_2$ and (for $M = K = 3$) $d_1 = d_2 = d_3$ or
- asymmetrical cases, where $d_1 = 0.8 - d_2$ and (for $M = K = 3$) $d_3 = 0.4$

We generally refer to $d_1 = d_2 = 0.3$ as a *cell-center* scenario, where the UEs are roughly in the middle between cell-edge and their BS. In the sequel, we denote with $\forall m \in \mathcal{M}, k \in \mathcal{K} : \lambda_{m,k}$ the linear path gain (in terms of power, not signal amplitude) between BS m and UE k . To compute these path gains as a function of the distance metrics d_k , we consider a simple flat-plane path loss model assuming omni-directional antennas, where the path loss is given as [PS95]

$$\text{PL}(d) = \theta \cdot 10 \cdot \log_{10} \left(\frac{d}{1\text{km}} \right) \quad [\text{dB}]. \quad (3.1)$$

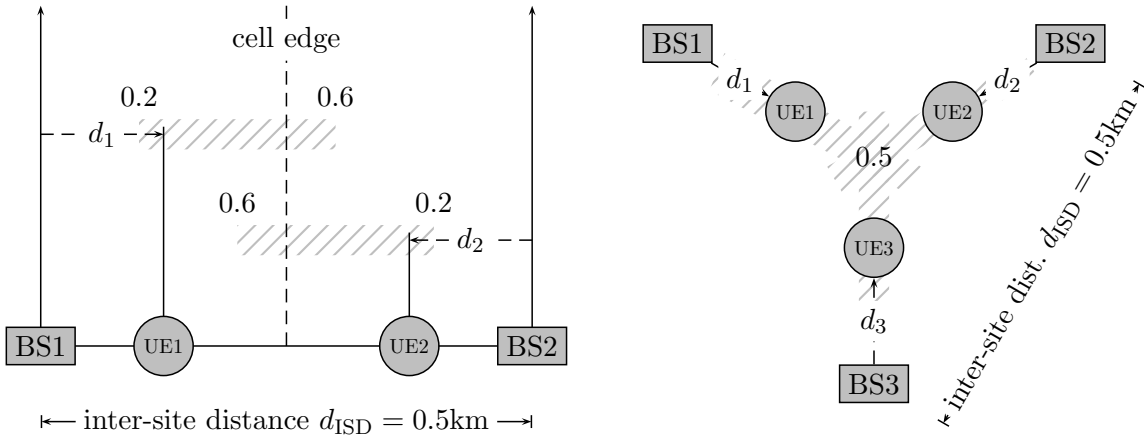


Figure 3.1: Scenarios considered in the uplink and downlink analysis in this chapter.

We use a path loss exponent of $\theta = 3.5$ in the remainder of this chapter, which is often used for the analysis of cellular systems with carrier frequencies around 2 GHz. The exact calculation of path gains $\lambda_{m,k}$ differs for uplink and downlink, and will be explained in the sequel.

3.1.1 Uplink

In the uplink of an LTE system, power control is applied, which means that UEs transmit in such a way that the receive power density at one single BS is constrained to within a certain region. We refer to this as *single-BS power control*. If the receive power is outside this region, the BSs send simple power control commands to the UEs to increase or decrease the transmit power, when necessary¹. Obviously, the maximum transmit power of a UE is limited, hence a UE in a deep fade might not be able to reach the target receive power density. For simplicity, we assume in this chapter that a UE can always achieve the receive power target, but will consider the power limitation in system level simulations in Chapter 4.

In this work, we furthermore observe *multi-cell power control* (mcpc.), where the transmit power of each UE is adjusted such that the *sum receive power density* at all observed BSs is controlled. We will see in Section 3.3.1 that this provides a more homogeneous performance regardless of the UE positions in conjunction with CoMP schemes.

In both cases, we model power control into the channel matrix, hence each channel column is scaled according to the assigned transmit power of the corresponding UE, assuming that the receive power target is exactly fulfilled. For our later analysis, we can then fix the (virtual) transmit power after channel normalization to $\hat{\mathbf{p}}^{\max} = \mathbf{1}_{[K \times 1]}$. For *single-BS power control*, we assume that the target receive power density is chosen such that each UE obtains a SISO SNR of 10 dB, a value which has been motivated through system level simulations in Chapter 4. Here, the noise component in the term SNR also contains the inter-cell interference generated

¹Note that the target receive power may be a function of the UE location, depending on an operator's exact implementation, but we assume here that the value is constant.

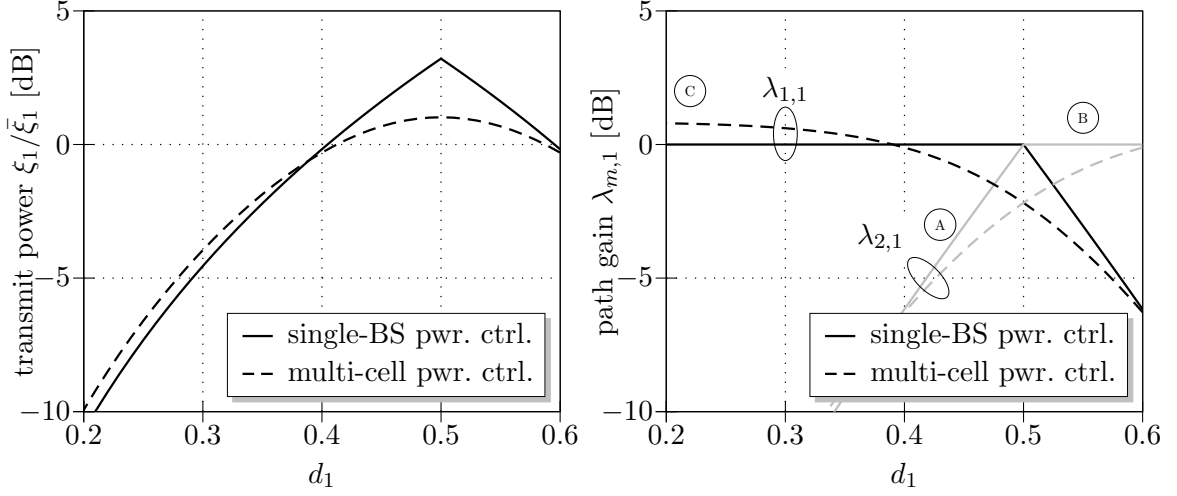


Figure 3.2: Uplink transmit power and path gain as a function of UE location.

by UEs outside the considered setup. Based on (3.1), we can now calculate the assigned transmit power ξ_k for each UE for $M = K = 2$ as

$$\forall k \in \{1, 2\} : \xi_k = \begin{cases} (\min(d_k, 1 - d_k) \cdot d_{\text{ISD}})^\theta & \text{single-BS pwr. ctrl.} \\ \chi_2 \cdot \left((d_k d_{\text{ISD}})^{-\theta} + ((1 - d_k) d_{\text{ISD}})^{-\theta} \right)^{-1} & \text{multi-cell pwr. ctrl.} \end{cases} \quad (3.2)$$

where $d_{\text{ISD}} = 0.5$ is the inter-site-distance (ISD) in km and θ the pathloss exponent introduced in Section 3.1. Obviously, the two different power control schemes as explained before differ not only in the assigned transmit power at a certain UE location d_k , but also in the *average* transmit power over all possible UE locations, such that we use the normalization factor χ_2 in (3.2) to ensure a fair comparison of both schemes. The factor is computed as

$$\chi_2 = 4 \cdot \int_0^{0.5} \frac{(d \cdot d_{\text{ISD}})^\theta}{\left((d \cdot d_{\text{ISD}})^{-\theta} + ((1 - d) d_{\text{ISD}})^{-\theta} \right)^{-1}} \cdot d \, dd \approx 1.21, \quad (3.3)$$

taking into consideration that, due to geometry, the probability that a UE is located at a certain distance $\min(d, 1 - d)$ from any BS increases proportionally to this distance. The corresponding path gains $\lambda_{m,k}$ can now be stated as

$$\forall k \in \{1, 2\} : \lambda_{k,k} = \xi_k \cdot (d_k d_{\text{ISD}})^{-\theta}, \quad \forall m, k \in \{1, 2\}, \quad m \neq k : \lambda_{m,k} = \xi_k \cdot ((1 - d_k) d_{\text{ISD}})^{-\theta}. \quad (3.4)$$

The impact of the two different power control schemes is illustrated in Figure 3.2, where the transmit power of UE 1 (normalized to its average transmit power $\bar{\xi}_1$ over the cell area) is shown as a function of its location d_1 in the left plot, and the resulting transmit-power-normalized path gain is shown in the right plot. For single-BS power control, we can see that for increasing d_1 , the path gain to BS 2 ($\lambda_{2,1}$) strongly increases (A). This is because not only the path loss decreases due to (3.1), but also the transmit power increases, as the UE becomes more distant to BS 1, to which the receive power is fixed. Beyond the cell edge ($d_1 \geq 0.5$), this path gain remains constant (B), as then the power control is performed w.r.t. BS 2, such

that the path loss is fully compensated. For multi-cell power control, the normalization factor χ_2 is visible close to the cell-center \odot , yielding a path gain of $10\log_{10}(1.21) \approx 0.8$ dB. For $M = K = 3$ and again a noise variance of $\sigma^2 = 0.1$, we state

$$\forall k \in \{1, 2, 3\} : \xi_k = \begin{cases} \left(\min(\bar{d}_k, \tilde{d}_k)\right)^\theta & \text{single-BS pwr. cntrl.} \\ \chi_3 \cdot \left(\bar{d}_k^{-\theta} + 2 \cdot \tilde{d}_k^{-\theta}\right)^{-1} & \text{multi-cell pwr. cntrl.} \end{cases} \quad (3.5)$$

where $\bar{d}_k = 2 \cdot \tan(\pi/6) \cdot d_{\text{ISD}} \cdot d_k$ is the distance from UE k to its BS with the same index $m = k$, and $\tilde{d}_k = \sqrt{(d_{\text{ISD}}/2)^2 + (\cos(\pi/6) \cdot d_{\text{ISD}} - \bar{d}_k)^2}$ is the distance from UE k to all BSs $m \neq k$. χ_3 is again a normalization factor ensuring a fair comparison of the power control schemes, calculated upon the same geometrical considerations as before as

$$\chi_3 = 4 \cdot \int_0^{0.5} \frac{\left(\min(\bar{d}_k, \tilde{d}_k)\right)^\theta}{\left(\bar{d}_k^{-\theta} + 2 \cdot \tilde{d}_k^{-\theta}\right)^{-1}} \cdot d \, dd \approx 1.48. \quad (3.6)$$

The path gains $\lambda_{m,k}$ are then given as

$$\forall k \in \{1, 2, 3\} : \lambda_{k,k} = \xi_k \cdot \bar{d}_k^{-\theta}, \quad \forall m, k \in \{1, 2, 3\}, m \neq k : \lambda_{m,k} = \xi_k \cdot \tilde{d}_k^{-\theta}. \quad (3.7)$$

3.1.2 Downlink

In the downlink, power control is typically not applied [McC07], hence we calculate the path gains directly from (3.1) without normalization w.r.t. assigned transmit power. We assume that the SISO SNR at the cell edge is 10 dB, which means that the thermal noise and the interference from outside the system of M cells that we are observing now is 10 dB weaker than the received signal if one of the BS antennas transmits at unit power. Again, the choice of SISO SNR at this point is motivated through system level observations in Chapter 4. For the case of $M = K = 2$, the stated SNR normalization at the cell edge given a noise variance of $\sigma^2 = 0.1$ and using (3.1) leads to

$$\forall k \in \{1, 2\} : \lambda_{k,k} = \left(\frac{0.5}{d_k}\right)^\theta, \quad \text{and} \quad \forall m, k \in \{1, 2\}, m \neq k : \lambda_{m,k} = \left(\frac{0.5}{1 - d_k}\right)^\theta, \quad (3.8)$$

due to the simple symmetry of the setup. For the case of $M = K = 3$, we can derive

$$\forall k \in \{1, 2, 3\} : \lambda_{k,k} = \left(\frac{0.5}{d_k}\right)^\theta, \quad \text{and} \\ \forall m, k \in \{1, 2, 3\}, m \neq k : \lambda_{m,k} = \left(\frac{\tan \frac{\pi}{6}}{\sqrt{\frac{1}{4} + (\cos \frac{\pi}{6} - d_k \cdot \tan \frac{\pi}{6})^2}}\right)^\theta. \quad (3.9)$$

Note that as long as we fix the cell-edge SNR, the path gains in both (3.8) and (3.9) are independent of the inter-site distance. The system level simulations, however, on which our assumptions here are based, used a specific inter-site distance of $d_{\text{ISD}} = 500$ m.

3.1.3 Channel Matrices

Based on the derived path gains, we now define representative channel matrices for both uplink and downlink as

$$\mathbf{H} = \begin{bmatrix} \sqrt{\lambda_{1,1}} & \sqrt{\lambda_{1,2}}e^{j(-\varphi_{Ab}/2-\varphi_{AB}/2)} \\ \sqrt{\lambda_{1,1}} & \sqrt{\lambda_{1,2}}e^{j(+\varphi_{Ab}/2-\varphi_{AB}/2)} \\ \sqrt{\lambda_{2,1}}e^{j(-\varphi_{Ba}/2-\varphi_{AB}/2)} & \sqrt{\lambda_{2,2}} \\ \sqrt{\lambda_{2,1}}e^{j(+\varphi_{Ba}/2-\varphi_{AB}/2)} & \sqrt{\lambda_{2,2}} \end{bmatrix} \quad (3.10)$$

for the case of $M = K = 2$, and

$$\mathbf{H} = \begin{bmatrix} \sqrt{\lambda_{1,1}} & \sqrt{\lambda_{1,2}}e^{j(-\varphi_{Ab}/2-\varphi_{AB}/2)} & \sqrt{\lambda_{1,3}}e^{-j(\varphi_{Ac}/2-\varphi_{AC}/2)} \\ \sqrt{\lambda_{1,1}} & \sqrt{\lambda_{1,2}}e^{j(+\varphi_{Ab}/2-\varphi_{AB}/2)} & \sqrt{\lambda_{1,3}}e^{j(+\varphi_{Ac}/2-\varphi_{AC}/2)} \\ \sqrt{\lambda_{2,1}}e^{j(-\varphi_{Ba}/2-\varphi_{AB}/2)} & \sqrt{\lambda_{2,2}} & \sqrt{\lambda_{2,3}}e^{j(-\varphi_{Bc}/2-\varphi_{BC}/2)} \\ \sqrt{\lambda_{2,1}}e^{j(+\varphi_{Ba}/2-\varphi_{AB}/2)} & \sqrt{\lambda_{2,2}} & \sqrt{\lambda_{2,3}}e^{j(+\varphi_{Bc}/2-\varphi_{BC}/2)} \\ \sqrt{\lambda_{3,1}}e^{j(-\varphi_{Ca}/2-\varphi_{AC}/2)} & \sqrt{\lambda_{3,2}}e^{j(-\varphi_{Cb}/2-\varphi_{BC}/2)} & \sqrt{\lambda_{3,3}} \\ \sqrt{\lambda_{3,1}}e^{j(+\varphi_{Ca}/2-\varphi_{AC}/2)} & \sqrt{\lambda_{3,2}}e^{j(+\varphi_{Cb}/2-\varphi_{BC}/2)} & \sqrt{\lambda_{3,3}} \end{bmatrix} \quad (3.11)$$

for $M = K = 3$, in both cases for $N_{\text{bs}} = 2$. Angles φ_{Ab} and φ_{Ba} (and for $M = K = 3$ also φ_{Ac} , φ_{Ca} , φ_{Bc} and φ_{Cb}) are connected to the orthogonality of the channel as seen by BSs 1 and 2, respectively, hence they are a measure for the capability of the BSs to spatially separate the UEs without BS cooperation. Angles φ_{AB} , φ_{BC} and φ_{AC} are measures for the orthogonality of the joint channel between two BSs, hence for the additional spatial multiplexing gain that cooperation between these two BSs can yield. Note that other authors use the *orthogonality defect* [MG02] of a channel as a measure, but this does not enable such an illustrative differentiation of local and compound orthogonality. As in our simplified channel matrices the links from the two antennas of a BS to any UE have equal path gain, we have removed additional degrees of freedom, and *per-antenna* power constraints in the sequel in fact correspond to *per-BS* power constraints. Still, we believe that we have captured the most important aspects connected to a channel realization in a strongly limited set of parameters. An extension of the conclusions in the next sections to larger scenarios will be discussed in Section 5.3.

3.1.4 Sum Rate and Common Rate

In both the uplink and downlink analysis, we will not observe complete constrained rate regions as before in Chapter 2, but consider the point of operation (e.g. a power allocation, certain cooperation strategy or possibly a time-share between strategies) where either the *sum rate* or the *common rate* of the involved UEs is maximized for a given sum backhaul β . These quantities are written as

$$f_s(\mathcal{R}_\beta) = \max_{\mathbf{r} \in \mathcal{R}_\beta} \mathbf{r}^T \mathbf{1} \quad \text{and} \quad f_c(\mathcal{R}_\beta) = \max_{\mathbf{r} \in \mathcal{R}_\beta} \min_{k \in \mathcal{K}} r_k, \quad (3.12)$$

respectively, where \mathcal{R}_β is the K -user backhaul-constrained capacity region of the cooperation scheme under observation. Obviously, optimizing the sum rate can cause certain UEs to have bad (or zero) rates, but we will see later in Chapter 4 that scheduling can be used to obtain long-term fairness. Optimizing the common rate provides instantaneous fairness in each channel access, which might be necessary for particular applications. As we consider both extremes, we can extend our conclusions to any arbitrary optimization metric an operator might chose in between.

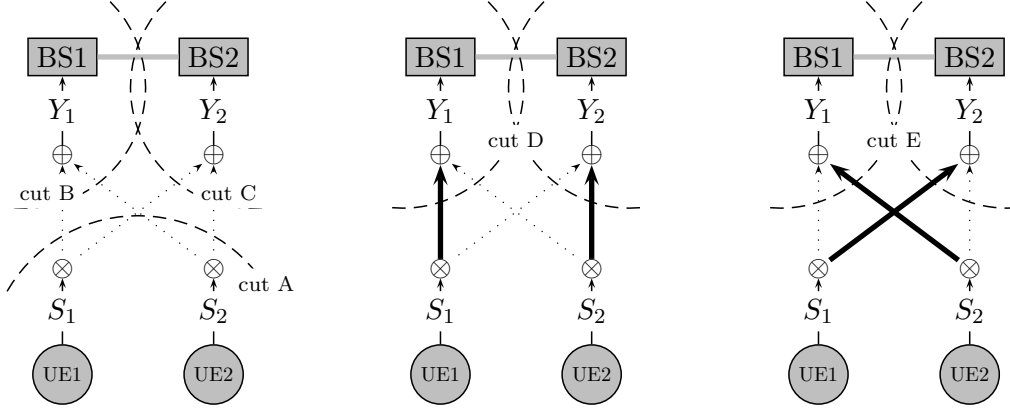


Figure 3.3: Illustration of the cut-set bound.

3.2 Cut-Set Bound

In the next sections, we will also make use of the *cut-set bound* [CT06] as an upper-bound on the rate/backhaul trade-off achievable with any CoMP scheme. This basically states that an achievable sum rate is upper-bounded through two constraints, which we want to explain for the uplink here. An extension to the downlink is then straightforward.

On one hand, the sum rate in the uplink can obviously not exceed MAC performance, i.e. the performance achievable with infinite BS cooperation. On the other hand, the sum rate achievable given a certain extent of sum backhaul β cannot be larger than the sum rate without cooperation *plus* the backhaul β provided. This would be the case where each bit of backhaul results in one bit of sum rate increase. While this is intuitive and easy to describe in such a way, a mathematical notation and illustration of the cut-set bound as done in [CT06] is slightly more involved, as we have to consider different possible decoding strategies. For a scenario with $M = K = 2$, we can upper-bound the sum rate r_{sum} of the two UEs as

$$r_{\text{sum}} \leq I(S_1, S_2; Y_1, Y_2) \quad (\text{cut A, MAC bound}) \quad (3.13)$$

$$r_{\text{sum}} \leq \max(\nu_{1,2 \rightarrow 1}, \nu_{1,2 \rightarrow 2}, \nu_{1 \rightarrow 1,2 \rightarrow 2}, \nu_{1 \rightarrow 2,2 \rightarrow 1}) \quad \text{where} \quad (3.14)$$

$$\nu_{1,2 \rightarrow 1} \leq I(S_1, S_2; Y_1) + \beta \quad (\text{cut B}) \quad (3.15)$$

$$\nu_{1,2 \rightarrow 2} \leq I(S_1, S_2; Y_2) + \beta \quad (\text{cut C}) \quad (3.16)$$

$$\nu_{1 \rightarrow 1,2 \rightarrow 2} \leq I(S_1; Y_1) + I(S_2; Y_2) + \beta \quad (\text{cut D}) \quad (3.17)$$

$$\nu_{1 \rightarrow 2,2 \rightarrow 1} \leq I(S_1; Y_2) + I(S_2; Y_1) + \beta \quad (\text{cut E}). \quad (3.18)$$

Clearly, the constraint given through (3.13) is the MAC bound, stating the sum rate achievable if both BSs jointly decode both UEs under infinite backhaul. The second bound in (3.14) is connected to the backhaul, and is defined by the best of four different decoding strategies. In (3.15), BS 1 aims at decoding both UEs, where the sum rate is limited by the mutual information between BS 1 and both UEs *plus* the backhaul rate. Note that this is based on the assumption that the information passed over the backhaul is uncorrelated from the received signals at BS 1, which is possible in theory if source coding concepts are employed. Equation (3.16) states a sum rate bound for the case that BS 2 performs the decoding.

Equations (3.17) and (3.16) finally capture the cases where each BS decodes exactly one UE, and both share the backhaul for assisting each other in the decoding process. Each of the five bounds stated above corresponds to a certain information flow in the CoMP setup. Using the concept of *max-flow min-cut* [FF62], we can hence express the cut-set bound as

$$r_{\text{sum}} = \min(\text{cut A}, \max(\text{cut B}, \text{cut C}, \text{cut D}, \text{cut E})), \quad (3.19)$$

where the cuts are illustrated in Figure 3.3. Note that the authors in [dCS08, dS08] also define a cut-set bound for backhaul-constrained CoMP, but only consider centralized decoding concepts at a fixed BS. In their model, the cut-set bound hence reduces to $\min(\text{cut A}, \text{cut B})$.

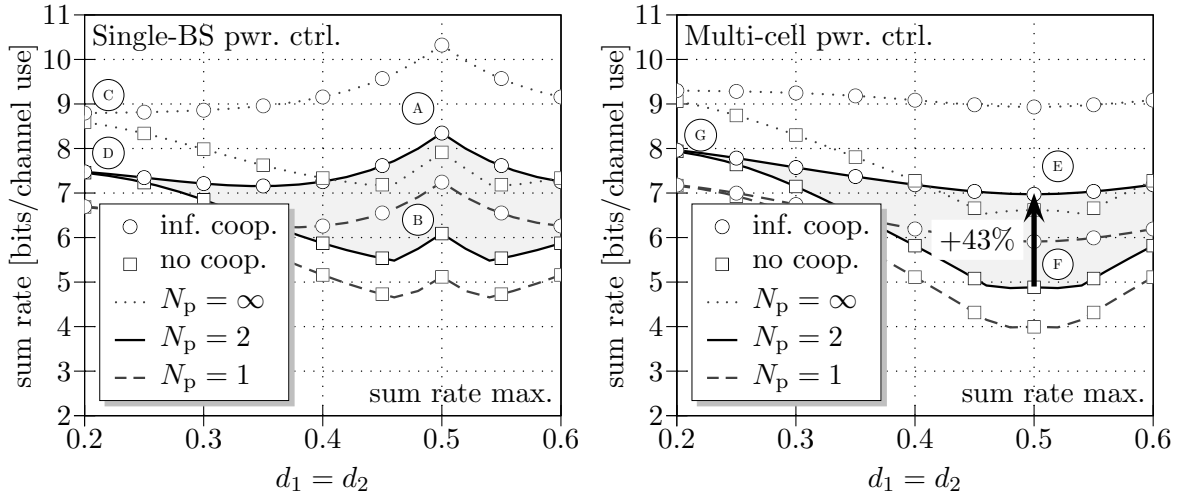
3.3 Uplink Analysis

We will now investigate the uplink CoMP schemes introduced in Section 2.2.5 in detail. Specifically, we want to find answers to the questions

- Which CoMP gains can generally be expected in the scenarios observed, and how do these gains depend on CSIR and on the pathloss exponent? → see Section 3.3.1
- How do uplink CoMP schemes introduced in the last chapter perform in different channel scenarios? → see Section 3.3.2
- How large is the benefit of exploiting inter-BS signal correlation through source coding concepts, or using superposition coding at the UE side? → see Section 3.3.3
- What is the gain of using iterative BS cooperation concepts? → see Section 3.3.4
- Does it make sense to adaptively switch between different cooperation concepts? If yes, on which thresholds should this adaptation be based? → see Section 3.3.5
- To which extent are the schemes affected by the channel orthogonality or background noise level? → see Section 3.3.6
- How do the schemes perform in scenarios with $M = K = 3$, and what is the benefit of combining different BS cooperation schemes in such setups? → see Section 3.3.7

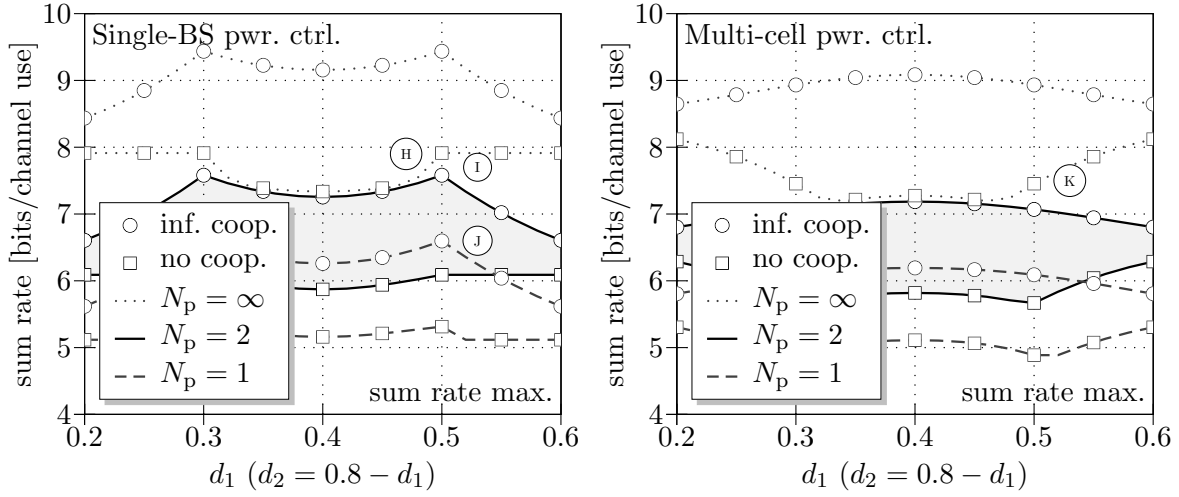
3.3.1 Capacity Gains through CoMP in the Uplink

In this section, we want to analyze the potential capacity gains possible through CoMP in the uplink, in order to later focus our attention on those scenarios where the largest gains are expectable. Figure 3.4 shows lower bounds on sum rates achievable with no or infinite BS cooperation, based on (2.17) and (2.11) from Sections 2.2.4 and 2.2.3, respectively. Note that we do not consider superposition coding at this point, as we will do this separately in Section 3.3.3. We here hence assume that each UE $k \in \mathcal{K}$ invests its transmit power completely into one message \hat{F}_k . As stated in Section 3.1.1, we consider a SISO SNR of 10 dB on the main UE-BS links (i.e. $\hat{\mathbf{P}}^{\text{max}} = \mathbf{I}$ and $\sigma^2 = 0.1$, as single-BS power control from (3.4) normalizes the links to unit gain). We furthermore consider the case of perfect CSI, or two different cases of imperfect CSI, with $N_p = 1$ or $N_p = 2$, where the latter value corresponds to observations in Appendix E. The left plots are based on single-BS power



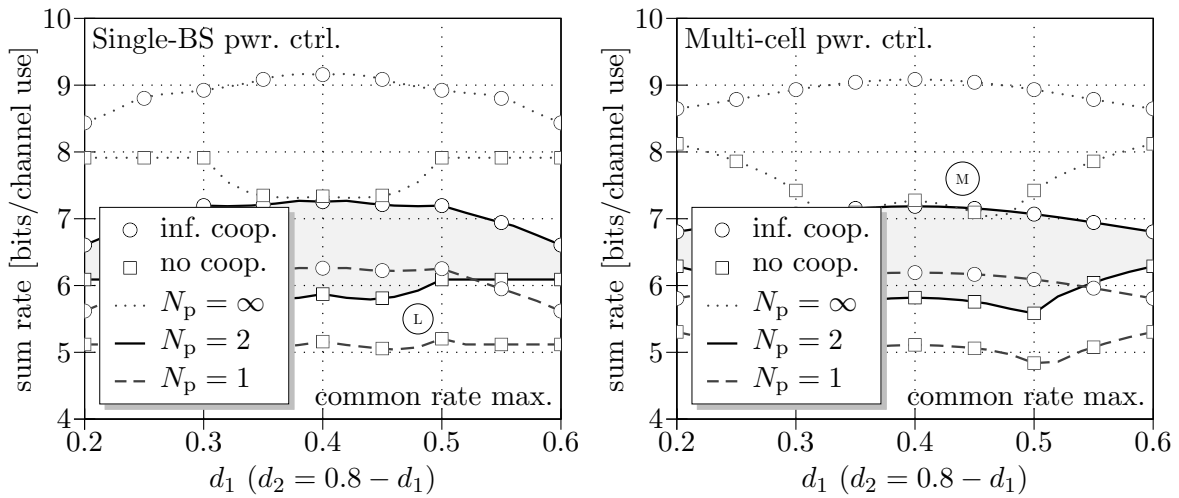
(a) Symmetrical interference, sum rate maximized.

(b) Symmetrical interference, sum rate maximized.



(c) Asymmetrical interference, sum rate maximized.

(d) Asymmetrical interference, sum rate maximized.



(e) Asymmetrical interf., common rate maximized.

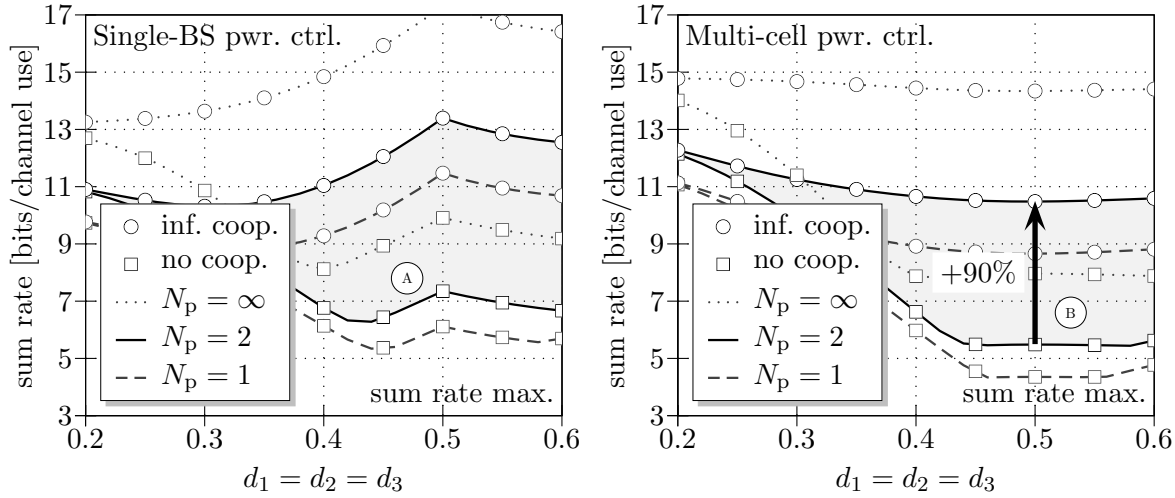
(f) Asymmetrical interf., common rate maximized.

Figure 3.4: CoMP gain in uplink scenarios with $M = K = 2$ of average orthogonality.

control, the right plots on the multi-cell power control described in Section 3.1. The upper two plots consider a symmetrical channel with $d_1 = d_2$, all other plots an asymmetrical channel with $d_1 = 0.8 - d_2$. We pursue a maximization of the UE *sum rate*, i.e. we observe $f_s(\hat{\mathcal{R}}_\infty)$, $f_s(\hat{\mathcal{R}}_0)$, except for the lower two plots, where the *common rate* is maximized ($f_c(\hat{\mathcal{R}}_\infty)$, $f_c(\hat{\mathcal{R}}_0)$). For all plots, a channel matrix corresponding to (3.10) has been used with moderate orthogonality, i.e. $\varphi_{Ab} = \varphi_{Ba} = \varphi_{AB} = \pi/2$. Such exemplary channel matrices allow us to illustrate certain aspects better than e.g. Monte-Carlo simulation results, but we have also performed such simulations to verify that the chosen angles do indeed represent channels of average orthogonality (not shown here).

We first want to observe to which extent the sum rate of the UEs change depending on the UE locations. Clearly, under single-BS power control, the power level at which a UE is received by its dominant BS remains constant, while the extent of interference increases towards the cell-edge. Under infinite BS cooperation, we can now identify two phenomena: On one hand, rates tend to decrease towards the cell-edge, as a growing extent of interference can not be canceled. This effect is especially pronounced if the compound channel orthogonality is low, i.e. φ_{Ab} , φ_{Ba} , φ_{AB} are small. On the other hand, array gain increases in this regime of interference. For our example of moderate channel orthogonality, the latter effect is dominant, hence the UE sum rate increases towards the cell-edge $\textcircled{\text{A}}$. Without BS cooperation, non-cancelable interference generally lets the UE rates decrease towards the cell-edge, especially for low φ_{Ab} , φ_{Ba} . A small performance peak, however, can be observed at the cell-edge $\textcircled{\text{B}}$, which is the regime where it is beneficial to let one BS decode both UEs, applying SIC. This effect is most prominent if $\max(\varphi_{Ab}, \varphi_{Ba})$ is low, hence if none of the BSs is able to spatially separate the UEs well with linear detection. Considering the observations made before for both infinite and no BS cooperation, we can see that the relative gain of BS cooperation is typically largest at the cell-edge [KRF07]. An exception are cases where the compound channel has a major orthogonality defect, e.g. for $\varphi_{Ab} = \varphi_{Ba} = \varphi_{AB} = \pi/4$, which will be shown later in Figure 3.12. An aspect not captured by our current observations is that cell-edge scenarios also yield the largest diversity gain [SSZ04]. Regardless of the channel orthogonality, cooperation yields only marginal benefit if both UEs are located in their cell-center $\textcircled{\text{C}}$, where this gain reduces further under imperfect channel knowledge $\textcircled{\text{D}}$. Here, the weak interference links are not only of little importance, but also subject to a major estimation error.

Under *multi-cell* power control, the sum rate under infinite BS cooperation in fact drops at the cell-edge $\textcircled{\text{E}}$, as power-control compensates for the potential array gain. The non-cooperative performance suffers equally at this point $\textcircled{\text{F}}$, as the UEs obtain 3 dB less power than in the conventional power control case. Here, even SIC-decoding of both UEs by one BS can hardly improve performance, as a weak SNR is the main problem. The better asymptotic performance for the interference-free cell-center case $\textcircled{\text{G}}$ than under single-BS power control is due to transmit power normalization. For asymmetrical channels and single-BS power control, the sum rate increases when the asymmetry increases $\textcircled{\text{H}}$, but decreases beyond the point $d_1 \geq 0.5$, where both UEs are closer to the same BS and SIC decoding by this BS is preferable $\textcircled{\text{I}}$. Non-cooperative performance clearly remains the same beyond $d_1 \geq 0.5$ $\textcircled{\text{J}}$, as the path gain to the dominant BS remains constant. For multi-cell power control, the effects noticed before are shifted in favor of cell-center UEs, enabling a similar performance over all UE locations $\textcircled{\text{K}}$. We can see that there is marginal difference between maximizing the *sum rate* or the *common rate* in the uplink, as power control compensates for a UE's path loss disadvantages. We will hence focus on maximizing sum rates in the remainder of this section.



(a) Symmetrical interference, sum rate maximized. (b) Symmetrical interference, sum rate maximized.

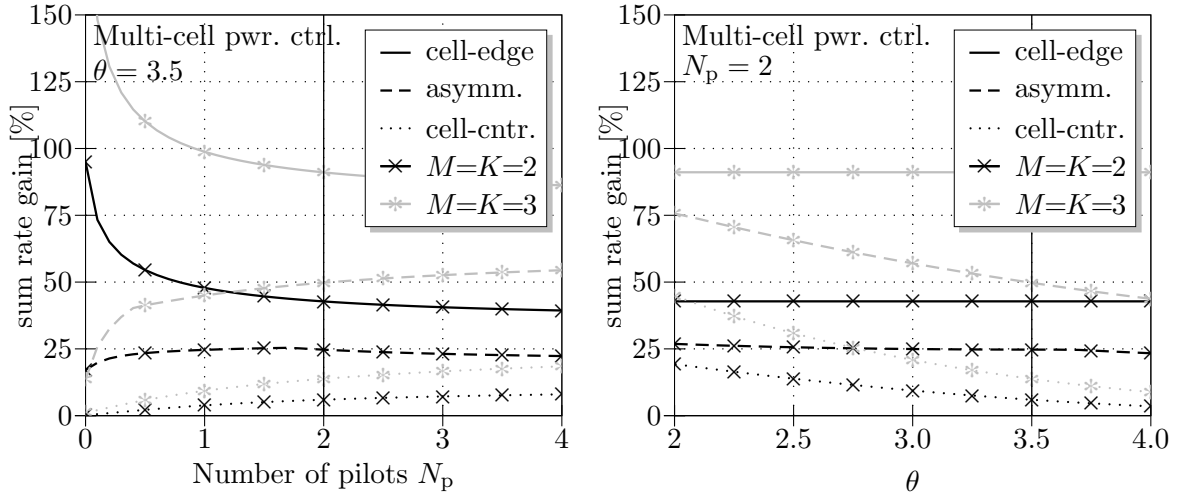
Figure 3.5: CoMP gain in uplink scenarios with $M = K = 3$ of average orthogonality.

Clearly, single-BS power control leads to good fairness without BS cooperation \textcircled{L} , whereas multi-cell power control improves fairness under infinite BS cooperation \textcircled{M} .

In Figure 3.5, we show the gain of BS cooperation for a larger scenario with $M = K = 3$, again for a moderately orthogonal channel, in this case with $\varphi_{Ac} = \varphi_{Ba} = \varphi_{Cb} = 3/4\pi$, $\varphi_{Ab} = \varphi_{Bc} = \varphi_{Ca} = 3/2\pi$ and $\varphi_{AB} = \varphi_{BC} = \varphi_{AC} = \pi/2$. Now, the cooperation gains are significantly larger, as each BS by itself does not have enough receive antennas to spatially separate all three UEs. As in the two-cell case, the non-cooperative performance generally decreases when the UEs are moved towards the cell-edge, except for a slight increase for $d \geq 0.45$ \textcircled{A} , where local SIC is applied to (at least) two of the three UEs here. With multi-cell power control, the decreased SINR at the cell-edge again renders SIC less attractive, leading to a flat performance \textcircled{B} . Note that the results for $d_1 = d_2 = d_3$ are now not symmetrical around $d_i = 0.5$, as moving a UE beyond the cell-edge means that it is moved *in between* the two other BSs, as shown in Figure 3.1(a). All other observations, e.g. considering common rate maximization, are similar to the two-cell case and hence not repeated here. In general, multi-cell power control appears to be the desirable choice when BS cooperation is enabled, offering a more homogeneous performance over the cell area. In addition, it leads to the fact that radiated power is shifted towards cell centers, where it is less harmful to adjacent cells.

Impact of Imperfect CSIR and Pathloss Exponent

While Figures 3.4 and 3.5 reveal a large drop in capacity if channel knowledge is erroneous, we can observe that the *relative* sum rate gain of CoMP at the cell-edge even increases when CSI is less accurate. This is shown in Figure 3.6(a), where the CoMP gain is plotted for cell-edge ($d_1 = d_2 = d_3 = 0.5$), asymmetrical ($d_1 = 0.3, d_2 = 0.5, d_3 = 0.4$) and cell-center ($d_1 = d_2 = d_3 = 0.3$) scenarios as a function of N_p . The gain increase at the cell-edge can be explained through the fact that BS cooperation alleviates the impact of imperfect CSI through multi-path array gain. In other words, using more BS antennas for UE detection (with uncorrelated channel estimation errors) makes the detection process more robust against



(a) Symmetrical interference, sum rate maximized. (b) Symmetrical interference, sum rate maximized.

Figure 3.6: Impact of imperfect CSIR and pathloss exponent on uplink CoMP.

these errors. Towards the cell-center, however, BS cooperation gains decrease with less CSI, as then the estimation of the interference links becomes too erroneous to provide any benefit.

Figure 3.6(b) finally shows the BS cooperation gain as a function of pathloss exponent θ . Obviously, the gain at the cell-edge is independent of θ , as our model normalizes the SINR at this point to a constant value (see (3.2) and (3.5)). In the other cases, the cooperation gain strongly decreases for an increasing pathloss exponent, as then the inter-cell interference becomes insignificant. Let us conclude that

- Significant capacity gains are possible through uplink CoMP, especially at the cell-edge, where we can achieve rate improvements of +43% in a two-cell setup, or +90% in a three-cell setup, in both cases based on a channel of average orthogonality.
- The CoMP gains strongly decrease towards the cell-center, in particular under imperfect CSIR, as then the weak interference links cannot be exploited.
- The relative gains of CoMP at the cell-edge, however, increase for a decreasing extent of CSIR, as jointly using the receive antennas of both BSs yields array gain.

We will analyze the sensitivity of achievable sum rates to, e.g. the channel orthogonality or SNR in Section 3.3.6.

3.3.2 Performance of Uplink CoMP Schemes for Specific Channels

We will now analyze the performance of the uplink BS cooperation schemes introduced in Section 2.2.5 for a setup with $M = K = 2$ and $N_{bs} = 2$ under a sum backhaul constraint, where it is possible to strongly simplify the models derived in Section 2.2.5. The antenna configuration is the base-line setup considered for LTE [McC07]. Clearly, one could argue that $K = 4$ UEs could be served on the same resource, as $N_{BS} = 4$ BS antennas are available, but this would render an analysis complex. We will, however, discuss the extension of our observations to setups with more UEs in Section 5.3.1. For now, we will initially consider cooperation

schemes with *one phase of information exchange* between BSs, corresponding to our model in Section 2.2.5, and look into *iterative* BS cooperation schemes later in Section 3.3.4.

Distributed Interference Subtraction (DIS)

A pure DIS scheme in a scenario of two cells implies that each BS aims at decoding exactly one UE. If only one phase of information exchange is possible, this means that one of the BSs decodes the transmission connected to one of the UEs and forwards the decoded data to the other BS, such that this can decode the other UE under a lesser extent of interference. The degrees of freedom in the role of the BSs and the assignment of UEs to BSs give us 4 possible modes of BS cooperation, which have to be jointly considered, as an optimal operation point might be a time-share thereof. Without loss of generality, we now constrain ourselves to one of these possibilities, and assume that UE 1 transmits a superposition of two messages \hat{F}_1^1 and $\hat{F}_1^{1 \rightarrow 2}$, mapped onto sequences \hat{X}_1^1 and $\hat{X}_1^{1 \rightarrow 2}$. Both messages are decoded by BS 1, after which message $\hat{F}_1^{1 \rightarrow 2}$ is forwarded to BS 2, as illustrated in Figure 3.10(a). As we know from Section 2.2.5, source coding can optionally be applied to exploit side-information at the DIS-receiving BS. The concept of superposition coding here allows us to adjust the rate/backhaul trade-off. We will see in Section 3.3.3, however, that a gain over simple schemes, where the complete transmission of UE 1 is decoded and forwarded to BS 2 (i.e. message \hat{F}_1^1 is assigned zero power), only exists for weak interference and very low backhaul [SSPS08b, SSPS09b]. For a given power allocation $\mathcal{P} = \{\rho_{\hat{F}_1^1}, \rho_{\hat{F}_1^{1 \rightarrow 2}}, \rho_{\hat{F}_2^2}\}$ and a sum backhaul β , the rate expressions from Theorem 2.2.5 can now be simplified such that we obtain an inner bound on the capacity region as all $\mathbf{r} \in \hat{\mathcal{R}}^{\text{dis}}(\mathcal{P}, \beta)$ that fulfill $\forall k \in \{1, 2\} : r_k \geq 0$ and

$$\begin{aligned}
 r_1 &\leq \nu_{\hat{F}_1^1} + \nu_{\hat{F}_1^{1 \rightarrow 2}} & (3.20) \\
 \nu_{\hat{F}_1^1} &\leq \log_2 \left| \mathbf{I} + \left(\sigma^2 \mathbf{I} + \mathbf{\Phi}_1^{\text{hh}} + \mathbf{H}_1^e \mathbf{P} \left(\hat{F}_2^2 \right) \left(\mathbf{H}_1^e \right)^H \right)^{-1} \mathbf{H}_1^e \mathbf{P} \left(\hat{F}_1^1 \right) \left(\mathbf{H}_1^e \right)^H \right| \\
 \nu_{\hat{F}_1^{1 \rightarrow 2}} &\leq \log_2 \left| \mathbf{I} + \left(\sigma^2 \mathbf{I} + \mathbf{\Phi}_1^{\text{hh}} + \mathbf{H}_1^e \mathbf{P} \left(\left\{ \hat{F}_1^1, \hat{F}_2^2 \right\} \right) \left(\mathbf{H}_1^e \right)^H \right)^{-1} \mathbf{H}_1^e \mathbf{P} \left(\hat{F}_1^{1 \rightarrow 2} \right) \left(\mathbf{H}_1^e \right)^H \right| \\
 \nu_{\hat{F}_1^{1 \rightarrow 2}} &\leq \underbrace{\beta + \log_2 \left| \mathbf{I} + \left(\sigma^2 \mathbf{I} + \mathbf{\Phi}_2^{\text{hh}} + \mathbf{H}_2^e \mathbf{P} \left(\left\{ \hat{F}_1^1, \hat{F}_2^2 \right\} \right) \left(\mathbf{H}_2^e \right)^H \right)^{-1} \mathbf{H}_2^e \mathbf{P} \left(\hat{F}_1^{1 \rightarrow 2} \right) \left(\mathbf{H}_2^e \right)^H \right|}_{=0 \text{ without Slepian-Wolf source coding}} \\
 r_2 &\leq \log_2 \left| \mathbf{I} + \left(\sigma^2 \mathbf{I} + \mathbf{\Phi}_2^{\text{hh}} + \mathbf{H}_2^e \mathbf{P} \left(\hat{F}_1^1 \right) \left(\mathbf{H}_2^e \right)^H \right)^{-1} \mathbf{H}_2^e \mathbf{P} \left(\hat{F}_2^2 \right) \left(\mathbf{H}_2^e \right)^H \right|,
 \end{aligned}$$

where $\mathbf{\Phi}_1^{\text{hh}}$ and $\mathbf{\Phi}_2^{\text{hh}}$ are channel estimation related noise covariances connected to BS 1 and 2, respectively, as defined in (2.9). We can see that the rate of UE 1 is the sum of the rates of the two superimposed messages. The rate of the first message $\hat{F}_1^{1 \rightarrow 2}$ is constrained on one hand through the fact that it has to be decoded by BS 1 (suffering from the interference from messages \hat{F}_1^1 and \hat{F}_2^2), and on the other hand by the rate of the backhaul plus the rate at which it could be decoded by BS 2 without cooperation. Message \hat{F}_2^2 can then be decoded free of interference from UE 1. Note that the decoding order at BS 1 is important, i.e. the forwarded message has to be decoded first such that its rate is low compared to the extent of interference power it represents. The performance region for this simplified DIS setup is then given as $\hat{\mathcal{Z}}^{\text{dis}} = \bigcup \{ \langle \mathbf{r}, \beta \rangle : \mathbf{r} \in \hat{\mathcal{R}}^{\text{dis}}(\mathcal{P}, \beta) \}$, where the convex hull is taken over all BS-UE assignments, cooperation directions, power allocations, and extents of backhaul β .

Compressed Interference Forwarding (CIF)

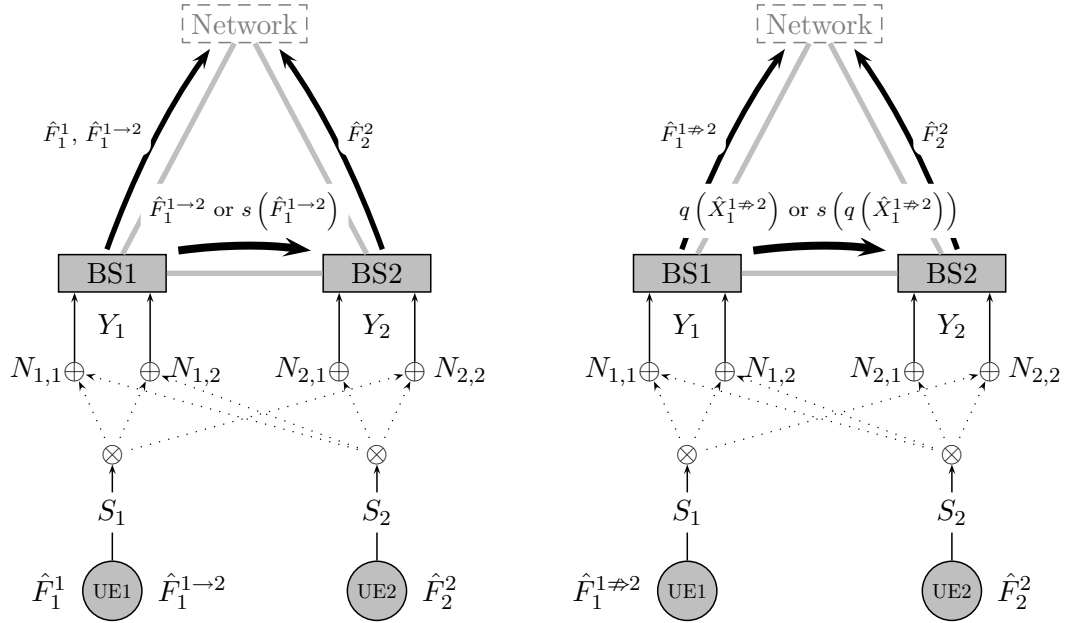
CIF is similar to DIS in the way that both BSs aim at decoding their UE individually, while one BS offers the other BS a certain extent of interference subtraction. In this case, however, the BSs exchange *quantized transmit sequences* instead of decoded messages. Using CIF schemes, the rate/backhaul operation point can be adjusted through choosing an appropriate degree of quantization, rather than using superposition, as in the case of DIS. This renders CIF more suitable for practical implementation. It hence suffices if the UEs transmit messages $\hat{F}_1^{1\neq 2}$ and \hat{F}_2^2 , respectively, mapped to $\hat{X}_1^{1\neq 2}$ and \hat{X}_2^2 , as depicted in Figure 3.7(b). Having the same degrees of freedom as in DIS, we again constrain ourselves to one cooperation case, where BS 1 decodes message $\hat{F}_1^{1\neq 2}$, calculates the originally transmitted sequence $\hat{X}_1^{1\neq 2} = \sqrt{\rho_{\hat{F}_1^{1\neq 2}}}e^{j\hat{F}_1^{1\neq 2}}$ and forwards a quantized version $q(\hat{X}_1^{1\neq 2})$ of this sequence to BS 2. Optionally, a source-encoded version $s(q(\hat{X}_1^{1\neq 2}))$ can be forwarded, exploiting side-information at BS 2. The latter BS then reconstructs $q(\hat{X}_1^{1\neq 2})$ and computes a version of its received signals $\tilde{Y}_2 = Y_2 - \mathbf{h}_{2,1}^e q(\hat{X}_1^{1\neq 2})$ with a reduced extent of interference from UE 1, after which message \hat{F}_2^2 can finally be decoded. An achievable rate region for a fixed power allocation $\mathcal{P} = \{\rho_{\hat{F}_1^{1\neq 2}}, \rho_{\hat{F}_2^2}\}$ and sum backhaul β can be simplified from Theorem 2.2.5 to all rates $\mathbf{r} \in \hat{\mathcal{R}}^{\text{cif}}(\mathcal{P}, \beta)$ with $\forall k \in \{1, 2\} : r_k \geq 0$ and

$$\begin{aligned}
 r_1 &\leq \log_2 \left| \mathbf{I} + \left(\sigma^2 \mathbf{I} + \mathbf{\Phi}_1^{\text{hh}} + \mathbf{H}_1^e \mathbf{P} \left(\hat{F}_2^2 \right) \left(\mathbf{H}_1^e \right)^H \right)^{-1} \mathbf{H}_1^e \mathbf{P} \left(\hat{F}_1^{1\neq 2} \right) \left(\mathbf{H}_1^e \right)^H \right| & (3.21) \\
 r_2 &\leq \log_2 \left| \mathbf{I} + \left(\sigma^2 \mathbf{I} + \mathbf{\Phi}_2^{\text{hh}} + \mathbf{H}_{2,1}^e \xi_{\hat{F}_1^{1\neq 2}} \left(\mathbf{H}_{2,1}^e \right)^H \right)^{-1} \mathbf{H}_2^e \mathbf{P} \left(\hat{F}_2^2 \right) \left(\mathbf{H}_2^e \right)^H \right| \\
 \xi_{\hat{F}_1^{1\neq 2}} &\geq \underbrace{\frac{\rho_{\hat{F}_1^{1\neq 2}} \left(1 + \rho_{\hat{F}_1^{1\neq 2}} \left(\mathbf{h}_{2,1}^e \right)^H \left(\sigma^2 \mathbf{I} + \mathbf{\Phi}_2^{\text{hh}} + \mathbf{H}_2^e \mathbf{P} \left(\hat{F}_2^2 \right) \left(\mathbf{H}_2^e \right)^H \right)^{-1} \mathbf{h}_{2,1}^e \right)^{-1}}{2^{\beta-1} + \left(1 + \rho_{\hat{F}_1^{1\neq 2}} \left(\mathbf{h}_{2,1}^e \right)^H \left(\sigma^2 \mathbf{I} + \mathbf{\Phi}_2^{\text{hh}} + \mathbf{H}_2^e \mathbf{P} \left(\hat{F}_2^2 \right) \left(\mathbf{H}_2^e \right)^H \right)^{-1} \mathbf{h}_{2,1}^e \right)^{-1}}}_{\text{with Slepian-Wolf source coding}}
 \end{aligned}$$

or $\xi_{\hat{F}_1^{1\neq 2}} \geq \rho_{\hat{F}_1^{1\neq 2}}/2^\beta$ if source coding is not applied. The performance region for CIF can be stated as $\hat{\mathcal{Z}}^{\text{cif}} = \bigcup \{(\mathbf{r}, \beta) : \mathbf{r} \in \hat{\mathcal{R}}^{\text{cif}}(\mathcal{P}, \beta)\}$, where the convex hull is again computed over all BS-UE assignments, cooperation directions, power allocations, and extents of backhaul β .

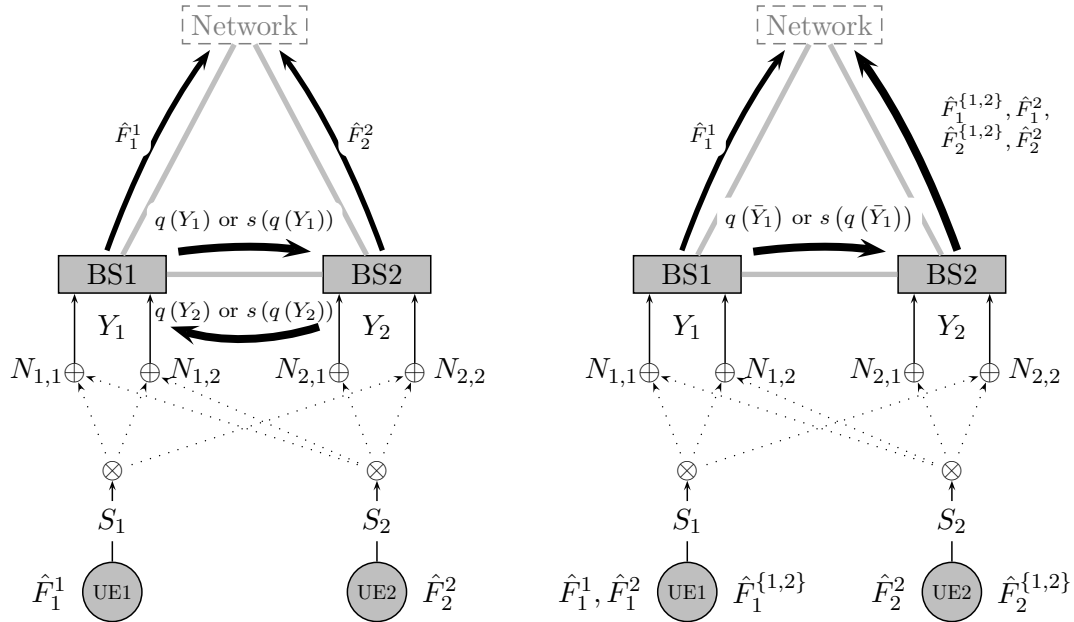
Distributed Antenna System (DAS) - Decentralized Decoding

Let us first consider a *decentralized* DAS setup where both BSs still aim at decoding their UEs locally, but assisted by an exchange of quantized receive signals between the BSs. Each UE transmits exactly one message \hat{F}_1^1 and \hat{F}_2^2 , respectively, mapped onto sequences \hat{X}_1^1 and \hat{X}_2^2 . Both BSs now create quantized versions $q(Y_1)$, $q(Y_2)$ of their received signals, and forward these over the backhaul. Optionally, as usual, source coding can be applied, such that $s(q(Y_1))$, $s(q(Y_2))$ are exchanged. Both BSs then use their received signals plus the information provided over the backhaul to reconstruct $q(Y_1)$, $q(Y_2)$, and then decode messages \hat{F}_1^1 , \hat{F}_2^2 , respectively. This process is illustrated in Figure 3.7(c). An achievable rate region for a given power allocation \mathcal{P} and backhaul β can then be stated as all rates $\mathbf{r} \in \hat{\mathcal{R}}^{\text{dasd}}(\mathcal{P}, \beta)$ that



(a) **DIS**: One BS forwards a decoded message to the other BS for (partial) interference subtraction.

(b) **CIF**: One BS forwards quantized interference to the other BS for (partial) interference subtraction.



(c) **DAS (Decentr.)**: Both BSs simult. exchange quantized receive signals, but decode UEs locally.

(d) **DAS (Centr.)**: One BS forwards quant. receive signals to the other BS for joint UE decoding.

Figure 3.7: Non-iterative uplink CoMP schemes for $M = K = 2$ analyzed in this chapter.

fulfill $\forall k \in \{1, 2\} : r_k \geq 0$ and

$$r_1 \leq \log_2 \left| \mathbf{I} + \left(\mathbf{H}^e \mathbf{P} \left(\hat{F}_2^2 \right) \left(\mathbf{H}^e \right)^H + \begin{bmatrix} \mathbf{0} & \mathbf{0} \\ \mathbf{0} & \Phi_2^{\text{qq}} \end{bmatrix} + \Phi^{\text{hh}} + \sigma^2 \mathbf{I} \right)^{-1} \mathbf{H}^e \mathbf{P} \left(\hat{F}_1^1 \right) \left(\mathbf{H}^e \right)^H \right| \quad (3.22)$$

$$r_2 \leq \log_2 \left| \mathbf{I} + \left(\mathbf{H}^e \mathbf{P} \left(\hat{F}_1^1 \right) \left(\mathbf{H}^e \right)^H + \begin{bmatrix} \Phi_1^{\text{qq}} & \mathbf{0} \\ \mathbf{0} & \mathbf{0} \end{bmatrix} + \Phi^{\text{hh}} + \sigma^2 \mathbf{I} \right)^{-1} \mathbf{H}^e \mathbf{P} \left(\hat{F}_2^2 \right) \left(\mathbf{H}^e \right)^H \right| \quad (3.23)$$

under the backhaul constraint

$$\underbrace{\log_2 \left| \mathbf{I} + \left(\Phi_1^{\text{qq}} \right)^{-1} \Phi_{1|2}^{\text{yy}} \right| + \log_2 \left| \mathbf{I} + \left(\Phi_2^{\text{qq}} \right)^{-1} \Phi_{2|1}^{\text{yy}} \right|}_{\text{Wyner-Ziv source coding}} \leq \beta \quad (3.24)$$

$$\text{or } \underbrace{\log_2 \left| \mathbf{I} + \left(\Phi_1^{\text{qq}} \right)^{-1} \Phi_1^{\text{yy}} \right| + \log_2 \left| \mathbf{I} + \left(\Phi_2^{\text{qq}} \right)^{-1} \Phi_2^{\text{yy}} \right|}_{\text{No source coding}} \leq \beta, \quad (3.25)$$

where $\forall m \in \{1, 2\} : \Phi_m^{\text{yy}} = \mathbf{H}_m^e \mathbf{P} \left(\hat{\mathcal{F}}_{\text{all}} \right) \left(\mathbf{H}_m^e \right)^H + \Phi_m^{\text{hh}} + \sigma^2 \mathbf{I}$ is the received signal covariance at BS m , and $\forall m, m' \in \{1, 2\} :$

$$\begin{aligned} \Phi_{m|m'}^{\text{yy}} &= E \{ Y_m Y_m^H | Y_{m'} \} \\ &= \mathbf{H}_m^e \left(\mathbf{I} + \mathbf{P} \left(\hat{\mathcal{F}}_{\text{all}} \right) \left(\mathbf{H}_{m'}^e \right)^H \left(\Phi_{m'}^{\text{hh}} + \sigma^2 \mathbf{I} \right)^{-1} \mathbf{H}_{m'}^e \right)^{-1} \mathbf{P} \left(\hat{\mathcal{F}}_{\text{all}} \right) \left(\mathbf{H}_m^e \right)^H + \Phi_m^{\text{hh}} + \sigma^2 \mathbf{I} \end{aligned} \quad (3.26)$$

is the same covariance, but conditioned on the signals received by the other BS. Note that we here have the degree of freedom of investing different portions of the backhaul into the two UEs, which could be exploited to increase fairness. One could further imagine that one BS could first decode its UE, subtract the corresponding receive signals, and then forward quantized signals to the other BS - a scheme we will observe separately in Section 3.3.4. The performance region of decentralized DAS can be stated as $\hat{\mathcal{Z}}^{\text{dasd}} = \bigcup \{ \langle \mathbf{r}, \beta \rangle : \mathbf{r} \in \hat{\mathcal{R}}^{\text{dasd}}(\mathcal{P}, \beta) \}$, where the convex hull is computed over all BS-UE assignments, backhaul distributions, power allocations, and extents of backhaul β .

Distributed Antenna System (DAS) - Centralized Decoding

We will see later that for most channel realizations, it is better to perform DAS such that the receiving BS decodes both UEs employing SIC. We will here again use the concept of superposition coding and assume without loss of generality that the UEs transmit messages $\hat{F}_1^{\{1,2\}}$ and $\hat{F}_2^{\{1,2\}}$, respectively, that are to be decoded individually by both BSs, superimposed by messages \hat{F}_1^2 and \hat{F}_2^2 , respectively, to be jointly decoded by BS 2. In addition, UE 1 may invest part of its transmit power into a message \hat{F}_1^1 that is only locally decoded by BS 1. This model hence reflects the concept of *common messages*, known to expand the capacity region of the interference channel [HK81], and also known to be beneficial in connection with DAS [MF08b], as well as the concept of local, non-cooperative decoding [SSS07a, SSS09]. For our considered cooperation direction, BS 1 hence decodes messages \hat{F}_1^1 , $\hat{F}_1^{\{1,2\}}$ and $\hat{F}_2^{\{1,2\}}$, and subtracts the corresponding transmitted sequences from the received signals to construct

$$\bar{Y}_1 = Y_1 - \mathbf{h}_{1,1}^e \left(\sqrt{\rho_{\hat{F}_1^{\{1,2\}}}} \hat{X}_1^{\{1,2\}} + \sqrt{\rho_{\hat{F}_1^1}} \hat{X}_1^1 \right) - \mathbf{h}_{1,2}^e \cdot \sqrt{\rho_{\hat{F}_2^{\{1,2\}}}} \cdot \hat{X}_2^{\{1,2\}}. \quad (3.27)$$

This is then quantized to $q(\bar{Y}_1)$ (and optionally source-encoded to $s(q(\bar{Y}_1))$) and forwarded to BS 2. The latter BS also decodes messages $\hat{F}_1^{\{1,2\}}$ and $\hat{F}_2^{\{1,2\}}$ and subtracts their impact on the received signals Y_2 . It then uses the remaining signals plus the information provided by BS 1 to finally decode messages \hat{F}_1^2 and \hat{F}_2^2 . For a fixed power allocation \mathcal{P} and backhaul β , the achievable rate region from Theorem 2.2.5 simplifies to all rates $\mathbf{r} \in \hat{\mathcal{R}}^{\text{dasc}}(\mathcal{P}, \beta)$ that fulfill $\forall k \in \{1, 2\} : r_k \geq 0$ and

$$r_1 = \nu_{\hat{F}_1^1} + \nu_{\hat{F}_1^{\{1,2\}}} + \nu_{\hat{F}_1^2} \quad (3.28)$$

$$r_2 = \nu_{\hat{F}_2^{\{1,2\}}} + \nu_{\hat{F}_2^2}$$

$$\forall \mathcal{F} \subseteq \left\{ \hat{F}_1^1, \hat{F}_1^{\{1,2\}}, \hat{F}_2^{\{1,2\}} \right\} :$$

$$\sum_{F \in \mathcal{F}} \nu_F \leq \log_2 \left| \mathbf{I} + \left(\mathbf{H}_1^e \mathbf{P} \left(\left\{ \hat{F}_1^2, \hat{F}_2^2 \right\} \right) \left(\mathbf{H}_1^e \right)^H + \Phi_1^{\text{hh}} + \sigma^2 \mathbf{I} \right)^{-1} \mathbf{H}_1^e \mathbf{P}(\mathcal{F}) \left(\mathbf{H}_1^e \right)^H \right| \quad (3.29)$$

$$\forall \mathcal{F} \subseteq \left\{ \hat{F}_1^{\{1,2\}}, \hat{F}_2^{\{1,2\}} \right\} :$$

$$\sum_{F \in \mathcal{F}} \nu_F \leq \log_2 \left| \mathbf{I} + \left(\mathbf{H}_2^e \mathbf{P} \left(\left\{ \hat{F}_1^1, \hat{F}_1^2, \hat{F}_2^2 \right\} \right) \left(\mathbf{H}_2^e \right)^H + \Phi_2^{\text{hh}} + \sigma^2 \mathbf{I} \right)^{-1} \mathbf{H}_2^e \mathbf{P}(\mathcal{F}) \left(\mathbf{H}_2^e \right)^H \right| \quad (3.30)$$

$$\forall \mathcal{F} \subseteq \left\{ \hat{F}_1^2, \hat{F}_2^2 \right\} :$$

$$\sum_{F \in \mathcal{F}} \nu_F \leq \log_2 \left| \mathbf{I} + \left(\underbrace{\begin{bmatrix} \Phi^{\text{qq}} & \mathbf{0} \\ \mathbf{0} & \rho_{\hat{F}_1^1} \mathbf{h}_{2,1}^e \left(\mathbf{h}_{2,1}^e \right)^H \end{bmatrix}}_{\text{Quant. noise / res. intrf.}} + \Phi^{\text{hh}} + \sigma^2 \mathbf{I} \right)^{-1} \mathbf{H}^e \mathbf{P}(\mathcal{F}) \left(\mathbf{H}^e \right)^H \right|, \quad (3.31)$$

with the backhaul constraint

$$\log_2 \left| \mathbf{I} + \left(\Phi^{\text{qq}} \right)^{-1} \Phi_{2|1}^{\text{yy}} \right| \leq \beta \quad \text{or} \quad \log_2 \left| \mathbf{I} + \left(\Phi^{\text{qq}} \right)^{-1} \Phi_2^{\text{yy}} \right| \leq \beta, \quad (3.32)$$

assuming source coding or no source coding, respectively. In (3.31), we can see that decoding is impaired not only by the quantization noise Φ^{qq} introduced, but also by residual interference $\rho_{\hat{F}_1^1} \mathbf{h}_{2,1}^e \left(\mathbf{h}_{2,1}^e \right)^H$ that BS 2 sees, as it does not decode \hat{F}_1^1 . Analogue to the other schemes, the performance region of centralized DAS is given as $\hat{\mathcal{Z}}^{\text{dasc}} = \bigcup \{(\mathbf{r}, \beta) : \mathbf{r} \in \hat{\mathcal{R}}^{\text{dasc}}(\mathcal{P}, \beta)\}$, where the convex hull is computed over all BS-UE assignments, choices of decoding BS, power allocations, and extents of backhaul β .

Numerical Results

Figure 3.8 shows the sum rate achievable for different BS cooperation schemes as a function of available sum backhaul for different, exemplary UE locations. As before, the sum rate itself is maximized, assuming a SISO SNR in the cell-center of SNR = 10 dB, and $N_p = 2$. As in Section 2.4, the performance of the schemes DIS, CIF, DAS (Dec.) and DAS (Ctr.) is not displayed as a single line, but as an area, illustrating the range between theory and practice. More precisely, all upper bounds correspond to schemes making use of inter-BS signal correlation through source coding techniques, the thick line in between denotes operation on the rate-distortion bound, but without source coding, while the lower bounds are based on the practical quantizer referred to in Section 2.2.5. As DIS schemes do not employ any

quantization, we only have two performance lines, either employing Slepian-Wolf source coding or not. To all plots, we have added the cut-set bound, which was introduced in Section 3.2. Recall that this indicates the sum rate that would be achieved if every additional quantity of backhaul would result in the same increase in sum rate, until MAC-capacity is reached. Clearly, only a centralized DAS scheme *always* reaches MAC performance asymptotically for a large backhaul, as this is the only scheme that exploits the full potential of array, spatial multiplexing and interference cancellation gain of the compound channel².

In a scenario where both UEs are located at the cell-edge (see plot 3.8(a)), centralized DAS schemes (even assuming practical quantization schemes) are clearly superior, as they can make best use of the strong interference at this point [KRF07]. Source coding techniques bring an additional strong gain in the sum rate/backhaul trade-off (A), as the correlation of signals received at BS 1 and BS 2 is strong (under the chosen $\varphi_{AB} = \pi/2$). In theory, any redundancy between the signals received by one BS and the information provided by the other BS is avoided, and the only reason why the scheme does not reach the cut-set bound is that backhaul is wasted into the quantization of noise [dCS08]. It is shown in Appendix F.3 that centralized DAS with source coding does in fact approach the cut-set bound for $\text{SNR} \rightarrow \infty$. Further improvement is possible if superposition coding is employed (B) - in this case due to the usage of common messages that are individually decoded by both BSs before DAS is performed. Note that for zero backhaul, these concepts yield no gain, as we are here observing a *strong interference channel* [Kra04]. This is also the reason why for this particular cell-edge scenario DIS-concepts are not beneficial at all (C). Instead of passing decoded bits of one UE over the backhaul, each BS can individually decode both UEs and apply SIC, yielding the same sum rate. Decentralized DAS schemes (D) lack the capability of performing successive interference cancellation and are hence inferior to centralized schemes.

In an asymmetrical scenario (see Plot 3.8(b)), DIS concepts yield (limited) gain (E). For $d_1 = 0.5$, the performance of DIS with source coding in fact follows the cut-set bound in a regime of low backhaul. Here, the cell-edge UE, received with little interference by BS 1, is decoded first, and then the decoded bits are forwarded to BS 2, exploiting strong side-information at BS 2. A proof on the rate/backhaul trade-off optimality of the scheme in this backhaul regime has been stated in [Gri09]. In the cited work, the performance of DIS with source coding almost equals the complete cut-set bound for an example scenario, namely a *Z-interference channel* [ZY08] (with $d_1 = 0.5$, $d_2 \rightarrow 0$), where DIS can almost yield MAC performance. Plots 3.8(c)-3.8(f) consider scenarios of less interference, where the left plots refer to symmetrical scenarios and the right plots to asymmetrical ones. In all cases, BS cooperation schemes based on decentralized decoding now become interesting, as they can outperform centralized DAS in regimes of low backhaul (F). If one of the interference links becomes weak, DIS schemes can be improved through superposition coding (G). As before in Plot 3.8(b), the sum rate is maximized if the UE subject to less interference is decoded first, and the data then forwarded to the other BS. In this case, however, the total rate of the forwarded UE's transmission is large compared to the gain of interference cancellation. Hence, it is beneficial to let the UE transmit superimposed messages, of which only one is forwarded after decoding. Also for centralized DAS schemes, we can see a strong benefit of superposition coding in the regime of low backhaul, which was especially pointed out in [SSSK05, SSS07a]. However, we can see that this gain merely constitutes a smooth transition from centralized

²One can construct particular channel realizations, however, where any of the compared schemes may achieve MAC performance, possibly even under finite backhaul.

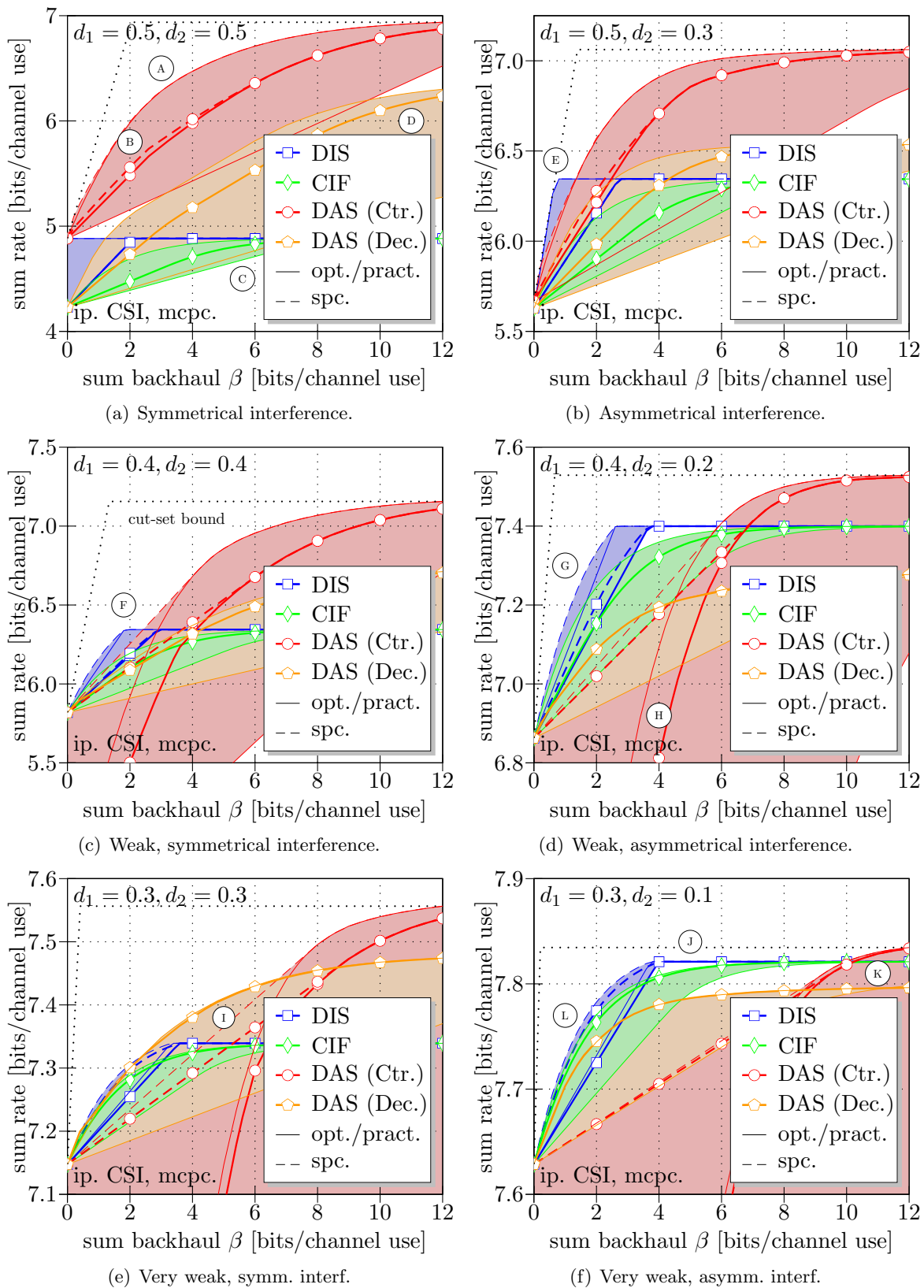


Figure 3.8: Sum rate vs. backhaul for uplink CoMP schemes and specific channels.

to decentralized decoding, which could also be achieved through a simple time-share between centralized DAS and non-cooperative, decentralized decoding. In fact, numerical evaluation has shown no benefit of using local decoding concepts in conjunction with DAS (i.e. where one BS decodes a message and only quantizes and forwards the remaining signals to the other BS) over the mentioned time-share. For all BS cooperation schemes, source coding techniques become less attractive $\textcircled{\text{H}}$ when the signal correlation between the BSs is weak.

In regimes of very low interference (Plots 3.8(e) and 3.8(f)), we know from Section 3.3.1 that the gain of cooperation is limited. Here, decentralized schemes are clearly superior (in regimes of low to moderate backhaul), as any centralized scheme would always lead to the fact that one of the two UEs is detected inefficiently through a very weak link. Decentralized DAS schemes now become particularly interesting $\textcircled{\text{I}}$, as they allow to adjust the extent of interference cancellation each UE shall benefit from at fine granularity. In weak and asymmetrical scenarios, DIS and CIF almost achieve MAC performance $\textcircled{\text{J}}$, enabling the cancellation of the stronger interference link, while the additional array gain a centralized DAS would obtain is marginal. Note that decentralized DAS is inferior in regimes of large backhaul $\textcircled{\text{K}}$, as it enables array gain and interference mitigation, but lacks the possibility of decoding and subtracting interference. CIF schemes become particularly interesting in this scenario, as they achieve most of the interference cancellation performance of DIS schemes, while assuring that the amount of backhaul invested is in good relation to the interference cancellation gain. In fact, it can be shown that DIS in conjunction with superposition coding is always superior to CIF (see the proof in Appendix F.5). CIF, however, can be considered more suitable for practical usage, as it does not require any modification of the transmit strategy of the UE.

3.3.3 Benefit of Source Coding and Superposition Coding

In the uplink, all considered BS cooperation schemes can make use of the fact that the BSs have correlated observations of the UE transmissions, i.e. by employing source coding techniques to the discrete signals (i.e. quantized receive signals or decoded data) before relaying these over the backhaul. As such schemes are typically computationally expensive [XLC04, VAG05, NEH07], we now want to summarize in which scenarios we can expect to obtain the largest gains. Furthermore, we summarize the benefit of using superposition coding, as we have introduced it into DIS and centralized DAS concepts in Section 3.3.2.

Figure 3.9 shows the maximum relative sum rate gain (in percent) of DIS and centralized DAS with source coding / superposition coding techniques (or both), maximized over all regimes of backhaul, for symmetrical and asymmetrical channels. We can see that source coding techniques can deliver moderate gains over a wide range of channels for centralized DAS, in particular when both UEs have fairly strong links to both BSs. Source coding in conjunction with DIS can be even more beneficial, particularly in scenarios where both UEs are at the cell-center (though here, DIS is inferior to centralized DAS in most cases), or for asymmetrical links, where the potential DIS-receiving BS has strong side-information on both UEs' signals.

The benefit of superposition coding has to be observed in a differentiated way. On one hand, it seems that DAS schemes can profit strongly from these concepts, especially for cell-center scenarios. However, these strong gains mainly come from cases where one UE is partially decoded by one BS without cooperation, after which the involved BS then quantizes and forwards the remaining signals to the other BSs [SSS07a, SSS09]. As we have pointed out

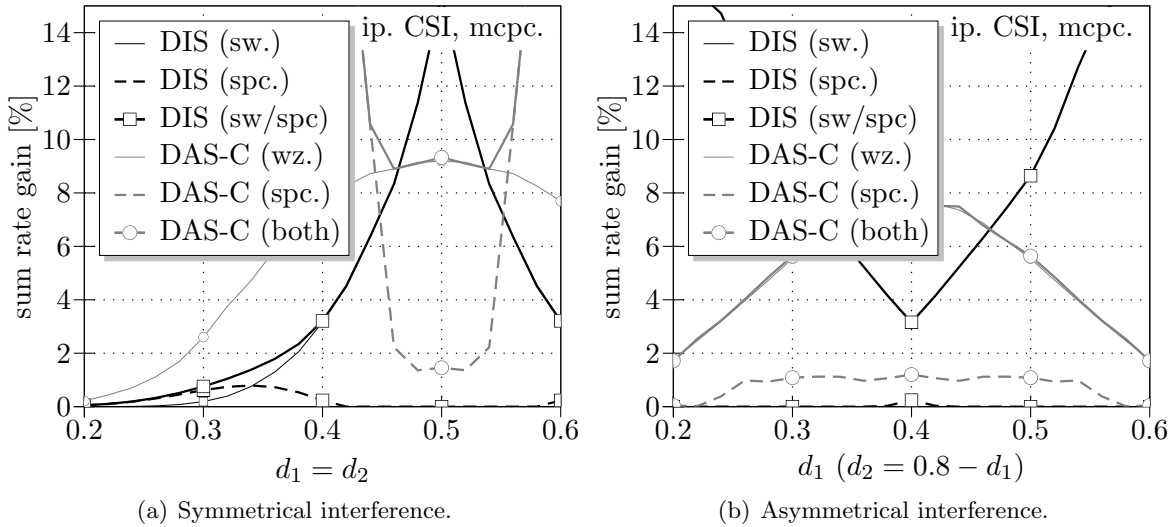


Figure 3.9: Gain through source coding or superposition coding in uplink CoMP.

in Section 3.3.2, however, such concepts perform equivalently to operating on a time-share between DIS and centralized DAS. At the cell-edge, we can observe a marginal gain from superposition coding that can have two reasons: Either **a**) both BSs individually decode a certain extent of common messages, such that the signal covariance of the remaining signals to be quantized and exchanged is reduced (as is visible in Figure 3.8(a)), or **b**) common message concepts already improve the non-cooperative sum rate, as known for the interference channel [HK81, Kra04]. This gain, however, only occurs for few interference scenarios and disappears as soon as a minimal extent of backhaul is available. DIS concepts can also profit from common message concepts where only part of a UE's transmission is forwarded over the backhaul [MF08b], as these allow to establish a concave rate/backhaul trade-off superior to a direct time-share between no and complete message forwarding. As this effect is most visible in scenarios of very weak interference, however, where the gains of CoMP are marginal, the relative rate gains of superposition coding in the context of DIS are generally small.

Based on these observations, we will continue to consider source coding concepts in the remainder of this work, but drop superposition coding schemes. Avoiding superposition coding also has the advantage that legacy UEs can be used in a system with BS cooperation.

3.3.4 Benefit of Iterative BS Cooperation Schemes

We now want to look into BS cooperation schemes where multiple phases of information exchange take place among the involved BSs, which requires an extension of our model from Section 2.2.5. Such schemes have been proposed by various authors, e.g. [AEH08, MJH06, BC07b, GHEM04, KF07]. We must first of all state that iterative schemes only make sense if both BSs are involved in decoding at least portions of the UE transmissions. If this were not the case, i.e. if only one BS would perform the decoding (as in the centralized DAS case before), there would be no point in iteratively exchanging information over the backhaul, as the other BS would not actually process its received signals to generate better knowledge on the transmitted sequences. In the sequel, we will hence only consider decentralized decoding.

Iterative Distributed Interference Subtraction (I-DIS)

Let us observe a cooperation scheme where the BSs iteratively decode a portion of their UE's transmission and then forward the decoded data according to the DIS concept. More precisely, let us assume that UE 1 transmits a superposition of N_1 messages $\hat{F}_1^{1[1]} \dots \hat{F}_1^{1[N_1]}$, and UE 2 messages $\hat{F}_2^{2[1]} \dots \hat{F}_2^{2[N_1]}$. At each iteration step $1 \leq i \leq N_1$, BS 1 decodes message $\hat{F}_1^{1[i]}$ and forwards the decoded bits to BS 2. The latter BS subtracts the impact of the corresponding sequence from its received signals, decodes message $\hat{F}_2^{2[i]}$, and forwards the decoded bits to BS 1. This is continued until all messages have been decoded, such that in each iteration a larger portion of interference is removed from the received signals. Each information exchange over the backhaul can be based on Slepian-Wolf source coding to exploit side information at the receiving BS. Note that in the last iteration, it is of course not necessary for BS 2 to forward decoded bits to BS 1, as the latter BS has already decoded all messages from UE 1. The achievable rates can be stated as follows:

$$\begin{aligned} r_1 &= \sum_{i=1}^{N_1} \nu_{\hat{F}_1^{1[i]}} \quad \text{and} \quad r_2 = \sum_{i=1}^{N_1} \nu_{\hat{F}_2^{2[i]}} \\ \nu_{\hat{F}_1^{1[i]}} &\leq \log_2 \left| \mathbf{I} + \left(\sigma^2 \mathbf{I} + \mathbf{\Phi}_1^{\text{hh}} + (\mathbf{\Phi}_1^{\text{ii}})^{[i]} \right)^{-1} \rho_{\hat{F}_1^{1[i]}} \mathbf{h}_{1,1}^e (\mathbf{h}_{1,1}^e)^H \right| \\ \nu_{\hat{F}_2^{2[i]}} &\leq \log_2 \left| \mathbf{I} + \left(\sigma^2 \mathbf{I} + \mathbf{\Phi}_2^{\text{hh}} + (\mathbf{\Phi}_2^{\text{ii}})^{[i]} \right)^{-1} \rho_{\hat{F}_2^{2[i]}} \mathbf{h}_{2,2}^e (\mathbf{h}_{2,2}^e)^H \right|, \end{aligned} \quad (3.33)$$

and the required sum backhaul in both directions is

$$\begin{aligned} \beta &= \sum_{i=1}^{N_1} \max \left(\underbrace{\nu_{\hat{F}_1^{1[i]}} - \log_2 \left| \mathbf{I} + \left((\mathbf{\Phi}_2^{\text{ii}})^{[i]} + \mathbf{h}_{2,2}^e \rho_{\hat{F}_2^{2[i]}} (\mathbf{h}_{2,2}^e)^H \right)^{-1} \rho_{\hat{F}_1^{1[i]}} \mathbf{h}_{2,1}^e (\mathbf{h}_{2,1}^e)^H \right|}_{{=0, \text{ without source coding concepts}}}, 0 \right) + \dots \\ &\quad \sum_{i=1}^{N_1-1} \max \left(\underbrace{\nu_{\hat{F}_2^{2[i]}} - \log_2 \left| \mathbf{I} + \left((\mathbf{\Phi}_1^{\text{ii}})^{[i]} - \mathbf{h}_{1,2}^e \rho_{\hat{F}_2^{2[i]}} (\mathbf{h}_{1,2}^e)^H \right)^{-1} \rho_{\hat{F}_2^{2[i]}} \mathbf{h}_{1,2}^e (\mathbf{h}_{1,2}^e)^H \right|}_{{=0, \text{ without source coding concepts}}}, 0 \right), \end{aligned} \quad (3.34)$$

with the interference terms

$$(\mathbf{\Phi}_1^{\text{ii}})^{[i]} = \sigma^2 \mathbf{I} + \mathbf{\Phi}_1^{\text{hh}} + \mathbf{H}_1^e \mathbf{P} \left(\left\{ \hat{F}_1^{1[i+1]} \dots \hat{F}_1^{1[N_1]}, \hat{F}_2^{2[i]} \dots \hat{F}_2^{2[N_1]} \right\} \right) (\mathbf{H}_1^e)^H \quad (3.35)$$

$$(\mathbf{\Phi}_2^{\text{ii}})^{[i]} = \sigma^2 \mathbf{I} + \mathbf{\Phi}_2^{\text{hh}} + \mathbf{H}_2^e \mathbf{P} \left(\left\{ \hat{F}_1^{1[i+1]} \dots \hat{F}_1^{1[N_1]}, \hat{F}_2^{2[i+1]} \dots \hat{F}_2^{2[N_1]} \right\} \right) (\mathbf{H}_2^e)^H. \quad (3.36)$$

The scheme, which we will abbreviate with I-DIS, can be interpreted in such a way that any new information on decoded bits is immediately forwarded to the other BS, such that the remaining remote decoding process is subject to less interference. The larger N_1 is chosen, the finer is the granularity of information exchanged between the BSs. The scheme is illustrated for $N_1 = 2$ in Figure 3.10(a). Note that I-DIS only leads to a marginal improvement of the rate/backhaul trade-off [GMF09], but it leads to an increase of achievable rates under asymptotically large backhaul, which we will investigate in the sequel.

Asymptotic I-DIS Performance for an Infinite Number of Information Exchanges

For I-DIS, it is difficult to determine the optimal power allocation connected to the super-imposed messages, as this is a non-convex optimization problem. However, we can derive a bound on the sum rate performance for I-DIS in a symmetrical channel scenario (and hence on the gain of I-DIS over DIS with one information exchange), and show that the gain will always be less for an asymmetrical scenario. Let us state the following lemma:

Lemma 3.3.1. *Assuming capacity-achieving codes, the sum rate achievable with an I-DIS cooperation scheme in a fully symmetrical two-cell scenario (i.e. $\lambda_{1,1} = \lambda_{2,2}$, $\lambda_{1,2} = \lambda_{2,1}$, $\varphi_{Ab} = \varphi_{Ba}$, $\hat{p}_1^{\max} = \hat{p}_2^{\max}$) is maximized if both UEs split their transmissions into an arbitrarily large number of messages that are assigned infinitesimally small power each, i.e. $N_I \rightarrow \infty$.*

Proof. The proof is based on recursion and stated in Appendix F.1. \square

Using Lemma 3.3.1, we can now compute the maximum sum rate for I-DIS in a symmetrical scenario based on (3.33) as

$$r \leq \lim_{N_I \rightarrow \infty} \sum_{m=1}^2 \sum_{i=1}^{N_I} \log_2 \left| \mathbf{I} + \left(\Phi_m^{\text{nn}} + \Phi_m^{\text{hh}} + \mathbf{H}_m^e \mathbf{P} \left(\mathcal{F}^{[i]} \right) \left(\mathbf{H}_m^e \right)^H \right)^{-1} \frac{\hat{p}_m^{\max}}{N_I} \mathbf{h}_{m,m}^e \left(\mathbf{h}_{m,m}^e \right)^H \right|, \quad (3.37)$$

where $\mathcal{F}^{[i]} = \{\hat{F}_1^{1[i+1]} \dots \hat{F}_1^{1[N_I]}, \hat{F}_2^{2[i+1]} \dots \hat{F}_2^{2[N_I]}\}$, and where we assume the transmit power of all messages to be \hat{p}_m^{\max}/N_I . Assigning equal power to each message is optimal for this asymptotic observation, as Lemma 3.3.1 has shown that any message of larger power can be split into more I-DIS iterations, yet still yielding an increase in sum rate. While it is difficult to find an analytical solution for (3.37) for an arbitrary number of BS antennas, such a solution has been stated for $N_{\text{bs}} = 1$ in [Gri09], which we recall in the following Lemma:

Lemma 3.3.2. *Assuming capacity-achieving codes, the sum rate achievable with an I-DIS cooperation scheme in a symmetrical two-cell scenario with $N_{\text{bs}} = 1$, where the main BS-UE links and interference links are of path gain γ and λ , respectively, both UEs transmit at power \hat{p}^{\max} , and both BSs observe thermal noise, interference and channel estimation related noise of variance σ^2 , can be bounded as*

$$r_{\text{sum}} \leq \frac{2}{1 + \frac{\lambda}{\gamma}} \log_2 \left(1 + \frac{(\lambda + \gamma) \hat{p}^{\max}}{\sigma^2} \right). \quad (3.38)$$

Proof. The proof is based on approximating (3.37) through a Taylor series expansion of the logarithm and solving the sum over all transmitted messages through an integral. The proof is given in [Gri09] and is revisited in Appendix F.1. \square

For symmetrical scenarios with $N_{\text{bs}} > 1$, we can calculate the maximum sum rate by solving (3.37) numerically, which we have done to observe the gain of I-DIS over DIS in Figure 3.11. The question is now to which extent I-DIS is also interesting in asymmetrical channels. Clearly, in the extreme case of a Z-interference channel [ZY08], it is optimal to let the non-interfered UE be decoded first and then forward the entire decoded message to the other BS, without any data exchange in the other direction. In general, it will be beneficial in any asymmetrical channel to decode larger portions of the less-interfered UE first, and decode a large portion of the more strongly interfered UE at the very end of the process, benefiting

most from interference cancellation. Hence, the concept of splitting UE power into many small messages, as in Lemma 3.3.1, can only be applied to the remaining smaller portion of power. This already suggests that the gain of iterative cooperation decreases, the more asymmetrical the scenario becomes, which we emphasize through simulation results in Figure 3.11 that we will discuss in Section 3.3.4. In general, the gains through I-DIS appear rather marginal. We will see in Section 5.1.4, however, that the theoretical concept of I-DIS stated in this section can be used for the discussion of practical schemes based on iterative interference subtraction.

Iterative Distributed Antenna System (I-DAS)

As the last uplink BS cooperation scheme considered in this chapter, we will now define an iterative DAS approach for the setup with $M = K = 2$, again built around decentralized decoding. We assume that both UEs transmit messages \hat{F}_1^1 and \hat{F}_2^2 , respectively. After receiving the transmissions, BS 1 forwards quantized receive signals $q(Y_1)$ (or source-encoded $s(q(Y_1))$) to BS 2. After BS 2 has reconstructed $q(Y_1)$, it decodes message \hat{F}_2^2 and subtracts its impact from the receive signals to obtain $\bar{Y}_2 = Y_2 - \mathbf{h}_{2,2}^s \sqrt{\rho_{\hat{F}_2^2}} e(\hat{F}_2^2)$. The resulting signal is then quantized to $q(\bar{Y}_2)$ and forwarded to BS 1, such that message \hat{F}_1^1 can be decoded there. The scheme, which we refer to as I-DAS, is illustrated in Figure 3.10(b). The achievable rates can be stated as

$$\begin{aligned}
r_1 &\leq \log_2 \left| \mathbf{I} + \left(\sigma^2 \mathbf{I} + \Phi^{\text{hh}} + \begin{bmatrix} \rho_{\hat{F}_2^2} \mathbf{h}_{1,2}^e (\mathbf{h}_{1,2}^e)^H & \mathbf{0} \\ \mathbf{0} & \Phi_2^{\text{qq}} \end{bmatrix} \right)^{-1} \mathbf{H}^e \mathbf{P} \left(\hat{F}_1^1 \right) (\mathbf{H}^e)^H \right| \quad (3.39) \\
r_2 &\leq \log_2 \left| \mathbf{I} + \left(\sigma^2 \mathbf{I} + \Phi^{\text{hh}} + \mathbf{H}^e \mathbf{P} \left(\hat{F}_1^1 \right) (\mathbf{H}^e)^H + \begin{bmatrix} \Phi_1^{\text{qq}} & \mathbf{0} \\ \mathbf{0} & \mathbf{0} \end{bmatrix} \right)^{-1} \mathbf{H}^e \mathbf{P} \left(\hat{F}_2^2 \right) (\mathbf{H}^e)^H \right| \\
\text{s.t.} &\quad \underbrace{\log_2 \left| \mathbf{I} + (\Phi_1^{\text{qq}})^{-1} \Phi_1^{\text{yy}} \right| + \log_2 \left| \mathbf{I} + (\Phi_2^{\text{qq}})^{-1} \bar{\Phi}_2^{\text{yy}} \right|}_{\text{Without source coding}} \leq \beta \\
\text{or} &\quad \underbrace{\log_2 \left| \mathbf{I} + (\Phi_1^{\text{qq}})^{-1} \Phi_{1|2}^{\text{yy}} \right| + \log_2 \left| \mathbf{I} + (\Phi_2^{\text{qq}})^{-1} \bar{\Phi}_{2|1}^{\text{yy}} \right|}_{\text{With source coding}} \leq \beta,
\end{aligned}$$

where $\Phi_1^{\text{yy}} = E \{ Y_1 Y_1^H \} = \mathbf{H}_1^e \mathbf{P}(\mathcal{F}_{\text{all}}) (\mathbf{H}_1^e)^H + \Phi_1^{\text{hh}} + \sigma^2 \mathbf{I}$ is the covariance of the signals received at BS 1, and $\bar{\Phi}_2^{\text{yy}} = E \{ \bar{Y}_2 \bar{Y}_2^H \} = \mathbf{h}_{2,1}^s \rho_{\hat{F}_1^1} (\mathbf{h}_{2,1}^s)^H + \Phi_2^{\text{hh}} + \sigma^2 \mathbf{I}$ is the covariance of the signals received at BS 2 after subtraction of the signals originating from UE 2. The conditional covariance terms $\Phi_{1|2}^{\text{yy}}$ and $\bar{\Phi}_{2|1}^{\text{yy}}$ can be derived from (D.18) in Appendix D.2. Compared to the decentralized DAS scheme introduced in Section 3.3.2, where the BSs make simultaneous use of the backhaul, the main advantage of an iterative scheme is that BS 1 obtains received and quantized signals from BS 2 that are already interference-free. This effect is of course most prominent if the involved signal covariance at BS 2 has significantly less entropy after the removal of the decoded signals of UE 2, which is the case if the interference link from UE 1 to BS 2 is weak. We will see this later in Section 3.3.4. Clearly, the performance of I-DAS is always at least as good as that of decentralized DAS, as it contains the latter as a subset. The price for the (marginal) rate gains over decentralized DAS that we will observe later is the additional latency that has been introduced into the decoding process.

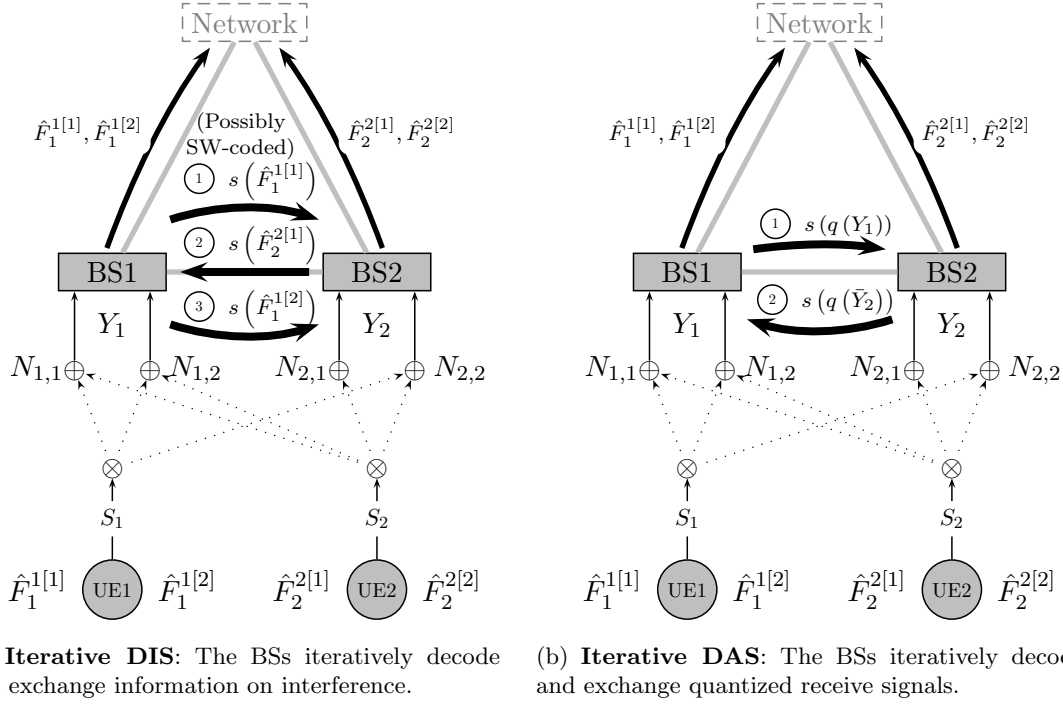


Figure 3.10: Iterative uplink CoMP schemes for $M = K = 2$ analyzed in this chapter.

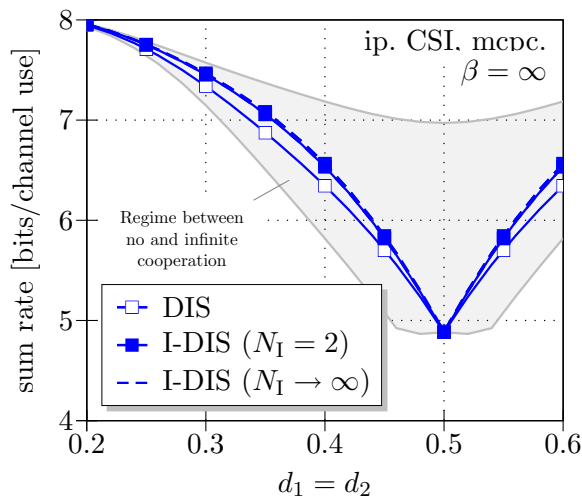
Iterative DAS Schemes with More Information Exchanges

Intuitively, one could think that it would also make sense to extend the I-DAS scheme to more information exchanges between the BSs. As for I-DIS, the UEs could transmit superpositions of messages which are successively decoded by the BSs. After each decoding step, a BS would forward quantized received signals to the other BS, freed from the signals of the messages already decoded. Ideally, each information exchange should be conditioned on previously forwarded and obtained signals in order to avoid a redundant exchange of information. However, we will show in the following theorem that (in our information theoretic model, under the assumption of large block lengths etc.) there is marginal benefit in terms of the rate/backhaul trade-off of having more than two information exchanges of quantized receive signals.

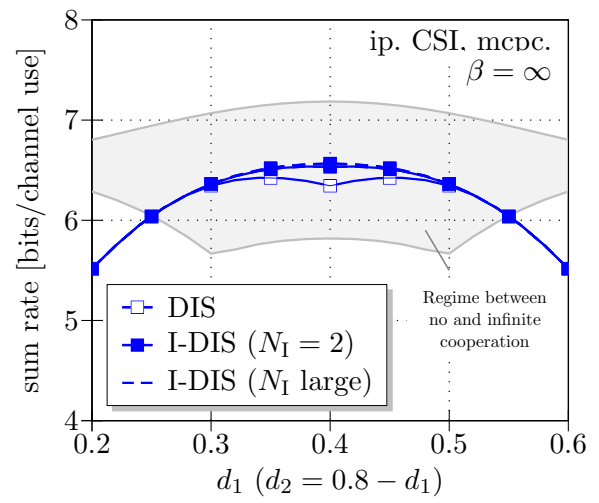
Theorem 3.3.3 (Marginal benefit of I-DAS with more than two information exchanges.). *In a scenario with $M = K = 2$, and assuming Gaussian, ergodic signals and large block lengths, the sum rate/backhaul trade-off cannot (or only marginally) be improved by I-DAS schemes with more than two information exchanges.*

Proof. The proof is stated in Appendix F.2. □

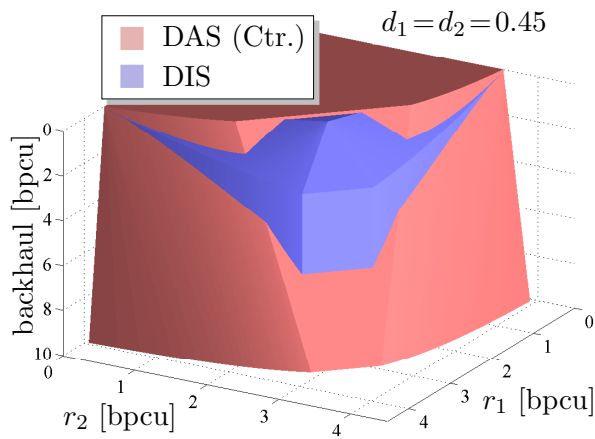
From an information theoretical point of view, especially under the assumption that complete codewords are subject to the same block-fading channel realization and to ergodic noise, schemes involving I-DAS with more than two information exchanges are hence quite unattractive. We will have more discussion on this observation, connected to the practical, iterative BS cooperation schemes suggested in [AEH08, MJH06, BC07b, GHEM04, KF07] in Section 5.1.4.



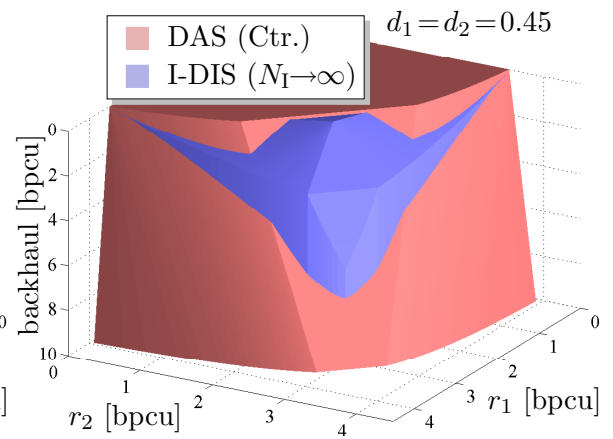
(a) Symmetrical interference.



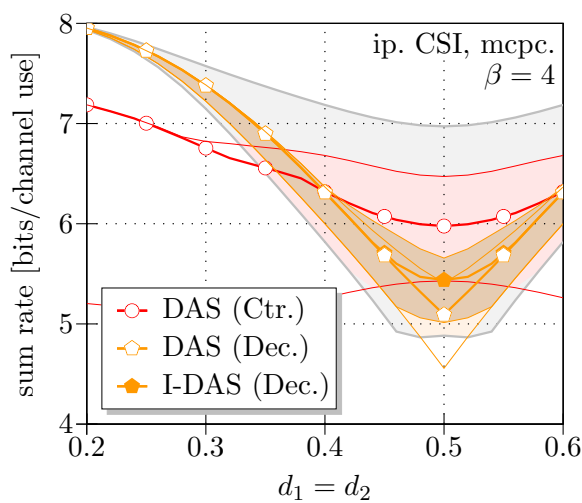
(b) Asymmetrical interference.



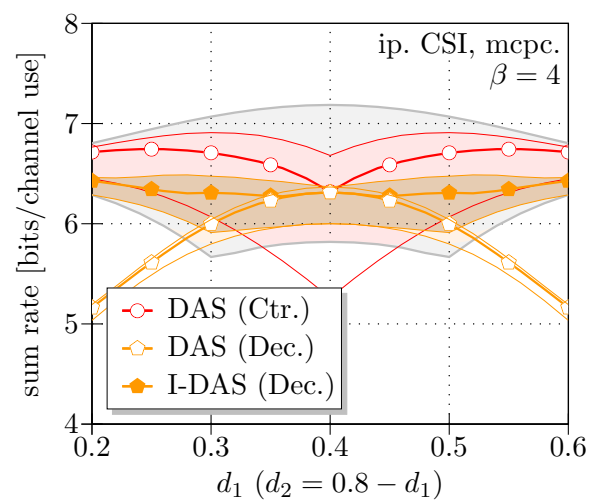
(c) Performance region with DIS.



(d) Performance region with I-DIS.



(e) Symmetrical interference.



(f) Asymmetrical interference.

Figure 3.11: Benefit of iterative uplink CoMP schemes for $M = K = 2$.

Numerical Results

Figure 3.11 shows simulation results for the iterative BS cooperation schemes discussed in this section, for the same channel, noise, and channel estimation parameters as previously used. As stated before, the benefit of I-DIS concepts is mainly that the asymptotic capacity for a large backhaul is increased, while the rate/backhaul trade-off itself is only marginally improved. To illustrate the first aspect, Plots 3.11(a) and 3.11(b) show the sum rate achievable under an infinite backhaul for DIS concepts with one BS information exchange, I-DIS concepts with $N_I = 2$, as well as the asymptotic bound for $N_I \rightarrow \infty$ derived in Section 3.3.4, for symmetrical or asymmetrical channels, respectively. The assumptions on imperfect CSI and SNR are the same as before. We can see that the sum rate gain through employing I-DIS as opposed to simple DIS is only in the order of a few percent, and these gains can only be achieved for fairly symmetrical channel conditions. Interestingly, using I-DIS concepts with $N_I = 2$ (i.e. with three information exchanges) already yields a performance close to the bound for an infinite number of information exchanges, as also observed in [Gri09, GMF09]. Note that the improved asymptotic sum rate of I-DIS for large backhaul makes decentralized cooperation concepts more attractive in regimes where otherwise DAS is dominant. This is illustrated in Plots 3.11(c) and 3.11(d), where the performance region for a symmetrical channel with $d_1 = d_2 = 0.45$ is shown for DIS and DAS concepts, and we can see that in the right plot the usage of I-DIS stretches the area in which decentralized schemes are superior into a regime of larger backhaul. The benefit of iterative DAS concepts is shown in Plots 3.11(e) and 3.11(f), again for symmetrical and asymmetrical channels and for an exemplary backhaul capacity of $\beta = 4$. We can see that the iterative scheme appears to be only attractive in cases of strong or asymmetrical interference, where centralized DAS schemes are superior, anyway.

3.3.5 Choice of Best Coop. Scheme and Cooperation Direction

In Section 3.3.2, we have already discussed the advantages and disadvantages of different uplink CoMP schemes under exemplary channel realizations. We now want to extend this work and investigate in which scenarios a system would ideally switch to a certain cooperation strategy. We are also interested in the optimal direction in which data should be exchanged over the backhaul, once a certain scheme has been chosen.

Figure 3.12 shows the best BS cooperation scheme and cooperation direction for sum rate maximization, where the x- and y-axes represent different UE locations. In all cases, we observe channels of average orthogonality, multi-cell power control and assume $\text{SNR} = 10$ dB in the cell-center and $N_p = 2$. All plots on the left side assume that source coding techniques can be used, while those on the right side are based on a practical quantizer, as introduced in Section 2.2.5. In Plots 3.12(a) and 3.12(b), the axes represent the location of the UEs, while the extent of available sum backhaul is fixed to 4 bpcu. As observed before in Figure 3.8, CIF and DIS schemes are superior in regimes of weak interference, where CIF dominates DIS under very weak interference. Decentralized DAS schemes are superior in regimes of very weak and symmetrical interference. At the cell-edge, or in strongly asymmetrical interference scenarios, centralized DAS concepts are superior. The hatched areas indicate where the benefit of using a decentralized decoding approach (DIS, CIF or decentralized DAS) over a centralized DAS, or vice versa, is a difference in sum rate of at least 10%. Clearly, DIS concepts become superior for a wider range of channels if source coding concepts are omitted and more practical quantization concepts are employed, as visible in the right plot.

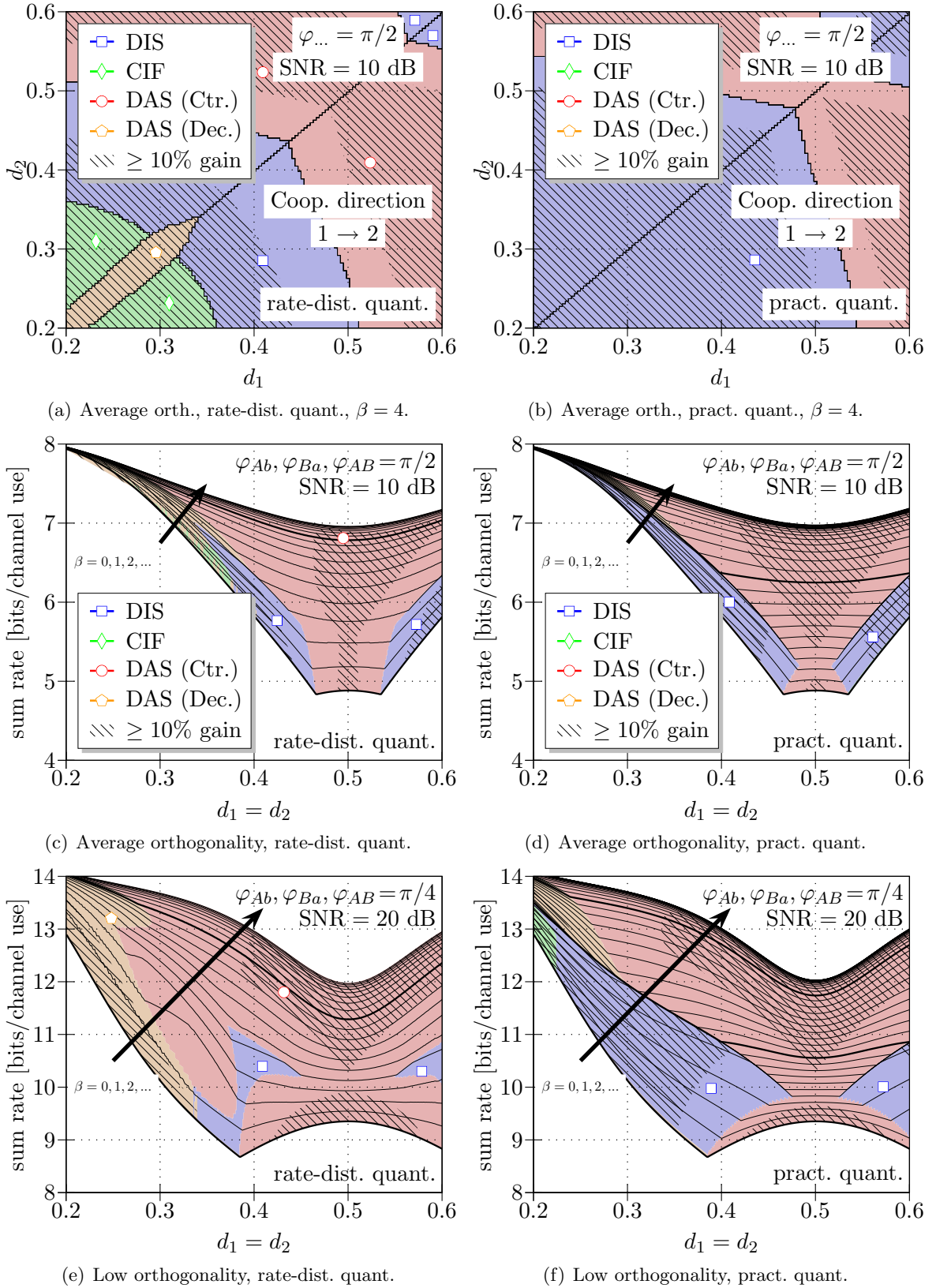


Figure 3.12: Best choice of BS cooperation scheme in uplink CoMP.

For all cooperation schemes, it is beneficial for BS 1 to forward signals to BS 2 if and only if $d_1 > d_2$. For DIS and CIF concepts, this is rather clear, as this means that the UE which is closer to the cell-edge is decoded first, as this is subject to less interference than the other UE. For decentralized DAS concepts, there is no preferred cooperation direction, as the main benefit of these schemes lies in the fact that the backhaul is used *simultaneously* in both directions. For centralized DAS schemes, we state the following theorem:

Theorem 3.3.4 (Optimal direction of cooperation for centralized DAS.). *For any (finite) extent of backhaul in a scenario with $M = 2$ BSs and an arbitrary number K of UEs, the sum rate is larger if the weaker BS forwards received signals to the stronger BS, hence to the BS that can achieve a better UE sum rate even without BS cooperation, than vice versa.*

Proof. The proof is stated in Appendix F.4. □

Clearly, Theorem 3.3.4 can easily be extended to the case of an arbitrary number of BSs, if all BSs forward signals to one BS. If, however, the common rate is to be maximized, then the optimal CoMP strategy will likely be a time-share between different cooperation directions. In this case, an analytical investigation is tedious and therefore omitted here.

Plots 3.12(c) and 3.12(d) show the superiority of different BS cooperation schemes in different regimes of sum rate. In addition, the black lines within the areas denote the extent of backhaul that has to be invested to achieve these rates, where each fine line denotes 1 bit of backhaul, and a bold line marks 10 bits of backhaul per channel use. Again, hatched areas indicate a gain of more than 10% between centralized or decentralized strategies. We can see that for our standard channel, DIS concepts pose a very backhaul-efficient solution, but cannot compete with DAS concepts if large sum rates are targeted. This is slightly different in the lower two Plots 3.12(e) and 3.12(f), where we observe a channel of low orthogonality ($\varphi_{Ab} = \varphi_{Ba} = \varphi_{AB} = \pi/4$) at a large SISO SNR of 20 dB. Here, the cooperation gain is in fact largest around $d \approx 0.38$, where DIS schemes can already yield about 50% of the possible cooperation again, while requiring very limited backhaul. Decentralized DAS schemes now become moderately interesting under practical considerations, as they provide the majority of cooperation gains for $d = 0.25$, requiring less backhaul than their centralized counterpart.

The results suggest that a practical system could switch between cooperation concepts based on simple rules, such as a look-up table at reasonable granularity. Even though MAC performance can only be achieved with centralized DAS concepts, there are scenarios where decentralized schemes, in particular DIS, appear to be an interesting low-backhaul option.

3.3.6 Sensitivity of Schemes to Channel Orthogonality and SNR

We have so far constrained ourselves to channels of moderate orthogonality ($\varphi_{Ab} = \varphi_{Ba} = \varphi_{AB} = \pi/2$) and a SISO SNR of 10 dB, motivated by system level simulations with particular clustering concepts in Chapter 4. We now want to observe the impact of these parameters on the absolute and relative performance of the discussed BS cooperation schemes. In Figure 3.13, we can see the maximum sum rates achievable for various schemes, for fixed UE locations $d_1 = d_2 = 0.4$ or $d_1 = 0.5, d_2 = 0.3$, respectively. In the upper plots, we vary the channel orthogonality on the x-axis, where angles φ_{Ab} and φ_{Ba} are changed from 0 up to π from left to right, while the additional compound channel orthogonality φ_{AB} is changed from π to 0. On the right side, we hence have channels where the BSs are already able to

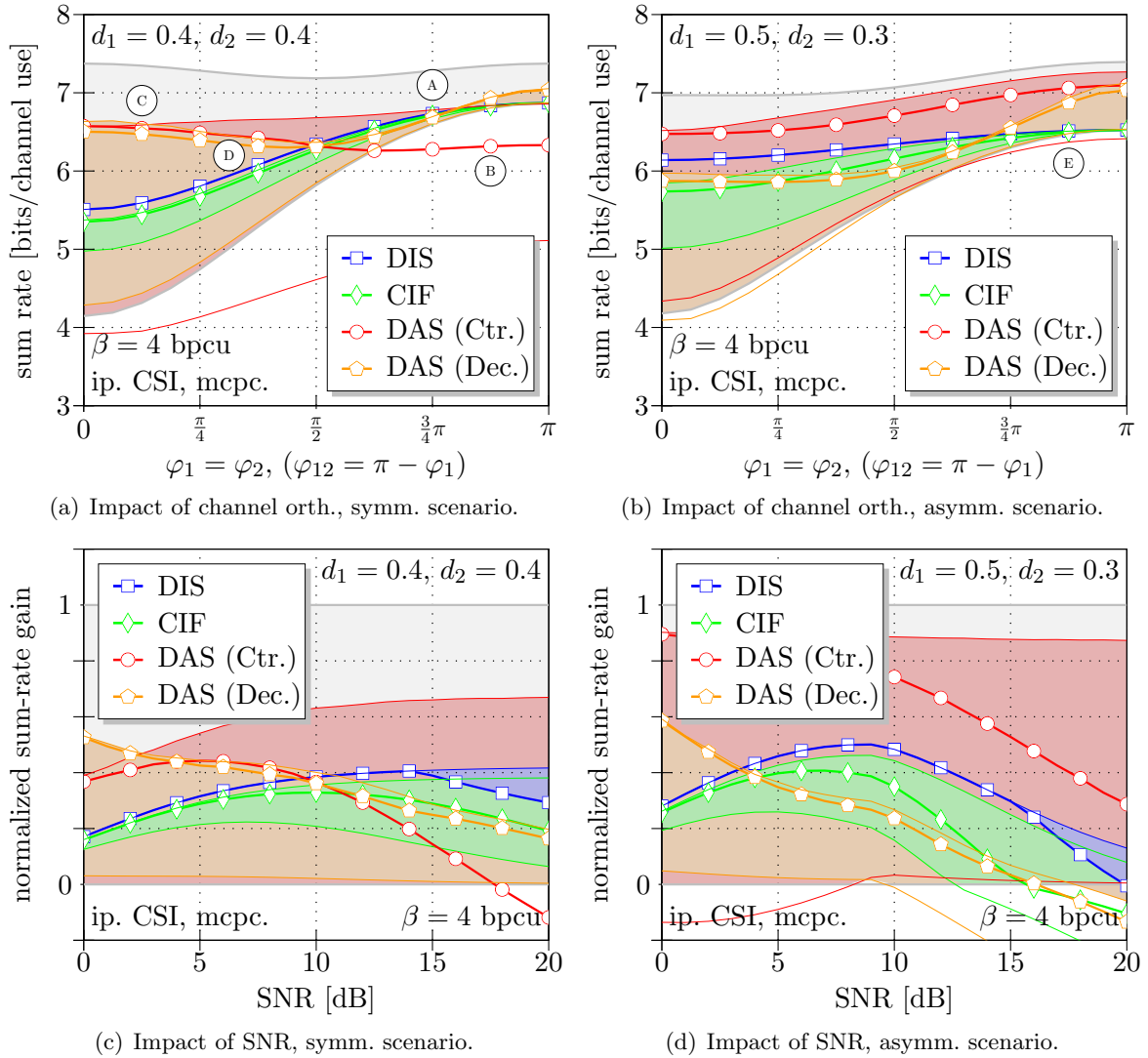


Figure 3.13: Impact of channel orthogonality and SNR on uplink CoMP schemes.

spatially separate both UEs without cooperation, while the compound channel of both BSs offers no additional orthogonality, and on the left side we have the opposite case. Obviously, the performance of a non-cooperative system increases from left to right, while that of a fully cooperative system stays roughly the same, as it does not matter which rows of the channel matrix provide orthogonality between the UEs. While the performance of schemes with decentralized decoding (DIS, CIF) improves for larger $\varphi_{Ab}, \varphi_{Ba}$ (A), that of DAS degrades (B), as this is mainly based on exploiting φ_{AB} . We can also observe that employing Wyner-Ziv yields no benefit for $\varphi_{Ab}, \varphi_{Ba} \rightarrow 0$ and $\varphi_{AB} \rightarrow \pi$, as then both BSs make orthogonal, uncorrelated observations of the UEs' transmissions (C). Decentralized DAS concepts (D) perform equally well in regimes of local or compound orthogonality, as they can exploit both sources of orthogonality. In the asymmetrical scenario in the right plot, centralized DAS schemes are superior over the whole range of orthogonalities, especially as they can exploit strong local orthogonality through local SIC, which is not the case for DIS (E).

Plots 3.13(c) and 3.13(d) show the sensitivity of the schemes towards background interference and noise. As the overall rates change strongly as a function of SNR, we plot *normalized sum rates* on the y-axis, showing the *relative* performance of any scheme between no and infinite BS cooperation. Note that we here assume that channel estimation is subject to the same extent of noise (i.e. $\sigma_{\text{pilots}}^2 = \sigma^2$), hence the impact of channel estimation also diminishes for $\text{SNR} \rightarrow \infty$. The backhaul is fixed to $\beta = 4$. The main observations are that decentralized schemes (in particular DIS) become more interesting in regimes of high SNR. This is mainly due to the fact that under larger SNR, non-cooperative decoding of the first UE to be forwarded is less subject to noise and interference. Further, DAS schemes operating on the rate distortion bound degrade under large SNR and for a fixed backhaul, as they require an additional bit of backhaul for each 3dB of SNR, to ensure that quantization noise stays in the order of background noise [SSPS08a]. Interestingly, source coding concepts enable to alleviate this problem, as of course the inter-BS signal correlation also increases with rising SNR. In particular, it appears that centralized DAS with Wyner-Ziv source coding and a fixed amount of backhaul can always obtain the same share of the cooperation gain, regardless of the SNR and hence also regardless of the high sum rates involved.

3.3.7 Performance of Uplink CoMP Schemes in Scenarios with $M = K = 3$

Even though we previously observed a minimalistic scenario with $M = K = 2$, we have seen that the degrees of freedom of BS cooperation and the dimensionality of the parameter space were already large. For practical systems, we consider cooperation scenarios with $M = K = 3$ to be more interesting, especially as Chapter 4 shows that cellular systems can be partitioned into such scenarios through simple clustering and resource partitioning concepts. In these cases, however, we know from (3.11) that the number of parameters required to fully characterize a channel is vast, and the number of possible combinations of BS cooperation schemes is sheer intractable. We hence constrain ourselves to

- Monte Carlo simulations with randomly generated channels.
- Basic BS cooperation concepts that have shown to be beneficial in our previous analysis (i.e. DIS and centr. DAS concepts *without* superposition coding, but *with* source coding).
- Combinations of these basic schemes that appear most interesting.

A framework to efficiently model combinations of DIS and centralized DAS for systems of arbitrary M, K was introduced in [MF08e], and used in e.g. [MF08d, MF09b]. We do not want to go into detail here, but state the key features in the sequel:

- The model supports any arbitrary assignment of UEs to BSs (yielding K^M different possibilities). We will see later that a flexible BS-UE assignment adapting to fast fading and local decoding of multiple UEs with SIC can yield substantial gains over a conventional system where the UE-BS assignment is typically based on large-scale fading.
- A BS that *does not* decode any UE itself can quantize and forward received signals (centralized DAS) to support another BS in decoding UEs, employing different numbers of quantization bits and (possibly) source coding concepts.
- A BS that *decodes* one or multiple UEs can forward the decoded bits (DIS) connected to all or a subset of these UEs to another BS that decodes one or multiple UEs. It is assured that such an information exchange is non-cyclic, as discussed in Section 2.2.5.

The model also allows a central network entity to decode UEs, as this has e.g. been proposed in [SSS07a]. In this case, which we refer to as *network DAS* (N-DAS), the network entity requires quantized received signals from at least one BS, as it has no received signals itself. To ensure a fair comparison of N-DAS to other BS cooperation schemes, we have to take into account that in N-DAS, the links from some BSs to the network will carry quantized receive signals, but not decoded messages, as in a conventional system. We hence have to subtract the conventional backhaul traffic in these cases to ensure that we only observe the *additional* backhaul infrastructure required compared to a non-cooperative system.

The model for $M = K = 3$ already yields large numbers of potential BS cooperation setups, but it is still feasible to perform a brute force search over all these possibilities for a given channel realization. We are particularly interested in the question whether it is beneficial to adaptively switch between DIS/DAS concepts or use hybrid cooperation concepts (i.e. DIS and centralized DAS concepts in parallel). Figure 3.14 shows the average sum rate/backhaul trade-off for a large number of channel realizations, where each channel coefficient has been drawn independently from a complex, zero-mean Gaussian distribution, where

$$\forall m \in \{1, 2\}, k \in \{1, 2\} : E \{|h_{2(m-1)+1,k}|^2\} = E \{|h_{2m,k}|^2\} = \lambda_{m,k}. \quad (3.40)$$

In the left plot of Figure 3.14, the chosen values for $\lambda_{m,k}$ represent a cell-edge scenario ($d_1 = d_2 = d_3 = 0.5$, see 3.7), whereas the right plot resembles a cell-center scenario ($d_1 = d_2 = d_3 = 0.3$). We compare the following detection or cooperation strategies:

- Detection as in a conventional system, where each UE k is decoded by BS $m = k$, without BS cooperation, and employing a *maximum ratio combining* (MRC) [KM98] filter at the receiver side. Such a scheme does *not* exploit the spatial properties of the interference.
- Detection as before, but employing interference rejection combining (IRC) filters [ER97], such that interference can be partially mitigated.
- Non-cooperative detection, exploiting the spatial interference properties, with an arbitrary BS-UE assignment, and the option of local multi-UE decoding with SIC.
- Pure DIS-based concepts.
- Pure (centralized) DAS-based concepts.
- Hybrid approaches of DIS and centralized DAS.
- Network DAS concepts (N-DAS), where all BSs forward quantized receive signals to a central network entity for further processing.

Figure 3.14 shows simulation results, based on the same assumptions w.r.t. imperfect CSIR ($N_p = 2$) and SNR (SNR = 10 dB). For a strong crosscoupling between cells in Plot 3.14(a), there is already a substantial gain if a system employs IRC (average sum rate increase from 3.78 bpcu by 16% to 4.38 bpcu), or especially if it allows an arbitrary assignment of UEs to BSs (increase by another 33% to 5.84 bpcu). Note that in all these cases we have no BS cooperation in the sense that received or decoded signals are exchanged among the BSs. Instead, the gains result purely from the fact that BSs are able to estimate interference and use IRC, and that in some cases multiple UEs are decoded by the same BS, employing SIC.

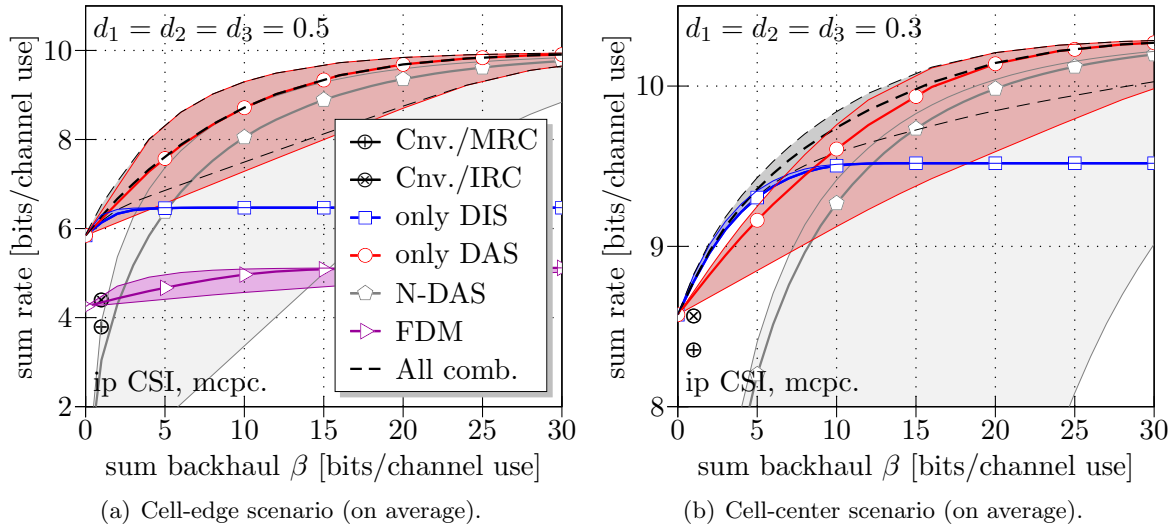


Figure 3.14: Monte Carlo simulation results for $M = K = 3$ in the uplink.

If backhaul is used to enable joint signal processing among BSs, the sum rate can be increased by another 71% in the asymptotic regime. Note that this corresponds well to observations in Section 3.3.1, where gains have been on the order of 90% in a symmetrical cell-edge scenario with moderate channel orthogonality. As the Monte-Carlo simulations observed now also yield instantaneous asymmetrical channels with less cell crosscoupling, the average gain is reduced. We can see that there is hardly any benefit of using DIS schemes, and that the rate/backhaul trade-off of centralized DAS schemes depends strongly on the assumptions made upon quantization. If inter-BS signal correlation is exploited, about 90% of the possible CoMP gains can be achieved with about 1.5 bits of additional backhaul per sum rate bit, while under the assumption of practical quantization schemes, the backhaul requirement is increased to a ratio of about 3. FDM schemes and network DAS schemes are inferior to the other observed schemes in all regimes of backhaul. In the first case, this is due to the fact that only array gain, but no spatial multiplexing or interference cancellation gain can be obtained by FDM. In the latter case, the rate/backhaul trade-off is fairly close to that of centralized DAS under optimistic assumptions w.r.t. quantization, but N-DAS is clearly inefficient under practical quantization [MF09b]. In large cellular systems, joint detection by a network entity appears even more questionable, as some BSs can cooperate without expensive backhaul (see Chapter 4), rendering centralized DAS even more attractive.

In the case of less crosscoupling between cells in Plot 3.14(b), the benefit of IRC and an arbitrary assignment of UEs to BSs of course diminishes, and the general gain of CoMP is less. However, we can now see that DIS schemes already allow us to achieve more than half of the possible CoMP gains, while requiring less backhaul than the sum rate achieved over the radio interface. Considering practical quantization schemes, it is beneficial to use a hybrid DIS/DAS approach, even in regimes of large backhaul. A frequently occurring example of such a hybrid approach is the case where centralized DAS concepts are used between two BSs, while the third BS is supplied with or provides decoded data bits. In general, we can see that cell-center scenarios are more backhaul-expensive than cell-edge scenarios, as the weak interference links render the usage of backhaul inefficient. If pure DAS schemes are

used, the backhaul required is on the order of 1.6 bits for each bit of data (assuming best possible quantization and source coding), or on the order of about 3.5 bits for each bit of data (assuming practical quantization), to obtain 90% of CoMP gains. The results are summarized in Table 4.2 at the end of Chapter 4.

3.3.8 Summary

In this section, we have observed the potential gains through uplink CoMP in scenarios of up to three BSs and UEs, assuming BSs with $N_{\text{bs}} = 2$ receive antennas each. We have seen that especially in the largest observed scenario, rate gains can be on the order of 70% to 90%, even though we incorporate into our calculations the detrimental effect of imperfect channel knowledge. In fact, we have observed that CoMP can partially mitigate the effects of imperfect CSI. We have further analyzed various BS cooperation schemes w.r.t. the achievable rate/backhaul trade-off, and can conclude that

- Centralized DAS schemes are mainly beneficial in regimes of strong interference, especially in cases of strong, asymmetrical interference. As these schemes are the only ones that can exploit all advantages of CoMP (i.e. spatial multiplexing, array and interference cancellation gain), centralized DAS schemes are always superior in regimes of large backhaul.
- Decentralized BS cooperation schemes (DIS, CIF or decentralized DAS) are interesting in regimes of weak, possibly asymmetrical interference and low backhaul. Here, CIF becomes relevant in cases of very weak interference, and decentralized DAS plays a role for very weak and symmetrical interference. As the differences between the schemes are quite subtle, and DIS appears most promising for practical implementation, we consider DIS as a good representative for decentralized BS cooperation schemes. We have also shown that DIS gains ground towards centralized DAS in regimes of larger SNR.
- Iterative BS cooperation schemes have shown to yield only marginal benefits in terms of rate/backhaul trade-off. Hence, it is usually better to exchange signals between BSs once, using a reasonable extent of backhaul, than to split the backhaul into multiple information exchanges. This aspect will be discussed further in Section 5.1.4.
- With Monte Carlo simulations, it has been shown that adaptive/hybrid DIS/DAS approaches can be highly beneficial in regimes of moderate interference. Further, the achievable rate/backhaul trade-off can be significantly improved if sophisticated quantization / source coding concepts are employed. Network DAS schemes or FDM have been shown to be of little interest and are hence omitted in the remainder of this work.

In total, we have shown that in uplink CoMP in a scenario with $M = K = 2$, we are operating in a regime of about 3.5 bits of backhaul per sum rate bit, if 90% of the total CoMP gain is to be achieved. Note that this ratio can easily double in practical systems, where the actually achieved data rates are significantly lower than the information theoretic values considered here [MKF06]. Significant reductions of this ratio are possible if more sophisticated quantization and source coding schemes are employed in cell-edge scenarios, or hybrid DIS/DAS are employed in cell-center scenarios, where 50% of the possible CoMP gain can be obtained with about 0.8 bits of backhaul per sum rate bit.

3.4 Downlink Analysis

In this section, we investigate the capacity gains that are generally possible through CoMP in the downlink (within clusters of no more than 3 cooperating cells), and observe the rate/backhaul trade-off of the BS cooperation schemes UMC, QSC and DAS introduced in Section 2.3.5 for different channels. We derive basic, qualitative thresholds according to which a system should ideally adapt between different cooperation strategies, and highlight the overall potential of backhaul reduction in the downlink. In particular, we address the following questions:

1. What are the capacity gains we can expect to achieve through CoMP in the downlink, and what is the impact of per-antenna power constraints on the sum rate or common rate of the UEs? Further, what is the impact of imperfect CSIT and CSIR in the downlink? \longrightarrow see Section 3.4.1
2. What is the performance of the downlink CoMP schemes introduced in Section 2.3.5 for specific or arbitrary channel examples, and in which interference and backhaul regimes are which schemes superior? \longrightarrow see Sections 3.4.2 and 3.4.4
3. Is there a benefit in terms of the rate/backhaul trade-off of transmitting a superposition of non-cooperatively and cooperatively transmitted messages? \longrightarrow see Section 3.4.3
4. Does it make sense to adaptively switch between different cooperation concepts, and on which thresholds should this adaptation be based? \longrightarrow see Section 3.4.5
5. To which extent are downlink CoMP schemes affected by the channel orthogonality or background noise level? \longrightarrow see Section 3.4.6
6. How do the schemes perform in scenarios with $M = K = 3$? \longrightarrow see Section 3.4.7

A summary of the analysis results for the downlink will be given in Section 3.4.8.

3.4.1 Capacity Gains through CoMP in the Downlink

As in the uplink, let us initially consider a scenario with $M = K = 2$ and $N_{\text{bs}} = 2$, for which a representative channel matrix was defined in (3.10). We assume that two messages \check{F}_1 and \check{F}_2 are to be transmitted to the two UEs, respectively. We want to observe the gains that are possible through cooperation, which we do by computing either the *sum rate* $f_s(\check{\mathcal{R}})$ or the *common rate* $f_c(\check{\mathcal{R}})$ of the two UEs for certain channel realizations for either infinite cooperation among BSs or no cooperation at all.

In the case of infinite BS cooperation, all transmit antennas can be used for the transmission to both UEs, hence we are observing a BC with imperfect channel knowledge. The rate region $\check{\mathcal{R}}_\infty$ is then taken from (2.62) in Section 2.3.3.

In the case of no cooperation, we have to consider 4 different assignments of UEs to BSs, represented by variable $\mathbf{m} \in \{1, 2\}^{[2 \times 1]}$. This determines which BS antennas can be used for the transmission to which UE, captured in variable Ψ , as defined in Section 2.3.4. If both UEs are served by the same BS, then the BS can perform local DPC, as it knows both messages to be transmitted to the UEs. In this case, the transmission to one of the two UEs can be encoded non-linearly, such that it can be decoded by the UE as if there was no interference from the transmission to the other UE at all. The relation between \mathbf{m} and Ψ is illustrated for two of the four BS-UE assignments in Table 3.1, and the rate region $\check{\mathcal{R}}_0$ is taken from (2.67) in Section 2.3.4.

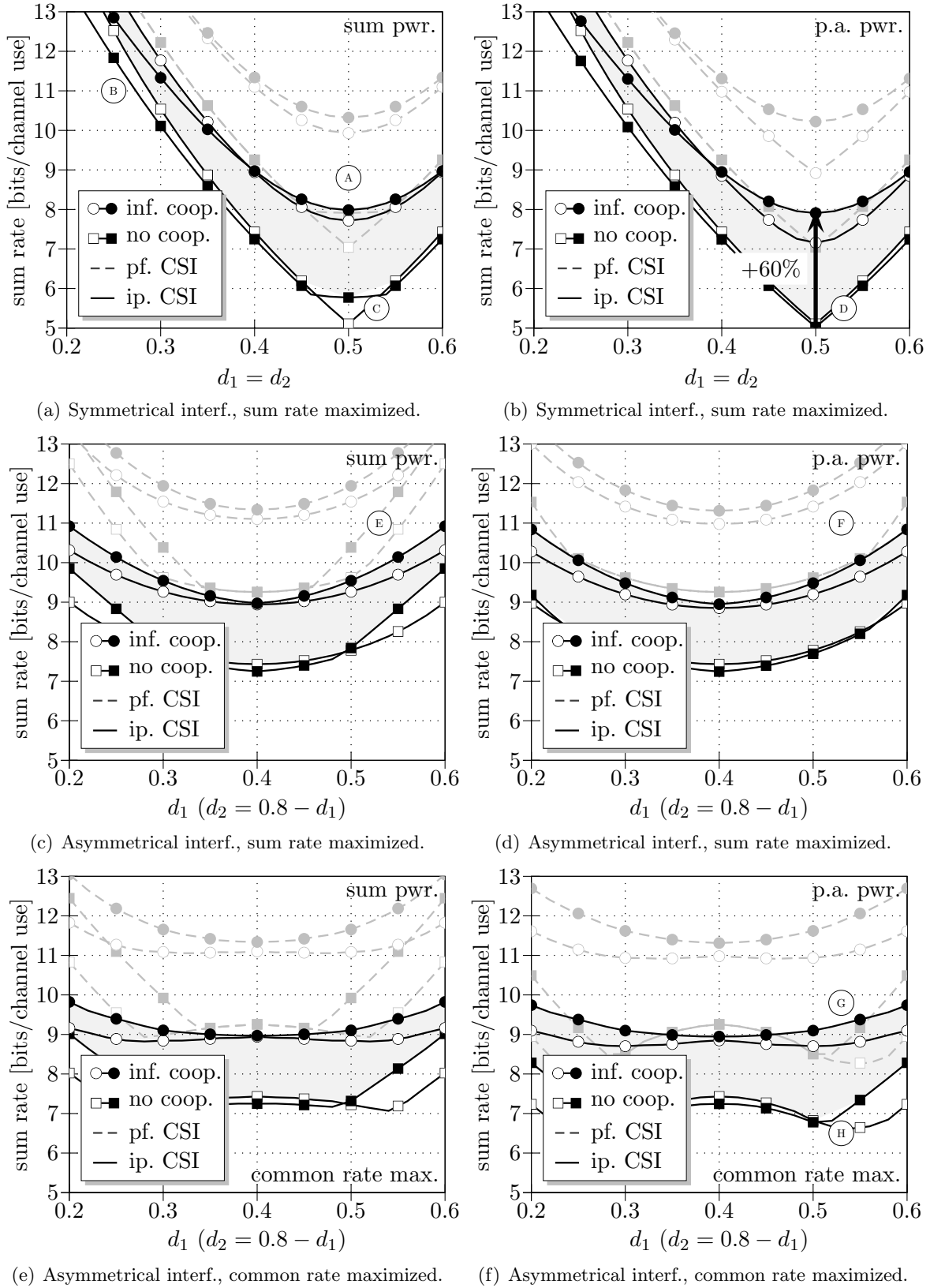
Both UEs served by their BS	$\mathbf{m} = \begin{bmatrix} 1 \\ 2 \end{bmatrix}$	$\Psi = \begin{bmatrix} 1 & 0 \\ 1 & 0 \\ 0 & 1 \\ 0 & 1 \end{bmatrix}$	No DPC possible
Both UEs served by BS 1	$\mathbf{m} = \begin{bmatrix} 1 \\ 1 \end{bmatrix}$	$\Psi = \begin{bmatrix} 1 & 1 \\ 1 & 1 \\ 0 & 0 \\ 0 & 0 \end{bmatrix}$	Local DPC possible

Table 3.1: Relation between BS-UE assignment \mathbf{m} and Ψ for non-coop. DL transmission.

Let us now observe simulation results in Figure 3.15. In all plots, we show the sum rate achievable without BS cooperation (based on $\check{\mathcal{R}}_0$) and infinite BS cooperation (based on $\check{\mathcal{R}}_\infty$). As in Section 2.3.5, filled-out markers mean that DPC is considered (where applicable), whereas hollow markers denote linear precoding techniques. We observe a SISO SNR of 10 dB at the cell edge, motivated by system level simulations in Chapter 4, and hence choose $\sigma^2 = 0.1$, assuming the transmission of one BS antenna at unit power and the fact that the channel at this UE location is normalized to unit gain according to (3.8). Based on an analysis of practical channel prediction and CSI feedback schemes in Appendix E, we further choose $N_p = 2$ and $N_b = 6$. In all plots on the left side, we consider a sum power constraint with $\check{P}^{\max} = 2$, whereas on the right side we have a per-antenna power constraint with $\check{\mathbf{P}}^{\max} = 0.5 \cdot \mathbf{I}$, such that the overall sum power budget in both cases corresponds to unit power per BS. Besides the before mentioned observation of imperfect CSIT and CSIR, we also provide results for perfect CSI at both sides of the link, i.e. $N_p = N_b = \infty$.

In Plots 3.15(a) and 3.15(b), the *sum rate* of the UEs is maximized, and we observe *symmetrical* interference cases, moving both UEs equally from their cell center ($d_k = 0.2$) to the cell-edge ($d_k = 0.5$) and slightly beyond ($d_k = 0.6$). As our model allows the assignment of UEs to BSs to be swapped, the results are symmetrical around $d_k = 0.5$. Clearly, the sum rate at the cell-edge (A) (with or without cooperation) is significantly lower than when the UEs are in their cell centers (B), as the links suffer from strong signal attenuation due to the fairly large path-loss exponent θ , which is *not* compensated via power control as in the uplink. We can see that regardless of the extent of CSI available, we have a gain of about 1 bpcu/user at the cell-edge through cooperation. This rather small gain is due to the fact that each BS is equipped with $N_{bs} = 2$ transmit antennas and can hence already perform *interference-aware* local beamforming [HS07] without BS cooperation (note that such a scheme requires multi-cell CSI at the BSs, but no exchange of messages \check{F}_k). With cooperation, the slightly better orthogonality of the overall channel matrix and an additional array gain can be exploited.

At the cell center, we see that DPC is inferior to linear precoding under limited CSI (B). This is due to the inner capacity bounds that we have derived for linear or non-linear precoding in Section 2.3.2. If the UEs are at the cell-center, where the inter-cell links are weak and hence difficult to estimate, this detrimental aspect then outweighs the actual benefit of DPC, namely the possibility of pre-cancelling a certain extent of interference. An optimal transmission scheme would of course adapt between linear and non-linear techniques, but our results suggest that in the channel scenarios considered here, DPC generally only appears marginally attractive, taking into consideration the complexity of any practical scheme approaching DPC. This is due to its sensitivity to imperfect CSI and the fact that in the case

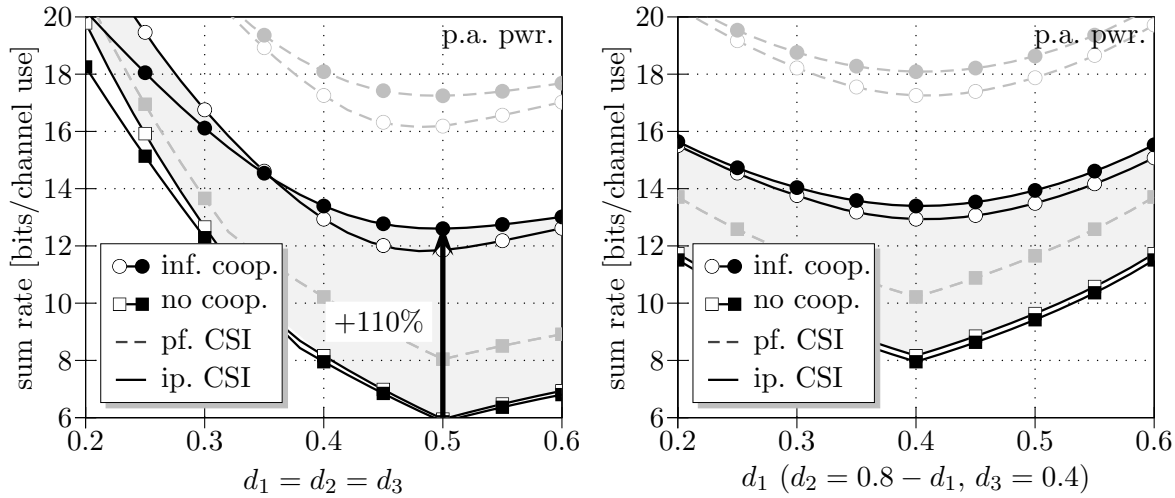
Figure 3.15: CoMP gain in downlink scenarios with $M = K = 2$ of average orthogonality.

of moderate cooperation, the system of 4 transmit antennas already offers enough degrees of freedom to spatially separate the users well enough through linear precoding. One advantage of DPC techniques, though, is that these can help mitigate the impact of per-antenna power constraints. We can see when comparing Plots 3.15(a) and 3.15(b) that the performance of linear precoding schemes is degraded by per-antenna power constraints, while DPC performance remains almost constant [MF08a]. Finally, we can see in Plot 3.15(a) that DPC outperforms linear schemes in the case of no cooperation and a cell-edge scenario (C). Here, both UEs are served by the same BS, such that local DPC can be applied. This only makes sense in the context of a sum-power constraint, as then one BS can transmit to both UEs at double power, while the other BS is simply turned off. In the case of per-antenna power constraints, this implies giving up transmit power, which is not attractive (D). This aspect leads to the fact that under a per-antenna power constraint, the gain through cooperation is even larger (about 60% rate improvement under imperfect CSI at the cell-edge).

In Plots 3.15(c) and 3.15(d), we now observe *asymmetrical* interference cases, where one UE is moved towards the cell-edge, while the other is moved towards the cell-center. For $d_1 < 0.3$ or $d_1 > 0.5$, we are now looking at scenarios where both UEs are close to the same BS. Under a sum-power constraint and perfect CSI, we can see that non-cooperative rates strongly grow when the UEs approach one of the BSs (E). In this case, both UEs can be served by the same BS, and the performance of both linear precoding and DPC is good due to the large SNR at this point. As expected, this phenomenon is not so dominant any more under limited CSI, and in particular under per-antenna power constraints, where turning one BS off would again mean sacrificing transmit power (F). Under infinite BS cooperation, there is hardly any impact of per-antenna power constraints, suggesting that cooperation is a good mean to overcome such power constraints.

While the results in Plots 3.15(a)-3.15(d) were based on a maximization of the *sum rate* of the UEs, Plots 3.15(e) and 3.15(f) now consider a maximized *common rate*. While both optimization metrics obviously lead to the same result for symmetrical interference scenarios, maximizing the common rate in asymmetrical scenarios means shifting transmit power towards (and possibly using a BS cooperation scheme in favor of) the weaker UE, and hence trading off sum rate for fairness. This *instantaneous* fairness can be interesting for applications where a certain SINR has to be guaranteed for each channel access. If it is sufficient to have fairness on a larger time-scale, we will see in Chapter 4 that it is possible to obtain long-term fairness through scheduling. Nevertheless, Plots 3.15(e) and 3.15(f) show that BS cooperation enables an almost constant common rate over all UE locations considered (G), while a non-cooperative system is rather unfair (H). Hence, also downlink CoMP can be used to improve the fairness of cellular systems.

Figure 3.16 now shows the gain of BS cooperation for a scenario with $M = K = 3$ and $N_{\text{bs}} = 2$ under a per-antenna power constraint with $\mathbf{P}^{\text{max}} = 0.5 \cdot \mathbf{I}$, again under perfect or imperfect CSIT and CSIR with the same parameters as before. We again observe a channel with moderate orthogonality, precisely with $\varphi_{Ab} = \varphi_{Bc} = \varphi_{Ca} = 2\pi/3$, $\varphi_{Ba} = \varphi_{Cb} = \varphi_{Ac} = 4\pi/3$ and $\varphi_{AB} = \varphi_{BC} = \varphi_{AC} = \pi/2$, the choice of which has been validated through Monte Carlo simulations. In Plot 3.16(a), we consider a symmetrical scenario where all UEs are equally moved from the cell-center to the cell-edge and beyond. In Plot 3.16(b), we have an asymmetrical scenario where UE 1 is moved towards the cell-edge, while UE 2 is moved to the cell-center, and UE 3 is always placed at the same location between cell-edge and cell-center ($d_3 = 0.4$). We can make similar observations as before, but are now looking at a gain through



(a) Symmetrical interf., sum rate maximized.

(b) Asymmetrical interf., sum rate maximized.

Hollow \circ and filled \bullet markers denote linear precoding and DPC, respectively.

Figure 3.16: CoMP gain in downlink scenarios with $M = K = 3$ of average orthogonality.

cooperation of around 110% when all UEs are at the cell-edge, which is mainly due to the fact that without cooperation, each BS observes a rank-deficient channel and has too few antennas to spatially separate the UEs. When the *common rate* is considered (not shown here), we can see that cooperation also improves instantaneous *fairness* over a non-cooperative system, as observed for $M = K = 2$.

As noted before in Section 2.3.5, the performance of infinite BS cooperation in the downlink can in fact be achieved with a finite extent of backhaul. Precisely, it is sufficient if all involved BSs are supplied with all messages $\tilde{F}_1 \dots \tilde{F}_K$ to be transmitted to all UEs, and share common CSI, as we assume in general. This implies that the backhaul traffic *per BS* scales linearly with the number of cooperating BSs or, more specifically, for $M = K = 2$ the backhaul network has to carry *in total* twice the traffic of all UEs, or for $M = K = 3$ three times the traffic of all UEs. In the next section, we will see that the BS cooperation schemes introduced in Section 2.3.5 enable a further, significant reduction in backhaul traffic, but we have to keep in mind that the backhaul issue in the downlink is generally not as critical as in the uplink, due to the upper bound on the required backhaul stated before.

Impact of Imperfect CSIT and CSIR

We now investigate the sensitivity of downlink CoMP towards imperfect CSIR and CSIT in more detail. In Figure 3.17, the upper two plots show the absolute sum rates achievable for no or infinite BS cooperation at the cell-edge ($d_1 = d_2 = 0.5$) or cell-center ($d_1 = d_2 = 0.3$), under a varying number of pilots N_p or CSI feedback bits N_b . In Plot 3.17(a), the latter has been fixed to $N_b = 6$, whereas the number of pilots in Plot 3.17(b) has been fixed to $N_p = 2$. Recall that both parameter choices are motivated through the analysis of a particular channel estimation and CSI feedback scheme in Appendix E. As usual, we are operating at a SISO SNR at the cell-edge of 10 dB. Obviously, the rates tend to zero for $N_p \rightarrow 0$ or $N_{bs} \rightarrow 0$, due to our model in Section 2.2.2. In the former case, this is quite intuitive, as the lack of CSIR renders decoding impossible, while in the latter case, our model underestimates performance

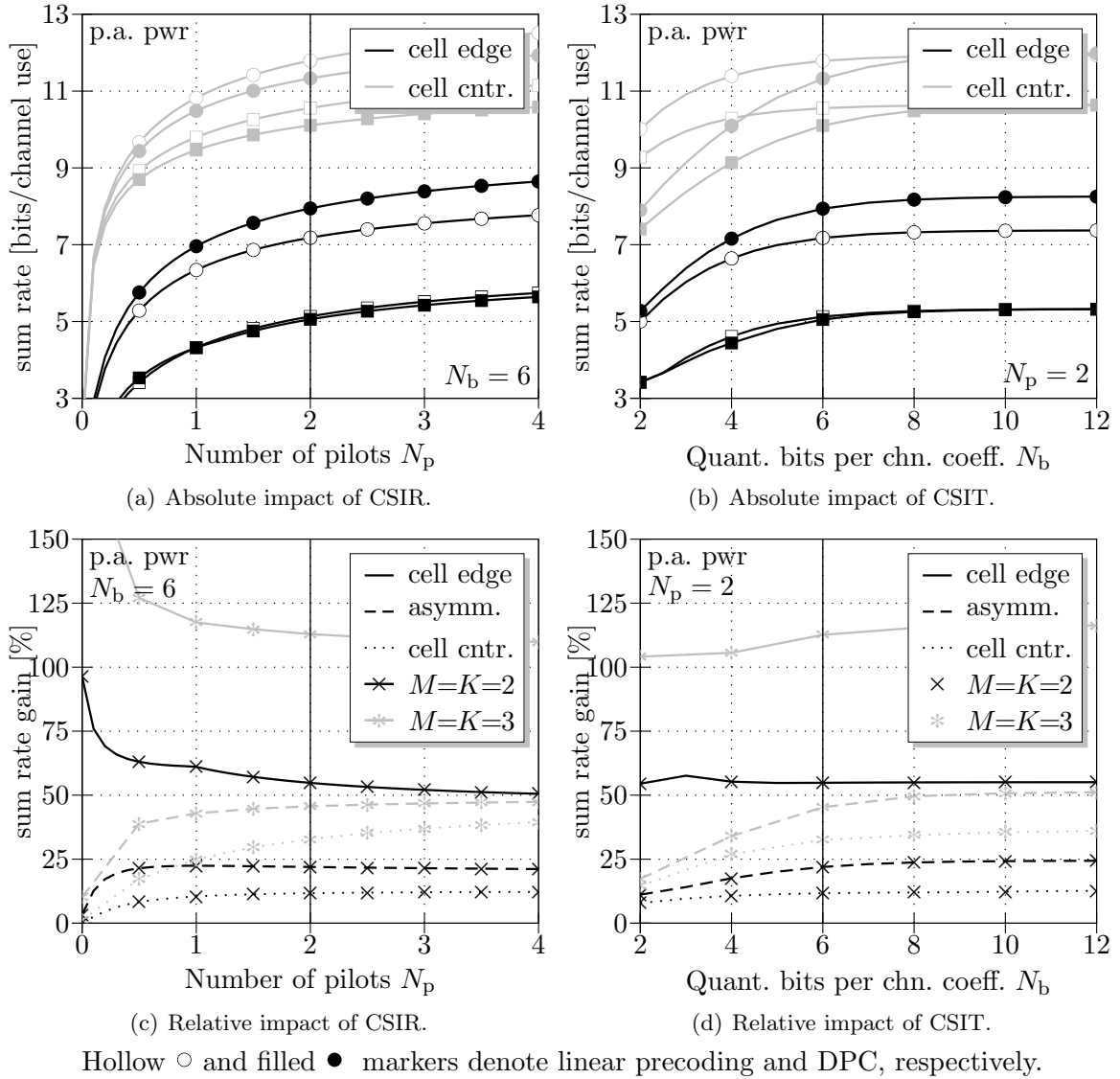


Figure 3.17: Impact of imperfect CSIT and CSIR on downlink CoMP.

for small N_b , as also discussed in Section 2.2.2. We can see in Plot 3.17(a) that our choice of $N_p = 2$ based on pilot patterns used in LTE Release 8 already leads to a strong reduction in performance, hence it could be beneficial to use a higher density of pilots³. Parameter N_b , however, already yields more than 90% of the possible CoMP performance. This shows that at least for the low UE speed and short CSI feedback delay considered in Appendix E, it is possible to obtain a large portion of downlink CoMP gain at reasonable feedback effort.

Similarly as in the uplink, Plots 3.17(c) and 3.17(d) show how the relative CoMP gain is affected by different extents of CSIR and CSIT. We can again see that BS cooperation in fact becomes more beneficial in cases of less CSIR in cell-edge scenarios, but decreases at the cell-

³Note that we always assume that $\sigma_{\text{pilots}}^2 = \sigma^2$, i.e. that channel estimation is subject to the same extent of background noise as the actual data transmission. In a practical system, channel estimation performance could most likely be further improved by using pilots that are orthogonal across large numbers of cells.

center. The right plot shows that the gain is rather independent of CSIT at the cell-center. This is due to the fact that adjusting N_b has an equal impact on all channel coefficients in our model, hence having the same effect on both CoMP schemes as also non-cooperative closed-loop transmission. One could argue that a smart CSI feedback concept should invest more quantization bits into those links that are more relevant for CoMP, rendering the whole situation different. This, however, would go beyond the scope of this thesis.

We can summarize the observations in this section as follows:

- BS cooperation offers the strongest performance gains when all UEs are located at the cell-edge, with 60% improvement for $M = K = 2$ and 110% improvement for $M = K = 3$ for moderately orthogonal channels, under per-antenna power and imperfect CSI.
- Within our regime of interest, the relative cooperation gains appear to remain the same or even increase with the decrease of CSI.
- DPC suffers from imperfect CSI especially when interference links are weak, but can mitigate the effects of per-antenna power constraints.
- BS cooperation can improve instantaneous fairness by offering a similar common rate over a wide set of UE locations.
- For the number of cooperating cells considered in this work, the backhaul infrastructure has to carry maximum three times the traffic delivered to the UEs, which shows that the backhaul issue is not as crucial in the downlink as it is in the uplink.

3.4.2 Performance of Downlink CoMP Schemes for Specific Channels

Knowing that the required backhaul in the downlink is clearly upper-bounded, we now want to explore the improved rate/backhaul trade-offs that can be achieved through the BS cooperation schemes UMC, QSC and DAS introduced in Section 2.3.5. As in the uplink analysis in this chapter, we are only interested in the *sum backhaul* required in addition to a non-cooperative system. As a non-cooperative reference system, we consider the case where for each UE $k \in \mathcal{K}$ only exactly one BS $m \in \mathcal{M}$ is provided with the corresponding message \check{F}_k . For the scenarios observed in this chapter, we can simplify the models from Section 2.3.5 in the following way:

Time-share between no and Infinite Cooperation (TS)

If the available sum backhaul is less than that required for infinite BS cooperation, the most straight-forward approach is to operate on a time-share between no and infinite BS cooperation, the latter of which is illustrated for $M = K = 2$ in Figure 3.18(a). In this case, the performance region can be stated as the convex hull around tuples of rates achievable with no cooperation, and tuples of rates achievable with infinite cooperation and a backhaul greater or equal to the UE sum rate, i.e.

$$\check{\mathcal{Z}} = \bigcup \{ \langle \mathbf{r}, \beta \rangle : (\mathbf{r} \in \check{\mathcal{R}}_0) \vee (\mathbf{r} \in \check{\mathcal{R}}_\infty \wedge \beta \geq \mathbf{r}^T \mathbf{1}) \}, \quad (3.41)$$

Unquantized Message based Cooperation (UMC)

For most channels, a better rate/backhaul trade-off can be achieved if BSs can selectively participate in the transmission to certain UEs. If a BS is involved in the transmission to a UE k , this means that the network needs to provide message \check{F}_k to the corresponding BS. For our small scenarios, we can reduce the range of variable \mathbf{C} introduced in Section 2.3.5 to

$$\mathbf{C} \in \mathcal{C}^{\text{UMC}} = \{0, \infty\}^{[2 \times 2]} \quad \text{and} \quad \mathbf{C} \in \mathcal{C}^{\text{UMC}} = \{0, \infty\}^{[3 \times 3]} \quad (3.42)$$

for $M = K = 2$ and $M = K = 3$, respectively. For $M = K = 2$, this cooperation scheme is illustrated in Figure 3.18(b). We here already have $2^{MK} = 16$ possibilities, of which only 9 are meaningful, as at least one BS must be involved into the transmission to a UE k to achieve a non-zero rate for this UE. As mentioned in Section 2.3.5, we do not consider DPC in the context of UMC. The reason is that DPC requires all BSs involved in the transmission to a UE k benefiting from DPC to know the corresponding message \check{F}_k , and to have a reasonable common knowledge of the interference to be canceled. This would require observing many special cases, which is tedious, and we will also see later that UMC is mainly superior to a simple time-share between no and infinite cooperation in the regime of weak interference. In this regime, however, we have already shown in Section (3.4.1) that DPC performs badly. Obviously, the definition of \mathbf{C} in (3.42) includes the cases of no cooperation and infinite cooperation as a subset, and implicitly covers all possible assignments of UEs to BSs. The performance region can then be stated as $\check{\mathcal{Z}}^{\text{umc}}$ with

$$\check{\mathcal{Z}}^{\text{umc}} = \bigcup_{\mathbf{C} \in \mathcal{C}^{\text{UMC}}} \left\{ \langle \mathbf{r}, \beta \rangle : \mathbf{r} \in \check{\mathcal{R}}^{\text{umc}}(\mathbf{C}) \wedge \beta \geq \sum_{k=1}^K \sum_{m=1}^M \min(r_k, c_{m,k}) - \mathbf{r}^T \mathbf{1} \right\} \quad (3.43)$$

where the term $-\mathbf{r}^T \mathbf{1}$ assures that the conventional case where each BS m is provided with only the message \check{F}_m corresponds to zero backhaul. $\check{\mathcal{R}}^{\text{umc}}(\mathbf{C})$ can be simplified from (2.71).

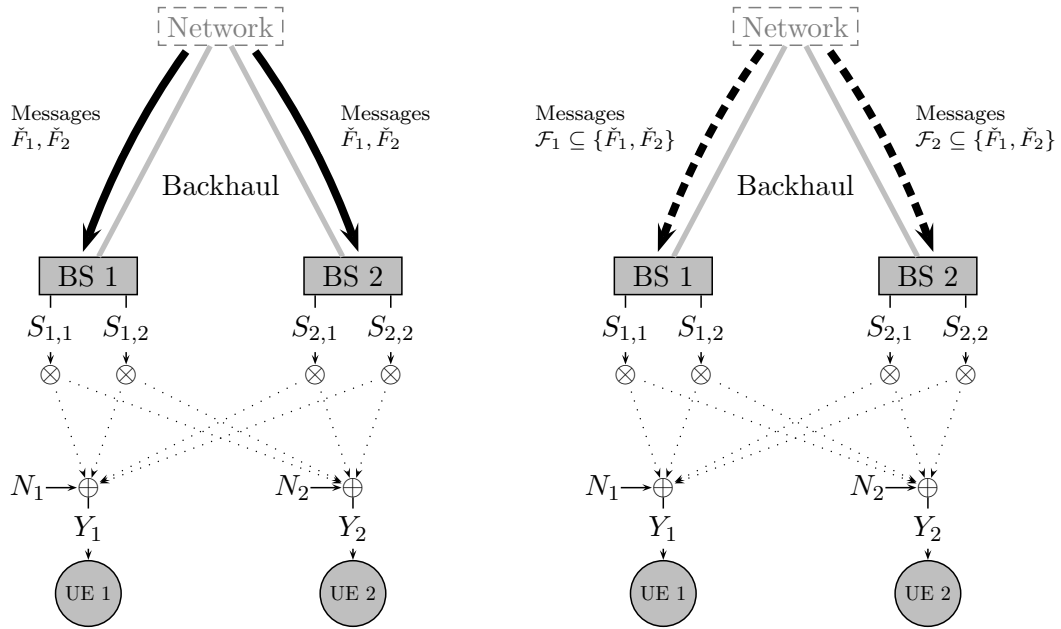
Quantized Sequence based Cooperation (QSC)

While UMC constrains a BS to have either full or no information about a message \check{F}_k , QSC allows BSs to be provided with *quantized* messages $q_c(\check{F}_k)$ employing c quantization bits per channel access⁴. For our considered scenarios, we capture the choice of quantization resolutions through variables

$$\mathbf{C} \in \mathcal{C}^{\text{QSC}} = \mathbb{R}_0^+[2 \times 2] \quad \text{and} \quad \mathbf{C} \in \mathcal{C}^{\text{QSC}} = \mathbb{R}_0^+[3 \times 3] \quad (3.44)$$

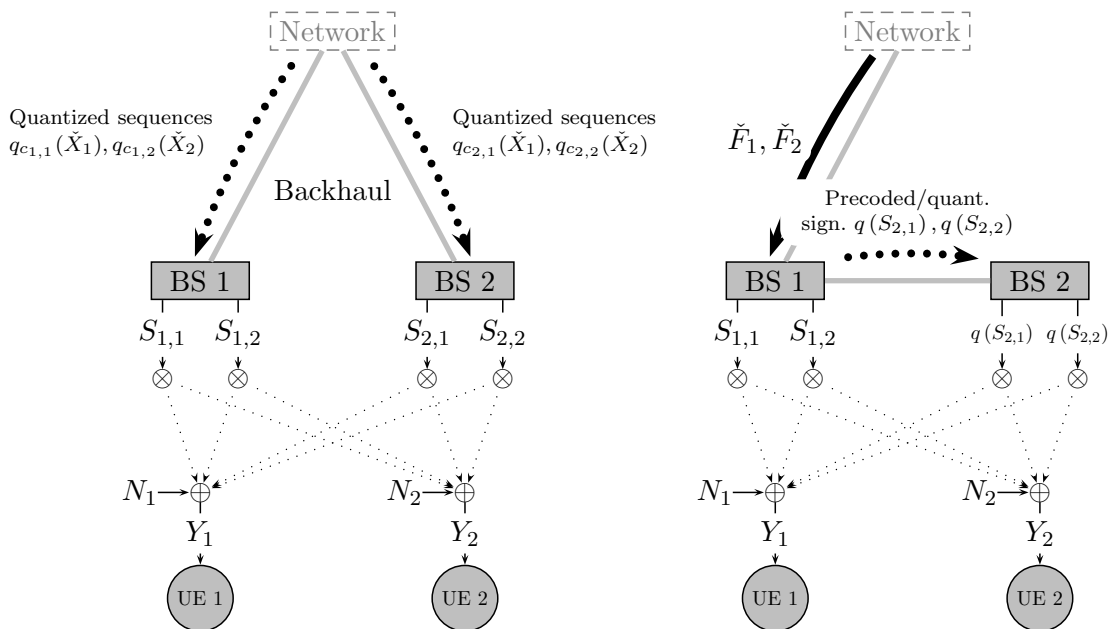
for the 2-cell and 3-cell case, respectively. Clearly, for each message \check{F}_k , at least one BS should be provided with full knowledge of the message. Furthermore, it is generally not beneficial to employ more quantization bits than the rate of the message itself, hence the set of reasonable values for \mathbf{C} is strongly limited. The performance region $\check{\mathcal{Z}}^{\text{qsc}}$ connected to QSC within our small scenarios is again given as in (3.43), except that \mathbf{C} is now taken from \mathcal{C}^{QSC} . QSC is illustrated for $M = K = 2$ in Figure 3.18(c).

⁴Note that different from the uplink, we can here connect a certain number of backhaul bits to each quantization process, as source coding concepts are not applicable.



(a) Infinite BS cooperation.

(b) UMC: Both BSs have knowledge on arbitrary subsets $\mathcal{F}_1, \mathcal{F}_2$ of messages.



(c) **QSC**: BSs have quantized knowledge on sequences \tilde{X}_1 and \tilde{X}_2 .

(d) **DAS**: One BS knows both \tilde{F}_1 and \tilde{F}_2 , and forwards precoded, quantized signals to the other BS.

Figure 3.18: Downlink CoMP schemes for $M = K = 2$ analyzed in this chapter.

Distributed Antenna System (DAS)

We finally observe the case where one of the BSs is provided with all messages \check{F}_1, \check{F}_2 (and for $M = K = 3$ also \check{F}_3), performs precoding, and forwards quantized transmit signals to the other BSs, as depicted in Figure 3.18(d) for $M = K = 2$. As the BS has knowledge of all messages, DPC is possible, and analog to UMC and QSC, parameter \mathbf{C} is now constrained to

$$\mathbf{C} \in \mathcal{C}^{\text{DAS}} = \left\{ \begin{bmatrix} \infty & \infty \\ \gamma & \gamma \end{bmatrix} \right\} \cup \left\{ \begin{bmatrix} \gamma & \gamma \\ \infty & \infty \end{bmatrix} \right\}, \quad \gamma \in \mathbb{R}_0^+ \quad (3.45)$$

for the case of $M = K = 2$ and

$$\mathbf{C} \in \mathcal{C}^{\text{DAS}} = \left\{ \begin{bmatrix} \infty & \infty & \infty \\ \gamma_1 & \gamma_1 & \gamma_1 \\ \gamma_2 & \gamma_2 & \gamma_2 \end{bmatrix} \right\} \cup \left\{ \begin{bmatrix} \gamma_1 & \gamma_1 & \gamma_1 \\ \infty & \infty & \infty \\ \gamma_2 & \gamma_2 & \gamma_2 \end{bmatrix} \right\} \cup \left\{ \begin{bmatrix} \gamma_1 & \gamma_1 & \gamma_1 \\ \gamma_2 & \gamma_2 & \gamma_2 \\ \infty & \infty & \infty \end{bmatrix} \right\}, \quad (3.46)$$

with $\gamma_1, \gamma_2 \in \mathbb{R}_0^+$ for the case of $M = K = 3$. Note that in the latter case, we constrain ourselves to scenarios where one BS takes over the role of a master BS and forwards precoded and quantized signals to both other BSs. A degree of freedom lies in the number of quantization bits chosen for each of the other BSs. The performance region for DAS within our small scenarios is then given as

$$\check{\mathcal{Z}}^{\text{das}} = \bigcup_{\mathbf{C} \in \mathcal{C}^{\text{DAS}}} \left\{ \langle \mathbf{r}, \beta \rangle : \mathbf{r} \in \check{\mathcal{R}}^{\text{das}}(\mathbf{C}) \wedge \beta \geq N_{\text{bs}} \left(\sum_{m=1}^M c_{m,1} - \max_m c_{m,1} \right) \right\}. \quad (3.47)$$

Note that in (3.47), we treat ∞ as an arbitrarily large, but finite number.

Numerical Results

We now provide numerical results on the different downlink CoMP schemes. Figure 3.19 shows the maximum sum rate as a function of backhaul for selected example channels. In general, the plots on the left side refer to a channel of moderate orthogonality, i.e. $\varphi_{Ab} = \varphi_{Ba} = \varphi_{AB} = \pi/2$, while on the right side, we observe channels with $\varphi_{Ab} = \varphi_{Ba} = \pi/4$ and $\varphi_{AB} = 3\pi/4$. In the latter case, the channel orthogonality is low without BS cooperation, but the compound channel orthogonality is high, such that the gain of CoMP is over average. In all cases, we observe per-antenna power constraints with $\check{\mathbf{P}}^{\text{max}} = 0.5 \cdot \mathbf{I}$, a cell-edge SISO SNR of 10 dB, and imperfect CSIT and CSIR as before, i.e. $N_p = 2$, and $N_b = 6$. As in the uplink, we always also plot the cut-set bound, which is defined as the performance if every bit of backhaul leads to an equal increase of sum rate, until the BC performance is reached.

In Plots 3.19(a) and 3.19(b), both UEs are placed at the same location slightly closer to BS 2 than to BS 1. In this scenario, TS and DAS schemes are of particular interest (A), as we know from Section 3.4.1 that DPC is beneficial here. In general, TS schemes are attractive if the gain of CoMP as well as the sum rate under infinite BS cooperation is low. In cases of larger CoMP gain, as in Plot 3.19(b), DAS schemes can become (marginally) superior (B), yielding a better rate/backhaul trade-off in a regime of moderate backhaul. In cases of less interference, UMC and QSC strategies become interesting (C). In Plots 3.19(c) and 3.19(d), for example, showing an asymmetrical interference channel where one UE is placed at the cell-edge, these two strategies are already superior to TS and DAS in regimes of low backhaul.

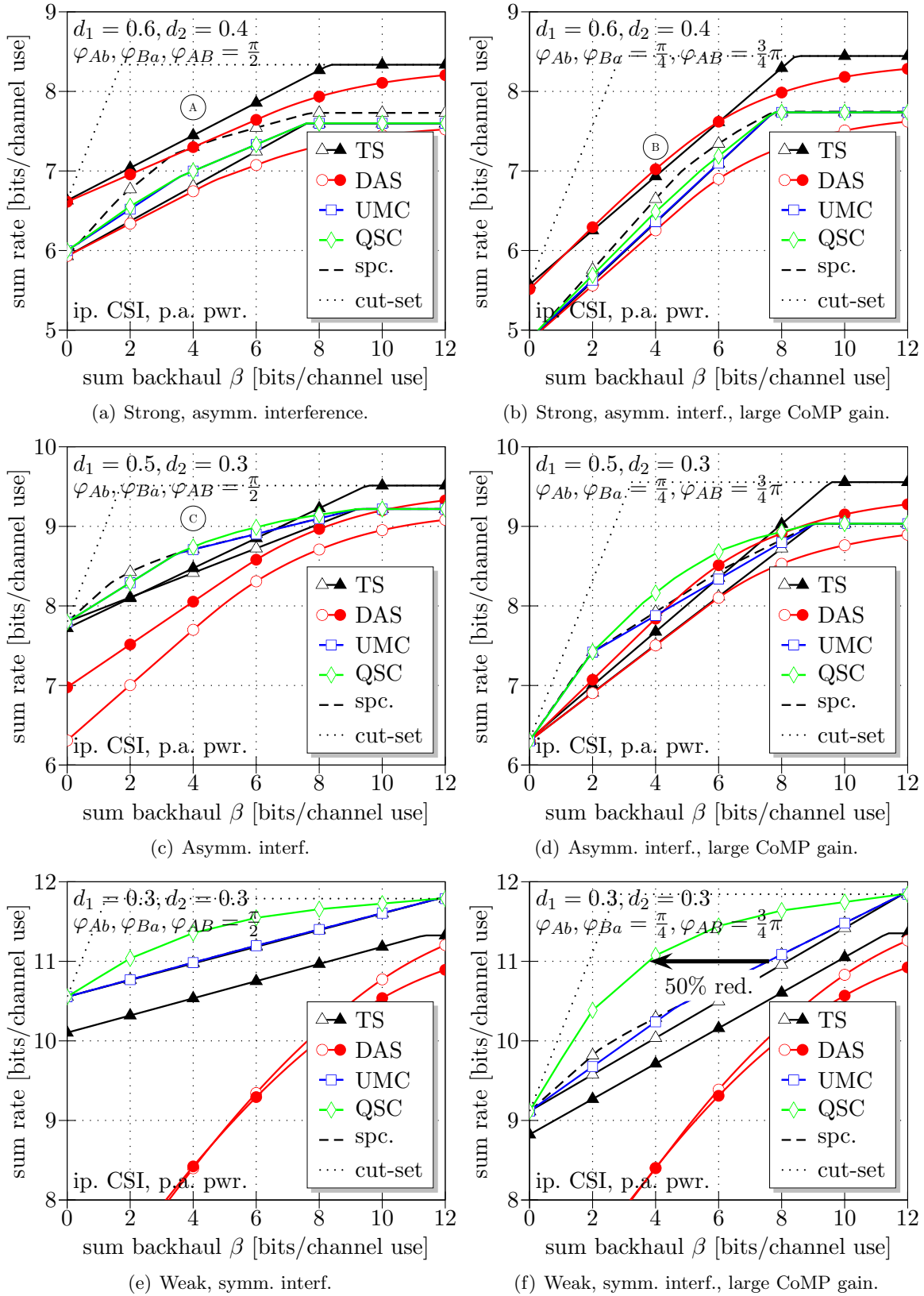


Figure 3.19: Sum rate vs. backhaul for downlink CoMP schemes and specific channels.

This is due to the fact that these schemes allow the backhaul to be invested alternately into supporting both UEs, rather than supporting both simultaneously, which becomes inefficient in regimes of weaker interference. A strong benefit of QSC becomes visible in Plots 3.19(e) and 3.19(f), where both UEs are placed in their cell-center, hence creating weak interference. Here, QSC can invest small portions of backhaul into supporting single UEs, assuring that the backhaul invested is in reasonable relation to the potential beamforming contribution of the weak interference links. DPC is inferior to linear precoding in these regimes due to imperfect CSIT, removing one of the main benefits from using TS and DAS concepts. In the right case, where the gain of CoMP is larger, using QSC can save up to 50% backhaul as opposed to TS (as illustrated for a target sum rate of 11 bits/channel use in Plot 3.19(f)). DAS concepts are clearly unattractive in this regime, as they introduce strong noise onto the signals originating from one BS and hence sacrifice the rate of the UE close to this BS.

3.4.3 Benefit of Superposition Coding in the Downlink

The downlink transmission model initially introduced in Section 2.3 also provides the possibility of using multiple superimposed messages per UE. This option was already used in the context of common message concepts in Section 2.3.4, and shown to enlarge the non-cooperative capacity region in the downlink in Figure 2.7. The same concept, however, can also be used to observe superimposed transmissions of conventionally and jointly transmitted messages. This appears attractive from an intuitive point of view, as a UE can for example receive a non-cooperative transmission from its assigned BS while at the same time receiving a joint transmission from 2 BSs, as for example considered in [SSSP08]. In this case, additional backhaul is only needed for the latter transmission. Interestingly, the uplink/downlink duality from Section 2.3.5 can also be used in this case. One simple way is to introduce *virtual UEs* by doubling the channel matrix in the UE dimension (i.e. $\mathbf{H}^{\text{virt}} := [\mathbf{H}\mathbf{H}]$). Each *real* UE is then expressed through one virtual UE decoding the conventionally transmitted message, and one virtual UE decoding the jointly transmitted one. Terms $\mathcal{J}_i(k)$ from Section 2.3.3 can then be defined such as to model the impact of a particular decoding order of the two desired messages (employing SIC) at each UE. While this procedure leads to a capacity region with $2K$ virtual UEs, one can then obtain the desired K -UE capacity region by simply adding the rates of the conventional and jointly transmitted message of each *real* UE. Indeed, this can lead to an improvement of the rate/backhaul trade-off, as indicated through dashed lines in Figure 3.19, in particular in cases of strong, asymmetrical interference and low backhaul. In principal, it can be beneficial to create superpositions not only between no and full cooperation, but also between arbitrary CoMP schemes, though capacity region calculation can easily become numerically intractable due to the enlarged parameter space, and has hence not been done here.

In a practical system, the usage of such superpositions appears questionable in the downlink, as this would strongly increase UE complexity, and a large portion of the benefit would be compensated by rate losses inherent in the usage of practical codes and finite block lengths with an SINR gap to capacity [FU98]. Furthermore, such concepts would be strongly sensitive to link adaptation, and would most likely require an increased pilot overhead, as each UE would have to estimate the effective channel resulting from (local or joint) precoding for each superimposed message it is supposed to decode. In the remainder of this work, we will hence omit downlink cooperation concepts based on superposition coding.

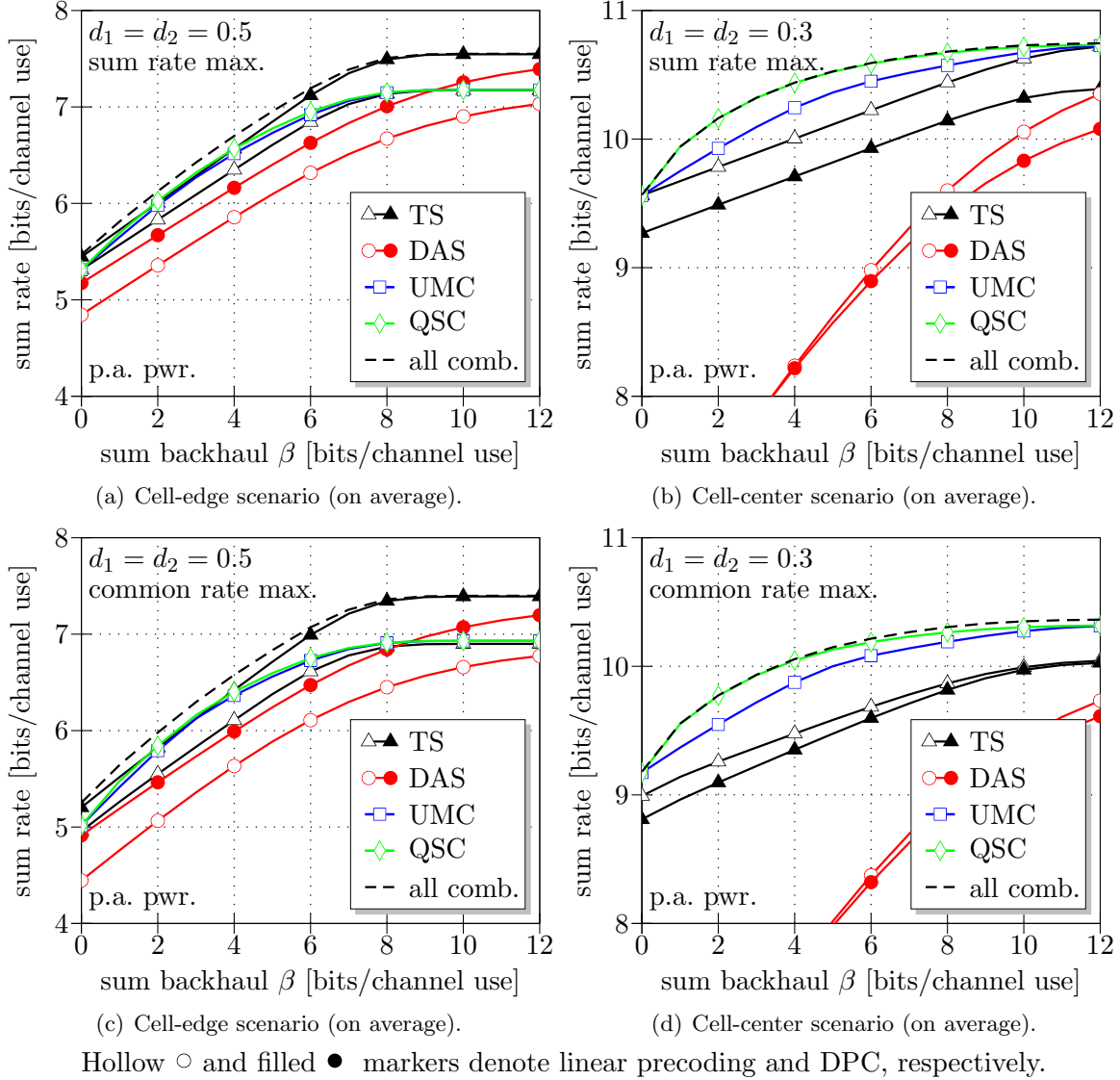


Figure 3.20: Monte Carlo simulation results for $M = K = 2$ in the downlink.

3.4.4 Performance of Downlink CoMP Schemes for Arbitrary Channels

To assure that the example channels from the last section are representative for the channel realizations that can occur under fast fading, we observe Monte Carlo simulation results for scenarios of $M = K = 2$ in Figure 3.20. Similarly to the Monte Carlo simulations performed in the uplink, the matrix coefficients are independently drawn from a zero-mean complex Gaussian distribution, so that (for $N_{\text{bs}} = 2$)

$$\forall m \in \{1, 2\}, k \in \{1, 2\} : E \{ |h_{2(m-1)+1,k}|^2 \} = E \{ |h_{2m,k}|^2 \} = \lambda_{m,k} \quad (3.48)$$

where $\lambda_{m,k}$ depends on the average UE distances to their BSs, and is computed as in (3.8). To capture the benefit of adaptively switching between CoMP strategies, we also consider all schemes combined, where the performance region is simply the convex hull around those of all cooperation schemes considered. In the upper two plots, the *sum rate* of the UEs

has been maximized, whereas the lower two plots refer to a maximization of *common rate*. We can basically draw the same conclusions as in Section 3.4.2, showing that the exemplary channels before have indeed captured the main advantages and disadvantages of the compared BS cooperation schemes. In cell-edge scenarios (see Plots 3.20(a) and 3.20(c)), a time-share between no and infinite BS cooperation (TS) is superior to all other schemes, and adaptation yields only marginal benefit. This is different when the UEs are placed in the cell-center on average (see Plots 3.20(b) and 3.20(d)), where UMC and especially QSC can exploit weak interference more efficiently. Note that QSC can effectively reduce the required backhaul by a factor of 2, while achieving almost BC performance. An adaptive approach is now of course useless, as QSC is always superior to UMC, and DAS and TS not of interest in this scenario, anyway. Plots 3.20(c) and 3.20(d) show another benefit of UMC and QSC, namely the possibility to promote fairness. This can be seen by the fact that a larger performance gap appears between QSC, UMC schemes and TS, DAS, when the common rate is of interest.

3.4.5 Choice of Best Cooperation Scheme

The previously discussed aspects are observed from a different perspective in Figure 3.21, where the best cooperation strategy is stated as a function of UE locations and/or available backhaul. As in Section 3.4.2, the plots on the left side refer to a moderately orthogonal channel, whereas those on the right side refer to a channel with an over-average gain through CoMP. As QSC contains UMC as a subset and is hence always superior to UMC (but more complex), we select QSC only in those cases where the sum rate is at least 5% larger than that of UMC. Furthermore, in order to emphasize the value of adaptively switching between schemes, we show hatched areas where one group of strategies (TS or DAS) is more than 5% better in terms of sum rate than the remaining strategies (UMC or QSC), or vice versa.

In Figures 3.21(a) and 3.21(b), we have fixed the sum backhaul to 3 bits/channel use and show the best cooperation strategy for different values of d_1 and d_2 . Clearly, both plots are symmetrical both w.r.t. a line $d_1 = d_2$ (as the UE indices can simply be swapped) and a line $d_1 = 0.5 - d_2$ (as the BS indices can be swapped). As discussed before, UMC and QSC are beneficial in regimes of low interference (where QSC becomes especially valuable in regimes of very low interference), whereas DAS is best for scenarios of strong, asymmetrical interference. We can see that especially in the right case, where the CoMP gain is large, switching between schemes is beneficial, whereas in the left case, performing a time-share between no and infinite cooperation (TS) performs well for most interference cases. The *direction* of BS cooperation, as investigated in the uplink, is of minor interest in the downlink, as we assume that the BSs are generally provided with messages by the network. Only in the case of DAS, signal exchange over the backhaul takes place directly between BSs. In this case, we can easily see that the sum rate is maximized if the BS with the stronger link to the involved UEs performs preprocessing, equivalent to our observations in the uplink in Section 3.3.5.

Plots 3.21(c) and 3.21(d) show the best possible scheme as a function of symmetrical interference power and achievable sum rate, whereas Plots 3.21(e) and 3.21(f) show the same for *asymmetrical* interference cases. As in the uplink, each black line within the areas indicates one bit of backhaul, and thick lines indicate 10 bits of backhaul. In all cases, we can clearly see that the fully cooperative sum rate can be achieved if the amount of backhaul corresponds to this sum rate. In the case of moderate channel orthogonality, it appears beneficial to adapt between UMC and TS. The reason for this is mainly because the former scheme provides a

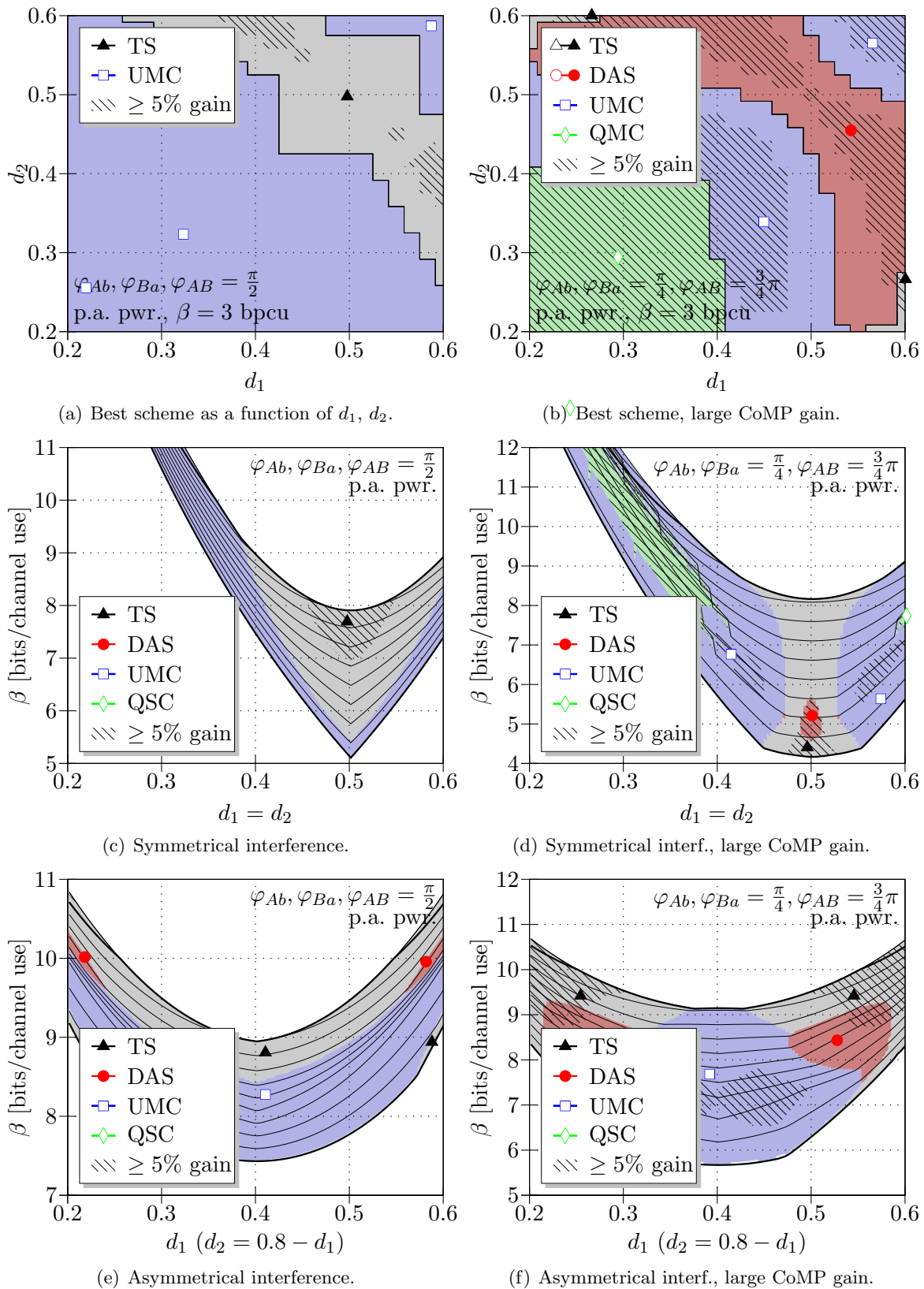


Figure 3.21: The best choice of BS cooperation scheme in downlink CoMP.

slightly better rate/backhaul trade-off, while the latter enables DPC, which is beneficial in regimes of strong crosscoupling. For channels with a stronger CoMP gain, it is beneficial to use DAS concepts in regimes of asymmetrical interference and moderate backhaul, or UMC concepts otherwise. QSC can give an additional, significant gain in regimes of very weak interference and a low or moderate extent of backhaul, as we have seen before. Clearly, the plots show that benefit of switching between cooperation strategies in the case of $M = K = 2$ as rather limited, as opposed to in the uplink. This will be different when we observe Monte Carlo simulations for large scenarios in Section 3.4.7, as then UMC and QSC schemes allow an effective adaptation of the cooperation strategy to the channel.

3.4.6 Sensitivity of Schemes to Channel Orthogonality and SNR

Analogous to our uplink analysis, we now investigate the sensitivity of the downlink CoMP schemes to the channel orthogonality and the extent of background noise. We assume the same parameters connected to imperfect CSIT and CSIR as before (SISO cell-edge SNR of 10 dB, $N_p = 2$ and $N_b = 6$), and that a fixed extent of backhaul $\beta = 4$ is available in the sequel. Plots 3.22(a) and 3.22(b) show sum rates achievable for different channel orthogonalities, for symmetrical, i.e. $d_1 = d_2 = 0.3$, and asymmetrical scenarios, respectively. As in Section 3.3.6, the channel orthogonality as seen by the BSs without cooperation is increased from left to right, while the additional compound orthogonality is decreased. Clearly, the CoMP gain is largest if the local channel orthogonality is low, but the compound orthogonality is large, and this is also the regime where we expect UMC and QSC schemes to be superior to TS and DAS concepts ^(A). In cases of stronger, asymmetrical interference, DPC concepts start becoming interesting ^(B), especially if a low compound channel orthogonality deteriorates the performance of linear precoding schemes. As observed in Section 3.4.2, DAS schemes become interesting in asymmetrical scenarios, particularly in cases where the CoMP gain is large ^(C).

Plots 3.22(c) and 3.22(d) show the performance of different CoMP strategies as a function of SNR. As in the uplink, we normalize achievable rates such that they can be observed relative to the performance achievable with no or infinite BS cooperation. As we have observed linear precoding schemes to be superior under imperfect CSI in cell-center scenarios in Section 3.4.1, the left plot is normalized to the performance without DPC. Here, we can see that the gap between QSC and other strategies such as UMC and TS is largest for regimes of moderate SNR. This is due to the following two phenomena: For low SNR, the sum rates in general are low, such that TS schemes become efficient. For high SNR, however, we know from rate-distortion theory that for each SNR increase of 3 dB, we need an additional bit of backhaul to ensure that the ratio of quantization noise over thermal noise stays constant. UMC schemes are also of particular interest only in regimes of moderate SNR, as in the high SNR regime, the extent of residual interference not cancelable through UMC becomes more dominant compared to thermal noise. In the scenario of stronger, asymmetrical interference shown in Plot 3.22(d), all schemes are normalized to the performance of no or infinite BS cooperation using DPC, as this is superior here. We can see that the gap between DPC and linear precoding decreases for increasing SNR ^(D), as then linear precoding concepts such as ZF asymptotically achieve BC performance. Otherwise, similar observations can be made as in the weak interference case, except that TS and DAS schemes are significantly more attractive now ^(E).

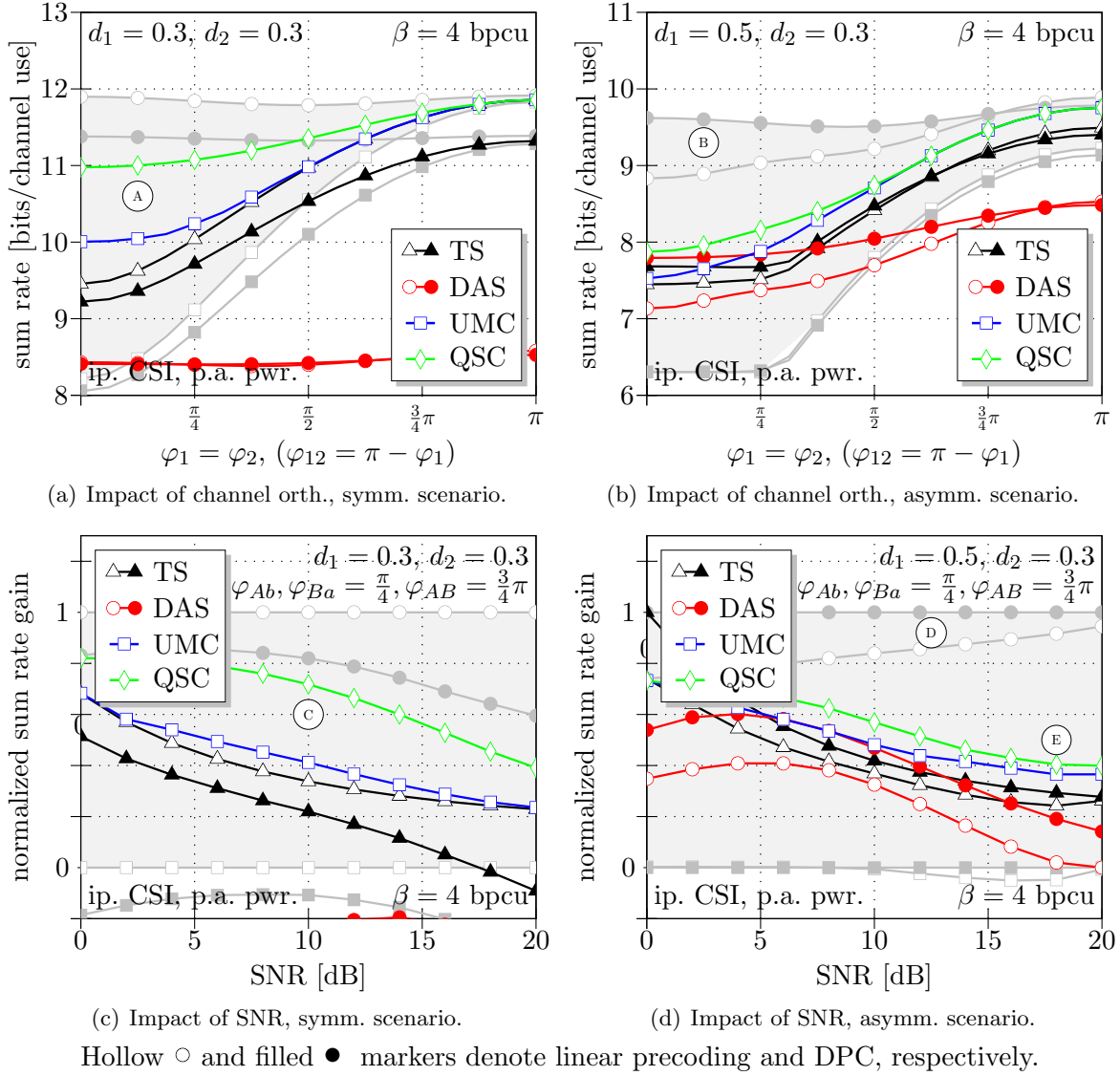
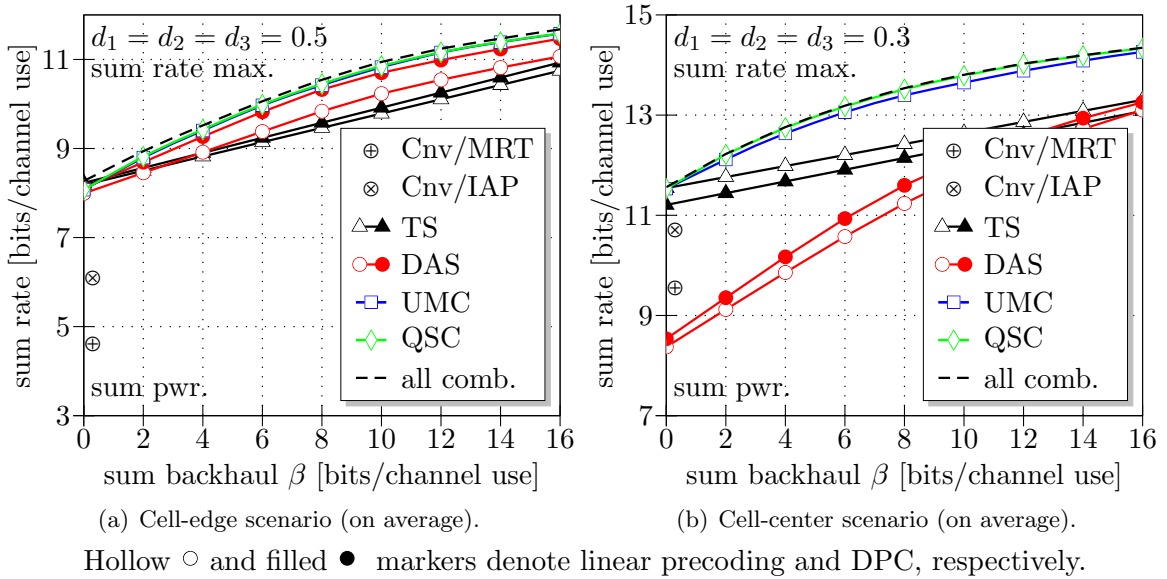


Figure 3.22: Impact of channel orthogonality and SNR on downlink CoMP schemes.

3.4.7 Performance of Downlink CoMP Schemes in Scenarios with $M = K = 3$

We now observe the performance of the downlink BS cooperation schemes for scenarios with $M = K = 3$ and $N_{\text{bs}} = 2$. As we have noted for the uplink, the number of parameters required to representatively characterize a channel becomes large in this case. We hence use Monte Carlo Simulations to obtain results averaged over a large number of randomly generated channel matrices \mathbf{H} according to (3.48). We can see the results in Figure 3.23, where we observe a cell-edge scenario in plot 3.23(a), and a cell-center scenario in plot 3.23(b). Note that we here assume a sum-power constraint with $\tilde{P}^{\max} = 3$, as simulations of channels of this dimensionality otherwise become tedious, and we know from our previous analysis that the impact of per-antenna power constraints almost equally affects all BS cooperation schemes. As usual, we assume a cell-edge SISO SNR of 10 dB and imperfect CSIR and CSIT with $N_p = 2$ and $N_b = 6$.



Hollow \circ and filled \bullet markers denote linear precoding and DPC, respectively.

Figure 3.23: Monte Carlo simulation results for $M = K = 3$ in the downlink.

Similarly as for the uplink results presented in Section 3.3.7, we here also include conventional schemes into the comparison. For example, we consider a scheme where each UE k is served by its dominant BS $m = k$ through *maximum ratio transmission* (MRT), hence where the precoding vector \mathbf{w}_k is chosen as the Hermitian of the channel between the BS and the UE, normalized to unit power. This scheme can make use of array gain (subject to imperfect CSIT), but basically ignores the fact that the chosen precoder might lead to strong interference for a UE in an adjacent cell. As an improved scheme, we consider the case of conventional transmission, but this time performing *interference-aware precoding* [HS07] (IAP), where the precoders are computed to optimize the non-cooperative sum rate based on (2.67) in Section 2.3.4. Note that all other schemes also incorporate an arbitrary assignment of UEs to BSs, hence they can already achieve better sum rates than a conventional system without requiring backhaul. This is strongly visible in the case of $d_1 = d_2 = d_3 = 0.5$, as they enable local precoding with DPC if multiple UEs are served by the same BS. More precisely, in the cell-edge scenario, average sum rates can be improved from 4.6 bpcu by 32% to 6.1 bpcu, and by another 32% to 8.1 bpcu with a flexible BS-UE assignment. The gain through using IAP is much larger in the downlink than that of the uplink counterpart IRC, due to the fact that the downlink does not use power control. Investing into backhaul can bring another sum rate improvement of about 51% in the asymptotic regime of large backhaul. Here, the rate/backhaul trade-off can be reduced significantly from 1.8 sum rate bits per backhaul bit to a ratio of 1.3 using UMC instead of a time-share between no and full BS cooperation (TS).

In a cell-center scenario, the gains through CoMP are obviously strongly reduced, and the benefit of IAP is less. Here, however, UMC can further reduce the backhaul required for cooperation, as compared to TS. For instance, 50% of the possible CoMP gains can already be obtained requiring only 0.5 bits of backhaul for each bit of sum rate. The additional gain through using QSC, however, is small, as UMC in this scenario already provides many degrees of freedom of adapting the cooperation scheme to the channel. The key results are summarized in Table 4.2 at the end of Chapter 4.

3.4.8 Summary

In this section, we have observed the potential gains through downlink CoMP in scenarios of up to three BSs and UEs, assuming BSs with $N_{\text{bs}} = 2$ receive antennas each. We have seen that in the largest observed scenario, rate gains can be on the order of 50% to 110%, which is similar to the gains observed in the uplink. Though absolute rates of course decrease strongly with imperfect CSI at the UE side, we have seen that the gain of cooperation actually increases with decreasing CSI at the UE, and is fairly independent of the number N_b of bits used for feeding back each channel coefficient to the BS side. The backhaul issue, however, is not as problematic as in the uplink, as the backhaul required in addition to that of a non-cooperative system corresponds to at most two times the sum rate of all jointly served UEs in the case of $M = K = 3$. The rate/backhaul trade-off can be further improved through the usage of different BS cooperation schemes, where we have made the key findings that

- DAS schemes are only interesting in few scenarios of strong, asymmetrical interference, such that the general usage of such schemes appears questionable.
- UMC schemes appear best over a wide set of channels, though (at least according to the considered model) they cannot provide any DPC gain. These schemes are also superior from an implementation point of view, as they do not involve any signal quantization.
- In cases of weak, symmetrical interference, QSC schemes can provide an additional gain over UMC, as they allow to employ approximate beamforming over links that are too weak to invest large quantities of backhaul. In a setup with $M = K = 3$, however, the gain over UMC appears marginal.
- In theory, there can be a benefit of using a superposition of conventionally and cooperatively transmitted messages, but a significantly increased UE complexity and other issues make the usage of such schemes in practical systems appear questionable.

In general, we have shown that in downlink CoMP in scenarios with $M = K = 3$, it is possible to operate in a regime of about 1.3 bits of backhaul for each bit of throughput if UMC schemes are applied, instead of a ratio of 1.8 for a time-share between no and full cooperation (in both cases aiming at 90% of possible CoMP gains).

Chapter 4

System Level Simulation

In this chapter, the gain of CoMP and the trade-off between throughput and required backhaul for different base station cooperation schemes is evaluated in the context of large cellular systems. Novel clustering and resource partitioning concepts are introduced as one approach to extract reasonably sized CoMP setups from a cellular system. We observe that these yield strong spectral efficiency gains and substantial fairness improvements over non-cooperative systems, while posing moderate requirements on the backhaul infrastructure.

4.1 Simulation Setup

In this chapter, we generally consider a cellular system consisting of 57 cells or sectors, laid out in a hexagonal pattern as depicted in Figure 4.1. As typical for most practical deployments, groups of three cells are served from BSs co-located at so-called *sites*, such that three-fold sectorization with corresponding antenna patterns is employed. We assume two antennas with orthogonal polarization per BS, such that uncorrelated fast fading can be assumed [NEBP02]. As in a typical urban scenario, an *inter-site-distance* (ISD) of 500 m is used. As shown in the diagram, we assume that there is a logical backhaul mesh between all sites, i.e. each site is connected to its adjacent neighbors at least through a logical backhaul link. BSs belonging to the same site are assumed to have infinite backhaul connectivity, as these are typically located in the same server room. We will see later that this has a strong impact on our results, as major CoMP gains can already be achieved without an expensive inter-site backhaul infrastructure.

4.1.1 Channel Model

The simulations in this work are based on an implementation of the 3GPP *spatial channel model* (SCM) [3GP09] provided by [SDS⁺05], which is commonly used for simulations connected to LTE and LTE-Advanced. The model provides a framework for calculating path losses based on a flat-plane model, and fast fading based on a scattering model with particular power delay profiles. Such models tend to yield more pessimistic results w.r.t. the number of weak interferers (i.e. the background interference floor) seen by each transmission as compared to a practical urban signal propagation, while underestimating strong interferers [SJ09]. This is due to the fact that in urban areas, building structures obstruct a large portion of the background interference, while some near interferers can become even more dominant

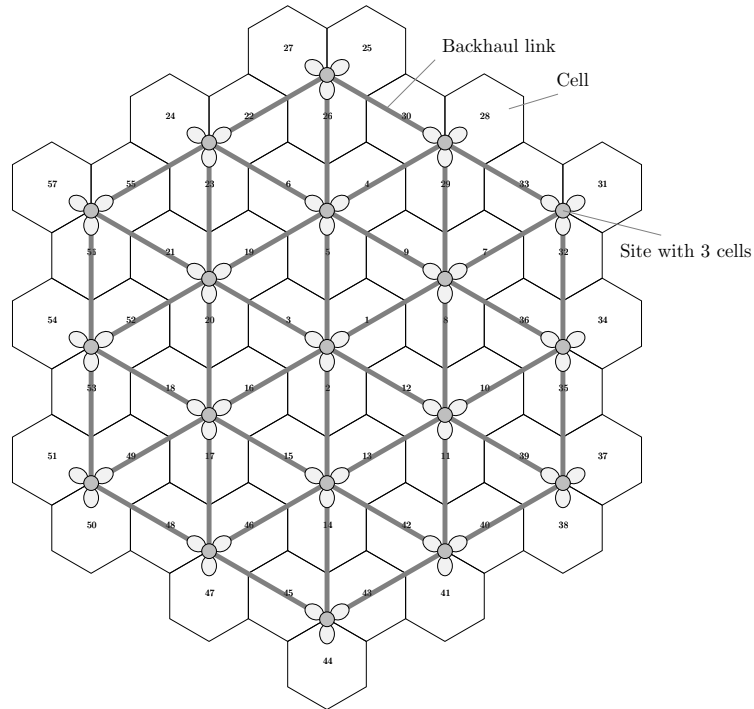


Figure 4.1: Cellular setup considered for system level simulations.

through signal reflection in street corridors, in effect reducing the path loss exponent. For this reason, the model used in this work has been adjusted such that links with a distance of more than 600 m (hence interferers outside the first two tiers of neighboring cells) are attenuated by an additional 3 dB, and those longer than 1200 m by an additional 3 dB. This approach is similar to that used in WINNER channel models [WIN03], where different path loss exponents are used beyond certain thresholds of distance. We do *not* consider shadow fading for a reason that will be explained in Section 4.5. To limit the complexity of our simulations, we only compute one channel realization per *transmit time interval* (TTI) and per *physical resource block* (PRB), consisting of 12 sub-carriers, which corresponds to the granularity of the scheduler. The main simulation parameters are summarized in Table 4.1.

4.1.2 Simulation Flow

All results presented in this chapter are based on a large number of *user drops*, where 570 UEs are generated with equal probability density over the complete simulation area of 57 cells, leading to an average of 10 UEs per cell. For each user drop, UEs are initially assigned to clusters of cells based on the average path loss over time. A user drop is repeated if there is a cluster with less UEs in it than the number of cells it spans. For each user drop, 12 statistically independent fast fading realizations are calculated (by choosing a large UE speed in the SCM), and the UE throughput is observed under a proportional fair scheduler. The independence of the fast fading realizations allows us to emulate the behavior of a system with channels slowly changing over many fading realizations, while only a subset of these need to be computed. As some particular assumptions are made w.r.t. scheduling and power

System Setup	
Number of sites / cells	19 / 57, employing three-fold sectorization
Number of terminals	570, equally distributed
Inter-site-distance	500 m
Backhaul topology	Logical mesh between adjacent BSs
Media Access Scheme (OFDMA)	
System bandwidth	5 MHz
FFT Size	512
Sub-carrier spacing	15 kHz
Symbol rate	14 kHz
Scheduler granularity	1 PRB (=12 sub-carriers) \times 1 TTI (=1 ms)
Number of usable PRBs	25
Channel Model	
Model used	SCM (urban macro)
Number of paths / sub-paths	8 / 20
Pathloss [dB]	$130.5 + 37.6 \cdot \log_{10}(d[\text{km}])$, assuming $f_c = 2.6$ GHz
Additional attenuation	3 dB for links > 600 m, +3 dB for links > 1200 m
Shadow fading	not used
Number of antennas	2 per BS, 1 per UE, assumed uncorrelated
BS antenna pattern (angle-dependent path loss)	$A(\theta)_{\text{dB}} = \min \left[12 \left(\frac{\theta}{\theta_{3\text{dB}}} \right), 30\text{dB} \right]$, $\theta_{3\text{dB}} = 70$
Antenna gain	14 dBi (BS), 0 dBi (UE)
BS / UE Characteristics	
BS transmit power	43 dBm (sum power over both antennas)
Max. UE transmit power	24 dBm
Noise floor (incl. rx noise figure)	-169 dBm/Hz (BS), -165 dBm/Hz (UE)

Table 4.1: Parameters used for system level simulations.

control, the steps taken for each user drop are described in detail in the sequel:

- **Calculation of CQI values.** For the link between each UE k and each BS m that could potentially serve this UE (according to clustering concepts explained later in Section 4.2), a *channel quality indicator* (CQI) is calculated for each TTI t and resource r . This value takes into account fast fading, but no interference, and is given as a linear SISO SNR value w.r.t. thermal noise and denoted as $\text{CQI}_{k,m}^{t,r}$.
- **Proportional fair scheduling** is performed based on instantaneous CQI values of infinite resolution. A scheduler, being responsible for one cluster of M cells, faces the problem of assigning a set of UEs \mathcal{K} to a set of resources \mathcal{R} . In order to achieve a full reuse factor of 1, each resource has to be assigned to exactly M terminals. In each TTI t , the scheduler calculates a metric for each potential UE to be scheduled, each resource, and each BS $m \in \mathcal{M}$, calculated as

$$\text{METRIC}_{k,m}^{t,r} = \frac{\log_2 \left(1 + \text{CQI}_{k,m}^{t,r} \right)}{\sum_{t'=t-6}^{t-1} \text{TP}_k^{t'}} \quad (4.1)$$

where $\text{TP}_k^{t'}$ is the actual throughput that UE k has achieved in TTI t' . The scheduler hence bases its decision on the link quality between the BSs and the UEs, but also takes into account the previous throughput of the UEs within a certain time window to obtain proportional fairness. The following steps are then repeated until all resources have been assigned to M terminals:

1. Choose the best UE, resource and BS as

$$k^*, r^*, m^* = \arg \max_{k \in \mathcal{K}, r \in \mathcal{R}, m \in \mathcal{M}} \text{METRIC}_{k,m}^{t,r} \quad (4.2)$$

and assign the terminal to the resource.

2. Ensure that the UE cannot be assigned to the same resource again, and ensure that no other UE can be assigned to the same resource *and* the same BS, by setting

$$\forall m \in \mathcal{M} : \text{METRIC}_{k^*,m}^{t,r^*} := -\infty \quad \text{and} \quad \forall k \in \mathcal{K} : \text{metric}_{k,m^*}^{t,r^*} := -\infty, \quad (4.3)$$

ensuring that M UEs are grouped that have dominant links to different BSs. Otherwise, both non-cooperative and cooperative performance would be deteriorated.

- **Power control** (in the uplink) is also performed based on instantaneous channel measures in such a way that the mean receive power density of the UEs to all BSs within the cluster reaches a certain threshold on each assigned resource. If this exceeds the maximum transmit power of the UE of 24 dBm, the transmit power invested into all resources is equally scaled down, such that the power constraint is met with equality. For the different clustering concepts observed in this work, the target receive power is set such that in each TTI, roughly 5% of UEs operate at their transmit power limit. In the downlink, the maximum BS transmit power is equally invested into all resources.
- **Throughput calculation**, depending on the chosen cooperation scheme. Instead of observing concrete modulation and coding schemes, we here again assume Gaussian modulation, and simply multiply the lower rate bounds obtained through our models in Chapters 2 and 3 with the symbol rate. In this work, we do not consider throughput losses due to pilots, synchronization or control channel overhead, as we are interested in *relative* performance improvements and throughput/backhaul trade-offs, which are both not affected by such overhead.

The rather idealistic assumptions w.r.t. scheduling and power control based on instantaneous channel measures in conjunction with a rather simplistic scheduler have been chosen to ensure that different clustering and CoMP concepts are not given an a priori scheduling advantage. We will see later in Section 5.2.3 that scheduling for CoMP remains an extensive research topic yet to be fully addressed.

In all cases of CoMP, the operation point on the constrained capacity region is chosen that maximizes instantaneous sum rate, while long-term fairness is obtained via scheduling. For all schemes that require backhaul, the rate/backhaul trade-off is first calculated for each resource separately, and then the overall available backhaul is successively invested into the resources that provide the largest gradient of sum rate improvement over backhaul increase. This corresponds to the approach proposed in [MF07c, MF07b, MF07a], where the backhaul is invested first into the UEs that profit most.

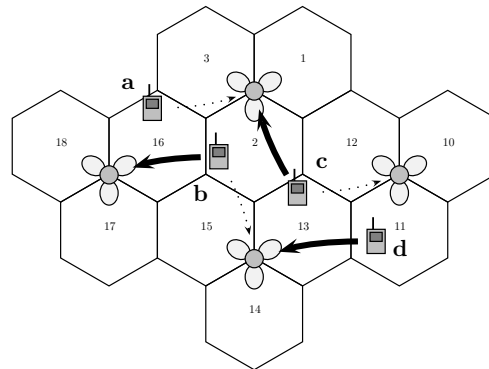


Figure 4.2: Example of a highly asymmetric uplink interference scenario.

4.2 Clustering and Resource Partitioning

In the previous chapters of this thesis, we have analyzed small CoMP setups with few cooperating BSs and UEs - for the sake of simplicity and analytical tractability. But also in a practical system, CoMP will be constrained to small cooperation sizes, mainly because

- Synchronization in time can become an issue due to signal propagation delays [KF10].
- The resources that have to be invested into orthogonal pilot sequences in uplink and downlink grow linearly with the cooperation size.
- The resources to be invested into CSI feedback for a cooperative downlink transmission grow at least linearly, or in the worst case quadratically with the cooperation size, depending on whether the number of channel coefficients fed back can be reduced (e.g. through UMC schemes), and whether the CSI feedback from all UEs can be sent on the same resources, exploiting joint detection in the uplink.
- The signaling overhead increases with increasing cooperation size, as more BSs have to agree upon (or exchange information connected to) the scheduling of users.

The question is hence: How can subsets of BSs and UEs be chosen in a cellular system, such that we obtain reasonably sized scenarios as in Chapter 3 where CoMP can be applied efficiently? Ideally, this means that we have to group UEs such that their strongest interferers are captured in the same group, while interference from outside the group is minimized. In [MF07a], it has been pointed out that this is a non-trivial problem, as interference is often of asymmetric nature. Consider, for example, the uplink scenario in Figure 4.2, where UE *a* is strongly interfered by UE *b*, but not vice versa (due to the BS antenna pattern), UE *b* is interfered by UE *c*, which itself is mainly interfered by UE *d*, while the interference in the other direction is marginal. In this case, assuring that all UEs get their strongest interferer canceled would mean that all UEs have to be jointly processed (i.e. through one joint DAS procedure spanning all four cells), or successively (i.e. through a chain of DIS steps). Whereas the first strategy would be problematic due to the large number of cells involved, the second would lead to a large latency, as each BS can only forward data after it has decoded its assigned UE. In the downlink, the situation is the same, but with reciprocal interference. With the additional constraint that the number of BSs involved must equal the number of

UEs served (otherwise resources in one cell are solely used to support UEs in other cells, hence the reuse factor is increased), this problem can become arbitrarily complex. In fact, this topic can be described through graph theory, where the UEs are the vertices, and a certain level of interference one UE poses towards another is denoted through a directed edge. An optimal, backhaul-efficient system would then aim at finding as many closed graphs with as few vertices as possible. As a practical cellular system does not have a central coordinator which can tackle such optimization problems, we need a different strategy to determine which UEs are to be jointly processed by which BSs. In principal, two approaches are thinkable:

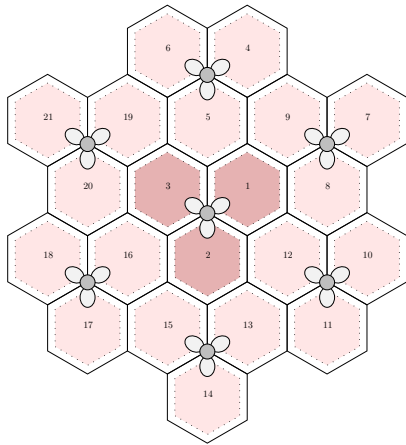
Ad-hoc cooperation between BSs [PGH08]. BSs could negotiate on a short to mid-term time scale which terminals are to be served on the same physical resources and are to be jointly processed. This would most likely require BSs to exchange basic channel information about their assigned UEs, and then agree based on some distributed decision protocol whether UEs are to be placed on orthogonal resources, in order to avoid interference, or served through CoMP. The decision process would probably also require the UEs to provide the BSs a list of the cells to which they have the strongest links (so-called *neighbor relation tables* (NRT)), as this is already done in conventional systems to facilitate hand-off procedures.

Fixed definition of cooperation areas (clusters) [MF07a, ZCA⁺08]. An alternative strategy is to pre-determine groups of BSs that are most likely to cooperate, and define an easy rule for the assignment of UEs to these groups (or *clusters*). A main benefit is that these clusters can then act almost autonomously, without requiring interaction with neighboring clusters¹. A concrete clustering concept proposed in [MF07a] foresees that each cluster has a subset of system resources that it can freely schedule to assigned UEs. Scheduling would still require an information exchange between the BSs within the cluster, but the corresponding protocol could be fixed, with one BS defined a priori as a cluster leader.

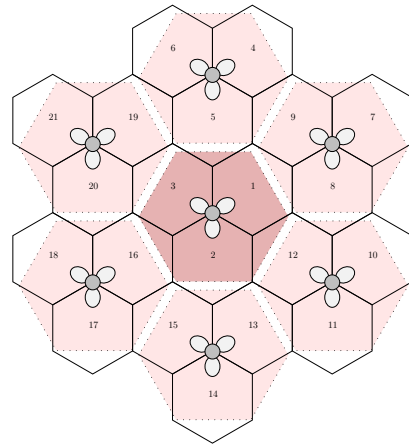
Multiple fixed clustering concepts considered in our work are illustrated in Figure 4.3, where subsets of the cellular system from Figure 4.1 are shown. Let us first pay our attention to Plot 4.3(c). Here, UEs are assigned to clusters according to the *average link quality* (or average receive power) they have w.r.t. tuples of three BSs. For example, all UEs which have stronger average links to BSs 1, 3 and 5 than e.g. to BSs {1, 2, 12} or {1, 8, 9}, are assigned to the red cluster spanning cells 1, 3 and 5. Within this cluster, the BSs can then decide on how to treat the UE, i.e. to schedule it such as to minimize interference, or to perform joint signal processing of this and other UEs. The small letters 'a', 'b' and 'c' and corresponding colors red, brown and green indicate the subsets of system resources that are assigned to the clusters, in order to assure that clusters using the same resources are maximally spaced in the system. Note that this resource partitioning does not change the overall reuse-factor of 1, as resources are split into three partitions, but at the same time each BS is involved into exactly three clusters, so that the complete system bandwidth is fully reused in each cell.

In another clustering concept shown in Plot 4.3(d), the spectrum is divided into 5 different blocks, as almost each cell edge between three adjacent cells is treated as an individual cluster. Again, the overall reuse factor of 1 is maintained, as each BS is now involved in 5 clusters. Note that in both presented clustering concepts, it is not foreseen for all three BSs located at the same site to cooperate. The reason is that this is typically not very useful due to the large back-attenuation of the simulated antennas, as we will see later.

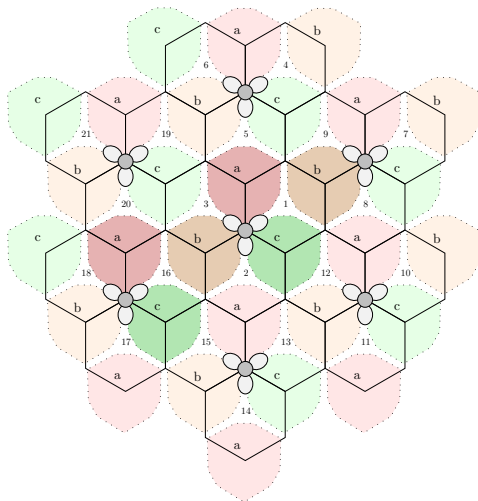
¹The only required information exchange between clusters might be for negotiating the shared usage of a common backhaul infrastructure.



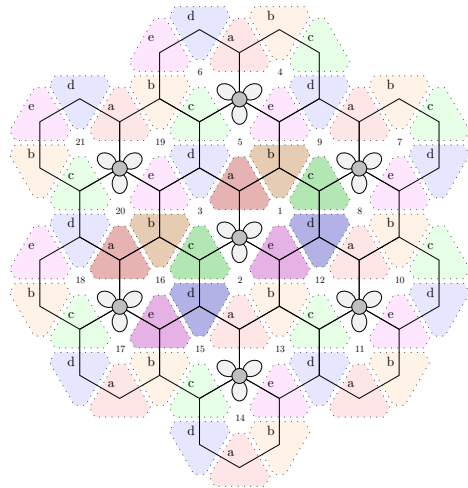
(a) Conv. system (each cell a cluster, no coop.).



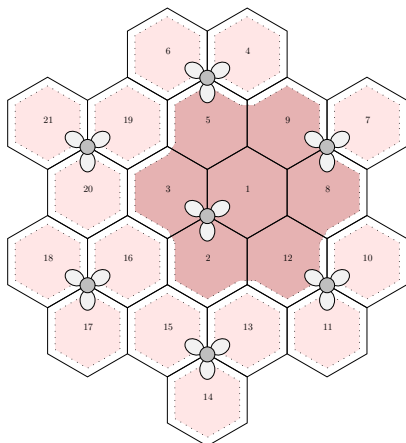
(b) Intra-site coop. (coop. size 3, no backh. req.).



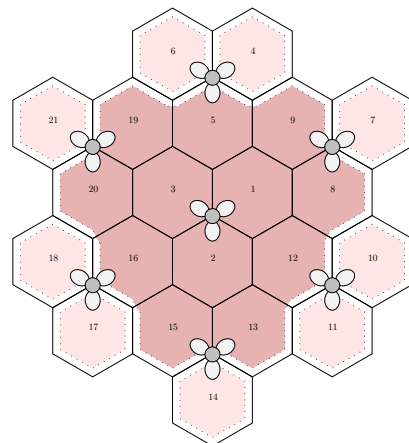
(c) Coop. between max. 2 sites (coop. size 3).



(d) Coop. between max. 3 sites (coop. size 3).



(e) Large cluster with cooperation size 7.



(f) Large cluster with cooperation size 12.

Figure 4.3: Clustering concepts compared through system level simulations.

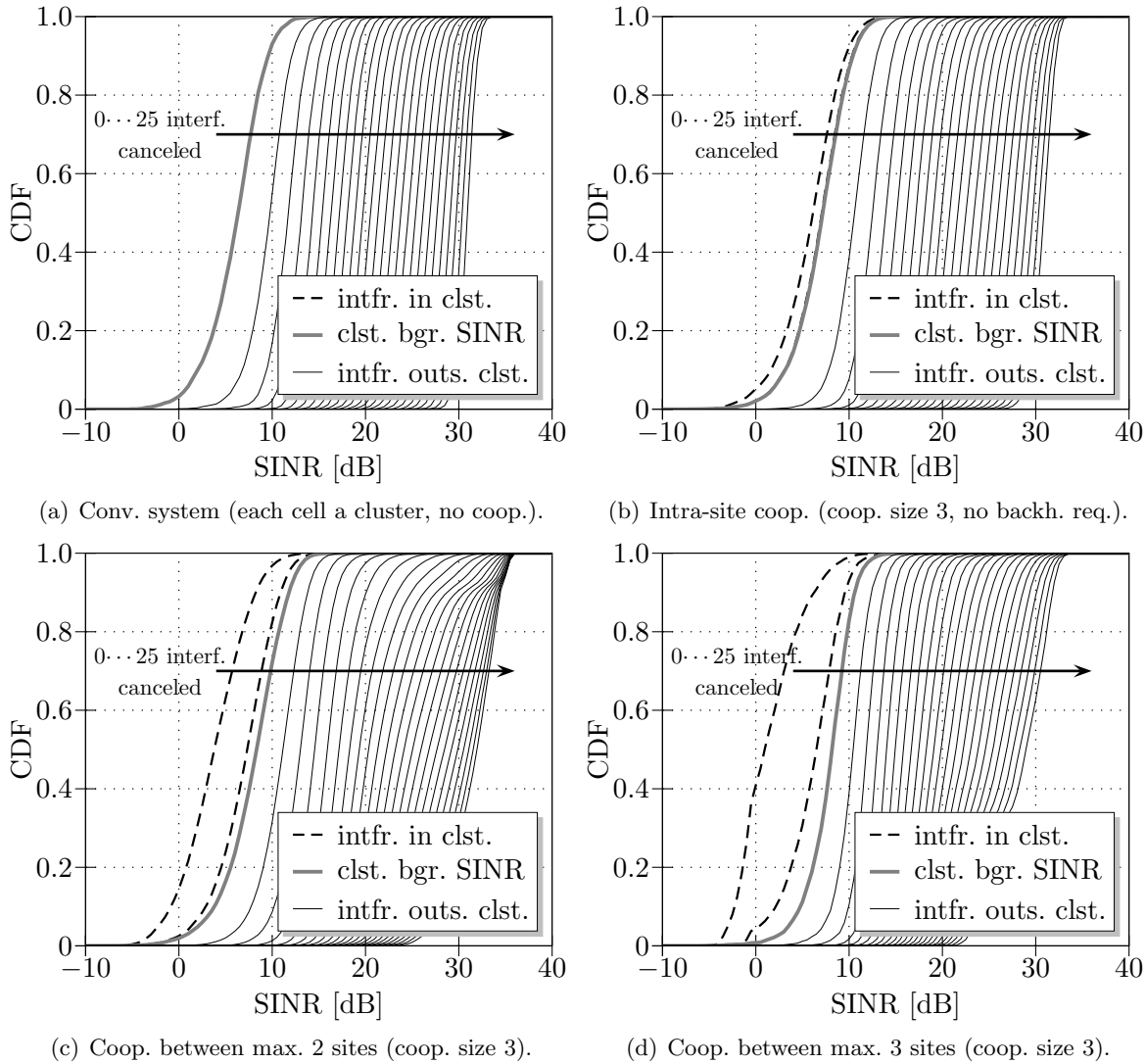


Figure 4.4: Uplink SINRs obtainable through clustering and interference cancellation.

The remaining clustering concepts in Figure 4.3 are simply for the purpose of comparison. Plot 4.3(a) shows a conventional system where each cell is a cluster by itself, hence multi-cell cooperation is not enabled. In Plot 4.3(b), all three sectors of one site are defined as a cluster within which CoMP is possible [BH07]. Even though this is inferior to inter-site cooperation, as discussed before, we here have the benefit that this cooperation does not require expensive backhaul infrastructure. Plots 4.3(e) and 4.3(f) show cases where large numbers of cells may cooperate. Such large-scale clustering concepts are of course rather unfair, as UEs in the cluster center can strongly benefit from CoMP, while users at the cluster edge might perform only marginally better than in a non-cooperative system. Still, such clustering concepts can be attractive in conjunction with scheduling, as then all UEs may profit from the increased spectral efficiency of a few UEs directly benefiting from CoMP.

In all plots in Figure 4.3, dark clusters indicate where throughput is finally evaluated, while all other clusters are simulated, scheduled etc. only to generate representative interference.

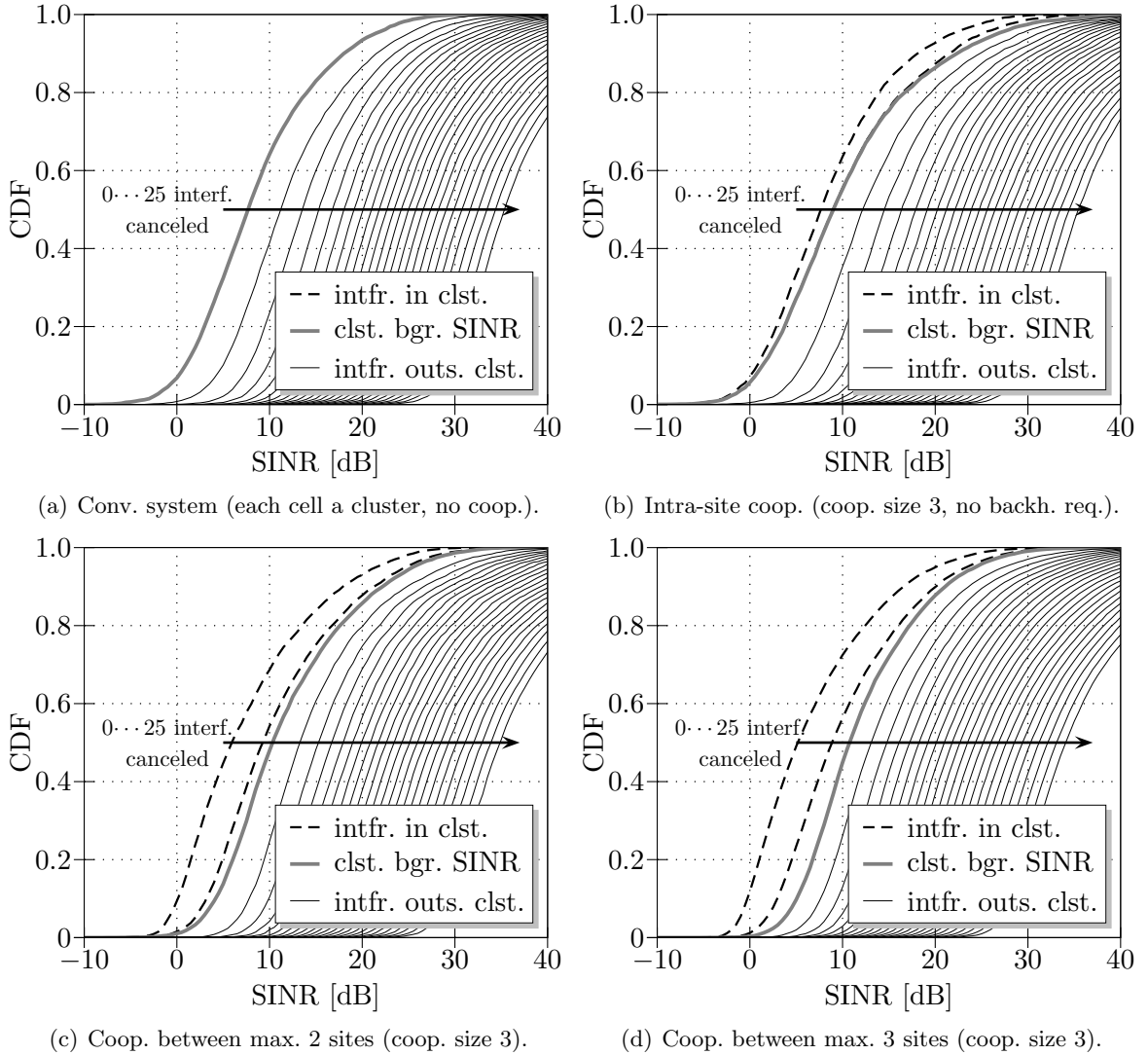


Figure 4.5: Downlink SINRs obtainable through clustering and interference cancellation.

4.2.1 The Benefit of Resource Partitioning

The benefit of using clustering in conjunction with resource partitioning - as done in above cases (c) and (d) - is that interference is reshaped such that we obtain 1-2 *strong* interferers inside a cluster (which can be efficiently canceled or even exploited through CoMP), while the background interference from outside the cluster is attenuated. This is emphasized in Figures 4.4 and 4.5, for the uplink and downlink, respectively. The plots show the cumulative distribution function of the SINRs that the UEs can obtain, for the clustering concepts (a)-(d) as explained before. Here, SINR is defined as the ratio of the desired signal at the receiving end over any interference and noise, assuming that a certain number of interferers is perfectly canceled, but not taking into account array gain through cooperation. The SINRs do, however, take into account the effect of scheduling and power control, as specified in section 4.1.2, and model the impact of imperfect CSIR, as usual based on a practical pilot concept observed in Appendix E. For the latter aspect, we here assume that all communicating entities use

orthogonal pilot sequences, such that in principle each BS can estimate the channel to each UE. Where applicable, we assume that interferers *within* clusters are canceled first (ordered by decreasing impact), after which the interferers outside the cluster are canceled, again starting with the strongest interferers first.

In Plot 4.4(a), we can see that in a conventional system, the median uplink SINR can be improved from about 6 dB to almost 10 dB, if for each user the strongest interferer is removed. Plot 4.4(b) now shows the case where all three sectors of a site are treated as a cluster. The performance without interference cancellation remains the same, and we can see that canceling the interference within the cluster only yields a gain of about 1 – 2 dB in SINR. This means that for most users, there must be at least one dominant interferer which is *not* included in the cluster. Hence, this clustering strategy - besides having the benefit of requiring no inter-site backhaul - is strongly suboptimal in terms of interference cancellation. This is improved in scenarios (c) and (d), covered in Plots 4.4(c) and 4.4(d), respectively, where the removal of the two interferers within the cluster provides significantly stronger gain. Especially clustering scheme (d) leads to the fact that we obtain one very strong interferer within the cluster, which is received at a power similar to that of the desired signal. As the statistics are the same for the other UEs in the cluster, we have here constructed a scenario with fairly strong and symmetric interference links between the cells and attenuated background interference, where DAS is efficiently applicable, and CoMP gains are maximized. Both clustering schemes enable an extent of interference cancellation that corresponds to the cancellation of the strongest interferer for each UE, while also providing maximum array gain.

Figure 4.5 principally shows the same impact of resource partitioning in the downlink. Note, however, that we here have a main difference to the uplink, namely the aspect that no power control is used. This leads to the fact that SINR distributions in general have a larger variance, i.e. UEs experience very different interference scenarios depending on their location. Furthermore, cell-edge UEs will always be subject to a certain extent of long-distance interference that cannot be combated within small clusters. Comparing plot 4.5(d) to 4.4(d), we can also see that clustering cannot yield as strong interference scenarios as in the uplink. All these aspects lead to the fact that the average gains from both intra-site and also inter-site BS cooperation are smaller in the downlink, as we will see in Section 4.4.

In both uplink and downlink, the clustering schemes (c) and (d) lead to a mean background SINR (regarding outer-cluster-interference) of ≈ 8 -10 dB, which we have used as assumptions for the simplified scenarios in Chapter 3. As stated before, we assume these values to be larger in practical urban deployments, as buildings obstruct many distant interferers.

4.3 Uplink Simulation Results

Figure 4.6 shows simulation results for the compared clustering concepts in the uplink. In the upper two plots, we can see the cumulative distribution functions of UE throughput assuming infinite backhaul (where applicable), whereas the lower two plots show the average throughput as a function of backhaul per UE. The noise each detection process is subject to is determined through the background interference from outside the considered cluster as well as thermal noise. In the left plots, we observe the case with perfect CSIR, whereas the right plots show results under the extent of CSIR expectable under a practical channel estimation observed in Appendix E, now assuming that channel estimation itself is subject to

the same noise variance as the data transmission. This implies that the system uses orthogonal pilots enabling CoMP solely within clusters, and the usage of pilots in different clusters is subject to mutual interference. The throughput/backhaul trade-off of the schemes is as usual displayed as an area, where the upper bound refers to schemes exploiting inter-BS correlation, whereas the lower bounds indicate the performance of schemes based on a practical quantizer. While clustering concept (a) only allows single UE detection at one BS, concept (b) enables the joint detection of three UEs by three BSs without requiring backhaul, such that MAC performance has been computed here. For concepts (c) and (d), all DIS and DAS combinations offered by the model from Section 3.3.7 have been observed, while for concepts (e) and (f) only centralized DAS schemes have been considered, as otherwise the degrees of freedom of cooperation strategies would have been intractable.

We can see that intra-site cooperation can already yield throughput gains of 63% under imperfect CSIR, with similar gains under perfect CSIR. Also, such cooperation yields a large fairness gain, which can be seen in an increase of the 10th percentile throughput by 72%. If clustering concepts (c) or (d) are used without backhaul, these are only slightly inferior to intra-site cooperation. This shows that there is usually little value in letting all three sectors of a site cooperate, due to the large back-attenuation of the antennas considered. If backhaul is then invested into cooperation with one or more additional sites, an additional mean throughput increase of about 14% is possible under imperfect CSIR. Observing the complete gain from a non-cooperative system (a) to clustering concept (c) or (d), which is about 85%, we realize that this corresponds well to our Monte Carlo simulations on a simplified scenario with $M = K = 3$ in Section 3.3.7. This shows that the proposed clustering concepts do in fact create scenarios of moderately strong interference on average, corresponding to our observations on SINRs in Section 4.2.1. Further, it suggests that our conclusions from Chapter 3 can be translated quite well to a system level perspective, at least for the uplink.

Clearly, the additional throughput gain by introducing inter-site CoMP appears quite marginal. However, one must point out that if e.g. clustering concept (c) is employed, the 10th percentile throughput can be increased by an additional 79% over that of intra-cell CoMP. A closer look at Plot 4.6(b) reveals that concept (c) only increases the throughput of the weaker UEs, while the performance of the better UEs is almost identical to that of intra-cell CoMP. The reason is that in most cases, two out of three UEs using the same resources in a cluster created through concept (c) can be served well through on-site CoMP. As we consider $N_{\text{bs}} = 2$, the two cooperating BSs will be able to reject the interference from the third UE quite well for most channel realizations. If backhaul is now used for multi-site CoMP, mainly the third UE will profit from this, leading to the observed fairness gain. This is different for clustering concept (d), where some clusters involve 3 different sites. Here, symmetric scenarios of even stronger interference are generated, and all UEs see a more similar background interference (i.e. the SINR distribution is steeper, see Plot 4.4(d)). Using this concept, all UEs profit more or less equally from CoMP, but the fact that the system bandwidth is split into more blocks leads to a loss in multi-user diversity and scheduling gain, as each scheduler faces less UEs and less resources. This leads to the fact that concept (d) is inferior to concept (c), even though it creates 'better' CoMP scenarios w.r.t. our observations in Section 3.3.7.

We can further see from Figure 4.6 that cooperation in a cluster of 7 cells under imperfect CSIR is only marginally superior to the proposed resource partitioning concepts. This shows that smart clustering concepts enable the cancellation of the most dominant interferers. While cooperation in a cluster of 12 cells still provides significant throughput improvements, the

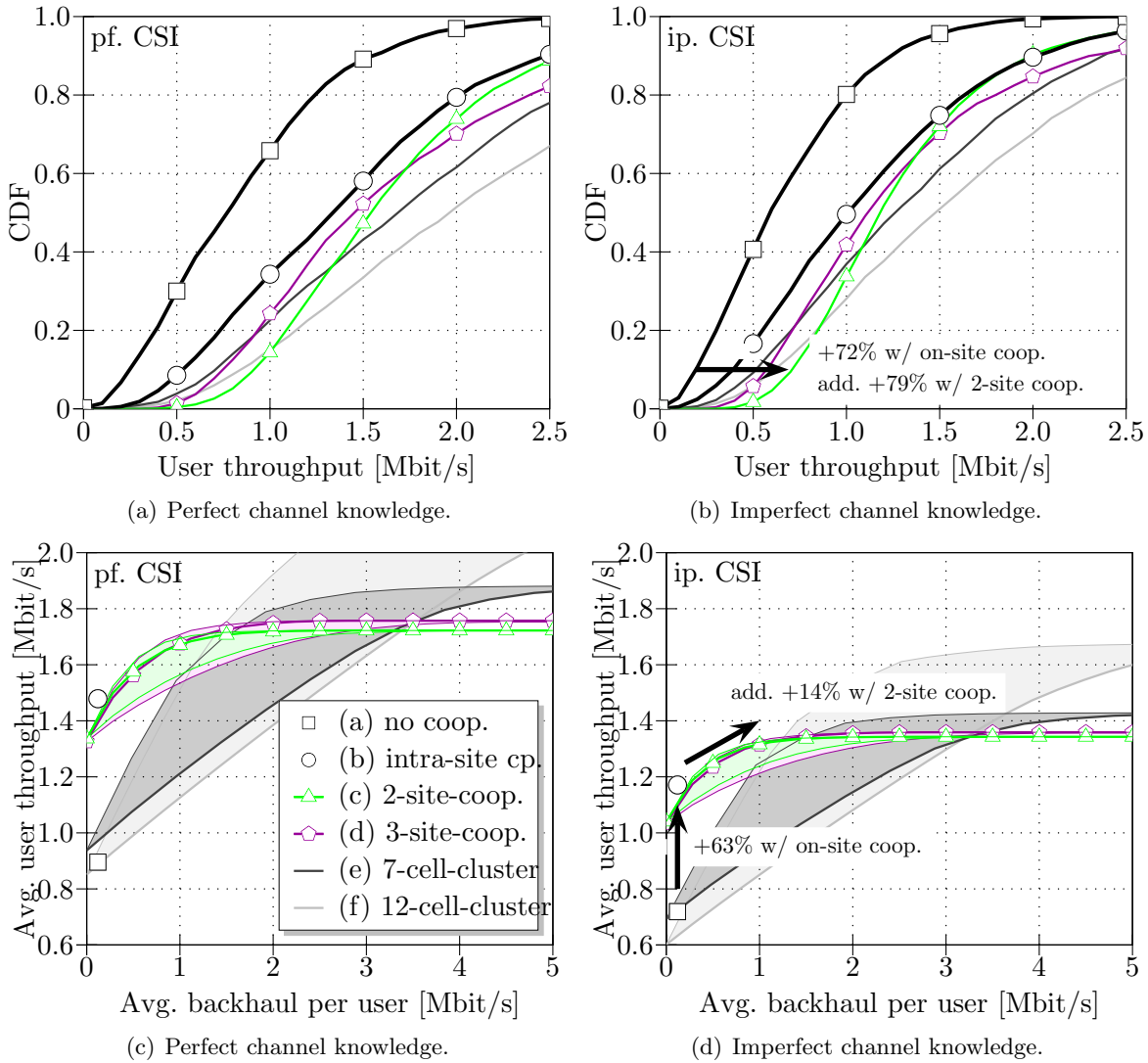


Figure 4.6: User throughput distribution and average user throughput vs. backhaul for different cooperation sizes and strategies (uplink).

throughput/backhaul trade-off of both clustering concepts (e) and (f) is strongly inferior to that of concepts (c) and (d), in particular when considering practical quantization schemes.

As the proposed clustering concepts (c) and (d) create CoMP scenarios with strong cross-coupling, decentralized CoMP schemes as well as hybrid DIS/DAS approaches are of marginal benefit and hence omitted in Figure 4.6. As observed in Sections 3.3.3 and 3.3.7, backhaul can be reduced through more sophisticated quantization concepts. The fairly small benefit of source coding schemes in the cellular uplink corresponds quite well to our observations in Figure 3.9, taking into consideration that not all three UEs in a cluster can have strong mutual interference, as seen in Figure 4.4. Even without source coding concepts, and under the assumption of a realistic quantizer, we can see that the option of performing part of the cooperation over intra-site links improves the overall rate/backhaul trade-off, such that now only about 1.5 bits of backhaul are required for 1 bit of throughput.

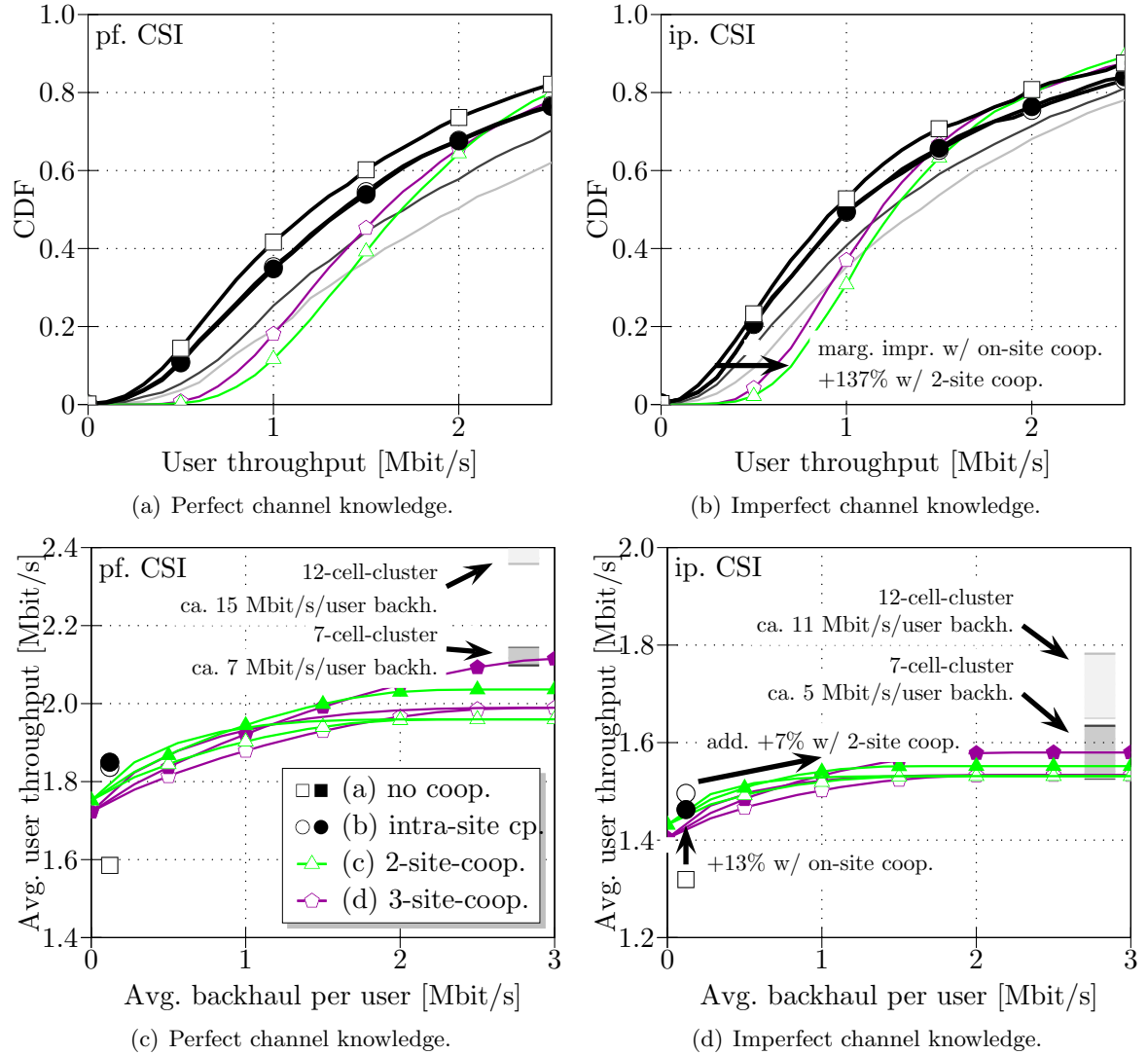


Figure 4.7: User throughput distribution and average user throughput vs. backhaul for different cooperation sizes and strategies (downlink).

4.4 Downlink Simulation Results

Figure 4.7 finally shows results for a downlink employing the clustering concepts stated before, where again the left plots refer to the case with perfect CSIT and CSIR, and the right plots are connected to imperfect CSIT and CSIR. As in the uplink, the noise at each UE is computed individually as the interference originating from outside the cluster and thermal noise. In the case of imperfect CSIT and CSIR, we as usual consider the concrete channel estimation and CSI feedback scheme from Appendix E, assuming as in the uplink that channel estimation is subject to the same noise as the actual data transmission. In general, we observe a sum-power constraint for simplicity, assuming that in an OFDMA system, the *peak-to-average power ratio* (PAPR) in time domain is of significantly more importance than a per-antenna

power constraint on a particular sub-carrier². For clustering concept (a), MRT is performed, while for concept (b), where full BS cooperation is possible without backhaul, the BC capacity region from Section 2.3.3 is computed. For concepts (c) and (d), we observe the performance of UMC and TS schemes, as done in Section 3.4.7, while for concepts (e) and (f), we constrain ourselves to a time-share between zero-backhaul and full BS cooperation (TS) for simplicity.

In general, the gains through CoMP in the downlink predicted by system level simulations appear significantly smaller than in the isolated scenarios observed in Section 3.4.7, in particular under imperfect CSI. This is mainly due to two effects: On one hand, we have already stated before that we are facing a larger variance of (possibly long-distance) background noise, and the proposed clustering concepts do not yield as strong interference scenarios as in the uplink. On the other hand, we have to consider the following: While in the uplink, a cell-edge user creates strong interference to multiple BSs, and hence impairs the detection of multiple other UEs, a cell-edge user in the downlink only suffers for himself. If then backhaul is invested to enable joint transmission to this UE under imperfect CSI, the performance of other UEs involved can even be degraded, which is for example visible in Plot 4.7(d). This leads to the fact that introducing intra-site CoMP improves the average throughput by only 13%, and clustering concepts (c) and (d) yield an additional 7%. However, exactly the effect stated before leads to a vast 10th percentile throughput improvement of 137% if clustering concept (c) is employed, while slightly deteriorating the performance of better users. As observed before in the uplink, concept (d) leads to a more equal improvement of all UEs, while the reduced scheduling gain leads to a performance deterioration again. Concept (c) hence appears most attractive in this comparison, at least if an operator strongly values system fairness. As this concept only establishes cooperation between two adjacent sites, the worst case extent of backhaul required corresponds exactly to the system throughput, i.e. 1 backhaul bit per throughput. Through UMC concepts, this ratio can be reduced to about 0.8. Note that the tendency of concept (d) to create stronger interference scenarios renders DPC schemes more valueable, while these perform badly under intra-site cooperation.

We can further see from Plot 4.7(d) that there is little benefit of using large cooperation clusters, especially as these require a large extent of backhaul. More precisely, clustering concept (e) with cooperation size 7 involves 4 sites per cluster, and hence the messages to be transmitted to all UEs require 3 backhaul bits per throughput bit. For cooperation size 12, this increases to 6 backhaul bits per throughput bit.

4.5 Summary

In this section, we have observed large cellular systems within which CoMP is applied. We have seen that clustering and resource partitioning concepts can be used to create small CoMP scenarios, as treated in Chapter 3. In particular, these concepts allow to create scenarios with strong intra-cluster interference, while the background interference is attenuated.

In both uplink and downlink, major throughput gains can already be achieved if intra-site CoMP is applied, which does not require backhaul. Further, limited average throughput

²Note that this does not put our model from Section 2.3 in question, as per-antenna power constraints are important in single-carrier systems or for cooperation between entities of different transmit power. In principle, it is for example thinkable that CoMP is used among macro and micro BSs in future cellular systems.

improvements are possible if cooperation clusters span a maximum of two sites. More importantly, such techniques can significantly improve fairness, as highlighted in a summary of the numerical results of this Chapter in Table 4.3. Clearly, the option of intra-site BS cooperation without backhaul improves the overall throughput/backhaul trade-off obtained. If 90% of the gains through intra-site CoMP are to be achieved, this requires roughly 1.5 bits of backhaul per throughput bit in the uplink, assuming practical quantization schemes, and a ratio of about 0.8 in the downlink, if UMC is employed. Note that the ratio in the uplink can easily double in a practical system, as actually achieved rates are usually much lower than the information theoretic quantities observed here [MKF06], while the backhaul effort for DAS remains the same. As UMC or TS schemes in the downlink require backhaul rates that scale with the actual data rates, this problem does not arise here. In general, it appears that larger cooperation sizes are not attractive, as additional gains are limited, and the complexity and backhaul consumption of such approaches increases drastically. As previously mentioned, large cooperation sizes also require an increased pilot overhead and increased effort for CSI feedback, reducing overall improvements of spectral efficiency [MRF10].

In Section 4.1, it was mentioned that shadow fading is not used in the observed simulations. While for the simulation of non-cooperative systems, such fading reflects very well the statistical impact that structures, buildings etc. have on point-to-point links, but the standard shadow fading models are questionable in the context of CoMP, where multi-cell signal propagation plays a major role. In this context, it is of course generally difficult to draw major conclusions from system level simulations based on a flat plane model, even though this is the standard simulation model used by 3GPP. In a practical urban deployment, it is likely that useful cooperation clusters are naturally constrained through the morphology of surrounding buildings. An operator could hence use signal propagation measurements or simulations based on, e.g., raytracing to identify such clusters. Alternatively, the BSs could find suitable cooperation partners on a large time-scale by themselves, corresponding to the concept of a *self-organizing network* (SON). In fact, CoMP field trials [I⁺09] suggest that in an urban environment, a transmission is typically subject to a few strong interferers, but little background noise. Hence, it can be expected that CoMP within small clusters yields even stronger gains than predicted through the results in this chapter, as a larger portion of the overall interference can be canceled. Under real-world signal propagation, it might also be possible and reasonable to create CoMP scenarios with asymmetrical interference, in which decentralized and backhaul-efficient BS cooperation schemes can be used in the uplink.

	Uplink		Downlink	
Monte Carlo analysis in an isolated scenario with $M = K = 3, N_p = 2, N_p = 6$				
	Sum rate [bpcu]	backh./tp.	Sum rate [bpcu]	backh./tp.
Cell-edge				
Conv. MRC/MRT	3.8	-	4.6	-
Conv. IRC/IAP	4.4 (+16%)	-	6.1 (+32%)	-
CoMP ($\beta = 0$)	5.8 (+32%)	-	8.1 (+32%)	-
CoMP (50% gain)	·	0.5 (DAS, th.)	·	0.8 (UMC)
	·	2.0 (DAS, pr.)	·	1.0 (TS)
CoMP (90% gain)	·	1.5 (DAS, th.)	·	1.3 (UMC)
	·	3.0 (DAS, pr.)	·	1.8 (TS)
CoMP ($\beta = \infty$)	9.9 (+71%)	∞	12.2 (+51%)	2.0
Cell-center				
Conv. MRC/MRT	8.4	-	9.6	-
Conv. IRC/IAP	8.6 (+2%)	-	10.7 (+11%)	-
CoMP ($\beta = 0$)	8.6 (+0%)	-	11.6 (+8%)	-
CoMP (50% gain)	·	0.8 (DIS/DAS)	·	0.5 (UMC)
	·	0.8 (DAS, th.)	·	1.0 (TS)
	·	2.0 (DAS, pr.)	·	
CoMP (90% gain)	·	1.6 (DAS, th.)	·	1.1 (UMC)
	·	3.5 (DAS, pr.)	·	1.8 (TS)
CoMP ($\beta = \infty$)	10.3 (+20%)	∞	14.7 (+27%)	2.0

Table 4.2: Summary on Monte-Carlo simulation results for scenarios with $M = K = 3$.

	Uplink			Downlink		
System level simulation	tp./UE [Mbit/s]	10th% tp. [Mbit/s]	bh./tp.	tp./UE [Mbit/s]	10th% tp. [Mbit/s]	bh./tp.
Non-cooperative	0.72	0.22	-	1.32	0.29	-
Intra-site CoMP	1.18 (+63%)	0.38 (+72%)	-	1.49 (+13%)	0.31 (+7%)	-
2-site CoMP (90%)	·	·	0.5 (DAS, th.)	·	·	0.8 (UMC)
	·	·	1.5 (DAS, pr.)	·	·	1 (TS)
2-site CoMP	1.35 (+14%)	0.68 (+79%)	-	1.59 (+7%)	0.69 (+123%)	-

Table 4.3: Summary on system level simulation results.

Chapter 5

Implications on Practical Systems

In this chapter, we discuss the impact of the analysis and the key findings in the last chapters on practical CoMP systems. We draw the connection between the theoretical models observed in this work and practical BS cooperation schemes proposed in literature. We further look into various additional aspects that have to be considered when introducing CoMP into cellular systems, and provide an outlook onto backhaul-aware scheduling and ad-hoc CoMP.

5.1 General Implications of our Work

After discussing the general value of the information-theoretic models used in previous chapters in the context of practical CoMP, we discuss the specific impact of our conclusions on network organization, backhaul topology, and the value of iterative CoMP schemes.

5.1.1 Fundamental Trade-Offs in the Context of CoMP

Clearly, this thesis uses strongly simplified and information-theoretic models to evaluate different CoMP concepts. However, these models still yield an important insight into general trade-offs and considerations that have to be made in the context of CoMP. For example, Section 3.3 has revealed that there are two principle ways of performing CoMP in the uplink. On one hand, information connected to UE messages may be exchanged among BSs (in the case of DIS or CIF). This typically enables an efficient usage of backhaul, but only yields a limited extent of interference cancellation. On the other hand, only the quantization of received signals (i.e. centralized DAS) may approach MAC performance, but this always involves wasting backhaul into a useless quantization of noise. Practical CoMP algorithms will typically be combinations of the concepts discussed in this work, but the general trade-offs identified in this work still apply, and can help to evaluate the appropriateness of particular CoMP algorithms in certain scenarios. We will continue this discussion throughout the remainder of this chapter.

5.1.2 Mobile Network Organization

In both uplink and downlink, we have seen that major capacity gains can already be achieved without backhaul, if

- the assignment of UEs to BSs is performed flexibly on a short term basis, and

- multiple UEs can be served jointly by one BS on the same resource without cooperation.

Chapter 4 has furthermore shown that these gains can already be obtained within reasonably sized clusters of BSs. This suggests that there might be a major paradigm shift in next generation mobile networks, where entities called *cells* could be replaced by entities called *clusters*. Ideally, a UE would be assigned to a cluster of cells, not a single cell, where most likely one of the involved BSs would take over the role of a cluster master. This master would then be responsible for the scheduling of all UEs assigned to the cluster. The decision on which BS should decode which UEs (and using which extent of BS cooperation) could be performed ad-hoc, *after* transmission has taken place, an aspect we will discuss later in Section 5.2.4. Such a change of paradigm will of course also have a major impact on the general network architecture, i.e. the role of BSs, network entities etc.

5.1.3 Backhaul Topology

Section 3.3.7 has shown that the uplink benefits from a direct cooperation between different base stations, as opposed to cooperation through a centralized network entity. Hence, the best possible backhaul topology would be a mesh connecting at least those adjacent cells with a strong cross-coupling. In a practical system, an operator would surely also consider reusing existing infrastructure to create *logical* links between base stations, which would, however, lead to a larger latency. Especially the latter aspect can be crucial if CoMP schemes are to be used in conjunction with *automatic repeat request* (ARQ) concepts [Tan89], as in LTE.

In the downlink, we have always used the wording that *a network entity provides a BS with the message to be transmitted to a certain UE*. Clearly, a star topology with network entities in the center would be the most intuitive solution, and at the same time minimize latency. As it is probably inefficient to establish both a mesh infrastructure for the uplink and a star topology for the downlink, the latter could, however, also be solved through a backhaul mesh. In this case, each BS would by default be supplied with the message to be transmitted to its assigned UEs by the network, and provide this information *on demand* to neighboring BSs, possibly in connection with channel information. This would increase the initial latency of providing data to the BSs, but have no impact on ARQ latency, as the ARQ process can be based on the data already available at all BSs, and does not involve the network. We will discuss ARQ in conjunction with CoMP in Section 5.2.2.

5.1.4 On the Value of Iterative BS Cooperation Schemes

In Section 3.3.4, it has been shown that iterative signal exchange between BSs (I-DIS or I-DAS) is of little value. Clearly, one has to keep in mind that this aspect was proved under typical information theoretical assumptions, i.e.

- A complete transmission of N_{sym} symbols sees the same channel.
- N_{sym} is chosen large enough such that noise and interference are ergodic in the wide sense, i.e. can be fully characterized through a zero-mean and a certain variance.

The situation is of course different in a practical OFDM system, where the symbols belonging to a codeword are spread out in time and frequency, and are hence subject to different channel realizations. This is especially the case under a strongly frequency selective channel

that occurs in urban scenarios with many scatterers [ECS⁺98]. In this case, it would theoretically be beneficial to let each part of a UE's transmission be decoded by the BS to which it has the better link on the corresponding sub-carriers. This would, however, require the usage of special coding strategies, as the codes employed in LTE use strong interleavers to make best possible usage of frequency diversity [McC07]. Furthermore, we have to consider that such a situation will occur most likely when a UE is located close to the cell-edge, where we know from Section 3.3.2 that centralized DAS concepts are superior to decentralized schemes, which is also confirmed in [MJH06]. In such a DAS concept, the number of quantization bits invested into groups of sub-carriers could be adapted to the SINR on these sub-carriers (if this is measurable at such granularity), further improving the rate/backhaul trade-off.

Let us now consider the case where interference links are weak, such that above situation does not occur, and such that decentralized cooperation schemes become interesting. Under these assumptions, it is clear that as soon as a BS attempts to decode a UE in an interfering cell (without being provided side-information by the other BS), this poses a stronger constraint on the interfering UE's rates [HK81]. Hence, let us assume as in Section 3.3.4 that each BS only decodes its assigned UE, and observe the following two cooperation schemes:

The BSs only exchange information on their own assigned terminals (I-DIS), where practical algorithms have been proposed in, e.g. [MJH06, KF07, KF08, KRF08]. Recall that in this case the performance is upper-bounded by the interference-free case, as no array or spatial multiplexing gain can be exploited. In a practical system, the UE rates have to be chosen conservatively enough to ensure that the first (non-cooperative) decoding process at the BSs already yields a reasonably low number of falsely decoded bits. If this is not the case, exchanging information on these bits among the BSs leads to error propagation. Then, the convergence of the iterative cooperation scheme requires more iterations [KRF08] (if convergence is given at all), leading to a redundant and hence inefficient usage of backhaul. Ideally, the BSs would only exchange information on subsets of bits, for example those that appear to be known with high reliability, or only those that have changed since the last iteration [KF07]. Clearly, this means that the BSs have to inform each other which bits have been exchanged, requiring additional backhaul, and still not avoiding error propagation.

To this respect, we can consider the information theoretical model in Section 3.3.4 as an idealistic case of a practical I-DIS approach. Although using superpositions of many transmitted messages is clearly unfeasible in a practical system [FU98], the model serves as an example where in each iteration a BS is able to reliably decode a further part of its UE's transmission. Also, the BS knows exactly which bits it can decode. This part can then be forwarded to the other BS at the highest possible backhaul efficiency if Slepian-Wolf source coding is employed. Note that a scheme where the BSs also aim at decoding the interference [KF07, KF08, KRF08], can be seen as a kind of (suboptimal¹) source coding, as the BSs only exchange the portion of information that the receiving BS needs to decode the interference by itself. In this case, an efficient backhaul usage is possible, as the exchanged bits are *reliably known* and hence no quantization of an LLR value or other measure of reliability [KRF08, Rav09] is needed. Further, each decoded bit needs to be exchanged only once, such that the required backhaul can be upper-bounded by the sum rate of the UEs, and error propagation does not occur. Still, we have seen in Section 3.3.4 that even this kind of optimal I-DIS scheme hardly performs

¹In the sense that a certain extent of redundancy between forwarded data and side-information at the receiving BS cannot be avoided.

better than DIS with one information exchange. We hence conclude that *any* practical I-DIS algorithm brings marginal benefit over a single-shot DIS.

The BSs exchange information on received signals (I-DAS), where practical algorithms have been proposed in [GHEM04, AEH06, MJH06, BC07b, AEH08]. Clearly, Section 3.3.2 has shown that such decentralized DAS schemes are only beneficial in scenarios of very weak interference, and that DIS or centralized DAS are superior otherwise. The authors in [AEH08] motivate the usage of a decentralized scheme by considering a large number of cooperating BSs, for which joint decoding at a central entity would become computationally infeasible. However, the system level results from Section 4.3 suggest that a fairly good rate/backhaul trade-off can already be achieved for reasonably-sized clusters of cooperating BSs, where centralized approaches are not only feasible from a computational point of view, but in most cases also better in terms of backhaul. This viewpoint is confirmed when the simulation results in [AEH08] are observed - the required backhaul appears to be orders of magnitude larger than the achieved rates.

Note that the authors in [KF08, KRF08] have also considered schemes where BSs exchange information on their decoded UEs, as well as on one or multiple interferers. While the scheme makes use of array and spatial multiplexing gain, it has to be pointed out that the scheme cannot approach MAC performance, as again rates have to be chosen conservatively to facilitate convergence. It further requires a large extent of backhaul [KRF08], and is strongly inferior to a centralized DAS scheme in this respect. The authors in [NEH07, NEHA08] suggest to use iterative BS cooperation schemes in the downlink. Here, the symbols to be transmitted from the BS antennas after precoding are distributed via message passing concepts. This concept also appears rather questionable, as in the downlink the BSs are dealing with discrete messages or continuous sequences that are *not* subject to noise as in the uplink. Hence, an iterative exchange of information cannot be superior to a single-shot exchange. One could only imagine that the exchange of *channel knowledge* among BSs could be performed in such an iterative way, such that the BSs inform each other about changes in their channels to certain UEs. This is an aspect we will discuss later in Section 5.2.2.

We conclude that iterative BS cooperation schemes are not only questionable from an information theoretical point of view, but also under practical considerations, if the rate/backhaul trade-off is observed. Only for large cooperation clusters, iterative schemes can be an option to distribute computational complexity over the network.

5.2 Practical Considerations

In this section, we revisit the BS cooperation concepts considered in the last chapters, and evaluate them from practical points of view. We further look into additional signaling required between BSs to enable CoMP, and briefly point out the potential of scheduling for CoMP and *ad-hoc CoMP* after transmission has taken place.

5.2.1 Practical Implementation of BS Cooperation Schemes

In the last chapters, we have seen that the performance of all cooperation schemes based on quantization depends strongly on the quantization scheme assumed. Especially source coding schemes exploiting signal correlation between BSs have shown to enable a significant backhaul

reduction. Though the practical implementation of distributed Wyner-Ziv source coding has been researched in, e.g., [XLC04, VAG05, NEH07], for example based on *low density parity check codes* (LDPC) [Gal63], it still appears questionable to which extent these schemes can be used in a cellular context. The stated papers typically assume that a quantization codebook is designed for a fixed extent of signal correlation. In a practical cellular system, channels are constantly changing over time, and hence also the correlation between BSs. Furthermore, scheduling leads to the fact that UEs are frequently assigned to new resources, such that both the channel conditions and interference conditions change. The computation of a new source coding codebook for each realization of correlation, which always has to be exchanged among the BSs or redundantly computed at both sides, would render these schemes unfeasible.

On the other hand, DIS schemes (without Slepian-Wolf source coding) are rather straightforward to implement, as decoded bits are exchanged that require no quantization. Furthermore, inter-BS signal correlation can quite easily be exploited if only a limited number of bits is handed over to the cooperating BS, but the latter uses these in conjunction with the own received signals to fully decode the interference. An additional benefit of DIS schemes is that the amount of backhaul required scales down with the practically achieved rates [MF08e]. These are typically significantly lower than the information theoretical quantities observed in this work [MKF06], as losses through non-Gaussian signaling, a finite set of modulation and coding schemes, imperfect rate adaptation to the channel etc. cannot be avoided. For a DAS scheme, however, the backhaul required is fixed due to the employed quantization scheme.

The previous remarks on quantization and DIS schemes clearly emphasize the practical advantages of DIS schemes. As we have seen in Section 3.3.2, however, these concepts are mainly interesting in scenarios of weak interference, and are limited to canceling a certain extent of interference. An interesting future research topic is hence whether clustering concepts as in Section 4.2 can be used in practical signal propagation environments that create exactly the weak, asymmetrical interference scenarios interesting for DIS.

In the downlink, we have concluded from Section 3.4.2 that UMC schemes, i.e. schemes *not* based on sequence quantization are in fact preferable for most scenarios. Introducing the same thoughts on practical quantization issues as in the last section further pronounces the superiority of these schemes.

5.2.2 CSI Exchange, ARQ and Complexity Issues

An additional, perhaps minor advantage of DIS and CIF schemes in the uplink is the fact that these require only the local channel knowledge from a BS to all involved UEs, whereas DAS schemes (both decentralized and centralized) require global channel knowledge in order to exploit the received signals provided by other BSs. In the latter cases, however, it appears feasible to assume that BSs not only exchange quantized receive signals connected to data, but also those connected to pilots, which are usually embedded therein. Then, the DAS-receiving BS can perform the channel estimation based on the quantized signals itself². A more sophisticated approach yielding a better rate/backhaul trade-off would be to use successive vector quantization approaches [Jin06a, LJ07, HWS09] for the pilots, where the BSs only update each other on the change of the channel over time.

²Obviously, it could make sense to invest more bits into the quantization of pilots than into the quantization of data, as we have seen the sensitivity of performance to the accuracy of CSIR in Section 3.3.1.

UPLINK	DIS	CIF	DAS Decentralized	DAS Centralized
Decoding	decentralized			centralized
Exchanged signals	decoded messages	quantized sequences	quantized receive signals	
Achievable gains	SIC gain (interference cancellation)	partial interference cancellation	array + spat. mult. gain	array + spat. mult. + SIC gain
Suitable in scenarios	weak, asymm. interference low backh. high SNR	very weak, asymm. interf. low backh. high SNR	very weak, symm. interf. low backh. low SNR	strong interference large backh. low SNR
Source coding concepts	provide little gain, but possible if interference is also decoded	provide little gain, and are highly questionable from implementation point of view		major potential gains, but highly questionable
Channel knowl. req.	local knowledge from each BS to all UEs sufficient		global CSIR at <i>all</i> BSs	global CSIR at <i>one</i> BS
Complexity	<i>moderate</i> , if interf. only needs re-encoding / SIC (w/o src. coding), <i>high</i> if dec. of mult. UEs / SIC (w/ src. coding)	<i>low</i> , due to simple signal subtraction	<i>low</i> , as only one UE is decoded	<i>high</i> , as all UEs are successively or jointly decoded + SIC
CoMP usage	possibly ad-hoc decision after transmission			ideally decided in advance
ARQ	possibly independent ARQ process for each BS-UE link			multi-cell ARQ processes

Table 5.1: Comparison of uplink BS cooperation schemes, considering practical aspects.

DOWNLINK	DAS	TS	UMC	QSC
Encoding	centralized	local		
Exchanged signals	quantized transmit signals	unquantized messages		quantized or unquantized messages
Achievable gains	array + spatial multiplexing + DPC gain		array + spatial multiplexing gain	
Suitable in scenarios	strong, asymm. interference	strong, symm. interference	any, in particular weak interference	any, in particular very weak interference
Channel knowledge required	global CSI needed at <i>one</i> BS	global CSI needed at <i>all</i> BSs	each BS req. local CSI to all UEs and that from other BSs to all UEs, if jointly serving UEs	
Complexity	<i>moderate</i> , as quantization required, <i>high</i> if DPC is applied before quant.	<i>high</i> , if DPC is applied	<i>low</i> , as only linear schemes considered	<i>moderate</i> , as quantization is involved
CoMP usage	in the downlink, it has to be decided in advance whether CoMP is used or not			
ARQ	All BSs participating in the transmission to a UE have to be aware of ARQ processes			

Table 5.2: Comparison of downlink BS cooperation schemes, considering practical aspects.

In the downlink, all compared BS cooperation schemes need more than just local channel information. For TS, each BS requires global channel knowledge, and for UMC and QSC, each BS requires the CSI connected to its links to *all* involved UEs (as it is already required for interference-aware precoding), plus the CSI from each other BS to *all* UEs, whenever the BSs have a non-empty set of UEs they jointly transmit to. This is required for the (redundant) calculation of precoders at each BS. In addition, the BSs have to agree on the transmit power to be invested into each transmission. While this appears to require a comprehensive exchange of channel information between BSs, one must however consider that in an FDD system, the major bottleneck is the fact that the UEs have to feed back CSI over the air. Regardless of increasing backhaul cost for an operator [Chu08], we assume that radio interface bandwidth will always be significantly more valuable than backhaul bandwidth. Also, one could argue that, as downlink CoMP is mainly interesting for cell-edge users, it is also feasible to assume that all involved BSs are able to decode the CSI feedback of all involved UEs (possibly also using CoMP in the uplink), provided the channel gains in uplink and downlink are roughly symmetrical, such that global channel knowledge is inherently available at all BSs. For DAS schemes in the downlink, global channel knowledge is required solely at the BS that performs the centralized precoding.

A main issue is the usage of CoMP schemes in connection with ARQ, especially in the uplink. For decentralized schemes, we could imagine independent ARQ processes on each BS-UE communication link. In the easiest case, the BSs would not be aware about retransmissions triggered by other BSs, but this would be suboptimal in the way that the redundancy in re-occurring interference patterns is not exploited. For centralized schemes, it might be necessary to request the retransmission of one UE, such that multiple UEs can then be jointly decoded³. In this case, the received signals or any other intermediate decoding result connected to multiple UEs would have to be stored until the ARQ process is completed, meaning that ARQ buffer times are in general enlarged. Further, the DAS-based cooperation might also have to be repeated. In the downlink, it is obvious that each BS involved in the transmission to a UE must also participate in a potential ARQ process, creating an additional signaling overhead. It appears that ARQ in conjunction with CoMP still requires a vast amount of future research.

The previously discussed practical aspects connected to uplink and downlink CoMP schemes are summarized in Tables 5.1 and 5.2, respectively. Here, we have also stated our observations from the last sections, and looked into the aspect of complexity. In the uplink, complexity mainly depends on the number of messages to be decoded by a single entity. For DIS schemes with source coding and centralized DAS schemes, BSs need to decode the messages connected to multiple UEs, applying SIC or joint decoding. For CIF, this is not required, as a CIF-receiving BS simply multiplies the quantized interference sequence with the channel towards the interferer, and subtracts the result from the own received signals prior to decoding an assigned UE. In this case, the CIF-receiving BS does not require code knowledge w.r.t. the removed interference. Also, decentralized DAS schemes are fairly simple, as each BS decodes only its own UE. In the downlink, the complexity of the schemes mainly depends on whether non-linear precoding schemes are applied, for example Tomlinson-Harashima precoding, which was initially proposed for ISI cancellation in [Tom71, HM72] and where concrete algorithms were proposed for the broadcast channel in, e.g., [FWLH02, KJUB05].

³This can occur, for example, if UE rates are chosen under the assumption of a particular SIC order, and the decoding process of the very first UE fails.

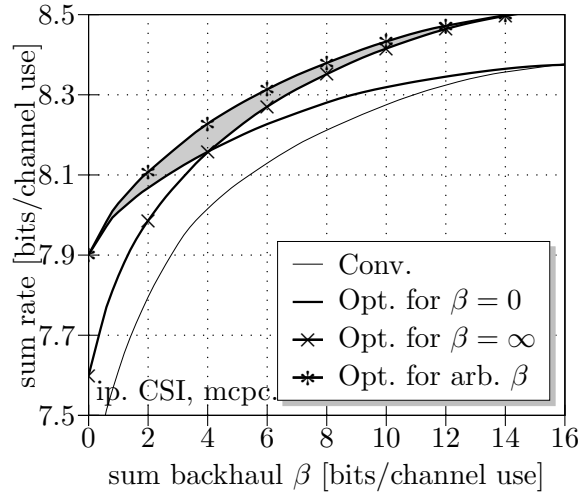


Figure 5.1: Benefit of backhaul-aware CoMP scheduling in a scenario with $M = K = 2$.

5.2.3 Scheduling for CoMP

The issue of scheduling for CoMP has been observed in, e.g. [KPKG05, MK06, KdFG⁺07, MK07]. The aim is to find groups of UEs that can be served efficiently with CoMP, which is usually done by observing the compound channel properties of the UEs. The main challenge is that this has to be performed in such a way that the multi-user diversity offered by a non-cooperative system (e.g. LTE Rel. 8) is not sacrificed too strongly. At the same time, the scheduling decision has to be based on as little channel information as possible, to avoid an excessive CSI signaling overhead between UEs and BSs, as well as among BSs themselves. A crucial aspect can also be complexity, which was addressed in, e.g., [MK07].

While the previously cited work dealt with scheduling for CoMP systems under the assumption of infinite backhaul, little research has yet been performed on scheduling for backhaul-constrained CoMP. In [Die09, DMFR09], a backhaul-constrained scenario with two BSs and a multitude of UEs to be scheduled onto multiple resources was considered, where a significant improvement of the rate/backhaul trade-off for regimes of moderate backhaul could be shown. This is possible as the proposed algorithm chooses the best group of users for each resource under different regimes of backhaul, and then invests the backhaul into the resources where the gradient of rate improvement over backhaul is maximized, inherently choosing the best user group for the respective backhaul regime.

The benefit of such backhaul-aware scheduling is briefly illustrated in Figure 5.1, where the average sum rate per resource is shown, assuming a simultaneous transmission over 5 orthogonal resources. For each resource, the best 2 UEs out of a set of 8 UEs are chosen and assigned to the resource, depending on the backhaul available. The simulations have been performed for a large number of Monte Carlo user drops, with an equally probable distribution of UEs over the area. We compare the following scheduling strategies:

- Assignment of UEs to the resources where BS-UE links are strongest (as in a conventional system).
- Maximization of the sum rate for the non-cooperative case ($\beta = 0$).

- Maximization of the sum rate for the case of infinite BS cooperation, as done in [KPKG05, MK06, KdFG⁺07, MK07] ($\beta = \infty$).
- Maximization of the sum rate for *any* extent of backhaul, as proposed in [Die09, DMFR09].

The gray area in Figure 5.1 illustrates the regime in which the latter scheme can improve the rate/backhaul trade-off. Intuitively, the benefit of backhaul-aware scheduling concepts increases in the number of resources and users [Die09].

5.2.4 Ad-hoc BS Cooperation after Transmission

We briefly want to mention a new research field connected to CoMP, where first steps have been undertaken in [GMF10a, GMF10b]. While this thesis has only considered capacity regions for quasi-block-static channels (assuming perfect rate adaptation to the instantaneous channel), a practical system will of course face the problem that the channel changes from the moment where a particular cooperation scheme and suitable UE rates are chosen to the moment the actual transmission takes place. Obviously, the channel can change to the worse or the better. In a conventional system without BS cooperation, the former case will lead to the fact that the transmission cannot be decoded, and an ARQ will be triggered. In the latter case, the transmission is successful, but a certain extent of channel capacity has then been wasted. From a network point of view, each transmission can be characterized through a boolean value stating whether the transmission was successful or not.

In a CoMP system, each transmission is not characterized solely through a boolean, but through a rate/backhaul trade-off. This allows the system to respond in many ways to a channel varying over time. In the case the channel has deteriorated in the time between scheduling and transmission, an additional extent of CoMP can be activated (e.g. the received signals from an additional BS could be exploited, or an additional DIS strategy could be used) to hopefully enable successful decoding. On the other hand, if the channel has improved, a lesser extent of BS cooperation (or none at all) might suffice for successful decoding.

One could for example envision a system where scheduling and the choice of cooperation strategy is based on the assumption of a moderate extent of backhaul. After the transmission has taken place, the involved BSs initially try to decode the UEs without cooperation, and only in the case of unsuccessful decoding, cooperation is successively established. It is for example possible that a BS initially DAS-forwards strongly quantized signals to a partnering BS, and then iteratively sends *refinements* (i.e. less significant quantization bits) to the other side, until decoding is possible [GMF10b]. By doing so, backhaul is traded against latency, and the system can compensate for the changes in channel just by investing more or less backhaul. Obviously, the more accurate this compensation is to be performed, the more complexity is invested into a large number of decoding attempts or other evaluation and decision steps performed by the BSs. In fact, such a procedure could have an impact on ARQ concepts, as the ARQ loop could be shifted from the UE-BS communication to inter-BS communication. It appears that this opens a very new perspective on cellular systems, where the interested reader is referred to [GMF10a].

5.3 Extension of the Work to other Scenarios

5.3.1 Intra-cell CoMP in the Uplink

LTE Release 8 [McC07] also foresees *intra-cell CoMP* in the uplink, hence the joint detection of up to 2 UEs by one BS, exploiting the fact that each BS is equipped with at least two receive antennas. Clearly, the models introduced in Chapters 2 and 3 also allow to observe such schemes, and all cooperation setups considered in system level simulations in Chapter 4 can also be extended to twice the number of UEs. In a cluster of $M = 3$ cooperating BSs with $N_{\text{bs}} = 2$, a maximum of 6 terminals could hence be jointly served on the same resource. In this case, however, we will often observe channels that are rank-deficient, hence the system would have to instantaneously adjust the number of UEs scheduled to the same resource. Such adaptation, however, goes beyond the scope of this thesis, and the degrees of freedom in BS cooperation for a scenario as stated before would render any analytical investigation intractable. However, the conclusions in the last chapters can be extended to intra-cell uplink CoMP through the following argumentation:

- Both non-cooperative and cooperative rates can be improved through the usage of intra-cell CoMP, regardless of the inter-BS cooperation size.
- Detection without BS cooperation will more often suffer from non-cancellable interference than with BS cooperation, hence the gain of BS cooperation should be larger.
- The crosscoupling between UEs will be larger in this setup, as spatial degrees of freedom in the channel formerly used for interference rejection are now used for spatial multiplexing. This renders centralized DAS schemes even more important than decentralized schemes such as DIS.
- DAS quantization will in addition become more backhaul-efficient, as more UEs can benefit from the same quantization process, without having to increase the number of quantization bits accordingly.

Hence, it can be expected that DAS strategies become more important in systems using intra-cell-CoMP. Further, the overall rate/backhaul trade-off will improve, while a significant extent of additional complexity is added to the system.

5.3.2 Terminals with more Receive Antennas in the Downlink

LTE Release 8 furthermore considers the usage of multiple receive antennas per terminal. These can be used for the downlink transmission of multiple data streams to each UE through spatial multiplexing, e.g. [HVKS03, DLS05], or to enable a certain extent of interference rejection at the terminal side [TSS⁺08].

In the first case, a capacity-achieving strategy would be to use an $N_{\text{mt}} \times N_{\text{mt}}$ receive filter at each UE, if N_{mt} is the number of receive antennas, applying local SIC or joint decoding of N_{mt} streams at each UE. Clearly, an adaptation in the number of schemes will be necessary if the channel is rank-deficient. For fixed UE-side receive filters, the system can then be seen as a transmission to $N_{\text{MT}} = K \cdot N_{\text{mt}}$ virtual terminals with one antenna each, if the channel matrix and receive filters are merged into an *effective* channel [VJG03, VT03, YL07]. In this case, it is easy to see that the uplink/downlink duality used in Section 2.3.3 still holds, even under an

equivalent transmission equation due to imperfect CSI, as introduced in Section 2.3.2. The receive filters in the downlink then correspond to UE-side transmit filters in the dual uplink. The calculation of the transmit filters in the uplink in conjunction with determining the optimal uplink power allocation was addressed in, e.g. [JJVG02, VRJG03, Yu03, JRV⁺05] for a sum-power constrained downlink. Per-antenna power constraints can also be incorporated into this model [YL07], but then convergence can become an issue. Recently, the authors in [HJ08, HJU09] have proposed a filter-based solution to decorrelate every point-to-point link in such a setup, such that an independent optimization is possible. The work could also be used to model the case where multiple receive antennas at the UE side are used solely for interference rejection, as then a certain subset of dual uplink power values is simply set to zero. An extension of the concepts in [HJ08, HJU09] to per-antenna power constraints and the impact of imperfect channel knowledge would be straightforward, but beyond the scope of this thesis. We hence constrain ourselves to a brief discussion on the impact of $N_{\text{mt}} > 1$ in the context of backhaul-efficient CoMP:

- If multiple receive antennas at the UE are used for *spatial multiplexing*
 - Non-cooperative schemes will suffer more strongly from non-cancellable interference, hence the gain through CoMP can be expected to be larger.
 - Due to less unused degrees of freedom in precoding, the effective crosscoupling between cells will increase, rendering TS and DAS schemes more important, according to our observation in 3.4.2.
 - Similar to intra-cell CoMP in the uplink, DAS schemes will become more efficient, as a larger number of streams can be served at only a minimal increase in quantization bits. The rate/backhaul trade-off is hence expected to improve.
- If multiple receive antennas are used for *interference rejection*
 - The effective cross-coupling between cells will decrease, as the UEs can reject a certain extent of interference.
 - Non-cooperative performance will increase, while cooperative performance will only marginally improve, hence diminishing the gain of CoMP.
 - UMC and especially QSC schemes will become superior, due to the reduced cross-coupling, and also because DPC concepts play a minor role.

5.4 Summary

In this chapter, we have discussed the considered BS cooperation concepts under practical aspects, and stated the implications of our key findings in the last chapters on the practical usage of CoMP. We have seen that

- Though practical CoMP algorithms may be combinations of the CoMP concepts introduced in this work, the thesis still yields an important insight into fundamental trade-offs that have to be considered.
- CoMP might lead to a change in paradigm of mobile network organisation, with *clusters* replacing the concept of *cells*.

-
- Ideally, a mesh backhaul topology should be established between BSs to facilitate low-latency uplink CoMP, while a star topology would be more suitable for the cooperative downlink.
 - Iterative uplink CoMP schemes appear questionable under both theoretical and practical considerations.
 - From a practical point of view, decentralized uplink CoMP schemes provide many benefits, such as less complexity, only local CSI requirements, and most likely an easier usage in conjunction with ARQ and ad-hoc CoMP.
 - In the downlink, UMC schemes cover not only a wide range of scenarios, but also offer low complexity.
 - Scheduling for CoMP is an important (yet hardly investigated) topic, as cooperation gains can be increased, or scenarios created for a particular cooperation concept. The option of ad-hoc CoMP in the uplink, i.e. on demand cooperation *after* transmission has already taken place, promises further improvements of the rate/backhaul trade-off and a shift of ARQ concepts into the network.

Chapter 6

Conclusions

6.1 Contribution of this Work

In this work, novel information-theoretic models for the analysis of rate/backhaul trade-offs achievable with a multitude of CoMP schemes under imperfect channel knowledge have been derived. For downlink CoMP, a major theoretical contribution has been made in the field of uplink/downlink duality, which allows an easier calculation of capacity regions under no or partial BS cooperation and imperfect CSI. The concepts of performance regions and backhaul-constrained capacity regions have been introduced, which enable a joint observation of achievable rates and the corresponding backhaul required.

After a detailed analysis of the capacity gains achievable through CoMP techniques under imperfect channel knowledge and the identification of scenarios where CoMP appears most beneficial, a comprehensive study and comparison of various base station cooperation concepts has been performed for small, analytically tractable scenarios.

The most promising cooperation techniques have then been observed in the context of large cellular systems, where clustering and resource partitioning schemes are used to break such a system down into CoMP scenarios of reasonable size and complexity. The results provide a good basis for mobile operators to assess the rate/backhaul trade-off of various CoMP strategies, and determine suitable cooperation sizes.

A bridge between theory and practice has been drawn through a comprehensive discussion of practical aspects connected to the cooperation schemes. Further, implicit requirements of different CoMP schemes have been pointed out, and a brief insight has been given on the gain of scheduling for CoMP and ad-hoc CoMP concepts.

6.2 Main Conclusions

The work has shown that the strongest CoMP gains in both uplink and downlink can typically be expected for cell-edge scenarios, where the benefit of CoMP in fact increases, the less channel knowledge is available. All CoMP schemes compared are in principle equally sensitive to imperfect channel knowledge, but the fact that imperfect CSI strongly decreases the CoMP gains in scenarios of weak interference narrows down the regimes in which particular schemes are otherwise attractive.

In both *uplink* and *downlink*, significant throughput gains over conventional systems can already be obtained if interference rejection combining or interference-aware precoding are performed. Additional gains are possible - still requiring no additional backhaul between base stations compared to an LTE Release 8 system - if the assignment of base stations to terminals is adjusted flexibly on a short-term basis, or if base stations can serve multiple UEs on the same resource through local joint decoding or joint preprocessing.

In the *uplink*, DIS strategies, where base stations exchange information on decoded data, appear to be of interest in regimes of weak or asymmetrical interference, and low background noise. These schemes provide a limited extent of interference cancellation at a very efficient usage of backhaul. From a practical point of view, a main benefit of these schemes is their low complexity, and that all BSs only require local channel knowledge. In regimes of strong interference, or if a moderate extent of backhaul is available, DAS strategies are superior, where quantized signals are exchanged between base stations and centralized decoding at an involved BS is performed, however requiring larger complexity. For both concepts, a mesh backhaul topology is preferred. Iterative cooperation approaches, i.e. with multiple phases of information exchange, yield only marginal benefit in terms of rate/backhaul trade-off.

In the *downlink*, UMC schemes, where only those base stations participate in the transmission to a terminal that have a reasonably strong link, have shown to be beneficial for most scenarios of low to moderate backhaul. If more backhaul is available, full BS cooperation can be used, facilitating the usage of DPC techniques. A superposition of conventionally and cooperatively transmitted messages appears beneficial in theory, but is questionable in practical systems due to a strongly increased UE complexity and other issues.

Simulation of large cellular systems has shown that in uplink as well as downlink, substantial capacity gains are already possible if co-located BSs perform cooperation without requiring an expensive backhaul infrastructure. Clustering and resource partitioning concepts that enable the cooperation of two adjacent sites have shown to yield a fairly marginal increase of average throughput, but major improvements of system fairness. In the downlink, such CoMP strategies require an additional backhaul traffic solely on the order of 80% of the system throughput, through the exploitation of intra-site CoMP in conjunction with UMC schemes. In the uplink, the proposed clustering concept yields scenarios of strong interference in which centralized DAS concepts are dominant, where the work has shown that the throughput/backhaul trade-off strongly depends on whether sophisticated signal quantization schemes are used. A practical system can be expected to require about 3 bits of additional backhaul for each bit of throughput in the uplink, if 90% of the potential CoMP gains are to be exploited. In total, the overall backhaul infrastructure required in addition to a non-cooperative system in uplink and downlink can hence be expected to carry less than *twice* the actual system capacity (under various optimistic assumptions, but assuming practical quantization schemes), if the downlink traffic is at least of the same order as the uplink traffic.

In general, the results suggest that there might be some major paradigm changes in future mobile communications. On one hand, cell concepts might be replaced through cluster concepts, as discussed in Chapter 4. On the other hand, it is thinkable that ARQ concepts could be shifted into the network, meaning that fluctuations of the wireless channel could be compensated through on-demand information exchanges and cooperation between base stations rather than re-transmission processes between terminals and base stations.

6.3 Future Outlook

In Chapter 4, it has been stated that the value of system-level simulations based on a flat-plane model might be questionable for a meaningful investigation of CoMP. Instead, a more conclusive system-level analysis of CoMP should be based on 3D-models of representative urban areas, where realistic interference scenarios can be captured through e.g. ray-launching techniques [RBL⁺91] and evaluated w.r.t. the suitability of different CoMP concepts. It can be expected that under practical signal propagation conditions, scenarios of highly asymmetrical interference with low background interference occur more often, rendering decentralized CoMP schemes more attractive than they appear in this work. A novel research topic in this context is to use sectorization in order to avoid or purposely create interference that can then be potentially addressed with CoMP [RHZF08]. In general, further practical field trials of CoMP schemes as in [I⁺09, GMRF10, HKF10] are necessary to obtain a better insight into the benefit vs. effort of CoMP under practical signal propagation conditions.

As pointed out in Section 5.2, major research is still necessary in the fields of scheduling for CoMP and *ad-hoc CoMP*. In general, the success of CoMP will strongly depend on whether systems can be built such that they use a reasonable extent of inter-BS signaling to decide

- *which* base stations should generally be considered for cooperation,
- *when* CoMP is to be used, and
- *what* kind of CoMP strategy is most efficient in the very situation.

These decisions and corresponding thresholds may depend strongly on whether spectral efficiency, energy or cost efficiency is to be optimized.

Further, it appears beneficial to use flexible pilot concepts and channel state information feedback schemes which are adapted to the current channel scenario, CoMP scheme and desired uplink/downlink throughput ratio [MRF10].

Finally, an interesting research field is the joint usage of *relaying* and CoMP concepts in heterogeneous deployments [RFL09]. For example, downlink CoMP appears highly suitable for the feeder link to a relay node, exploiting the fact that the latter is typically static, and hence very precise channel knowledge can be obtained at the transmitter at minimal effort. A major challenge then lies in the system design, given the many degrees of freedom in interference shaping and exploitation.

Appendix A

Literature Overview on CoMP

To our knowledge, CoMP was originally proposed for *Code Division Multiple Access* (CDMA) systems in [BMTT00, MBW⁺00, WBOW00, SZ01, WMSL02] and extended to *Orthogonal Frequency Division Multiplex* (OFDM) systems, which are of interest in our work, in [SWC⁺02]. Since then, major research has been performed on this topic, mainly centered around the following key questions or key challenges connected to CoMP:

- **Benefits through CoMP** have been addressed in a wide range of publications. Significant improvements of spectral efficiency have e.g. been predicted in [MKF06] for the uplink and [FKV06, KJV06, JTH⁺07, HT08] in the downlink. A good overview on the potential of interference cancellation through CoMP is given in [And05, CA07a]. The capability of CoMP to improve instantaneous rate fairness in a network was observed in, e.g., [KFVY06], whereas the trade-offs between obtaining spatial multiplexing gain, array gain and/or diversity have been explored for the downlink in, e.g., [ZD04].
- **Synchronization issues connected to CoMP** can be divided into the following fields: Frequency synchronization and timing synchronization of involved communication entities, as well as the phase-coherent synchronization of base stations required for downlink CoMP. It appears that the first issue is minor, as standard frequency synchronization and synchronization error compensation schemes from LTE can be employed [MKP07, SJ09, KHF09]. Timing synchronization poses a major constraint towards CoMP, as strongly differing signal propagation delays between base stations and jointly processed terminals can lead to inter-symbol interference (ISI) or inter-carrier interference (ICI) [KF10]. The aspect of phase synchronization appears to be solvable through GPS-based reference normals at the base stations [I⁺09] (at small CSI feedback delay), or through a network-based IEEE1588v2 time protocol [Dro05, Lim08]. To the knowledge of the authors, however, it has yet not been proved in field trials whether the latter approach offers sufficient accuracy.
- **Channel estimation for CoMP**, more specifically the impact of imperfect channel knowledge on the performance of CoMP was studied in, e.g., [SMW⁺01, WSM06]. It was pointed out in [MW04b] that this can indeed be a crucial problem connected to CoMP. Concrete pilot design for CoMP was done in, e.g., [MWSL02], and specific channel estimation algorithms proposed in [ZN04, MW04a]. A good overview on channel estimation for MIMO OFDM systems in general is found in [BLM03, MB05, CA07b]. An important aspect is also the estimation of signal-to-noise ratios for filter computation [ZM09]. In

the author's opinion, channel estimation for CoMP is a solvable problem, though the previously cited work will still have to be extended to specific multi-cell multi-user pilot sequences and corresponding estimation schemes for LTE-Advanced.

- **Feedback of channel knowledge** is an important aspect for downlink CoMP, but has already been widely investigated in the context of point-to-point MIMO systems. Obviously, such schemes can benefit strongly from the fact that channel realizations are typically strongly correlated in time and frequency. Whereas some authors focus on vector quantization techniques and the inherent codebook design [LJ06, LJ07], others approach the topic more from a source coding point of view, i.e. use decorrelation filters to obtain Gaussian quantities that can be quantized with standard codebooks [CJCU07, JCCU08]. CSI feedback implies that downlink rates are traded against uplink rates, suggesting an application-driven adaptation of the extent of CSI feedback [MRF10].
- **User selection/scheduling for CoMP** has e.g. been investigated in [KPKG05, MK06, KdFG⁺07, MK07], where the focus has been on finding terminals with compound channel properties that can be scheduled onto the same resource in time and frequency and served efficiently through CoMP, while minimizing the accuracy of information needed for performing this decision. Interference-aware scheduling for non-cooperative systems has been investigated in [JST⁺09]. While these publications provide a good basis, there still appears to be vast research required for the design of LTE Advanced systems that can decide ad-hoc when CoMP is to be applied, and to which terminals.
- **Practical CoMP algorithms** for the uplink have been proposed in e.g. [GHEM04, BC07b, BC07a, AEH08]- In these schemes, which can be seen as an extension of local interference-cancellation schemes [CCC00], to decentralized algorithms, the base stations perform individual decoding, but assist each other through the exchange of likelihood information on transmitted bits. Degrees of freedom lie in the question whether each BS only exchanges information on the transmission of an assigned terminal [KF07], or also information on interfering terminals [KF08]. In all cases, a mutual-information maximizing quantization of likelihood values [Rav09] can significantly reduce the required communication bandwidth between base stations. In [MJH06], the authors come to the conclusion that one single information exchange between base stations can in fact yield good decoding results, while further reducing the inter-base-station communication - an aspect we will also confirm later. For the downlink, concrete CoMP algorithms have been proposed in [NEHA08], also based on message passing, or [PHG08, PHG09], where each base station performs signal processing redundantly.
- **Clustering concepts for CoMP**, hence an a priori or ad-hoc definition of groups of base stations that are allowed to cooperate, possibly in conjunction with resource partitioning concepts, have been discussed in [MF07a, PGH08, ZCA⁺08]. All such schemes basically trade performance against signaling overhead. An interesting insight into an optimal frequency reuse factor for a cooperative system is provided in [LYG06], as the results are slightly controversial to most operator's target of reuse factor 1.
- **CoMP field trial results** are available from, e.g., the EASY-C project [I⁺09], where large-scale research test beds for LTE-Advanced have been established. Uplink results are presented in [JJT⁺09, GMRF10], whereas the downlink is covered in [JTW⁺09, HKF10].

Appendix B

Proofs connected to Imperfect Channel Knowledge

B.1 Modified Transmission Equation for UL under Imp. CSI

In this section, we prove Theorem 2.2.1. Let us recall from (2.4) that we assume the channel estimate at the receiver side to be

$$\hat{\mathbf{H}} = \mathbf{H} + \hat{\mathbf{E}}, \quad (\text{B.1})$$

and can hence re-write the transmission equation from (2.1) as

$$\mathbf{y} = (\hat{\mathbf{H}} - \hat{\mathbf{E}}) \mathbf{s} + \mathbf{n} = \left(\underbrace{\hat{\mathbf{H}} - \bar{\mathbf{E}}}_{\hat{\mathbf{H}}^e} - \mathbf{E}^e \right) \mathbf{s} + \mathbf{n}, \quad (\text{B.2})$$

in order to split the channel estimation error $\hat{\mathbf{E}}$ into a part $\bar{\mathbf{E}} \in \mathbb{C}^{[N_{\text{BS}} \times K]}$ which is fully correlated with the estimated channel $\hat{\mathbf{H}}$ (i.e. a kind of *bias*), and a part $\mathbf{E}^e \in \mathbb{C}^{[N_{\text{BS}} \times K]}$ which is completely uncorrelated [PSS04]. To compute the variance of the uncorrelated part (i.e. the *conditional variance* of the elements in $\hat{\mathbf{E}}$ given that $\hat{\mathbf{H}}$ is known), we observe the differential entropy relations [CT06]

$$\forall i, j : h(\hat{e}_{i,j} | \hat{h}_{i,j}) = h(\hat{e}_{i,j}, \hat{h}_{i,j}) - h(\hat{h}_{i,j}) = h(h_{i,j}) + h(\hat{e}_{i,j}) - h(\hat{h}_{i,j}) \quad (\text{B.3})$$

$$\log_2 \left(E \left\{ |\hat{e}_{i,j}|^2 \mid \hat{h}_{i,j} \right\} \right) = \log_2 \left(E \left\{ |h_{i,j}|^2 \right\} \right) + \log_2 \left(E \left\{ |\hat{e}_{i,j}|^2 \right\} \right) - \log_2 \left(E \left\{ |\hat{h}_{i,j}|^2 \right\} \right), \quad (\text{B.4})$$

considering that the channel is modeled as a Gaussian random variable in Section 2.2.1, from which we can follow that

$$\forall i, j : E \left\{ |e_{i,j}^e|^2 \right\} = E \left\{ |\hat{e}_{i,j}|^2 \mid \hat{h}_{i,j} \right\} = \frac{E \left\{ |h_{i,j}|^2 \right\} \cdot \sigma_E^2}{E \left\{ |h_{i,j}|^2 \right\} + \sigma_E^2}. \quad (\text{B.5})$$

As stated in (B.2), we can then merge the estimated channel $\hat{\mathbf{H}}$ and the correlated error term $\bar{\mathbf{E}}$ into a power-reduced *unbiased* channel estimate $\hat{\mathbf{H}}^e \in \mathbb{C}^{[N_{\text{BS}} \times K]}$ given as [PSS04]

$$\forall i, j : \hat{h}_{i,j}^e = \left(1 - \frac{\sigma_E^2}{E \left\{ |h_{i,j}|^2 \right\} + \sigma_E^2} \right) \hat{h}_{i,j}, \quad (\text{B.6})$$

which leads to the fact that the mean powers of the elements in $\hat{\mathbf{H}}^e$ and \mathbf{E}^e sum up to that of the actual channel \mathbf{H} again. Under the assumption that the receiver knows the statistics of the channel estimation error term \mathbf{E}^e , a typical receiver strategy would now be to multiply the received signals with the linear MMSE filter

$$\mathbf{M} = \mathbf{P} \left(\hat{\mathbf{H}}^e \right)^H \left(\hat{\mathbf{H}}^e \mathbf{P} \left(\hat{\mathbf{H}}^e \right)^H + E \left\{ \mathbf{E}^e \mathbf{P} \left(\mathbf{E}^e \right)^H \right\} + \sigma^2 \mathbf{I} \right)^{-1}, \quad (\text{B.7})$$

with $\mathbf{P} = \mathbf{P}(\hat{\mathcal{F}}_{\text{all}})$, in order to obtain estimates $\hat{s} = \mathbf{M}\mathbf{y}$ on the transmitted symbols. Let us now observe one instantaneous channel estimate $\hat{\mathbf{H}}^e$ and derive the average mutual information of the transmission over multiple estimation error realizations \mathbf{E}^e as

$$E_{\mathbf{E}^e} \left\{ I \left(S; \hat{S} | \hat{\mathbf{H}}^e \right) \right\} = h(S) - E_{\mathbf{E}^e} \left\{ h \left(S; \hat{S} | \hat{\mathbf{H}}^e \right) \right\}, \quad (\text{B.8})$$

where the second term can be upper-bounded as the entropy of the *mean-square error* (MSE) between the signals transmitted and estimated [JB03, YG06] as $E_{\mathbf{E}^e} \{ h(S; \hat{S} | \hat{\mathbf{H}}^e) \} =$

$$= E_{\mathbf{E}^e} \left\{ \log_2 \left| \pi e \cdot E_t \left\{ (s - \hat{s}) (s - \hat{s})^H \right\} \right| \right\} \quad (\text{B.9})$$

$$= E_{\mathbf{E}^e} \left\{ \log_2 \left| \pi e \left(\mathbf{P} + \mathbf{M} \left(\mathbf{H} \mathbf{P} \mathbf{H}^H + \sigma^2 \mathbf{I} \right) \mathbf{M}^H - \mathbf{M} \left(\hat{\mathbf{H}}^e + \mathbf{E}^e \right) \mathbf{P} - \mathbf{P} \left(\hat{\mathbf{H}}^e + \mathbf{E}^e \right)^H \mathbf{M}^H \right) \right| \right\} \quad (\text{B.10})$$

$$\leq \log_2 \left| \pi e \left(\mathbf{P} + \mathbf{M} \left(\hat{\mathbf{H}}^e \mathbf{P} \left(\hat{\mathbf{H}}^e \right)^H + \Phi^{\text{hh}} + \sigma^2 \mathbf{I} \right) \mathbf{M}^H - \mathbf{M} \hat{\mathbf{H}}^e \mathbf{P} - \mathbf{P} \left(\hat{\mathbf{H}}^e \right)^H \mathbf{M}^H \right) \right| \quad (\text{B.11})$$

$$= \log_2 \left| \pi e \left(\mathbf{P} - \mathbf{P} \left(\hat{\mathbf{H}}^e \right)^H \left(\hat{\mathbf{H}}^e \mathbf{P} \left(\hat{\mathbf{H}}^e \right)^H + \Phi^{\text{hh}} + \sigma^2 \mathbf{I} \right)^{-1} \hat{\mathbf{H}}^e \mathbf{P} \right) \right|, \quad (\text{B.12})$$

where (B.11) is based on Jensen's inequality, and $\Phi^{\text{hh}} = E_{\mathbf{E}^e} \{ \mathbf{E}^e \mathbf{P} \left(\mathbf{E}^e \right)^H \}$. Equation (B.12) now states the MSE of a transmission where the impact of channel estimation error is treated as a random variable that changes in each channel access. Using (B.12) with (B.8) now yields a lower bound on the mutual information

$$E_{\mathbf{E}^e} \left\{ I \left(S; \hat{S} | \hat{\mathbf{H}}^e \right) \right\} \geq \log_2 \left| \mathbf{I} + \left(\Phi^{\text{hh}} + \sigma^2 \mathbf{I} \right)^{-1} \hat{\mathbf{H}}^e \mathbf{P} \left(\hat{\mathbf{H}}^e \right)^H \right|. \quad (\text{B.13})$$

In this work, we are typically interested in the opposite case, i.e. the capacity of a fixed channel \mathbf{H} , averaged over many channel estimation realizations $\hat{\mathbf{H}}^e$, which we approximate as

$$I \left(S; \hat{S} \right) \geq E_{\hat{\mathbf{H}}^e} \left\{ I \left(S; \hat{S} | \hat{\mathbf{H}}^e \right) \right\} \approx \log_2 \left| \mathbf{I} + \left(\Phi^{\text{hh}} + \sigma^2 \mathbf{I} \right)^{-1} \mathbf{H}^e \mathbf{P} \left(\mathbf{H}^e \right)^H \right|, \quad (\text{B.14})$$

where \mathbf{H}^e is the *average channel estimate* at the receiver, which, considering an unbiased estimator, is a power-scaled version of the actual channel \mathbf{H} , given from (B.1) and (B.5) as

$$\forall i, j : h_{i,j}^e = \frac{h_{i,j}}{\sqrt{1 + \sigma_E^2 / E \left\{ |h_{i,j}|^2 \right\}}}. \quad (\text{B.15})$$

We will from now on refer to \mathbf{H}^e as the *effective*, power-reduced channel. Note that the right-hand side of the approximation in (B.14) is actually larger than the left-hand-side due to

Jensen's equality. However, numeric evaluation has shown that for most channels considered in this work, (B.14) can almost be treated as an equality. Only if the channel estimation noise is of the same power or larger than the channel itself (given unit pilot power), i.e. $\sigma_E^2 \geq E\{|h_{i,j}|^2\}$, the right-hand side of (B.13) may lead to an overestimation of the left-hand side of a few percent. This, however, is a regime in which the exploitation of a link is questionable, anyway. Considering, additionally, that the mutual information for a given channel estimate in (B.13) is already a strong underestimation due to the transformation in (B.11), we assume that in total, (B.15) is a valid lower bound.

Intuitively, this bound can be understood as follows. Initially, we assume both the channel and the estimation error to be random variables with a different realization per block. Then, assuming the latter to have a different realization per channel access, yields a multiplication of Gaussian random variables $\mathbf{E}^e \cdot \mathbf{s}$ in (B.2), which itself is non-Gaussian. Further assuming this product to be Gaussian (knowing that for a given covariance, a Gaussian distribution of a random variable is the one that maximizes entropy) overestimates the detrimental impact of channel estimation error [Med00]. Regardless of the particular BS cooperation scheme we observe in our work, we can hence conservatively estimate the performance of our original transmission in (2.1) by observing the transmission

$$\mathbf{y} = \mathbf{H}^e \mathbf{s} + \mathbf{v} + \mathbf{n}, \quad (\text{B.16})$$

where \mathbf{H}^e is given in (B.15), and $\mathbf{v} \in \mathbb{C}^{[N_{\text{BS}} \times 1]}$ is an additional, zero-mean Gaussian noise term caused by the channel estimation error, fulfilling

$$E\{\mathbf{v}\mathbf{v}^H\} = \mathbf{\Phi}^{\text{hh}} = E\left\{\mathbf{E}^e \mathbf{s} \mathbf{s}^H (\mathbf{E}^e)^H\right\} = \Delta \left(\bar{\mathbf{E}}^e \mathbf{P} \left(\hat{\mathcal{F}}_{\text{all}} \right) (\bar{\mathbf{E}}^e)^H \right), \quad (\text{B.17})$$

where $\forall i, j : \bar{e}_{i,j}^e = \sqrt{E\{|e_{i,j}^e|^2\}}$. The expression $E\{\mathbf{v}\mathbf{v}^H\}$ yields a diagonal covariance due to the fact that all elements of \mathbf{E}^e are uncorrelated. \square

B.2 Modified Transmission Equation for DL under Imp. CSI

In this section, we prove Theorem 2.3.1. Let us recall the transmission in (2.57), i.e.

$$\mathbf{y} = \left(\underbrace{(1 - 2^{-N_b})^{-\frac{1}{2}} (\hat{\mathbf{H}}^{\text{BS}} - \hat{\mathbf{E}}^{\text{BS}})}_{\hat{\mathbf{H}}^{\text{UE}}} - \hat{\mathbf{E}}^{\text{UE}} \right)^H \mathbf{W}\mathbf{x} + \mathbf{n}. \quad (\text{B.18})$$

As in the uplink, we want to transform this into an equation

$$\mathbf{y} = \left(\hat{\mathbf{H}}^e + \mathbf{E}^{\text{e,BS}} + \mathbf{E}^{\text{e,UE}} \right)^H \mathbf{W}\mathbf{x} + \mathbf{n}, \quad (\text{B.19})$$

where all terms $\hat{\mathbf{H}}^e$, $\mathbf{E}^{\text{e,BS}}$ and $\mathbf{E}^{\text{e,UE}}$ are uncorrelated from each other and sum up to the power of the original channel again. We can start by observing the variance of $\hat{\mathbf{E}}^{\text{UE}}$ conditioned on $\hat{\mathbf{H}}^{\text{BS}}$ and $\hat{\mathbf{E}}^{\text{BS}}$. Clearly, this is the same as conditioning the variable on $\hat{\mathbf{H}}^{\text{UE}}$, which we have already derived in Theorem 2.2.1 as

$$\forall i, j : E\left\{|e_{i,j}^{\text{e,UE}}|^2\right\} = E\left\{|\hat{e}_{i,j}^{\text{UE}}|^2 \mid \hat{h}_{i,j}^{\text{UE}}\right\} = \frac{E\{|h_{i,j}|^2\} \cdot \sigma_E^2}{E\{|h_{i,j}|^2\} + \sigma_E^2}. \quad (\text{B.20})$$

As in the uplink, we must consider the part of $\hat{\mathbf{E}}^{\text{UE}}$ which is correlated with $\hat{\mathbf{H}}^{\text{UE}}$, and which leads us to the unbiased channel estimate $\hat{\mathbf{H}}^{\text{e,UE}}$ [PSS04]

$$\forall i, j : \hat{h}_{i,j}^{\text{e,UE}} = \left(1 - \frac{\sigma_E^2}{E \{ |h_{i,j}|^2 \} + \sigma_E^2} \right) \hat{h}_{i,j}^{\text{UE}}. \quad (\text{B.21})$$

Now we need to determine the variances of the elements of $\hat{\mathbf{E}}^{\text{BS}}$ conditioned on $\hat{\mathbf{H}}^{\text{BS}}$, where we make use of the relation between estimated and real channel in (2.56) and state the differential entropy relations [CT06]

$$\begin{aligned} \forall i, j : h \left(\hat{e}_{i,j}^{\text{BS}} \mid \hat{h}_{i,j}^{\text{BS}} \right) &= h \left(\hat{e}_{i,j}^{\text{BS}}, \hat{h}_{i,j}^{\text{BS}} \right) - h \left(\hat{h}_{i,j}^{\text{BS}} \right) \\ &= h \left(\hat{h}_{i,j}^{\text{BS}} \mid \hat{e}_{i,j}^{\text{BS}} \right) + h \left(\hat{e}_{i,j}^{\text{BS}} \right) - h \left(\hat{h}_{i,j}^{\text{BS}} \right) \\ \log_2 \left(E \left\{ \left| \hat{e}_{i,j}^{\text{BS}} \right|^2 \mid \hat{h}_{i,j}^{\text{BS}} \right\} \right) &= \log_2 \left((1 - 2^{-N_b}) \left(E \left\{ |h_{i,j}|^2 \right\} + \sigma_E^2 \right) \right) \cdots \\ &\quad + \log_2 \left((2^{-N_b}) \left(E \left\{ |h_{i,j}|^2 \right\} + \sigma_E^2 \right) \right) \cdots \\ &\quad - \log_2 \left(\left(E \left\{ |h_{i,j}|^2 \right\} + \sigma_E^2 \right) \right) \\ &= \log_2 \left((1 - 2^{-N_b}) (2^{-N_b}) \left(E \left\{ |h_{i,j}|^2 \right\} + \sigma_E^2 \right) \right). \end{aligned} \quad (\text{B.22})$$

We can now conjecture from (B.18) and (B.22) that

$$\forall i, j : E \left\{ \left| \hat{e}_{i,j}^{\text{e,BS}} \right|^2 \right\} = 2^{-N_b} \frac{\left(E \left\{ |h_{i,j}|^2 \right\} \right)^2}{E \left\{ |h_{i,j}|^2 \right\} + \sigma_E^2}. \quad (\text{B.23})$$

We can now follow the argumentation from Section B.1 again and introduce an *effective channel*. This can be derived, such that the powers of all terms in parentheses in (B.19) sum up to the power of the actual channel again, as

$$\forall i, j : h_{i,j}^{\text{e}} = h_{i,j} \cdot \sqrt{\frac{E \left\{ |h_{i,j}|^2 \right\} (1 - 2^{-N_b})}{E \left\{ |h_{i,j}|^2 \right\} + \sigma_E^2}}. \quad (\text{B.24})$$

We can easily see that if the CSI at BS and UE side is the same (i.e. $N_b \rightarrow \infty$), the effective channel corresponds to that of the uplink in (2.8). Note that $\mathbf{E}^{\text{e,BS}}$ and $\mathbf{E}^{\text{e,UE}}$ are still assumed to be random variables that remain constant over a complete transmission block. If we now assume that these random variables have a different realization for each transmitted symbol, the expressions $\mathbf{E}^{\text{e,BS}} \mathbf{W} \mathbf{x}$ and $\mathbf{E}^{\text{e,UE}} \mathbf{W} \mathbf{x}$ have a *product normal distribution*, which is rather difficult to handle. If we assume these terms to be Gaussian random variables, we overestimate their impact on the transmission, as a Gaussian distribution maximizes entropy for a given variance. If we assure that both stated terms have a detrimental effect on our achievable rates in the remainder of this work (hence these terms are never exploited as useful signal power), we can hence inner-bound capacity regions of the initial transmission equation (2.54) by making the above mentioned assumptions. As all elements in $\mathbf{E}^{\text{e,BS}}$ and

$\mathbf{E}^{e, \text{UE}}$ are uncorrelated, we can further state

$$E \left\{ (\mathbf{E}^{e, \text{BS}})^H \mathbf{W}_x \left((\mathbf{E}^{e, \text{BS}})^H \mathbf{W}_x \right)^H \right\} = \Delta \left((\bar{\mathbf{E}}^{e, \text{BS}})^H \Phi^{\text{ss}} \bar{\mathbf{E}}^{e, \text{BS}} \right) \text{ and} \quad (\text{B.25})$$

$$E \left\{ (\mathbf{E}^{e, \text{UE}})^H \mathbf{W}_x \left((\mathbf{E}^{e, \text{UE}})^H \mathbf{W}_x \right)^H \right\} = \Delta \left((\bar{\mathbf{E}}^{e, \text{UE}})^H \Phi^{\text{ss}} \bar{\mathbf{E}}^{e, \text{UE}} \right), \quad (\text{B.26})$$

where $\forall i, j$: $\bar{e}_{i,j}^{\text{BS}} = \sqrt{2^{-N_b} \frac{(E\{|h_{i,j}|^2\})^2}{E\{|h_{i,j}|^2\} + \sigma_E^2}}$ and $\bar{e}_{i,j}^{\text{UE}} = \sqrt{\frac{|h_{i,j}|^2 \cdot \sigma_E^2}{|h_{i,j}|^2 + \sigma_E^2}}$. \square

B.3 Downlink SINRs under Imperfect CSI

In this section, we prove Lemma 2.3.2. Let us first observe a simplified SISO transmission

$$y = (h + \Delta h) s + n, \quad (\text{B.27})$$

where y , s and n are scalar Gaussian random variables, and h and Δh correspond to a (block static) channel and Gaussian random channel estimation error, where we assume h to be known to both transmitter and receiver, and Δh to be known only to the receiver. We are interested in the average mutual information of this transmission over all possible realizations of the channel component Δh only known to the receiver, which can easily be stated as

$$E_{\Delta h} \{I(S; Y)\} = E_{\Delta h} \{h(Y) - h(Y|S)\} \quad (\text{B.28})$$

$$= E_{\Delta h} \left\{ \log_2 \left(\frac{|h + \Delta h|^2 E\{|s|^2\} + E\{|n|^2\}}{E\{|n|^2\}} \right) \right\} \quad (\text{B.29})$$

$$\geq \log_2 \left(\frac{|h|^2 E\{|s|^2\} + E\{|n|^2\}}{E\{|n|^2\}} \right). \quad (\text{B.30})$$

Here, Y and S denote the sequences of all received and transmitted signals over all N_{sym} channel accesses, respectively. We can see from (B.28) that the mutual information can be lower-bounded by the case where the channel estimation error at the transmitter side (but known to the receiver side) simply does not exist. Clearly, this is not a very satisfactory lower bound, as it is intuitive to see that the receiver should actually benefit from the additional signal power connected to Δh , but this is difficult to state in compact notation (i.e. where all expectation values connected to channel estimation error appear in the logarithm, hence where a closed-form SINR can be stated), without conflicting with Jensen's inequality.

For the dirty-paper coding case, we state an even weaker lower bound by assuming that any channel estimation error at the transmitter side, despite being known at the receiver side, is treated as noise [MF09b], if the receiver is supposed to benefit from DPC.

With (B.28) and the previous considerations, (2.61) is directly derived from (2.58). Each UE k sees a useful signal term (based on the chosen precoding vector \mathbf{w}_k and the effective channel \mathbf{h}_k^e the BS can exploit with its limited CSI), and noise terms connected to interference or the impact of channel estimation error. In the case of pure linear precoding, each transmission is interfered by all other transmissions (hence $\mathcal{J}_1(k) = \{j \in \mathcal{K} : j \neq k\}$), but the fact of less CSI at the BS side than at the UE side has no effect for the useful signal directed towards k , as seen in (B.28) (hence also $\mathcal{J}_2(k) = \{j \in \mathcal{K} : j \neq k\}$). In the case of dirty paper coding, where the UEs are assumed to be encoded in the order $K..1$, the BSs can transmit

in such a way that all UEs are free of the interference of transmissions encoded successively (at least the extent of interference connected to the channel knowledge at the BSs, hence connected to \mathbf{H}^e), as proven in [Cos83] (hence $\forall k : \mathcal{J}_1(k) = \{j \in \mathcal{K} : j < k\}$). However, all UEs suffer from the imperfect CSI at both BS and UE side as well as the additional channel imperfectness at the BS side through additional noise terms. Only UE K , which is encoded first and hence does *not* benefit from DPC, does not suffer from its own noise term connected to additional CSIT imperfectness (hence $\mathcal{J}_2(K) = \{1..K-1\}$ and $\forall k < K : \mathcal{J}_2(k) = \mathcal{K}$). \square

Appendix C

Proofs connected to Uplink-Downlink Duality

In this appendix, we prove Theorem 2.3.3. The proof consists of proving two lemmas in the sequel.

C.1 DL SCO Problem with Per-Antenna Power Constraints

Lemma C.1.1. *A downlink beamforming problem from M fully cooperative BSs with N_{bs} antennas each to K UEs with one antenna each and noise covariance $\sigma^2\mathbf{I}$, individual SINR targets and per-antenna power constraints $\check{\mathbf{P}}^{\text{max}}$, has the same optimum solution (i.e. the same minimum sum transmit power) as an uplink transmission from K UEs to M BSs through the same (reciprocal) channel with the same SINR targets under a sum-power constraint and a least favorable noise covariance.*

More specifically, the downlink SINR-constrained optimization (SCO) problem

$$\begin{aligned} & \text{minimize} && \alpha \cdot \text{tr}\{\check{\mathbf{P}}^{\text{max}}\} \\ & \text{subject to} && \Delta(\mathbf{W}\mathbf{W}^H) \preceq \alpha\check{\mathbf{P}}^{\text{max}} \\ & && \text{and } \forall k \in \mathcal{K} : \text{SINR}_k^{\text{inf}} \geq \xi_k, \end{aligned} \tag{C.1}$$

where $\check{\mathbf{P}}^{\text{max}} = \text{diag}(\check{\mathbf{p}}^{\text{max}})$ contains the per-antenna power constraints on the diagonal as defined in Section 2.3.1, $\alpha \geq 0$ is a slack variable, and $\forall k \in \mathcal{K} : \text{SINR}_k^{\text{inf}}$ are the achievable downlink SINRs as given in Lemma 2.3.2, can be tackled by solving a dual uplink SCO problem

$$\begin{aligned} & \max_{\hat{\Phi}_{\text{nn}}} \min_{\hat{\mathbf{P}}} && \sum_{k=1}^K \hat{p}_k \\ & \text{subject to} && \forall k \in \mathcal{K} : \text{SINR}_k \geq \xi_k \\ & && \text{and } \text{tr}\{\hat{\Phi}_{\text{nn}}\check{\mathbf{P}}^{\text{max}}\} \leq \sigma^2 \text{tr}\{\check{\mathbf{P}}^{\text{max}}\}, \hat{\Phi}_{\text{nn}} \succeq 0, \end{aligned} \tag{C.2}$$

where $\hat{\mathbf{P}} = \text{diag}(\hat{\mathbf{p}})$ are dual uplink transmit powers and $\forall k \in \mathcal{K} : \text{SINR}_k$ are the achievable uplink SINRs.

Proof. The proof is partially based on work in [YL07], but extended to the case of imperfect CSIT and CSIR, due to our downlink transmission model in Section 2.3.2. We also believe that we have found a significantly more compact proof than the stated authors. Let us initially recall the achievable downlink SINR of each user $k \in \mathcal{K}$ based on Lemma 2.3.2 as

$$\text{SINR}_k^{\check{\text{inf}}} \geq \frac{\overbrace{\left| (\mathbf{h}_k^e)^H \mathbf{w}_k \right|^2}^{\text{Desired signal}}}{\underbrace{\sum_{j \in \mathcal{J}_1(k)} \left| (\mathbf{h}_k^e)^H \mathbf{w}_j \right|^2}_{\text{Inter-user interference}} + \underbrace{\sum_{j \in \mathcal{J}_2(k)} \sum_{a=1}^{N_{\text{BS}}} \left| \bar{e}_{a,k}^{\text{BS}} w_{a,j} \right|^2}_{\text{Impact of imp. CSI at BS}} + \underbrace{\sum_{j=1}^K \sum_{a=1}^{N_{\text{BS}}} \left| \bar{e}_{a,k}^{\text{UE}} w_{a,j} \right|^2}_{\text{Impact of imp. CSI at UE}} + \sigma^2}, \quad (\text{C.3})$$

where $\mathcal{J}_1(k)$ and $\mathcal{J}_2(k)$ were stated in the context of Lemma 2.3.2 and are not of particular interest here. By inserting (C.3) into the optimization problem (C.1), we can restate this as

$$\begin{aligned} & \text{minimize} && \alpha \cdot \text{tr}\{\check{\mathbf{P}}^{\text{max}}\} \\ & \text{subject to} && \Delta(\mathbf{W}\mathbf{W}^H) \preceq \alpha \check{\mathbf{P}}^{\text{max}} \\ & \text{and} && \forall k \in \mathcal{K} : \frac{1}{\xi_k} \left| (\mathbf{h}_k^e)^H \mathbf{w}_k \right|^2 \geq \left\| \begin{array}{c} (\mathbf{h}_k^e)^H \mathbf{W}_{\mathcal{J}_1(k)} \\ \text{vec} \left(\Delta \left(\bar{\mathbf{e}}_k^{\text{e,BS}} \right) \mathbf{W}_{\mathcal{J}_2(k)} \right) \\ \text{vec} \left(\Delta \left(\bar{\mathbf{e}}_k^{\text{e,UE}} \right) \mathbf{W} \right) \\ \sigma \end{array} \right\|^2, \end{aligned} \quad (\text{C.4})$$

where $\mathbf{W}_{\mathcal{J}}$ is the precoding matrix \mathbf{W} reduced to all columns connected to UEs $j \in \mathcal{J}$. As the achieved terminal SINRs are independent of phase rotations of complete columns of matrix \mathbf{H}^e , we can assume without loss of generality that $\forall k \in \mathcal{K} : \Im\{(\mathbf{h}_k^e)^H \mathbf{w}_k\} = 0$ [YL07], which allows us to write (C.4) as

$$\begin{aligned} & \text{minimize} && \alpha \cdot \text{tr}\{\check{\mathbf{P}}^{\text{max}}\} \\ & \text{subject to} && \Delta(\mathbf{W}\mathbf{W}^H) \preceq \alpha \check{\mathbf{P}}^{\text{max}} \\ & \text{and} && \forall k \in \mathcal{K} : \sqrt{\frac{1}{\xi_k}} \left| (\mathbf{h}_k^e)^H \mathbf{w}_k \right| \geq \left\| \begin{array}{c} (\mathbf{h}_k^e)^H \mathbf{W}_{\mathcal{J}_1(k)} \\ \text{vec} \left(\Delta \left(\bar{\mathbf{e}}_k^{\text{e,BS}} \right) \mathbf{W}_{\mathcal{J}_2(k)} \right) \\ \text{vec} \left(\Delta \left(\bar{\mathbf{e}}_k^{\text{e,UE}} \right) \mathbf{W} \right) \\ \sigma \end{array} \right\|. \end{aligned} \quad (\text{C.5})$$

This corresponds to the formulation of a *second order cone programming* (SOCP) problem [BV04, WES06] with a convex objective and convex constraints, for which it is known that if a Lagrangian dual problem can be formulated, strict duality holds, hence the optimum value of the dual problem is equal to the optimum value of the original problem [BV04]. We

can state the Lagrangian for the optimization problem in (C.1) as

$$\begin{aligned}
L(\alpha, \mathbf{W}, \mathbf{Q}, \mathbf{\Lambda}) = & \\
& \alpha \cdot \text{tr}\{\check{\mathbf{P}}^{\max}\} + \sum_{i=1}^{N_{\text{BS}}} q_i \left(\left[\sum_{j=1}^K \mathbf{w}_j \mathbf{w}_j^H \right]_{i,i} - \alpha \text{tr}\{\check{\mathbf{P}}^{\max}\} \right) + \sum_{k=1}^K \lambda_k \left(\sum_{j \in \mathcal{J}_1(k)} \left| (\mathbf{h}_k^e)^H \mathbf{w}_j \right|^2 + \dots \right. \\
& \left. \dots + \sum_{j \in \mathcal{J}_2(k)} \sum_{a=1}^{N_{\text{BS}}} |\bar{e}_{a,k}^{\text{BS}} w_{a,j}|^2 + \sum_{j=1}^K \sum_{a=1}^{N_{\text{BS}}} |\bar{e}_{a,k}^{\text{UE}} w_{a,j}|^2 + \sigma^2 - \frac{1}{\xi_k} \left| (\mathbf{h}_k^e)^H \mathbf{w}_k \right|^2 \right), \quad (\text{C.6})
\end{aligned}$$

where $\mathbf{q} \in \mathbb{R}_0^{+[N_{\text{BS}} \times 1]}$ with $\mathbf{Q} = \text{diag}(\mathbf{q})$ are the Lagrangian multipliers connected to the per-antenna power constraints, and $\forall k \in \mathcal{K} : \lambda_k \in \mathbb{R}$ with $\mathbf{\Lambda} = \text{diag}(\lambda_1 \dots \lambda_K)$ are the Lagrangian multipliers connected to the SINR constraints. These multipliers can be seen as *penalties* that are added to the objective function if the constraints are not met. Hence, the optimization problem with *explicit*, hard constraints from (C.1) has been modified to an optimization problem with *implicit*, soft constraints. The authors in [YL07] have shown that it is also possible to obtain the Lagrangian from the formulation of a SOCP directly, which can be easily extended to our model incorporating imperfect CSI. Equation (C.6) can be restated as

$$\begin{aligned}
L(\alpha, \mathbf{W}, \mathbf{Q}, \mathbf{\Lambda}) = & \\
& \sum_{k=1}^K \lambda_k \sigma_k^2 + \alpha \left(\underbrace{\text{tr}\{\check{\mathbf{P}}^{\max}\} - \text{tr}\{\mathbf{Q}\check{\mathbf{P}}^{\max}\}}_{\text{Must be non-negative}} \right) + \sum_{k=1}^K \mathbf{w}_k^H \left(\underbrace{\mathbf{Q} + \sum_{j \in \mathcal{J}_1^*(k)} \lambda_j \mathbf{h}_j^e (\mathbf{h}_j^e)^H}_{\text{Must be ...}} + \dots \right) \\
& \left. \dots + \underbrace{\sum_{j \in \mathcal{J}_2^*(k)} \lambda_j \Delta \left(\bar{\mathbf{e}}_j^{\text{e,BS}} (\bar{\mathbf{e}}_j^{\text{e,BS}})^H \right) + \sum_{j=1}^K \lambda_j \Delta \left(\bar{\mathbf{e}}_j^{\text{e,UE}} (\bar{\mathbf{e}}_j^{\text{e,UE}})^H \right) - \frac{\lambda_k}{\xi_k} \mathbf{h}_k^e (\mathbf{h}_k^e)^H}_{\dots \text{ positive semidefinite}} \right) \mathbf{w}_k, \quad (\text{C.7})
\end{aligned}$$

where $\forall i \in \{1, 2\} : \mathcal{J}_i^*(k) = \{j \in \mathcal{K} : k \in \mathcal{J}_i(j)\}$ are the dual sets to $\mathcal{J}_1(k)$, $\mathcal{J}_2(k)$, and the dual objective function [BV04] can then be written as

$$g(Q, \Lambda) = \min_{\mathbf{W}} \min_{\alpha} L(\alpha, \mathbf{W}, \mathbf{Q}, \mathbf{\Lambda}). \quad (\text{C.8})$$

As there is no constraint on parameter \mathbf{W} , and α is only constrained to be non-negative, we have to assure that \mathbf{Q} and $\mathbf{\Lambda}$ in (C.8) are constrained such that the objective function always yields a finite, non-negative value. As already indicated in (C.7), this is the case if we assure that $\text{tr}\{\check{\mathbf{P}}^{\max}\} - \text{tr}\{\mathbf{Q}\check{\mathbf{P}}^{\max}\} \geq 0$ and that the bulky expression in parentheses in (C.7)

is positive semidefinite. With these observations, we can finally state the dual problem as

$$\begin{aligned}
& \max_{\mathbf{Q}} \max_{\mathbf{\Lambda}} \quad \sum_{k=1}^K \lambda_k \sigma_k^2 \\
\text{subject to} \quad & \forall k \in \mathcal{K} : \mathbf{Q} + \sum_{j \in \mathcal{J}_1^*(k)} \lambda_j \mathbf{h}_j^e (\mathbf{h}_j^e)^H + \sum_{j \in \mathcal{J}_2^*(k)} \lambda_j \Delta \left(\bar{\mathbf{e}}_j^{\text{e,BS}} \left(\bar{\mathbf{e}}_j^{\text{e,BS}} \right)^H \right) + \dots \\
& \dots + \sum_{j=1}^K \lambda_j \Delta \left(\bar{\mathbf{e}}_j^{\text{e,UE}} \left(\bar{\mathbf{e}}_j^{\text{e,UE}} \right)^H \right) - \frac{\lambda_k}{\xi_k} \mathbf{h}_k^e (\mathbf{h}_k^e)^H \succeq 0 \\
\text{and} \quad & \text{tr}\{\mathbf{Q}\check{\mathbf{P}}^{\text{max}}\} \leq \text{tr}\{\check{\mathbf{P}}^{\text{max}}\}, \mathbf{Q} \succeq 0.
\end{aligned} \tag{C.9}$$

As the original problem has been shown to have a convex objective and convex constraints, we have already proved that (C.9) is strictly dual to the original optimization problem (C.1), hence they lead to the same optimum solution $\alpha \cdot \text{tr}\{\check{\mathbf{P}}^{\text{max}}\} = \sum_{k=1}^K \lambda_k \sigma_k^2$. However, we still have to prove that (C.9) is equivalent to the uplink SCO problem in (C.2). For this, let us re-write (C.9) as

$$\begin{aligned}
& \max_{\mathbf{Q}} \max_{\mathbf{\Lambda}} \quad \sum_{k=1}^K \lambda_k \sigma_k^2 \\
\text{subject to} \quad & \forall k \in \mathcal{K}, \forall \hat{\mathbf{w}}_k : \hat{\mathbf{w}}_k^H \left(\mathbf{Q} + \sum_{j \in \mathcal{J}_1^*(k)} \lambda_j \mathbf{h}_j^e (\mathbf{h}_j^e)^H + \sum_{j \in \mathcal{J}_2^*(k)} \lambda_j \Delta \left(\bar{\mathbf{e}}_j^{\text{e,BS}} \left(\bar{\mathbf{e}}_j^{\text{e,BS}} \right)^H \right) + \dots \right. \\
& \left. \dots + \sum_{j=1}^K \lambda_j \Delta \left(\bar{\mathbf{e}}_j^{\text{e,UE}} \left(\bar{\mathbf{e}}_j^{\text{e,UE}} \right)^H \right) - \frac{\lambda_k}{\xi_k} \mathbf{h}_k^e (\mathbf{h}_k^e)^H \right) \hat{\mathbf{w}}_k \geq 0 \\
\text{and} \quad & \text{tr}\{\mathbf{Q}\check{\mathbf{P}}^{\text{max}}\} \leq \text{tr}\{\check{\mathbf{P}}^{\text{max}}\}, \mathbf{Q} \succeq 0.
\end{aligned} \tag{C.10}$$

Now it is easy to see that at the optimum of (C.10), there must be at least one vector $\hat{\mathbf{w}}_k$ for each k for which the second line in (C.10) is met with equality. If this were not the case, λ_k as well as other lambda values could be increased, so that a better objective value would be achieved, while still fulfilling the constraints. Based on this knowledge, we can change the maximization over $\mathbf{\Lambda}$ in (C.10) to a minimization and state

$$\begin{aligned}
& \max_{\mathbf{Q}} \min_{\mathbf{\Lambda}} \quad \sum_{k=1}^K \lambda_k \sigma_k^2 \\
\text{subject to} \quad & \forall k \in \mathcal{K}, \exists \hat{\mathbf{w}}_k : \frac{\lambda_k \hat{\mathbf{w}}_k^H \mathbf{h}_k^e (\mathbf{h}_k^e)^H \hat{\mathbf{w}}_k}{\hat{\mathbf{w}}_k^H \left(\mathbf{Q} + \sum_{j \in \mathcal{J}_1^*(k)} \lambda_j \mathbf{h}_j^e (\mathbf{h}_j^e)^H + \sum_{j \in \mathcal{J}_2^*(k)} \lambda_j \Delta \left(\bar{\mathbf{e}}_j^{\text{e,BS}} \left(\bar{\mathbf{e}}_j^{\text{e,BS}} \right)^H \right) + \sum_{j=1}^K \lambda_j \Delta \left(\bar{\mathbf{e}}_j^{\text{e,UE}} \left(\bar{\mathbf{e}}_j^{\text{e,UE}} \right)^H \right) \right) \hat{\mathbf{w}}_k} \geq \xi_k \\
\text{and} \quad & \text{tr}\{\mathbf{Q}\check{\mathbf{P}}^{\text{max}}\} \leq \text{tr}\{\check{\mathbf{P}}^{\text{max}}\}, \mathbf{Q} \succeq 0.
\end{aligned} \tag{C.11}$$

If we now introduce $\hat{\Phi}_{\text{nn}} = \sigma^2 \mathbf{Q}$ and $\forall k \in \mathcal{K} : \hat{p}_k = \lambda_k \sigma^2$, we can write (C.12) as

$$\begin{aligned} \max_{\hat{\Phi}_{\text{nn}}} \min_{\hat{\mathbf{P}}} \quad & \sum_{k=1}^K \hat{p}_k \\ \text{subject to} \quad & \forall k \in \mathcal{K}, \exists \hat{\mathbf{w}}_k : \frac{\hat{p}_k \hat{\mathbf{w}}_k^H \mathbf{h}_k^e (\mathbf{h}_k^e)^H \hat{\mathbf{w}}_k}{\hat{\mathbf{w}}_k^H \left(\hat{\Phi}_{\text{nn}} + \sum_{j \in \mathcal{J}_1^e(k)} \hat{p}_j \mathbf{h}_j^e (\mathbf{h}_j^e)^H + \sum_{j \in \mathcal{J}_2^e(k)} \hat{p}_j \Delta \left(\mathbf{e}_j^{\text{e,BS}} (\mathbf{e}_j^{\text{e,BS}})^H \right) + \sum_{j=1}^K \hat{p}_j \Delta \left(\mathbf{e}_j^{\text{e,UE}} (\mathbf{e}_j^{\text{e,UE}})^H \right) \right) \hat{\mathbf{w}}_k} \geq \gamma_k \\ \text{and} \quad & \text{tr}\{\hat{\Phi}_{\text{nn}} \check{\mathbf{P}}^{\text{max}}\} \leq \sigma^2 \text{tr}\{\check{\mathbf{P}}^{\text{max}}\}, \hat{\Phi}_{\text{nn}} \succeq \mathbf{0}, \end{aligned} \quad (\text{C.12})$$

which corresponds to (C.2), an uplink problem where $\forall k \in \mathcal{K} : \hat{\mathbf{w}}_k$ are the BS-side receive filters, with imperfect *receiver-side* CSI and a least favorable noise covariance, i.e.

$$\begin{aligned} \max_{\hat{\Phi}_{\text{nn}}} \min_{\hat{\mathbf{P}}} \quad & \sum_{k=1}^K \hat{p}_k \\ \text{subject to} \quad & \forall k \in \mathcal{K} : \text{SINR}_k \geq \xi_k \\ \text{and} \quad & \text{tr}\{\hat{\Phi}_{\text{nn}} \check{\mathbf{P}}^{\text{max}}\} \leq \sigma^2 \text{tr}\{\check{\mathbf{P}}^{\text{max}}\}, \hat{\Phi}_{\text{nn}} \succeq \mathbf{0}. \end{aligned} \quad (\text{C.13})$$

For *per-base-station* power constraints (hence constraints on groups of antennas), it has been shown in [YL07] that the same concept of uplink/downlink duality can be applied, but that the matrix of Lagrangian multipliers \mathbf{Q} is of size $M \times M$, as the number of power constraints is less. This leads to the fact that the virtual uplink noise covariance matrix $\hat{\Phi}_{\text{nn}}$ must have equal values on all elements connected to BS antennas belonging to the same BS. In the case of a *sum-power* constraint in the downlink, all diagonal elements of the virtual uplink covariance matrix $\hat{\Phi}_{\text{nn}}$ must be equal, yielding the unique solution $\hat{\Phi}_{\text{nn}} = \sigma^2 \mathbf{I}$. \square

C.2 Equivalence of UL and DL Capacity Region under Per-Ant. Power Constr.

Lemma C.2.1. *The capacity region of a downlink transmission from M BSs with N_{bs} antennas each to K UEs with one antenna each, noise covariance $\sigma^2 \mathbf{I}$, per-antenna power constraints $\check{\mathbf{P}}^{\text{max}}$ and imperfect transmitter-sided CSI is equivalent to the capacity region of an uplink transmission from K UEs to M BSs through the same (reciprocal) channel under a sum-power constraint and a least favorable, diagonal noise covariance fulfilling $\text{tr}\{\hat{\Phi}_{\text{nn}} \check{\mathbf{P}}^{\text{max}}\} \leq \sigma^2 \text{tr}\{\check{\mathbf{P}}^{\text{max}}\}$, and the same extent of imperfect receiver-sided CSI.*

Proof. The proof follows directly from Lemma C.1.1. In both the original downlink SCO problem (C.1) and the dual uplink SCO problem (C.2) it is apparent that at the optimum point, all SINR constraints have to be met with equality. If this were not the case, i.e. if one UE would over-fulfill its SINR constraint, the corresponding transmit power could be reduced (and that connected to other UEs correspondingly), leading to an improved metric. For $N_{\text{mt}} = 1$, there is a direct relation between SINR and capacity $C = \log_2(1 + \text{SINR})$, assuming Gaussian modulation, perfect coding and infinite block lengths. Hence, if we observe all rate tuples for which the downlink SCO problem from Section C.1 is feasible (hence yielding $\alpha \leq 1$), the dual uplink SCO problem must also be feasible and yield $\sum_{k=1}^K \hat{p}_k \leq \text{tr}\{\check{\mathbf{P}}^{\text{max}}\}$. Hence, the capacity regions of the modified downlink transmission from (2.58) and of a dual uplink transmission with a sum power constraint and a least favorable noise covariance fulfilling $\text{tr}\{\hat{\Phi}_{\text{nn}} \check{\mathbf{P}}^{\text{max}}\} \leq \sigma^2 \text{tr}\{\check{\mathbf{P}}^{\text{max}}\}$ must be equivalent. \square

Appendix D

Proofs connected to Capacity Regions

D.1 Uplink Capacity Region under Infinite BS cooperation

In this section, we prove Theorem 2.2.2. For any power allocation $\mathbf{P} \preceq \mathbf{P}(\hat{\mathcal{F}}_{\text{all}})$, the mutual information of the modified transmission equation in (2.7) is given as [CT06]

$$I(S; Y) = h(Y) - h(Y|S) \quad (\text{D.1})$$

$$= \log_2 |\pi e \Phi^{yy}| - \log_2 |\pi e \Phi^{yy|s}|, \quad (\text{D.2})$$

where S and Y denote all transmitted and received signals during N_{sym} consecutive channel accesses, $\Phi^{yy} \in \mathbb{C}^{[N_{\text{BS}} \times N_{\text{BS}}]}$ denotes the signal covariance of the received signals at all BS antennas, and $\Phi^{yy|s} \in \mathbb{C}^{[N_{\text{BS}} \times N_{\text{BS}}]}$ denotes the same signal covariance, but conditioned on the fact that S is known. We can then follow from

$$\Phi^{yy}(\mathbf{P}) = \mathbf{H}^e \mathbf{P} \mathbf{H}^e + \Delta \left(\bar{\mathbf{E}}^e \mathbf{P} \left(\hat{\mathcal{F}}_{\text{all}} \right) \left(\bar{\mathbf{E}}^e \right)^H \right) + \sigma^2 \mathbf{I} \text{ and} \quad (\text{D.3})$$

$$\Phi^{yy|s}(\mathbf{P}) = \Delta \left(\bar{\mathbf{E}}^e \mathbf{P} \left(\hat{\mathcal{F}}_{\text{all}} \right) \left(\bar{\mathbf{E}}^e \right)^H \right) + \sigma^2 \mathbf{I}, \quad (\text{D.4})$$

and the fact that signals from some UEs can be decoded and subtracted from the system before the decoding of other UEs (i.e. successive interference cancellation), that the maximum sum-rate of any subset of messages $\forall \mathcal{F} \subseteq \hat{\mathcal{F}}_{\text{all}}$ is limited through

$$\sum_{F \in \mathcal{F}} \nu_F \leq \log_2 \left| \mathbf{I} + \left(\sigma^2 \mathbf{I} + \Delta \left(\bar{\mathbf{E}}^e \mathbf{P} \left(\hat{\mathcal{F}}_{\text{all}} \right) \left(\bar{\mathbf{E}}^e \right)^H \right) \right)^{-1} \mathbf{H}^e \mathbf{P}(\mathcal{F}) \left(\mathbf{H}^e \right)^H \right|. \quad (\text{D.5})$$

The overall capacity region considering all power allocations $\mathbf{P} \preceq \hat{\mathbf{P}}^{\text{max}}$ in (2.11) then follows through standard time-sharing arguments [CT06]. As the modified transmission equation in (2.7) overestimates the impact of imperfect channel knowledge at the receiver side as proved in section B.1, equation (2.11) states an inner bound to the capacity region of the original uplink transmission in (2.1). \square

D.2 UL Capacity Region with DIS/CIF/DAS BS Cooperation

In this section, we prove Theorem 2.2.5, stating inner bounds on the capacity regions of various uplink base station cooperation schemes.

Proof. Equation (2.31) is similar to (2.18) in Theorem D.4.1 in the way that we observe all subsets of messages that are actively decoded by a particular BS m , where the resulting rate constraints consider all possibilities of SIC decoding order of these messages (or, equivalently, joint decoding of subsets of these messages). However, we now also consider the fact that a BS can exploit signals received by other BSs and forwarded to BS m according to the DAS concept. In (2.31), we model this such that the decoding of messages is always based on the received signals of all $M - 1$ other BSs (or all M BSs in case decoding takes place at a central network entity), where in those cases where no DAS cooperation exists between pairs of BSs, an infinite quantization noise is introduced. Recall that we have defined the following four sets of messages $\forall m \in \mathcal{M}$:

$$\mathcal{F}^{[m]} = \left\{ F_j^{\mathcal{M}'}, F_j^{\mathcal{M}', m' \rightarrow \mathcal{M}''}, F_j^{\mathcal{M}', m' \not\rightarrow \mathcal{M}''} \in \hat{\mathcal{F}}_{\text{all}} : m \in \mathcal{M}' \right\} \quad (\text{D.6})$$

$$\bar{\mathcal{F}}^{[m]} = \left\{ F_j^{\mathcal{M}'}, F_j^{\mathcal{M}', m' \rightarrow \mathcal{M}''}, F_j^{\mathcal{M}', m' \not\rightarrow \mathcal{M}''} \in \mathcal{S}_{\text{all}} : m \notin \mathcal{M}' \wedge m \notin \mathcal{M}'' \right\} \quad (\text{D.7})$$

$$\bar{\mathcal{F}}^{[m]} = \left\{ F_j^{\mathcal{L}, l \rightarrow \mathcal{L}'} \in \hat{\mathcal{F}}_{\text{all}} : m \in \mathcal{L}' \right\} \quad (\text{D.8})$$

$$\bar{\mathcal{F}}^{[m]} = \left\{ F_j^{\mathcal{L}, l \not\rightarrow \mathcal{L}'} \in \hat{\mathcal{F}}_{\text{all}} : m \in \mathcal{L}' \right\}, \quad (\text{D.9})$$

where the first one denotes all messages that are purposely¹ decoded by BS m , the second one denotes the set of messages that are neither decoded by BS m itself nor forwarded to BS m via DIS or CIF concepts, and the latter two denote all messages forwarded to BS m according to the DIS or CIF concept, respectively. We will now derive all equations in Theorem 2.2.5 explained along the signal processing steps taken at a decoding BS, for which we have defined a specific order in Section 2.2.5.

DAS-based quantization

First, a BS $m \in \mathcal{M}$ (possibly) receives quantized receive signals from other BSs $\mathcal{M}' \subseteq \mathcal{M} \setminus m$. This information exchange between BSs is characterized through the fact that the quantized signals have already undergone signal processing at the quantizing BSs. For instance, interference might have been (partially) subtracted due to DIS and CIF concepts, and the BSs will have decoded messages and subtracted the corresponding sequences from their received signals, before quantizing the remaining signals and noise and forwarding these to BS m . We denote the corresponding, processed signals at BSs before quantization as $\forall m \in \mathcal{M}' : \bar{Y}_m$, and their covariances as

$$\forall m' \in \mathcal{M}' : \bar{\Phi}_{m'}^{\text{yy}} = \mathbf{H}_{m'}^e \mathbf{P} \left(\bar{\mathcal{F}}^{[m']} \right) (\mathbf{H}_{m'}^e)^H + \Phi_{m'}^{\text{cc}} + \Phi_{m'}^{\text{hh}} + \sigma^2 \mathbf{I}, \quad (\text{D.10})$$

which contain the remaining interference from all messages $\bar{\mathcal{F}}^{[m']}$ not decoded by the BSs themselves, nor provided by other BSs via DIS or CIF, as well as residual interference $\Phi_{m'}^{\text{cc}}$ after partial CIF-based interference cancellation, which will be explained later, channel estimation related noise $\Phi_{m'}^{\text{hh}}$ and background noise $\sigma^2 \mathbf{I}$. We will later also refer to the joint signal

¹The word 'purposely' means that decoding is *not* only performed for the sake of interference cancellation.

covariances of all BSs in set \mathcal{M}' after local decoding and interference cancellation as $\bar{Y}_{\mathcal{M}'}$. Note that the latter term is difficult to state in a compact way, as it has to be distinguished for each BS which signal has been decoded or otherwise canceled or not. On the other hand, the DAS-receiving BS m has not performed any signal processing yet, so that if any inter-BS signal correlation is to be exploited, this has to be based on the original, unprocessed signals of BS m , which we denote as Y_m . We denote the signals *after* quantization at any BS $m' \in \mathcal{M}'$ as $\tilde{Y}_{m' \rightarrow m}$, and the quantized signals connected to the complete set \mathcal{M}' of BSs as $\tilde{Y}_{\mathcal{M}' \rightarrow m}$. The notation $\rightarrow m$ is required here, as it is of course possible that BSs forward received signals to multiple recipients, possibly applying different quantization strategies. To our knowledge, the best known scheme for multiple BSs to forward quantized receive signals to another BS (or a central network entity) w.r.t. the rate/backhaul trade-off for UEs decoded by the receiving side is *distributed Wyner-Ziv* [Gas04]. Under such a distributed source coding concept, still assuming that all BSs in set $\mathcal{M}' \subseteq \mathcal{M}$ forward signals to BS m , the following information theoretical relations must hold [SSSK05, dCS08]:

$$\forall \mathcal{M}'' \subseteq \mathcal{M}' : I\left(\bar{Y}_{\mathcal{M}''}; \tilde{Y}_{\mathcal{M}'' \rightarrow m} \middle| Y_m, \tilde{Y}_{\mathcal{M}' \setminus \mathcal{M}'' \rightarrow m}\right) \leq \sum_{m' \in \mathcal{M}''} \hat{b}_{m, m'}^{\text{das}}, \quad (\text{D.11})$$

which means that for each subset $\mathcal{M}'' \subseteq \mathcal{M}'$ of BSs quantizing and forwarding signals, the mutual information between the signals $\bar{Y}_{\mathcal{M}''}$ and the quantized versions $\tilde{Y}_{\mathcal{M}'' \rightarrow m}$ forwarded to BS m , given the signals Y_m received by BS m itself as well as the quantized signals $\tilde{Y}_{\mathcal{M}' \setminus \mathcal{M}'' \rightarrow m}$ provided by all other BSs $\mathcal{M}' \setminus \mathcal{M}''$ to BS m must be less or equal to the *aggregate backhaul capacity* from the BSs in \mathcal{M}'' to BS m . Assuming that the quantized version of a receive signal is simply the received signal plus independent Gaussian quantization noise $\tilde{Y}_{\mathcal{M}'' \rightarrow m} = \bar{Y}_{\mathcal{M}''} + Z_{\mathcal{M}'' \rightarrow m}$, where the quantization noise has block-diagonal covariance matrix [dCS08],

$$E_t \left\{ \mathbf{z}_{\mathcal{M}'' \rightarrow m} (\mathbf{z}_{\mathcal{M}'' \rightarrow m})^H \right\} = \mathbf{\Phi}_{\mathcal{M}'' \rightarrow m}^{\text{qq}} = \text{diag} \left(\mathbf{\Phi}_{m'_1 \rightarrow m}^{\text{qq}}, \mathbf{\Phi}_{m'_2 \rightarrow m}^{\text{qq}}, \dots, \mathbf{\Phi}_{m'_{|\mathcal{M}''|} \rightarrow m}^{\text{qq}} \right) \quad (\text{D.12})$$

(as the quantization process at each BS is independent), we can now rewrite the mutual information term in (D.11) as

$$I\left(\bar{Y}_{\mathcal{M}''}; \tilde{Y}_{\mathcal{M}'' \rightarrow m} \middle| Y_m, \tilde{Y}_{\mathcal{M}' \setminus \mathcal{M}'' \rightarrow m}\right) \quad (\text{D.13})$$

$$= h\left(\tilde{Y}_{\mathcal{M}'' \rightarrow m} \middle| Y_m, \tilde{Y}_{\mathcal{M}' \setminus \mathcal{M}'' \rightarrow m}\right) - h\left(\tilde{Y}_{\mathcal{M}'' \rightarrow m} \middle| \bar{Y}_{\mathcal{M}''}, Y_m, \tilde{Y}_{\mathcal{M}' \setminus \mathcal{M}'' \rightarrow m}\right) \quad (\text{D.14})$$

$$= h\left(\tilde{Y}_{\mathcal{M}'' \rightarrow m} \middle| Y_m, \tilde{Y}_{\mathcal{M}' \setminus \mathcal{M}'' \rightarrow m}\right) - h\left(\mathbf{\Phi}_{\mathcal{M}'' \rightarrow m}^{\text{qq}}\right) \quad (\text{D.15})$$

$$= \log_2 \left(2\pi e \left| \bar{\mathbf{\Phi}}_{\mathcal{M}'' | m, \mathcal{M}' \setminus \mathcal{M}''}^{\text{yy}^*} + \mathbf{\Phi}_{\mathcal{M}'' \rightarrow m}^{\text{qq}} \right| \right) - \log_2 \left(2\pi e \left| \mathbf{\Phi}_{\mathcal{M}'' \rightarrow m}^{\text{qq}} \right| \right), \quad (\text{D.16})$$

such that we can finally rewrite (D.11) as

$$\forall \mathcal{M}'' \subseteq \mathcal{M}' : \log_2 \left| \mathbf{I} + \left(\mathbf{\Phi}_{\mathcal{M}'' \rightarrow m}^{\text{qq}} \right)^{-1} \bar{\mathbf{\Phi}}_{\mathcal{M}'' | m, \mathcal{M}' \setminus \mathcal{M}''}^{\text{yy}^*} \right| \leq \sum_{m' \in \mathcal{M}''} \hat{b}_{m, m'}^{\text{das}}, \quad (\text{D.17})$$

where $\bar{\mathbf{\Phi}}_{\mathcal{M}'' | m, \mathcal{M}' \setminus \mathcal{M}''}^{\text{yy}^*}$ is the joint covariance of the signals at all BSs in set \mathcal{M}'' before quantization, conditioned on the received signals at BS m and the quantized signals provided by

the BSs in set $\mathcal{M}' \setminus \mathcal{M}''$. Unfortunately, it is tedious to state general conditional covariance expressions for the model considered in our work. The main problem is that each BS in set \mathcal{M}'' can have a different mix of interference in its signal which is to be quantized, depending on the signal processing steps that have been undertaken before. The same also holds for the receiving BS m and the BSs in set $\mathcal{M}' \setminus \mathcal{M}''$. Hence, we will have the case that for each signal connected to a certain message, some BSs will have correlated observations, while other BSs will not, as they have already decoded or otherwise canceled the corresponding signals. In our work, we will hence constrain ourselves to scenarios where all BSs that jointly perform distributed Wyner-Ziv compression as well as the receiving BS have a common set of messages that have not been decoded or otherwise canceled yet at *any* of the involved BSs. The distributed source coding can then exploit the correlated observations connected to this set of messages, while all other sequences are (suboptimally) considered as uncorrelated interference. Note that this corresponds to the simplified model also used in [dCS08]. In Section 3.3.2, we observe the case where DAS-forwarding BSs do not decode or cancel any signals before performing DAS-quantization (hence, they are used as pure remote radio heads, and the common set of messages corresponds to all messages $\hat{\mathcal{F}}_{\text{all}}$ transmitted by the terminals), or (when observing iterative BS cooperation schemes) where only one DAS-forwarding and one DAS-receiving BS exist. In both cases, the beforementioned problem does not occur, and the calculated conditional covariances are hence optimal. If we denote the common set of (not yet decoded or otherwise canceled) messages between DAS-forwarding and DAS-receiving BSs as $\bar{\mathcal{F}}^{[\mathcal{M}', m]}$, the conditional covariance from (D.17) can now be derived as $\forall \mathcal{M}'' \subseteq \mathcal{M}'$ [dCS08]

$$\begin{aligned}
\bar{\Phi}_{\mathcal{M}''|m, \mathcal{M}' \setminus \mathcal{M}''}^{\text{yy}^*} &= \mathbf{H}_{\mathcal{M}''}^e \left[\mathbf{I} + \mathbf{P} \left(\bar{\mathcal{F}}^{[\mathcal{M}', m]} \right) \left(\dots \right. \right. \\
&\quad \left. \left. \dots (\mathbf{H}_m^e)^H \underbrace{\left(\mathbf{H}_m^e \mathbf{P} \left(\hat{\mathcal{F}}_{\text{all}} \setminus \bar{\mathcal{F}}^{[\mathcal{M}', m]} \right) (\mathbf{H}_m^e)^H + \Phi_m^{\text{hh}} + \sigma^2 \mathbf{I} \right)}_{\text{Interference and noise seen by BS } m} \right)^{-1} \mathbf{H}_m^e + \dots \right. \\
&+ \sum_{m' \in \mathcal{M}' \setminus \mathcal{M}''} (\mathbf{H}_{m'}^e)^H \left(\underbrace{\mathbf{H}_{m'}^e \mathbf{P} \left(\bar{\mathcal{F}}^{[m']} \setminus \bar{\mathcal{F}}^{[\mathcal{M}', m]} \right) (\mathbf{H}_{m'}^e)^H + \Phi_{m'}^{\text{cc}} + \Phi_{m'}^{\text{hh}} + \sigma^2 \mathbf{I} + \Phi_{m' \rightarrow m}^{\text{qq}}}_{\text{Noise and interference seen by BS } m'} \right)^{-1} \mathbf{H}_{m'}^e \dots \\
&\quad \left. \left. \dots \right) \right]^{-1} \mathbf{P} \left(\bar{\mathcal{F}}^{[\mathcal{M}', m]} \right) (\mathbf{H}_{\mathcal{M}''}^e)^H + \Phi_{\mathcal{M}''}^{\text{ii}} + \Phi_{\mathcal{M}''}^{\text{cc}} + \Phi_{\mathcal{M}''}^{\text{hh}} + \sigma^2 \mathbf{I}, \quad (\text{D.18})
\end{aligned}$$

where $\mathbf{H}_{\mathcal{M}''}^e$ is the effective channel matrix connected to all BSs in set \mathcal{M}'' , Φ_m^{hh} is the noise covariance due to imperfect CSI at BS m , as derived in (2.9) in Section 2.2.2, Φ_m^{cc} is the residual interference after CIF-based interference cancellation at BS m and $\Phi_{\mathcal{M}''}^{\text{ii}}$ is the interference from messages in set $\hat{\mathcal{F}}_{\text{all}} \setminus \bar{\mathcal{F}}^{[\mathcal{M}', m]}$ as seen by the BSs in \mathcal{M}'' . As for $\bar{Y}_{\mathcal{M}'}$, $\Phi_{\mathcal{M}''}^{\text{ii}}$ is difficult to state in compact form (and hence also omitted here), as for each BS in \mathcal{M}'' it has to be considered which interfering message has already been decoded or otherwise canceled. The algorithmic computation of this term, however, poses no problem. Note that the interference seen by the DAS-receiving BS m in (D.18) consists of the contributions of *all* messages not in set $\bar{\mathcal{F}}^{[\mathcal{M}', m]}$, under the assumption that BS m evaluates received DAS information first (i.e. reconstructs quantized receive signals \tilde{Y}) before performing any other signal processing steps

(e.g. DIS/CIF-based interference cancellation or decoding).

Note that we have now merely stated constraints on the quantization noise covariances $\forall m' \in \mathcal{M}' : \Phi_{m'}^{\text{qq}}$ for a given backhaul infrastructure, but it remains unclear how optimal quantization noise covariances can be computed. This problem has been dealt with in detail by [dCS08], where it has also been shown that these covariances can be chosen such as to trade-off the achievable rates of certain messages against those of other messages (i.e. by optimizing a weighted sum-rate of these rates). In our work, we have computed quantization noise covariances based on concrete algorithms proposed by [dCS08], and would like to refer the interested reader to the solid and comprehensive work of the stated authors.

CIF-related backhaul constraint

After a DAS-receiving BS has evaluated signals provided by other BSs, it can then (possibly) perform CIF-based partial interference cancelation. The CIF-related backhaul constraint in (2.35) is based on the following derivation. Let us assume in a simplified setup that BS 1 has decoded a message F , reconstructed the sequence transmitted from the UE as $X = \sqrt{\rho_F}e(F)$, and has created a quantized version $\tilde{X} = q(X)$ of this sequence that is to be forwarded to BS 2 for approximate interference subtraction². We assume in this case that the quantized sequence corresponds to a scaled version of the sequence plus quantization noise, such that the power before and after quantization remains the same, as e.g. modeled in [CT06], hence $\tilde{X} = \sqrt{(\rho_F - \xi_F)/\rho_F} \cdot X + Z$, where the quantization noise has a power of $E_t\{zz^H\} = \xi_F$. We know from Slepian-Wolf source coding [SW73], that it is sufficient to forward data at a rate $h(\tilde{X}|Y_2)$ per channel access to BS 2, such that the latter BS can perfectly reconstruct \tilde{X} , based on side information in its own received signals Y_2 . If we now state

$$h(\tilde{X}|Y_2) = h(\tilde{X}, Y_2) - h(Y_2) \quad (\text{D.19})$$

$$= h(Y_2|\tilde{X}) + H(\tilde{X}) - h(Y_2) \quad (\text{D.20})$$

$$= H(\tilde{X}) + \log_2 \left(2\pi e \left| \Phi_{2|\tilde{X}}^{\text{yy}} \right| \right) - \log_2 \left(2\pi e \left| \Phi_2^{\text{yy}} \right| \right) \quad (\text{D.21})$$

$$= \underbrace{\log_2 \left(\frac{\rho_F}{\xi_F} \right)}_{\text{Quantizer rate}} - \log_2 \left| \left(\Phi_{2|\tilde{X}}^{\text{yy}} \right)^{-1} \Phi_2^{\text{yy}} \right|, \quad (\text{D.22})$$

where $\Phi_2^{\text{yy}} = E_t\{\mathbf{y}_2\mathbf{y}_2^H\}$ is the receive signal covariance at BS 2, and $\Phi_{2|\tilde{X}}^{\text{yy}} = E_t\{\mathbf{y}_2\mathbf{y}_2^H|\tilde{X}\}$ is the same receive signal covariance, but given that the quantized sequence \tilde{X} is already known. As we can see, the required backhaul corresponds to the rate of the employed quantization, *minus* the rate with which BS 2 could decode \tilde{X} solely based on its received signals Y_2 . If BS 1 (or multiple BSs) should now forward quantized versions of multiple sequences $\mathcal{F} = \{F_1..F_N\}$ to BS 2, the sum backhaul capacity required on the involved links for each subset $\mathcal{F}' \subseteq \mathcal{F}$ must be at least

$$h(q(e(\mathcal{F}'))|Y_2) = \sum_{F \in \mathcal{F}'} h(q(e(F))|Y_2) = \sum_{F \in \mathcal{F}'} \log_2 \left(\frac{\rho_F}{\xi_F} \right) - \log_2 \left| \left(\Phi_{2|q(e(\mathcal{F}'))}^{\text{yy}} \right)^{-1} \Phi_2^{\text{yy}} \right|, \quad (\text{D.23})$$

where $e(\mathcal{F}') = \{X : \forall F \in \mathcal{F}' : X = e(F)\}$ is the set of sequences corresponding to the set of messages \mathcal{F}' , $q(\mathcal{X}) = \{\tilde{X} : \forall X \in \mathcal{X} : \tilde{X} = q(X)\}$ is the set of all quantized sequences corresponding to

²We know from [WZ76] that for Gaussian signaling the approach of quantization succeeded by Slepian-Wolf source coding is equivalent to performing Wyner-Ziv source coding on a sequence X directly.

the set of sequences \mathcal{X} , and $\Phi_{2|q(e(\mathcal{F}))}^{yy}$ is the receive signal covariance at BS 2, given that the quantized versions of all sequences corresponding to the messages in set \mathcal{F}' are known at BS 2. For our specific model of joint DIS/CIF/DAS concepts, we can first of all derive the residual interference a CIF-receiving BS is still subject to after partial interference cancellation as

$$\forall m \in \mathcal{M} : \Phi_m^{cc} = \mathbf{H}_m^e \Psi_m \left(\vec{\mathcal{F}}_m \right) \left(\mathbf{H}_{m'}^e \right)^H, \quad (\text{D.24})$$

where $\Psi(\mathcal{F}) \in \mathbb{R}_0^{+[K \times K]}$ is a power matrix containing the residual quantization noise power connected to the CIF-forwarded messages in set \mathcal{F} on the diagonal elements, i.e.

$$\forall k \in \mathcal{K} : [\Psi_m(\mathcal{F})]_{k,k} = \sum_{F \in \{\hat{\mathcal{F}}_k \cap \mathcal{F}\}} \xi_{F \neq m}. \quad (\text{D.25})$$

We have to consider that a CIF-receiving BS evaluates quantized sequences *after* it has received quantized signals according to the DAS concept from other BSs. Hence, the received DAS-signals can be seen as side-information that can be exploited for reconstructing quantized sequences. We further have to consider, however, that at this point in time, no messages have been decoded by the CIF-receiving BS yet, hence they still have to be counted as interference. The overall CIF-related backhaul constraint for our model can then be stated as $\forall m \in \mathcal{M}$:

$$\begin{aligned} \forall \mathcal{F} \subseteq \hat{\mathcal{F}}^{\neq[m]}, \mathcal{M}' = \underbrace{\left\{ m' \in \mathcal{M} : F_j^{\mathcal{L}, l \neq \mathcal{L}'} \in \mathcal{F} \wedge m' = l \right\}}_{\text{Set of BSs that CIF-forward messages in } \mathcal{F} \text{ to BS } m} : \\ \sum_{F \in \mathcal{F}} \log_2 \left(\frac{\rho_F}{\xi_{F \neq m}} \right) - \log_2 \left| \mathbf{I} + \bar{\Psi}_m(\mathcal{F}) \left(\sum_{m'=1}^M \left(\mathbf{H}_{m'}^e \right)^H \left(\Phi_{m' \rightarrow m}^{\text{ii, cif}} \right)^{-1} \mathbf{H}_{m'}^e \right) \right| \leq \sum_{m' \in \mathcal{M}'} \hat{b}_{m, m'}^{\text{cif}}, \end{aligned} \quad (\text{D.26})$$

Portion of quantized sequences $q(e(\mathcal{F}))$ decodeable by BS m by itself

where $\bar{\Psi}_m(\mathcal{F}) \in \mathbb{R}_0^{+[K \times K]}$ is a power matrix containing the scaled-down power of the CIF-forwarded messages in set \mathcal{F} after quantization on the diagonal elements, i.e.

$$\forall k \in \mathcal{K} : [\bar{\Psi}_m(\mathcal{F})]_{k,k} = \sum_{F \in \{\hat{\mathcal{F}}_k \cap \mathcal{F}\}} \rho_F - \xi_{F \neq m}, \quad (\text{D.27})$$

and we have the interference terms

$$\Phi_{m \rightarrow m}^{\text{ii, cif}} = \mathbf{H}_m^e \mathbf{P} \left(\hat{\mathcal{F}}_{\text{all}} \setminus \hat{\mathcal{F}}^{\neq[m]} \right) \left(\mathbf{H}_m^e \right)^H + \Phi_m^{cc} + \Phi_m^{\text{hh}} + \sigma^2 \mathbf{I} \quad \text{and} \quad (\text{D.28})$$

$$\Phi_{m' \rightarrow m}^{\text{ii, cif}} = \mathbf{H}_{m'}^e \mathbf{P} \left(\hat{\mathcal{F}}^{[m']} \setminus \hat{\mathcal{F}}^{\neq[m]} \right) \left(\mathbf{H}_{m'}^e \right)^H + \Phi_{m'}^{cc} + \Phi_{m'}^{\text{hh}} + \sigma^2 \mathbf{I} + \Phi_{m' \rightarrow m}^{\text{qq}}, \quad (\text{D.29})$$

where the signals received by BS m itself are subject to interference from all messages except the CIF-received ones (as BS m has not performed any decoding steps yet), whereas the signals provided by any other BS $m' \neq m$ to BS m via DAS-concepts are subject to interference from the messages *not* decoded by BS m' itself or otherwise provided to BS m' , again except the CIF-received ones.

DIS-related backhaul constraints After performing CIF-based partial interference cancellation, a BS may receive information from other BSs for complete interference cancellation. The DIS-related backhaul constraint in (2.39) is based on the following argumentation: Let us consider a simplified setup where e.g. BS 1 decodes a message F and forwards this to a BS 2 that has made the signal observation Y_2 . Similarly as before for CIF, we know that it is sufficient if BS 1 forwards information at rate $H(F|Y_2)$ to the other side in order for BS 2 to be able to fully reconstruct message F given the side information in the received signals Y_2 [SW73]. We can hence state

$$H(F|Y_2) = h(F, Y_2) - h(Y_2) \quad (\text{D.30})$$

$$= h(Y_2|F) + H(F) - h(Y_2) \quad (\text{D.31})$$

$$= \log_2 \left(2\pi e \left| \Phi_{2|F}^{yy} \right| \right) + \nu_F - \log_2 \left(2\pi e \left| \Phi_2^{yy} \right| \right) \quad (\text{D.32})$$

$$= \nu_F - \underbrace{\log_2 \left| \left(\Phi_{2|F}^{yy} \right)^{-1} \Phi_2^{yy} \right|}_{\text{Portion of message } F \text{ decodeable by BS } m \text{ by itself}}, \quad (\text{D.33})$$

where we denote as $\Phi_{2|F}^{yy} = E_t\{\mathbf{y}_2\mathbf{y}_2^H|F\}$ the conditional receive signal covariance at BS 2, given that message F is already known. We can see that (D.33) corresponds to the rate of message F minus the rate message F could obtain if it was decoded by BS 2 itself, hence without cooperation. Note that this expression cannot be negative, if we assume that the rate of message F is fixed such that it can be successfully decoded by BS 1. However, the backhaul requirement can be zero if e.g. BS 2 has a better link to the UE transmitting F than BS 1, in which of course the considered DIS concept is pointless. Similarly as in the CIF-case, we have to consider that if multiple messages $\mathcal{F} = \{F_1..F_N\}$ are forwarded to BS 2 according to the DIS-concept, the aggregate backhaul capacity on the involved backhaul links connected to any subset of messages $\mathcal{F}' \subseteq \mathcal{F}$ must be greater or equal to

$$\sum_{F \in \mathcal{F}'} \nu_F - \underbrace{\log_2 \left| \left(\Phi_{2|\mathcal{F}'}^{yy} \right)^{-1} \Phi_2^{yy} \right|}_{\text{Portion of messages in } \mathcal{F} \text{ decodeable by BS } m \text{ by itself}}, \quad (\text{D.34})$$

$\Phi_{2|\mathcal{F}'}^{yy}$ denotes the receive signal covariance at BS2 conditioned on all messages in set \mathcal{F}' . If we now extend this to our model, we have to consider that the receiving BS can make use of the fact that it has already obtained quantized received signals from other BSs (DAS concept) and performed partial interference cancellation (CIF concept). We can extend (D.34) to our general model as

$$\forall \mathcal{F} \subseteq \bar{\mathcal{F}}^{[m]} : \underbrace{\mathcal{M}' = \left\{ m' \in \mathcal{M} \mid F_j^{\mathcal{L}, l \rightarrow \mathcal{L}'} \in \mathcal{F} \wedge m' = l \right\}}_{\text{Set of BSs that forward messages in } \mathcal{F} \text{ to BS } m} :$$

$$\sum_{F \in \mathcal{F}} \nu_F - \log_2 \left| \mathbf{I} + \mathbf{P}(\mathcal{F}) \left(\sum_{m'=1}^M (\mathbf{H}_{m'}^e)^H \left(\Phi_{m' \rightarrow m}^{\text{ii, dis}} \right)^{-1} \mathbf{H}_{m'}^e \right) \right| \leq \sum_{m' \in \mathcal{M}'} \hat{b}_{m, m'}^{\text{dis}}, \quad (\text{D.35})$$

Portion of messages in \mathcal{F} already decodeable by BS m by itself

and we have the interference terms

$$\Phi_{m \rightarrow m}^{\text{ii, dis}} = \mathbf{H}_m^e \mathbf{P} \left(\hat{\mathcal{F}}_{\text{all}} \setminus \{ \vec{\mathcal{F}}^{[m]} \cup \vec{\mathcal{F}}^{\neq [m]} \} \right) (\mathbf{H}_m^e)^H + \Phi_m^{\text{cc}} + \Phi_m^{\text{hh}} + \sigma^2 \mathbf{I} \quad (\text{D.36})$$

$$\Phi_{m' \rightarrow m}^{\text{ii, dis}} = \mathbf{H}_{m'}^e \mathbf{P} \left(\vec{\mathcal{F}}^{[m']} \setminus \vec{\mathcal{F}}^{[m]} \right) (\mathbf{H}_{m'}^e)^H + \Phi_{m'}^{\text{cc}} + \Phi_{m'}^{\text{hh}} + \sigma^2 \mathbf{I} + \Phi_{m' \rightarrow m}^{\text{qq}}, \quad (\text{D.37})$$

where the signals considered as side-information at BS m contain interference connected to all messages except those already canceled through CIF concepts, and except the DIS messages considered now, whereas the signals provided by other BSs only contain interference from messages not remotely decoded or received from other BSs, again except the DIS messages considered now.

Actual decoding of messages

We finally consider constraints on the rates of the messages decoded by BSs after (partial) interference cancellation through DIS and CIF concepts. We can state these as $\forall m \in \mathcal{M}$:

$$\forall \mathcal{F} \subseteq \mathcal{F}^{[m]} : \sum_{F \in \mathcal{F}} \nu_F \leq \log_2 \left| \mathbf{I} + \mathbf{P}(\mathcal{F}) \left(\sum_{m'=1}^M (\mathbf{H}_{m'}^e)^H (\Phi_{m' \rightarrow m}^{\text{ii}})^{-1} \mathbf{H}_{m'}^e \right) \right|, \quad (\text{D.38})$$

with the interference term

$$\Phi_{m' \rightarrow m}^{\text{ii}} = \underbrace{\sigma^2 \mathbf{I}}_{\text{Noise}} + \underbrace{\Phi_{m'}^{\text{hh}}}_{\text{Chn. est.}} + \underbrace{\mathbf{H}_{m'}^e \mathbf{P} \left(\vec{\mathcal{F}}^{[m]} \cap \vec{\mathcal{F}}^{[m']} \right) (\mathbf{H}_{m'}^e)^H}_{\substack{\text{Intrfr. from msgs. neither decoded} \\ \text{by nor provided to BSs } m \text{ or } m'}} + \underbrace{\Phi_{m'}^{\text{cc}}}_{\substack{\text{Residual intrfr.} \\ \text{rel. to CIF}}} + \underbrace{\Phi_{m' \rightarrow m}^{\text{qq}}}_{\substack{\text{Quant. noise} \\ \text{rel. to DAS}}}. \quad (\text{D.39})$$

We here have to consider that signals provided by other BSs only contain interference that has not been decoded at the remote side, and where the corresponding messages are not already known by BS m itself.

Network-related backhaul constraint

We finally have to consider that messages decoded at BSs (and not by a central network entity) have to be forwarded to the network, in order to have a fair comparison between both kinds of BS cooperation and decoding strategies. For this, we state additional constraints on the message rates as

$$\forall \mathcal{F} \subseteq \hat{\mathcal{F}}_{\text{all}^*}, \mathcal{M}' = \underbrace{\left\{ m' \in \mathcal{M} : \exists F_j^{\mathcal{L}}, F_j^{\mathcal{L}, l \rightarrow \mathcal{L}'}, F_j^{\mathcal{L}, l \neq \mathcal{L}'} \in \mathcal{F} : m' \in \mathcal{L} \right\}}_{\text{Set of all BSs that decode messages in } \mathcal{F}} : \sum_{F \in \mathcal{F}} \nu_F \leq \sum_{m \in \mathcal{M}'} \hat{b}_{M+1, m}^{\text{net}}, \quad (\text{D.40})$$

where we recall that

$$\hat{\mathcal{F}}_{\text{all}^*} = \left\{ F_j^{\mathcal{L}}, F_j^{\mathcal{L}, l \rightarrow \mathcal{L}'}, F_j^{\mathcal{L}, l \neq \mathcal{L}'} \in \hat{\mathcal{F}}_{\text{all}} : M+1 \notin \mathcal{L} \right\} \quad (\text{D.41})$$

is the set of all messages that are *not* decoded by a central network entity. Equation (D.40) states that for each subset of messages involved in the transmission (and not decoded by a central network entity), the sum-rate of the messages must be less or equal to the aggregate capacity of the backhaul links from the BSs decoding these messages to the network. \square

D.3 Downlink Capacity Region Calculation

In this section, we introduce an algorithm for calculating inner bounds of the capacity regions connected to downlink transmissions under imperfect CSIT and CSIR and an arbitrary extent of BS cooperation. Let us initially recall the corresponding inner rate bound from (2.71) as

$$\sum_{k=1}^K \alpha_k r_k \leq \min_{\hat{\mathbf{\Phi}}_{\text{nn}}} \max_{\hat{\mathbf{P}}} \max_{\mathbf{C}: \check{\mathbf{B}}(\mathbf{C}) \preceq \check{\mathbf{B}}^{\max}} \sum_{k \in \mathcal{K}} \alpha_k \cdot \log_2 \left| \mathbf{I} + \frac{\mathbf{\Phi}^{\text{ss}}(k)}{\mathbf{\Phi}^{\text{ii}}(k) + \mathbf{\Phi}^{\text{qq}}(k) + \mathbf{\Phi}^{\text{CSI}}(k) + \hat{\mathbf{\Phi}}_{\text{nn}}} \right|$$

s.t. $\underbrace{\text{tr}\{\hat{\mathbf{P}}\} \leq \text{tr}\{\mathbf{P}^{\max}\}}_{\text{Dual uplink power constraint}}, \underbrace{\text{tr}\{\hat{\mathbf{\Phi}}_{\text{nn}} \check{\mathbf{P}}^{\max}\} \leq \sigma^2 \text{tr}\{\check{\mathbf{P}}^{\max}\}}_{\text{DL per-antenna power constraint}} \text{ or } \underbrace{\hat{\mathbf{\Phi}}_{\text{nn}} = \sigma^2 \mathbf{I}}_{\text{DL sum power constraint}}, \quad (\text{D.42})$

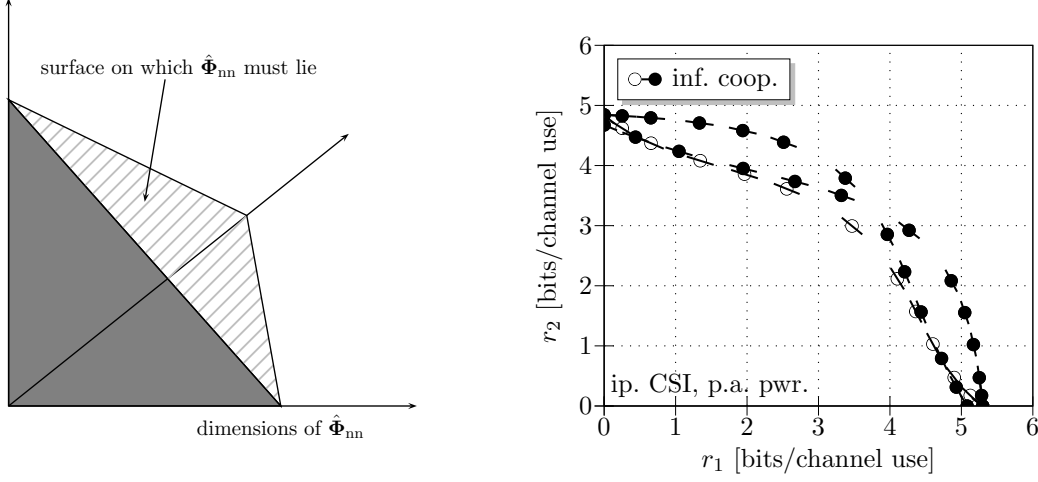
where $\mathbf{\Phi}^{\text{ss}}(k) = \hat{p}_k \sqrt{\mathbf{\Psi}_k} \mathbf{h}_k^e (\mathbf{h}_k^e)^H \sqrt{\mathbf{\Psi}_k}$ and the various other covariance terms are given in (2.71). It is now possible to approximate the inner bound on the capacity region through a polyhedron, where each side denotes a lower bound on a weighted sum-rate for a particular choice of weights $\alpha_1.. \alpha_K$. Clearly, the lower the number of weight tuples used for this computation is, the more the corners of the polyhedron will in fact *overestimate* possible rate tuples, hence it cannot be assured that we are still observing a lower bound. In order to avoid having to use too many tuples of weights for an accurate capacity region computation, we hence choose a different computation approach. The central idea is that we perform a brute force search over the parameter space $\hat{\mathbf{P}}$ and \mathbf{C} at reasonable granularity and compute for each choice of these parameters the least favorable noise w.r.t. the sum rate defined through the weights $\alpha_1.. \alpha_K$ that describe the *tangent* touching the capacity region inner bound in this point. By using this procedure, we can assure that if the granularity of the brute force search is low, we tend to underestimate capacities, but never overestimate these. The algorithm hence consists of the steps

1. Loop through different choices of $\hat{\mathbf{P}}, \mathbf{C}$ at reasonable granularity.
2. For each choice, initially set the uplink noise covariance to $\hat{\mathbf{\Phi}}_{\text{nn}} := \sigma^2 \cdot \mathbf{I}$.
3. Loop until desired extent of convergence:
 - (a) Calculate the weights $\alpha_1.. \alpha_K$ defining the tangent to the rate region for the current choice of $\hat{\mathbf{P}}, \mathbf{C}$ and $\hat{\mathbf{\Phi}}_{\text{nn}}$.
 - (b) Update the uplink noise covariance $\hat{\mathbf{\Phi}}_{\text{nn}}$ through a gradient technique.

The two main steps (3a) and (3b) are explained in the sequel. Without loss of generality, let us constrain ourselves to the case of $K = 2$ for brevity, and only consider no or infinite BS cooperation, UMC or QSC, hence where quantization noise (where applicable) is correlated over the antennas of one BS.

Calculate the weights $\alpha_1.. \alpha_K$ for a given $\hat{\mathbf{P}}, \mathbf{C}$ and $\hat{\mathbf{\Phi}}_{\text{nn}}$. We calculate the derivative of the UE rates towards \hat{p}_1 , knowing that $\hat{p}_2 = \text{tr}\{\check{\mathbf{P}}^{\max}\} - \hat{p}_1$, as

$$\forall k \in \{1, 2\} : \frac{\delta r_k}{\delta \hat{p}_1} = \underbrace{\text{tr} \left\{ \left(\hat{p}_1 \mathbf{\Omega}_k^{\text{sd}} + \mathbf{\Omega}_k^{\text{sf}} \right)^{-1} \mathbf{\Omega}_k^{\text{sd}} \right\}}_{\text{Desired signal, interference and noise}} - \underbrace{\text{tr} \left\{ \left(\hat{p}_1 \mathbf{\Omega}_k^{\text{id}} + \mathbf{\Omega}_k^{\text{if}} \right)^{-1} \mathbf{\Omega}_k^{\text{id}} \right\}}_{\text{Only interference and noise}}, \quad (\text{D.43})$$



(a) Illustration of the polyhedron within which $\hat{\Phi}_{nn}$ is constrained due to DL per-ant. power constraints.

(b) Illustration of rate tuples and tangents obtained for different $\hat{\mathbf{P}}$ after convergence.

with the following covariance terms $\forall k \in \{1, 2\}$:

$$\Omega_k^{\text{sd}} = \nabla \Phi_{1 \rightarrow k}^{\text{ii}} + \nabla \Phi_{1 \rightarrow k}^{\text{qq}} + \nabla \Phi_{1 \rightarrow k}^{\text{CSI}} - (\nabla \Phi_{2 \rightarrow k}^{\text{ii}} + \nabla \Phi_{2 \rightarrow k}^{\text{qq}} + \nabla \Phi_{2 \rightarrow k}^{\text{CSI}}) \quad (\text{D.44})$$

$$\Omega_k^{\text{sf}} = \text{tr}\{\check{\mathbf{P}}^{\text{max}}\} \cdot (\nabla \Phi_{2 \rightarrow k}^{\text{ii}} + \nabla \Phi_{2 \rightarrow k}^{\text{qq}} + \nabla \Phi_{2 \rightarrow k}^{\text{CSI}}) + \hat{\Phi}_{nn} \quad (\text{D.45})$$

$$\Omega_1^{\text{id}} = \nabla \Phi_{1 \rightarrow 1}^{\text{qq}} + \nabla \Phi_{1 \rightarrow 1}^{\text{CSI}} - (\nabla \Phi_{2 \rightarrow 1}^{\text{ii}} + \nabla \Phi_{2 \rightarrow 1}^{\text{qq}} + \nabla \Phi_{2 \rightarrow 1}^{\text{CSI}}) \quad (\text{D.46})$$

$$\Omega_2^{\text{id}} = \nabla \Phi_{1 \rightarrow 2}^{\text{ii}} + \nabla \Phi_{1 \rightarrow 2}^{\text{qq}} + \nabla \Phi_{1 \rightarrow 2}^{\text{CSI}} - (\nabla \Phi_{2 \rightarrow 2}^{\text{qq}} + \nabla \Phi_{2 \rightarrow 2}^{\text{CSI}}) \quad (\text{D.47})$$

$$\Omega_1^{\text{if}} = \text{tr}\{\check{\mathbf{P}}^{\text{max}}\} \cdot (\nabla \Phi_{2 \rightarrow 1}^{\text{ii}} + \nabla \Phi_{2 \rightarrow 1}^{\text{qq}} + \nabla \Phi_{2 \rightarrow 1}^{\text{CSI}}) + \hat{\Phi}_{nn} \quad (\text{D.48})$$

$$\Omega_2^{\text{if}} = \text{tr}\{\check{\mathbf{P}}^{\text{max}}\} \cdot (\nabla \Phi_{2 \rightarrow 2}^{\text{qq}} + \nabla \Phi_{2 \rightarrow 2}^{\text{CSI}}) + \hat{\Phi}_{nn}. \quad (\text{D.49})$$

Here, matrices $\nabla \Phi_{j \rightarrow k}^{\text{ii}}$, $\nabla \Phi_{j \rightarrow k}^{\text{qq}}$ and $\nabla \Phi_{j \rightarrow k}^{\text{CSI}}$ are signal, interference or noise covariance contributions *per unit power* w.r.t. \hat{p}_1 , given as

$$\nabla \Phi_{k \rightarrow j}^{\text{ii}} = \sum_{k' \in \{\mathcal{J}_1^*(j) \cap k\}} \sqrt{\Psi_j} \mathbf{h}_{k'}^e (\mathbf{h}_{k'}^e)^H \sqrt{\Psi_j} \quad (\text{D.50})$$

$$\nabla \Phi_{k \rightarrow j}^{\text{qq}} = \Delta \left(\sqrt{\mathbf{I} - \Psi_j} \mathbf{h}_k^e (\mathbf{h}_k^e)^H \sqrt{\mathbf{I} - \Psi_j} \right) \quad (\text{D.51})$$

$$\nabla \Phi_{k \rightarrow j}^{\text{CSI}} = \sum_{k' \in \{\mathcal{J}_2^*(j) \cap k\}} \Delta \left(\bar{\mathbf{e}}_{k'}^{\text{e,BS}} (\bar{\mathbf{e}}_{k'}^{\text{e,BS}})^H \right) + \Delta \left(\bar{\mathbf{e}}_k^{\text{e,UE}} (\bar{\mathbf{e}}_k^{\text{e,UE}})^H \right). \quad (\text{D.52})$$

From the rate derivatives in (D.43), we can now state the weights that define the tangent to the rate region for a given $\hat{\mathbf{P}}$, \mathbf{C} and $\hat{\Phi}_{nn}$ as

$$\alpha_1 = \frac{-\frac{\delta r_2}{\delta \hat{p}_1}}{\frac{\delta r_1}{\delta \hat{p}_1} - \frac{\delta r_2}{\delta \hat{p}_1}} \quad \text{and} \quad \alpha_2 = \frac{\frac{\delta r_1}{\delta \hat{p}_1}}{\frac{\delta r_1}{\delta \hat{p}_1} - \frac{\delta r_2}{\delta \hat{p}_1}}. \quad (\text{D.53})$$

The weights for different choices of $\hat{\mathbf{P}}$ for an example channel with $M = K = 2$, $N_{\text{bs}} = 1$ and infinite BS cooperation are illustrated in Figure D.1(b). Here, the different lines corre-

spond to the pure linear precoding case (hollow markers) and DPC (filled markers) with the two possible DPC encoding orders.

Update the uplink noise covariance $\hat{\Phi}_{\text{nn}}$ through a gradient technique. For this step, we can exploit the fact that regardless of the choice of $\check{\mathbf{P}}$, \mathbf{C} and weights $\alpha_1 \dots \alpha_K$, the weighted sum rate in (D.42) is convex in $\hat{\Phi}_{\text{nn}}$, hence a global minimum exists which can be approached through a gradient search. For this, we calculate the derivative of the weighted sum-rate towards $\hat{\Phi}_{\text{nn}}$ from (D.42) as

$$\begin{aligned} \nabla \hat{\Phi}_{\text{nn}} = \frac{\delta \left(\sum_{k \in \{1,2\}} \alpha_k r_k \right)}{\delta \hat{\Phi}_{\text{nn}}} = \sum_{k \in \{1,2\}} \alpha_k \left(\Phi^{\text{ss}}(k) + \Phi^{\text{ii}}(k) + \Phi^{\text{qq}}(k) + \Phi^{\text{CSI}}(k) + \hat{\Phi}_{\text{nn}} \right)^{-1} \\ - \alpha_k \left(\Phi^{\text{ii}}(k) + \Phi^{\text{qq}}(k) + \Phi^{\text{CSI}}(k) + \hat{\Phi}_{\text{nn}} \right)^{-1}. \end{aligned} \quad (\text{D.54})$$

Due to the connection of $\hat{\Phi}_{\text{nn}}$ to Lagrangian multipliers (see Appendix C), only the non-zero diagonal components $\Delta(\nabla \hat{\Phi}_{\text{nn}})$ are relevant for us. We must further consider the constraints $\hat{\Phi}_{\text{nn}} \succeq 0$ and $\text{tr}\{\hat{\Phi}_{\text{nn}} \check{\mathbf{P}}^{\text{max}}\} \leq \sigma^2 \text{tr}\{\check{\mathbf{P}}^{\text{max}}\}$ from (D.42), which geometrically mean that $\hat{\Phi}_{\text{nn}}$ must lie inside a polyhedron defined through the positive quadrant of the coordinate system, additionally bounded by the plane defined through point $\sigma^2 \text{tr}\{\check{\mathbf{P}}^{\text{max}}\} / N_{\text{BS}} \cdot (\check{\mathbf{P}}^{\text{max}})^{-1} \mathbf{1}$ and normal vector $\text{diag}(\check{\mathbf{P}}^{\text{max}})$ (see Figure D.1(a)). As the gradient search is supposed to yield the least favorable noise covariance, $\text{tr}\{\hat{\Phi}_{\text{nn}} \check{\mathbf{P}}^{\text{max}}\} \leq \sigma^2 \text{tr}\{\check{\mathbf{P}}^{\text{max}}\}$ must in fact be fulfilled with equality, and $\hat{\Phi}_{\text{nn}}$ hence lie *on* the hatched surface of the polyhedron. Hence, we are interested in the portion of $\nabla \hat{\Phi}_{\text{nn}}$ which is *orthogonal* to the normal vector $\text{diag}(\check{\mathbf{P}}^{\text{max}})$, which we can calculate as

$$\begin{aligned} \nabla_{\perp} \hat{\Phi}_{\text{nn}} = \mathbf{Q} \mathbf{Q}^H \cdot \Delta(\nabla \hat{\Phi}_{\text{nn}}) \\ \text{with } [\mathbf{e} \mathbf{Q}] \mathbf{R} = \text{qr} \left(\text{diag}(\check{\mathbf{P}}^{\text{max}}) \quad \mathbf{v}_2 - \mathbf{v}_1 \quad \mathbf{v}_3 - \mathbf{v}_1 \quad \dots \quad \mathbf{v}_{N_{\text{BS}}} - \mathbf{v}_1 \right) \\ \text{and } \mathbf{V} = \sigma^2 \text{tr}\{\check{\mathbf{P}}^{\text{max}}\} (\check{\mathbf{P}}^{\text{max}})^{-1}, \end{aligned} \quad (\text{D.55})$$

where $\text{qr}(\cdot)$ stands for a QR-decomposition of the operand and $\mathbf{Q} \in \mathbb{C}^{[N_{\text{BS}} \times N_{\text{BS}} - 1]}$ is a matrix containing $N_{\text{BS}} - 1$ vectors orthogonal to each other and to normal vector $\text{diag}(\check{\mathbf{P}}^{\text{max}})$. Terms $\mathbf{e} \in \mathbb{C}^{[N_{\text{BS}} \times 1]}$ and $\mathbf{R} \in \mathbb{C}^{[N_{\text{BS}} \times N_{\text{BS}}]}$ are parts of the decomposition result which are not needed for further computation. \mathbf{Q} could equivalently be obtained through a complex Householder transform of $\Delta(\nabla \hat{\Phi}_{\text{nn}})$ [CY97]. Finally, we update the uplink noise covariance through $\hat{\Phi}_{\text{nn}} := \hat{\Phi}_{\text{nn}} + t \cdot \nabla_{\perp} \hat{\Phi}_{\text{nn}}$, where t is determined by solving

$$\begin{aligned} t = \arg \min_{t' \in \mathbb{R}} \sum_{k \in \{1,2\}} \alpha_k \cdot \log_2 \left| \mathbf{I} + \frac{\Phi^{\text{ss}}(k)}{\Phi^{\text{ii}}(k) + \Phi^{\text{qq}}(k) + \Phi^{\text{CSI}}(k) + \hat{\Phi}_{\text{nn}} + t' \cdot \nabla_{\perp} \hat{\Phi}_{\text{nn}}} \right| \\ \text{s.t. } \hat{\Phi}_{\text{nn}} \succeq 0, \end{aligned} \quad (\text{D.56})$$

which is e.g. possible through bisection [WES06]. For all scenarios considered in our work (i.e. with up to 3 cooperating BSs serving up to 3 UEs), the algorithm has shown stable and fast convergence, though convergence could not yet be analytically proved. In the case of *per-base-station* power constraints, the same algorithm can be used, but it must be considered that M tuples of N_{bs} elements in $\hat{\Phi}_{\text{nn}}$ must be constrained to the same value, as mentioned in Appendix C.

D.4 Downlink Capacity Region with Common Messages

In this section, we derive an inner bound on the capacity region achievable in the non-cooperative downlink employing common message concepts.

As we have observed common message concepts in the downlink to be moderately beneficial in the regime of no or very limited backhaul [MF08c], we also consider these schemes in this work, but observe a sub-optimal approach, where we assume all messages connected to a specific UE k (but possibly decoded by other UEs as well) to be precoded with the same precoding vector \mathbf{w}_k . Further, we assume that common messages are only employed in the context of pure linear precoding, as they are to a certain extent a contradiction to DPC techniques, where interference is supposed to be pre-cancelled instead of being decoded. More precisely, we derive the optimal uplink power allocation $\hat{\mathbf{P}}$ for any point on the capacity region defined through Theorem 2.67. The optimal uplink receive filters $\forall k \in \mathcal{K} : \hat{\mathbf{w}}_k$, as introduced in Appendix C, can then be computed as the strongest generalized Eigenvectors to the signal and interference covariance of each UE individually. Based on the fact that the optimal uplink filters $\hat{\mathbf{w}}_k$ and downlink precoders $\forall k \in \mathcal{K} : \mathbf{w}_k$ must be the same except for a scaling factor \mathbf{d} [SB04], we calculate the optimal downlink precoding matrix \mathbf{W} as [BS02b, SB04, YL07]

$$\mathbf{W} = \hat{\mathbf{W}} \sqrt{\text{diag}(\mathbf{d})} \quad \text{with} \quad \mathbf{d} = \mathbf{A}^{-1} \sigma^2 \mathbf{1}_{[K \times 1]}, \quad (\text{D.57})$$

where $\mathbf{A} \in \mathbb{C}^{[K \times K]}$ is given as

$$\forall k \in \mathcal{K} : a_{k,k} = \frac{1}{\hat{\text{SINR}}_k} \left| (\mathbf{h}_k^e)^H \Psi_{m_k} \hat{\mathbf{w}}_k \right|^2 - \sum_{a=1}^{N_{\text{BS}}} \left| \bar{e}_{a,k}^{\text{UE}} \hat{w}_{a,k} \right|^2 \quad \text{and} \quad (\text{D.58})$$

$$\forall j, k \in \mathcal{K}, j \neq k : a_{k,j} = - \left| (\mathbf{h}_k^e)^H \Psi_{m_j} \mathbf{w}_j \right|^2 - \sum_{a=1}^{N_{\text{BS}}} \left(\left| \bar{e}_{a,k}^{\text{BS}} \hat{w}_{a,j} \right|^2 + \left| \bar{e}_{a,k}^{\text{UE}} \hat{w}_{a,j} \right|^2 \right) \quad (\text{D.59})$$

We then allow the downlink transmit power of each UE to be split into multiple messages, where $\tilde{F}_{\mathcal{K}':k}^m$ denotes a message transmitted from BS m to UE k with precoding vector \mathbf{w}_k , but decoded by all UEs in set $\mathcal{K}' \subseteq \mathcal{K}$. If we denote the set of all messages decoded by UE k as $\check{\mathcal{F}}^{[k]}$, the capacity region achievable can be stated as in the following theorem:

Theorem D.4.1 (DL capacity region without BS coop., under imp. CSI and lin. precoding, employing common message concepts). *The capacity region of a downlink transmission from M non-cooperative BSs with N_{bs} antennas each to K non-cooperative UEs with 1 antenna each, with imperfect CSIT and CSIR and per-antenna or sum power constraints, employing linear precoding and common message concepts, can be inner-bounded through the capacity region given through*

$$\check{\mathcal{R}}_0^{\text{hk}} = \bigcup_{\mathcal{R} \in \check{\mathcal{R}}_0, \check{\mathcal{P}}: \forall k \in \mathcal{K}: \sum_{F=\tilde{F}_{\mathcal{K}':k}^m} \rho_F = 1} \check{\mathcal{R}}_0^{\text{hk}}(\mathbf{W}(\mathcal{R}), \mathbf{m}(\mathcal{R}), \check{\mathcal{P}}), \quad (\text{D.60})$$

where $\check{\mathcal{R}}_0^{\text{hk}}(\mathbf{W}, \mathbf{m}, \check{\mathcal{P}})$ denotes an inner bound on the achievable rate region for a given precoding matrix \mathbf{W} , UE to BS assignment \mathbf{m} and power allocation $\check{\mathcal{P}}$, where all rate tuples

$\mathbf{r} \in \check{\mathcal{R}}_0^{\text{hk}}(\mathbf{W}, \mathbf{m}, \check{\mathcal{P}})$ fulfill $\forall k \in \mathcal{K} : r_k \leq \sum_{F=\check{F}_{\mathcal{K}:k}^m \in \check{\mathcal{F}}_{\text{all}}: k'=k} \nu_F$ and $\forall k \in \mathcal{K}, \forall \mathcal{F} \subseteq \check{\mathcal{F}}^{[k]} :$

$$\sum_{F \in \mathcal{F}} \nu_F \leq \log_2 \left(\mathbf{I} + \frac{\sum_{F=\check{F}_{\mathcal{K}:j}^m \in \mathcal{F}} \check{\rho}_F \left(\overbrace{\left| (\mathbf{h}_k^e)^H \Psi_m \mathbf{w}_j \right|^2}^{\text{Desired signal}} \right)}{\underbrace{\sum_{F=\check{F}_{\mathcal{K}:j}^m \in \check{\mathcal{F}}_{\text{all}} \setminus \check{\mathcal{F}}^{[k]}} \check{\rho}_F \left| (\mathbf{h}_k^e)^H \mathbf{w}_j \right|^2}_{\text{Inter-user interference}} + \sigma_{\text{CSIBS}}^2 + \sigma_{\text{CSIUE}}^2} \right)$$

$$\sigma_{\text{CSIBS}}^2 = \sum_{F=\check{F}_{\mathcal{K}:j}^m \in \check{\mathcal{F}}_{\text{all}} \setminus \check{\mathcal{F}}^{[k]}} \sum_{a=1}^{N_{\text{BS}}} \check{\rho}_F \left| \bar{c}_{a,k}^{\text{BS}} w_{a,j} \right|^2 \quad \text{and} \quad \sigma_{\text{CSIUE}}^2 = \sum_{F=\check{F}_{\mathcal{K}:j}^m \in \check{\mathcal{F}}_{\text{all}}} \check{\rho}_F \sum_{a=1}^{N_{\text{BS}}} \left| \bar{c}_{a,k}^{\text{UE}} w_{a,j} \right|^2$$
(D.61)

Proof. The proof is a straightforward extension of Theorem 2.3.3. □

Appendix E

Motivation of Simulation Parameters

In this appendix, we motivate the choice of N_p in both uplink and downlink, and that of N_b for the downlink in our models introduced in Chapter 2. Recall that in these models we assume that transmission takes place over a single, frequency-flat and block-static channel, where N_p denotes the the number of pilots used per codeword for a simple Kramer-Rao lower bound, while N_b denotes the number of feedback bits invested into each channel coefficient.

In a practical system, as e.g. LTE Release 8, coding is performed over channel accesses that are connected to different OFDM symbols and different sub-carriers. Hence, each channel access will see a slightly different channel realization, depending on the dispersiveness of the channel in time and frequency. In this section, we observe a more detailed and realistic transmission model than in Chapter 2 in order to take into account these aspects, and also consider the option of using channel estimation and CSI feedback schemes that can exploit the correlation of the channel realizations in time and frequency. The aim is to finally compute *realistic* values for N_p and N_b for practical scenarios which we can then plug into our simplified transmission models in Chapter 2.

Let us now observe an OFDMA system as it is used in the downlink of LTE Release 8 [McC07], with a symbol rate of $f_s = 14$ kHz and a sub-carrier spacing of $\Delta F = 15$ kHz. For simplicity, let us assume that OFDMA is used in both uplink and downlink¹, and that both channel estimation and CSI feedback are performed individually for so-called *physical resource blocks* (PRBs) that span $N_s = 14$ OFDM symbols times $N_c = 12$ sub-carriers, hence 168 channel accesses. Clearly, performance could be improved if the schemes would exploit a larger observation window in time and frequency, but then complexity could become an issue. Again for both link directions, we assume that a concrete pilot scheme from LTE Rel. 8 [Mot07] is employed, where for each point-to-point link to be estimated a total of $N_{\text{pos}} = 8$ pilots is multiplexed into one PRB, as illustrated in Figure E.2.

Choice of Parameter N_p

The channel estimation and CSI feedback model used in this section is illustrated in Figure E.1. Note that in some case our notation deviates from that used in the main part of this

¹This deviates from LTE Rel. 8, where single-carrier (SC)-FDMA is used in the uplink [McC07].

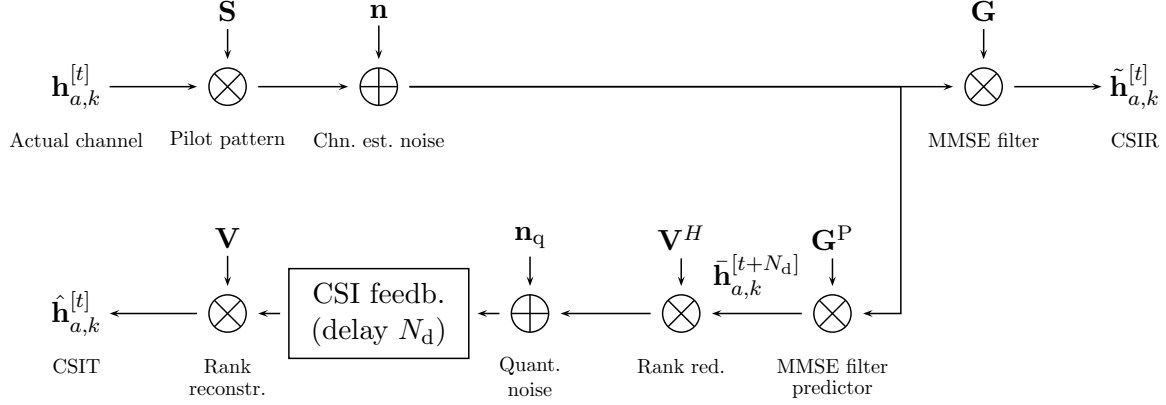


Figure E.1: Channel estimation and CSI feedback process.

thesis. Vector $\mathbf{h}_{a,k} \in \mathbb{C}^{[N_s N_c \times 1]}$, for instance, now stacks all channel realizations connected to the link between BS antenna a and UE k for all 168 channel accesses within an observed PRB of time index t . Matrix $\mathbf{S} \in \{0, 1\}^{[N_s N_c \times N_{\text{pos}}]}$ indicates the pilot positions as illustrated in Figure E.2, implying that the channel estimator only makes observations on the N_{pos} supporting points within the PRB, as well as unit transmit power per pilot. Channel estimation is assumed to be subject to uncorrelated Gaussian noise $\mathbf{n} \sim \mathcal{N}_{\mathbb{C}}(\mathbf{0}, \sigma_{\text{pilots}}^2 \mathbf{I}_{[N_{\text{pos}}]})$. Assuming a wide-sense stationary uncorrelated scattering (WSSUS) channel fading model [DBC93], the correlation of the channel realizations can be stated as [HKR97a, HKR⁺97b]

$$\Phi_{a,k}^{\text{hh}}(N_d) = E \left\{ \mathbf{h}_{a,k}^{[t]} \left(\mathbf{h}_{a,k}^{[t+N_d]} \right)^H \right\} = E \left\{ |h_{a,k}|^2 \right\} \cdot \mathbf{\Pi}_T(N_d) \otimes \mathbf{\Pi}_F, \quad (\text{E.1})$$

where \otimes denotes the Kronecker product,

$$\mathbf{\Pi}_T(N_d) = \begin{bmatrix} J_0\left(2\pi \frac{f_D N_d N_s}{f_s}\right) & J_0\left(2\pi \frac{f_D(N_d N_s + 1)}{f_s}\right) & \cdots & J_0\left(2\pi \frac{f_D(N_d N_s + N_s - 1)}{f_s}\right) \\ J_0\left(2\pi \frac{f_D(N_d N_s - 1)}{f_s}\right) & J_0\left(2\pi \frac{f_D N_d N_s}{f_s}\right) & \cdots & J_0\left(2\pi \frac{f_D(N_d N_s + N_s - 2)}{f_s}\right) \\ \vdots & \vdots & \ddots & \vdots \\ J_0\left(2\pi \frac{f_D(N_d N_s - N_s + 1)}{f_s}\right) & J_0\left(2\pi \frac{f_D(N_d N_s - N_s + 2)}{f_s}\right) & \cdots & J_0\left(2\pi \frac{f_D N_d N_s}{f_s}\right) \end{bmatrix} \quad (\text{E.2})$$

and

$$\mathbf{\Pi}_F = \begin{bmatrix} 1 & \text{si}(2\pi\tau_{\text{max}}\Delta F) & \cdots & \text{si}(2\pi\tau_{\text{max}}\Delta F(N_s - 1)) \\ \text{si}(2\pi\tau_{\text{max}}\Delta F) & 1 & \cdots & \text{si}(2\pi\tau_{\text{max}}\Delta F(N_s - 2)) \\ \vdots & \vdots & \ddots & \vdots \\ \text{si}(2\pi\tau_{\text{max}}\Delta F(N_s - 1)) & \text{si}(2\pi\tau_{\text{max}}\Delta F(N_s - 2)) & \cdots & 1 \end{bmatrix}. \quad (\text{E.3})$$

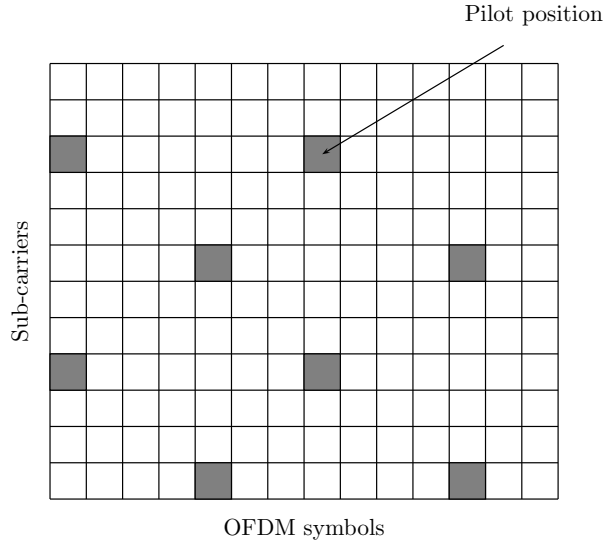


Figure E.2: Pilot structure in each PRB from the LTE downlink assumed in this appendix.

Here, $J_0(\cdot)$ is the zero-th order Bessel function of the first kind, $\text{si}(x)$ denotes $\sin(x)/x$, and f_D is the maximum Doppler frequency, given as $f_D = f_c \cdot v/c$ [DBC93], where f_c is the carrier frequency, v the UE speed, and c the speed of light. τ_{\max} is the maximum delay spread of the channel. N_d is a parameter that will be explained later in the context of CSI feedback and is simply set to zero for now. We assume that a channel estimate is computed for all $N_s \cdot N_c$ channel accesses by multiplying the received pilots with a linear MMSE filter matrix given as [HKR97a, HKR⁺97b]

$$\mathbf{G}_{a,k} = \mathbf{\Phi}_{a,k}^{\text{hh}}(0) \mathbf{S}^H \left(\mathbf{S} \mathbf{\Phi}_{a,k}^{\text{hh}}(0) \mathbf{S}^H + \sigma_{\text{pilots}}^2 \mathbf{I} \right)^{-1}. \quad (\text{E.4})$$

The mean-square error (MSE) of the obtained channel estimates $\tilde{\mathbf{h}}_{a,k} = \mathbf{G}(\mathbf{S}\mathbf{h}_{a,k} + \mathbf{n})$ at the receiver side is [HKR97a, HKR⁺97b, CJC07, JCCU08]

$$\begin{aligned} \text{MSE}_{a,k}^{\text{CSIR}} &= \text{diag} \left(E \left\{ \left(\mathbf{h}_{a,k}^{[t]} - \tilde{\mathbf{h}}_{a,k}^{[t]} \right) \left(\mathbf{h}_{a,k}^{[t]} - \tilde{\mathbf{h}}_{a,k}^{[t]} \right)^H \right\} \right) \\ &= E \left\{ |h_{a,k}|^2 \right\} \cdot \mathbf{1}_{[N_c N_s \times 1]} - \text{diag} \left(\mathbf{\Phi}_{a,k}^{\text{hh}}(0) \mathbf{S}^H \left(\mathbf{S} \mathbf{\Phi}_{a,k}^{\text{hh}}(0) \mathbf{S}^H + \sigma_{\text{pilots}}^2 \mathbf{I} \right)^{-1} \mathbf{S} \mathbf{\Phi}_{a,k}^{\text{hh}}(0) \right). \end{aligned} \quad (\text{E.5})$$

Based on (2.5), we can now translate the *average* MSE to a parameter N_p as

$$N_p \approx \sigma_{\text{pilots}}^2 \cdot \frac{N_s N_c \cdot E\{|h_{a,k}|^2\} - (\text{MSE}_{a,k}^{\text{CSIR}})^T \mathbf{1}}{E\{|h_{a,k}|^2\} \cdot (\text{MSE}_{a,k}^{\text{CSIR}})^T \mathbf{1}}. \quad (\text{E.6})$$

Note that $\text{MSE}_{a,k}^{\text{CSIR}}$ is connected to a particular choice of channel gain $E\{|h_{a,k}|^2\}$ and noise variance σ_{pilots}^2 , while N_p states a universal quantity that is only connected to the assumption that pilots are transmitted with the same power as data. Hence, parameter N_p is a very

convenient term in the context of our work, as it can be used for arbitrary link gains and noise levels, as they occur in CoMP setups. For a particular choice of parameters, namely a SISO SNR of 10 dB, a terminal speed of $v = 3$ km/h, an urban channel with a fairly large maximum delay spread $\tau_{\max} = 1\mu\text{s}$, and a carrier frequency of $f_c = 2.6$ GHz, we obtain $N_p \approx 2.63$. Considering that (E.4) and (E.5) were based on some idealistic assumptions (e.g. filters based on perfect knowledge of the channel correlation statistics), we have decided to use the more pessimistic value of $N_p = 2$ in our work. Note that the uplink performance for the chosen parameters is mainly limited through the frequency selectivity of the channel, and not so much through the terminal speed. In fact, the simulated uplink curves throughout this thesis would still be valid for UE speeds up to $v \approx 25$ km/h.

Choice of Parameter N_b

Let us now consider the case where CSI has to be fed back to the transmitter side (see the lower part of the signal processing chain in Figure E.1). As this feedback process creates a certain extent of delay, which we assume to be $N_d = 3$ TTIs, either the receiver or transmitter side will need to perform *channel prediction*. We assume that there is a channel estimator at the receiver side which inherently performs this prediction, hence the transmitter side can immediately apply the received feedback for the computation of precoding matrices. For simplicity, we further assume that the same downlink pilots are used both for channel estimation for data decoding (MMSE filter matrix \mathbf{G}), as well as for CSI feedback (filter matrix \mathbf{G}^P), even though in a practical CoMP setup one would typically distinguish between cell-specific and stream-specific (i.e. precoded) pilots. The channel prediction filter is given similarly to (E.4) as

$$\mathbf{G}_{a,k}^P = \Phi_{a,k}^{\text{hh}}(N_d) \mathbf{S}^H \left(\mathbf{S} \Phi_{a,k}^{\text{hh}}(0) \mathbf{S}^H + \sigma_{\text{pilots}}^2 \mathbf{I} \right)^{-1}, \quad (\text{E.7})$$

and the MSE of the predicted CSI after the filter is then given as

$$\begin{aligned} \text{MSE}_{a,k}^{\text{CSIR,pred.}} &= \text{diag} \left(E \left\{ \left(\mathbf{h}_{a,k}^{[t]} - \bar{\mathbf{h}}_{a,k}^{[t]} \right) \left(\mathbf{h}_{a,k}^{[t]} - \bar{\mathbf{h}}_{a,k}^{[t]} \right)^H \right\} \right) \\ &= E \left\{ |h_{a,k}|^2 \right\} \cdot \mathbf{1}_{[N_c N_s \times 1]} - \text{diag} \left(\Phi_{a,k}^{\text{hh}}(N_d) \mathbf{S}^H \left(\mathbf{S} \Phi_{a,k}^{\text{hh}}(0) \mathbf{S}^H + \sigma_{\text{pilots}}^2 \mathbf{I} \right)^{-1} \mathbf{S} \Phi_{a,k}^{\text{hh}}(N_d) \right), \end{aligned} \quad (\text{E.8})$$

which is equivalent to (E.5), except that delay N_d is now taken into account. As in [CJCU07, JCCU08], we assume that a decorrelation filter \mathbf{V}^H is applied to the vector of channel estimates $\bar{\mathbf{h}}_{a,k}$, such that we obtain a vector of only few uncorrelated quantities. Filter matrix $\mathbf{V} \in \mathbb{C}^{[N_s N_c \times N_{\text{rank}}]}$ is simply obtained through an Eigenvalue decomposition of the signal covariance at the output of the MMSE filter, i.e.

$$\Phi_{a,k}^{\bar{\text{hh}}} = \Phi_{a,k}^{\text{hh}}(N_d) \mathbf{S}^H \left(\mathbf{S} \Phi_{a,k}^{\text{hh}}(0) \mathbf{S}^H + \sigma_{\text{pilots}}^2 \mathbf{I} \right)^{-1} \mathbf{S} \Phi_{a,k}^{\text{hh}}(N_d) = \mathbf{U} \Sigma \mathbf{U}^H, \quad (\text{E.9})$$

after which \mathbf{V} is chosen such that it contains the N_{rank} column vectors from \mathbf{U} that correspond to the strongest Eigenvalues on the diagonal of Σ . The rank-reduced channel estimates are now quantized with a total number of b bits per PRB, leading to an introduction of quantization noise $\mathbf{n}_q \sim \mathcal{N}_{\mathbb{C}}(\mathbf{0}, \Phi^{\text{qq}})$, and fed back to the transmitter side through an error-free link, where

a multiplication with \mathbf{V} yields a vector of channel estimates again. We here assume that the number of strongest Eigenvalues used is fixed to $N_{\text{rank}} = 2$ (a value which has been determined empirically), and consider the same practical quantization approach as in Section 2.2.5, where an equal number of bits is invested into each of the N_{rank} decorrelated channel estimates, and one bit per real dimension is lost w.r.t. the rate-distortion bound [LBG80]. The quantization noise inherent in the feedback can then be stated as

$$\Phi^{\text{qq}} = 2^{-\max(0, \frac{b}{N_{\text{rank}}} - 2)} \mathbf{V}^H \Phi_{a,k}^{\bar{\text{h}}\bar{\text{h}}} \mathbf{V}. \quad (\text{E.10})$$

Finally, the MSE of the predicted channel at the transmitter side is given as [CJCU07]

$$\begin{aligned} \text{MSE}_{a,k}^{\text{CSIT}} &= \text{diag} \left(E \left\{ \left(\mathbf{h}_{a,k}^{[t]} - \hat{\mathbf{h}}_{a,k}^{[t]} \right) \left(\mathbf{h}_{a,k}^{[t]} - \hat{\mathbf{h}}_{a,k}^{[t]} \right)^H \right\} \right) = \\ &E \left\{ |h_{a,k}|^2 \right\} \cdot \mathbf{1}_{[N_c N_s \times 1]} + \text{diag} \left(\mathbf{V} \Phi^{\text{qq}} \mathbf{V}^H \right) - \dots \\ &- \text{diag} \left(\mathbf{V} \mathbf{V}^H \Phi_{a,k}^{\text{hh}}(N_d) \mathbf{S}^H \left(\mathbf{S} \Phi_{a,k}^{\text{hh}}(0) \mathbf{S}^H + \sigma_{\text{pilots}}^2 \mathbf{I} \right)^{-1} \mathbf{S} \Phi_{a,k}^{\text{hh}}(N_d) \mathbf{V} \mathbf{V}^H \right). \end{aligned} \quad (\text{E.11})$$

The simplified parameter N_b in our downlink transmission model in Section 2.3.2 can now be calculated from (2.56) as

$$N_b = \log_2 \left(\frac{N_s N_c \cdot E \left\{ |h_{a,k}|^2 \right\} - (\text{MSE}_{a,k}^{\text{CSIR}})^T \mathbf{1}}{(\text{MSE}_{a,k}^{\text{CSIT}})^T \mathbf{1} - (\text{MSE}_{a,k}^{\text{CSIR}})^T \mathbf{1}} \right). \quad (\text{E.12})$$

For the previously chosen terminal speed of $v = 3$ km/h, a maximum delay spread of $\tau_{\text{max}} = 1 \mu\text{s}$, a CSI feedback delay of $N_d = 3$ TTIs and $b = 25$ CSI feedback bits per PRB, we obtain $N_b = 5.266$. This time, we have chosen a slightly more optimistic value for our simulations, namely $N_b = 6$, considering that a practical system could benefit from *successive* CSI feedback. The choice of $N_d = 3$ TTIs is based on considerations in [Ass09], though it must be mentioned that some authors argue that $N_d = 4$ could be more realistic [KPK⁺07]. The choice of $b = 25$ feedback bits corresponds to less than 10% of the uplink capacity, assuming that at least QPSK with a code rate of 2/3 is employed in the uplink. We assume that such a sacrifice of uplink rates is reasonable, considering that some applications require significantly larger downlink rates than uplink rates. Determining the optimal extent of CSI feedback for a weighted sum rate optimization of both uplink and downlink rates was investigated in [MRF10]. The calculations in this appendix show that downlink CoMP performance degrades very quickly for increasing N_d and UE velocities, such that a practical system will be able to deliver CoMP only to e.g. static users with a moderately changing environment.

In this chapter, we have shown that the simulation parameters $N_p = 2$ and $N_b = 6$ used throughout large parts of this thesis are realistic for OFDMA-based uplink and downlink transmission under practical channel conditions, and where a reasonable extent of pilots and CSI feedback bits are employed.

Appendix F

Proofs connected to Specific BS Cooperation Schemes

F.1 Proofs Connected to Iterative DIS (I-DIS)

We first prove Lemma 3.3.1, stating that in a symmetrical two-cell scenario (i.e. $\lambda_{1,1} = \lambda_{2,2}$, $\lambda_{1,2} = \lambda_{2,1}$, $\varphi_{Ab} = \varphi_{Ba}$, $\hat{p}_1^{\max} = \hat{p}_2^{\max}$), the sum rate maximizing I-DIS strategy, regardless of the required backhaul, is to split the transmit power of the UEs into an infinite number of messages iteratively exchanged over the backhaul.

Proof. Let us first consider a symmetrical single-antenna setup ($N_{\text{bs}} = 1$), and let us denote the gain of the main links from the UEs to the BSs as $\gamma = \lambda_{1,1} = \lambda_{2,2}$, and the gain of the interference links as $\lambda = \lambda_{1,2} = \lambda_{2,1}$. Similarly, the equal power constraint is written as $\hat{p}^{\max} = \hat{p}_1^{\max} = \hat{p}_2^{\max}$. We here assume that a background noise of variance σ^2 contains thermal noise as well as interference from outside the system plus the impact of imperfect channel estimation (being symmetrical again for both BSs). In a non-iterative DIS case, one of the UEs would be completely decoded by its BS, and the decoded data forwarded to the other BS for a complete cancellation of interference. The sum rate would be the same as if we assumed that both UEs send a superposition of two messages $F_1^{1[1]}$, $F_1^{1[2]}$ and $F_2^{2[1]}$, $F_2^{2[2]}$ at half power $\hat{p}^{\max}/2$ each, such that both messages of one UE are decoded successively or jointly, and both forwarded to the other BS, where then both messages of the other UE are decoded. This is illustrated on the left side of Figure F.1. This is then compared to an iterative scheme where only message $F_1^{1[1]}$ of UE 1 is decoded and forwarded to the other BS, after which message $F_2^{2[1]}$ of UE 2 is decoded, and forwarded along the backhaul in opposite direction. Then the second message $F_1^{1[2]}$ of UE 1 is decoded and forwarded to BS 2, for an interference-free decoding of the second message $F_2^{2[2]}$ of UE 2, as illustrated on the right side of Figure F.1. Both schemes only differ in the rate of messages $F_1^{1[2]}$ and $F_2^{2[1]}$ (indicated through hatched messages in the figure), hence we only need to consider these rates for comparing the schemes. In the non-iterative case, the sum rate of these two messages would be:

$$r_{\text{sum, DIS}} = \log_2 \left(\frac{\gamma \frac{\hat{p}^{\max}}{2} + \lambda \hat{p}^{\max} + \sigma^2}{\lambda \hat{p}^{\max} + \sigma^2} \right) + \log_2 \left(\frac{\gamma \hat{p}^{\max} + \sigma^2}{\gamma \frac{\hat{p}^{\max}}{2} + \sigma^2} \right), \quad (\text{F.1})$$

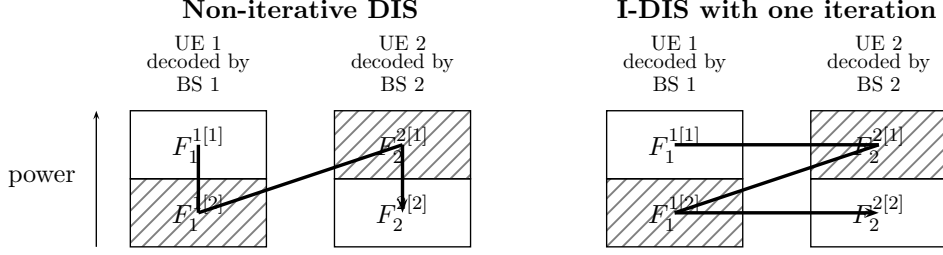


Figure F.1: Illustration of adding one iteration to a DIS cooperation and decoding process.

whereas in the second case, we obtain

$$r_{\text{sum, I-DIS}} = \log_2 \left(\frac{\gamma \frac{\hat{p}^{\max}}{2} + \lambda \frac{\hat{p}^{\max}}{2} + \sigma^2}{\lambda \frac{\hat{p}^{\max}}{2} + \sigma^2} \right) + \log_2 \left(\frac{\gamma \hat{p}^{\max} + \lambda \frac{\hat{p}^{\max}}{2} + \sigma^2}{\gamma \frac{\hat{p}^{\max}}{2} + \lambda \frac{\hat{p}^{\max}}{2} + \sigma^2} \right), \quad (\text{F.2})$$

As the logarithm is a strictly monotonic increasing function, $r_{\text{sum, I-DIS}} > r_{\text{sum, DIS}}$ holds if and only if

$$\begin{aligned} & \left(\frac{\gamma \frac{\hat{p}^{\max}}{2} + \lambda \frac{\hat{p}^{\max}}{2} + \sigma^2}{\lambda \frac{\hat{p}^{\max}}{2} + \sigma^2} \right) \left(\frac{\gamma \hat{p}^{\max} + \lambda \frac{\hat{p}^{\max}}{2} + \sigma^2}{\gamma \frac{\hat{p}^{\max}}{2} + \lambda \frac{\hat{p}^{\max}}{2} + \sigma^2} \right) - \dots \\ & \dots \left(\frac{\gamma \frac{\hat{p}^{\max}}{2} + \lambda \hat{p}^{\max} + \sigma^2}{\lambda \hat{p}^{\max} + \sigma^2} \right) \left(\frac{\gamma \hat{p}^{\max} + \sigma^2}{\gamma \frac{\hat{p}^{\max}}{2} + \sigma^2} \right) > 0, \quad (\text{F.3}) \end{aligned}$$

which can be simplified to

$$r_{\text{sum, I-DIS}} > r_{\text{sum, DIS}} \iff \frac{\gamma \lambda (\gamma - \lambda) \frac{(\hat{p}^{\max})^3}{4}}{(\gamma \frac{\hat{p}^{\max}}{2} + \sigma^2) (\lambda \frac{\hat{p}^{\max}}{2} + \sigma^2) (\lambda \hat{p}^{\max} + \sigma^2)} > 0 \wedge \gamma, \lambda > 0. \quad (\text{F.4})$$

As the condition in (F.4) holds for all $\gamma > \lambda > 0$, this means that splitting the UE transmissions into more messages and increasing the number of I-DIS iterations always leads to a strict increase in sum rate, if all links are of non-zero path gain and the interference links are weaker than the serving links. This is not really a constraint, as we would of course change the BS-UE assignment in the case of dominant interference links (i.e. if $\lambda > \gamma$), and for the case of $\gamma = \lambda$ (i.e. when both UEs are at the cell edge), we know from Section 3.3.2 that there is no gain in using DIS or I-DIS, anyway.

The proof can now be completed through recursion. Any of the split messages before can again be split into two messages with power $\hat{p}^{\max}/4$, and Equations (F.1)-(F.4) can be applied again (taking into account that the noise floor of variance σ^2 must then also contain the interference from the messages yet to be decoded), yet again yielding a sum rate increase. This power splitting can then be performed until we have an infinite number of messages of infinitesimally small power, hence an infinite number of information exchanges over the backhaul.

If we now observe a system with an arbitrary number N_{bs} of antennas per BS, the same proof can be applied, but γ and λ have to be set to the *effective* path gains after the application of an (information-theoretically) optimal *interference rejection combining* (IRC) filter before each decoding step. This makes notation tedious, but it can again be shown that the sum rate is maximized for $N_{\text{I}} \rightarrow \infty$. \square

We can now continue to prove Lemma 3.3.2, stating an upper bound on the sum rate of an I-DIS scheme in a symmetrical interference scenario and $N_{\text{bs}} = 1$. The proof follows the lines of [Gri09], but is slightly generalized to the case of main BS-UE links of gain γ .

Proof. The sum rate of both UEs can be stated as

$$r_{\text{sum}} \leq \lim_{N_{\text{I}} \rightarrow \infty} 2 \cdot \sum_{i=1}^{N_{\text{I}}} \log_2 \left(1 + \frac{\gamma \hat{p}^{\text{max}}}{N_{\text{I}}} \left(\frac{N_{\text{I}} - i}{N_{\text{I}}} (\gamma + \lambda) \hat{p}^{\text{max}} + \sigma^2 \right)^{-1} \right) \quad (\text{F.5})$$

$$\approx \lim_{N_{\text{I}} \rightarrow \infty} \frac{2}{\ln 2} \cdot \sum_{i=1}^{N_{\text{I}}} \left(\frac{\gamma \hat{p}^{\text{max}}}{N_{\text{I}}} \left(\frac{N_{\text{I}} - i}{N_{\text{I}}} (\gamma + \lambda) \hat{p}^{\text{max}} + \sigma^2 \right)^{-1} \right) \quad (\text{F.6})$$

$$= \lim_{N_{\text{I}} \rightarrow \infty} \frac{2}{\ln 2} \cdot \sum_{i=1}^{N_{\text{I}}} \left(\frac{1}{N_{\text{I}}} \left(\frac{N_{\text{I}} - i}{N_{\text{I}}} \left(1 + \frac{\lambda}{\gamma} \right) + \frac{\sigma^2}{\gamma \hat{p}^{\text{max}}} \right)^{-1} \right) \quad (\text{F.7})$$

$$= \frac{2}{\ln 2} \int_{\zeta=0}^1 \frac{1}{1 + \frac{\lambda}{\gamma} + \frac{\sigma^2}{\gamma \hat{p}^{\text{max}}} - \zeta \left(1 + \frac{\lambda}{\gamma} \right)} d\zeta \quad (\text{F.8})$$

$$= 2 \cdot \left[\frac{\log_2 \left(1 + \frac{\lambda}{\gamma} + \frac{\sigma^2}{\gamma \hat{p}^{\text{max}}} - \zeta \left(1 + \frac{\lambda}{\gamma} \right) \right)}{- \left(1 + \frac{\lambda}{\gamma} \right)} \right]_0^1 \quad (\text{F.9})$$

$$= \frac{2}{1 + \frac{\lambda}{\gamma}} \log_2 \left(1 + \frac{(\lambda + \gamma) \hat{p}^{\text{max}}}{\sigma^2} \right), \quad (\text{F.10})$$

where the approximation in (F.6) is due to a Taylor series expansion yielding $\ln(1+x) \approx x$ for small x , which can be applied in our case, as we let the transmit power of each single message go to zero. \square

Note that this proof is only valid for a symmetrical scenario, as here both UEs profit equally from the lower extent of interference provided through a larger number of I-DIS iterations¹. Also, the lemma only refers to maximizing the sum rate. Using an infinite number of exchanges messages is not necessarily optimal in terms of the achievable sum rate/backhaul trade-off. In [GMF09], it has been shown that using large N_{I} is especially detrimental if practical codes with a gap to capacity are used, as then each I-DIS iteration inserts an additional rate loss.

F.2 Benefit of Iterative DAS (I-DAS)

We now prove Theorem 3.3.3, stating that in a scenario with $M = K = 2$, and assuming Gaussian, ergodic signals and large block lengths, the sum rate/backhaul trade-off cannot (or

¹In asymmetrical scenarios, it is e.g. beneficial to let the UE profiting most from interference cancellation assign significantly more power to the message $\hat{F}_1^{1[N_{\text{I}}]}$ decoded last than to the other messages, such that it can be decoded completely free of the interference from the other UE.

only marginally) be improved by I-DAS schemes with more than two information exchanges.

Proof. As stated before, I-DAS concepts in general imply that each BS aims at decoding its own UE. This means that we are operating in a scenario where $d_1 < 0.5$ and $d_2 < 0.5$ (or $d_1 > 0.5$ and $d_2 > 0.5$, in which case the BS-UE assignment is simply swapped). In any other case, it would be more efficient to let one BS decode both UEs, as we have seen before in Section 3.3.2. We know that in such a *weak interference channel* (according to the definition in [Kra04]), we would always pose stronger constraints on one UE's rates if this UE would also (in part) be decoded by the BS in the neighboring cell (unless this BS is also provided information on the UE by the other BS, e.g. through DIS or CIF). Hence, we assume in the sequel that each BS only decodes parts of its *own* UE's transmissions.

Now the question is: What is the increment in information that a BS has obtained after each signal processing step in each single iteration? Clearly, it has decoded an additional portion of its own UE's transmission, and is thus able to distinguish more clearly between desired signal and interference/noise. In an iterative DAS setup, each BS would hence always forward an update on its (remaining) received signals to the other BS, freed from the signals connected to all previously decoded messages. This would mean that in each iteration, a BS would quantize the difference in received signals (equaling the received signals connected to the newest decoded messages). Clearly, this is highly inefficient, especially if the only new information inherent in the quantized signals is an improved removal of interference, and it is obviously better to exchange the decoded interference bits, as then the receiving BS can perform the subtraction itself (and even subtract the interference from its own received signals). Hence, it would be better to exchange reasonably well quantized receive signals at the beginning of the cooperation, and then iteratively update the other side on the own decoded signals (according to the I-DIS concept). The gain of such iterative and joint I-DIS/I-DAS concepts, however, is limited due to the same reasons that limit I-DIS, as we have seen in Lemmas 3.3.1 and 3.3.2. \square

Note that some authors have stated a benefit of multiple exchanges of information between cooperating receivers, but usually in a different context or narrowed down to very particular channels. The authors in [WT09], for example, observe the interference channel with cooperation at the receiver side, but constrain themselves to exemplary channels of strong interference and the regime of asymptotically high SNR, which is of little interest for practical systems. Other authors consider slightly different scenarios, where for example multiple BSs aim at decoding the same common information [DS06], or all BSs aim at decoding all transmissions of all UEs [SGP⁺09].

F.3 UL DAS with Source Coding Approaching Cut-set Bound

In this section, we state and prove the following theorem:

Theorem F.3.1. *Any concrete centralized DAS scheme employing Wyner-Ziv source coding approaches the cut-set bound for $SNR \rightarrow \infty$, if the cut-set bound is defined as the minimum of the performance of same DAS scheme under zero backhaul plus the extent of backhaul itself, and the MAC performance.*

Proof. Assuming a setup of an arbitrary number M of BSs with an arbitrary number N_{bs} of BS antennas, and an arbitrary number K of terminals, where all BSs in set $\mathcal{M}' = \mathcal{M} \setminus m$

forward quantized receive signals to BS m employing distributed Wyner-Ziv source coding, we can state the sum-rate achievable for a sum-backhaul β as [dCS08]

$$r_{\text{sum}} = \log_2 \left| \mathbf{I} + \mathbf{P} \left((\mathbf{H}_m^e)^H (\boldsymbol{\Phi}_m^{\text{hh}} + \sigma^2 \mathbf{I})^{-1} \mathbf{H}_m^e + \sum_{m' \neq m} (\mathbf{H}_{m'}^e)^H (\boldsymbol{\Phi}_{m'}^{\text{hh}} + \boldsymbol{\Phi}_{m' \rightarrow m}^{\text{qq}} + \sigma^2 \mathbf{I})^{-1} \mathbf{H}_{m'}^e \right) \right|$$

$$\text{s.t. } \log_2 \left| \mathbf{I} + (\boldsymbol{\Phi}^{\text{qq}})^{-1} \boldsymbol{\Phi}_{\mathcal{M}'|m}^{\text{yy}} \right| \leq \beta, \quad (\text{F.11})$$

with $\mathbf{P} = \mathbf{P}(\hat{\mathcal{F}}_{\text{all}})$ for brevity, and where $\boldsymbol{\Phi}_{\mathcal{M}'|m}^{\text{yy}}$ is the joint covariance of the signals received at all BSs in set \mathcal{M}' , given that the signals received by BS m are known. We can now rewrite (F.11) to

$$r_{\text{sum}} = \log_2 \underbrace{\left| \mathbf{I} + \mathbf{P} (\mathbf{H}_m^e)^H (\boldsymbol{\Phi}_m^{\text{hh}} + \sigma^2 \mathbf{I})^{-1} \mathbf{H}_m^e \right|}_{=R_0 \text{ (performance at zero backhaul)}} + \dots$$

$$\log_2 \left| \mathbf{I} + \left(\mathbf{I} + \mathbf{P} (\mathbf{H}_m^e)^H (\boldsymbol{\Phi}_m^{\text{hh}} + \sigma^2 \mathbf{I})^{-1} \mathbf{H}_m^e \right)^{-1} \mathbf{P} \left(\sum_{m' \neq m} (\mathbf{H}_{m'}^e)^H (\boldsymbol{\Phi}_{m'}^{\text{hh}} + \boldsymbol{\Phi}_{m' \rightarrow m}^{\text{qq}} + \sigma^2 \mathbf{I})^{-1} \mathbf{H}_{m'}^e \right) \right|, \quad (\text{F.12})$$

under the same backhaul constraint as in (F.11). We can see that the first term corresponds to the non-cooperative sum-rate R_0 , where BS m decodes all terminals on its own. We can further write

$$r_{\text{sum}} = R_0 + \log_2 \left| \mathbf{I} + \mathbf{H}_{\mathcal{M}'}^e \left(\mathbf{I} + \mathbf{P} (\mathbf{H}_m^e)^H (\boldsymbol{\Phi}_m^{\text{hh}} + \sigma^2 \mathbf{I})^{-1} \mathbf{H}_m^e \right)^{-1} \mathbf{P} (\mathbf{H}_{\mathcal{M}'}^e)^H (\boldsymbol{\Phi}_{\mathcal{M}'}^{\text{hh}} + \boldsymbol{\Phi}_{\mathcal{M}' \rightarrow m}^{\text{qq}} + \sigma^2 \mathbf{I})^{-1} \right|, \quad (\text{F.13})$$

by using the property that $|\mathbf{I} + \mathbf{AB}| = |\mathbf{I} + \mathbf{BA}|$, and stacking the BSs' channels, channel estimation noise covariances and quantization noise covariances into compound matrices

$$\mathbf{H}_{\mathcal{M}'}^e = \left[(\mathbf{H}_{m'_1}^e)^T, (\mathbf{H}_{m'_2}^e)^T, \dots, (\mathbf{H}_{m'_{|\mathcal{M}'|}}^e)^T \right]^T \quad (\text{F.14})$$

$$\boldsymbol{\Phi}_{\mathcal{M}'}^{\text{hh}} = \text{diag} \left(\boldsymbol{\Phi}_{m'_1}^{\text{hh}}, \boldsymbol{\Phi}_{m'_2}^{\text{hh}}, \dots, \boldsymbol{\Phi}_{m'_{|\mathcal{M}'|}}^{\text{hh}} \right) \quad \text{and} \quad (\text{F.15})$$

$$\boldsymbol{\Phi}_{\mathcal{M}'}^{\text{qq}} = \text{diag} \left(\boldsymbol{\Phi}_{m'_1}^{\text{qq}}, \boldsymbol{\Phi}_{m'_2}^{\text{qq}}, \dots, \boldsymbol{\Phi}_{m'_{|\mathcal{M}'|}}^{\text{qq}} \right), \quad (\text{F.16})$$

for $\mathcal{M}' = \{m'_1, m'_2, \dots, m'_{|\mathcal{M}'|}\}$. Equation (F.12) can now be simplified to

$$r_{\text{sum}} = R_0 + \log_2 \left| \mathbf{I} + \left(\boldsymbol{\Phi}_{\mathcal{M}'|m}^{\text{yy}} - \boldsymbol{\Phi}_{\mathcal{M}'}^{\text{hh}} - \mathbf{H}_{\mathcal{M}'}^e - \sigma^2 \mathbf{I} \right) \left(\boldsymbol{\Phi}_{\mathcal{M}'}^{\text{hh}} + \boldsymbol{\Phi}_{\mathcal{M}' \rightarrow m}^{\text{qq}} + \sigma^2 \mathbf{I} \right)^{-1} \right|$$

$$= R_0 + \log_2 \left| \boldsymbol{\Phi}_{\mathcal{M}'|m}^{\text{yy}} + \boldsymbol{\Phi}_{\mathcal{M}' \rightarrow m}^{\text{qq}} \right| - \log_2 \left| \boldsymbol{\Phi}_{\mathcal{M}'}^{\text{hh}} + \boldsymbol{\Phi}_{\mathcal{M}' \rightarrow m}^{\text{qq}} + \sigma^2 \mathbf{I} \right|, \quad (\text{F.17})$$

using the derivation of the conditional covariance from (D.18) in Appendix D.2. Merging this with the backhaul constraint in (F.11), we can finally write

$$\begin{aligned} r_{\text{sum}} &= R_0 + \beta + \log_2 |\Phi_{\mathcal{M}' \rightarrow m}^{\text{qq}}| - \log_2 \left| \Phi_{\mathcal{M}' \rightarrow m}^{\text{qq}} + \Phi_{\mathcal{M}'}^{\text{hh}} + \sigma^2 \mathbf{I} \right| \\ &= \underbrace{R_0 + \beta}_{\text{Cut-set bound}} - \underbrace{\log_2 \left| \mathbf{I} + (\Phi_{\mathcal{M}' \rightarrow m}^{\text{qq}})^{-1} (\Phi_{\mathcal{M}'}^{\text{hh}} + \sigma^2 \mathbf{I}) \right|}_{\text{Becomes zero for } \Phi_{\mathcal{M}'}^{\text{hh}} + \sigma^2 \mathbf{I} \rightarrow 0}. \end{aligned} \quad (\text{F.18})$$

From (F.18), we can see that for each value of β , the sum-rate corresponds to that of non-cooperative decoding plus the backhaul invested, *minus* the amount of backhaul that is wasted into the quantization of noise. For $\text{SINR} \rightarrow \infty$, thermal noise and hence also channel estimation related noise go to zero, and in this case the scheme would perform according to the cut-set bound (i.e. such that each additional bit of backhaul yields an additional bit of sum-rate, until MAC performance is reached). This suggests that DAS based on distributed Wyner-Ziv compression is in effect an optimal BS cooperation scheme (in the way that it avoids any redundant exchange of information connected to the UE's transmission over the backhaul), but it cannot avoid to invest parts of the backhaul into quantizing (useless) noise. This is in fact the only reason why for many channel conditions, DAS with source coding is inferior to other BS cooperation schemes such as DIS or CIF. \square

F.4 Best Cooperation Direction for Uplink DAS

In this section, we prove Theorem 3.3.4, stating that for any (finite) extent of backhaul in a scenario of $M = 2$ BSs and an arbitrary number K of terminals, the sum rate is larger if the *weaker* BS DAS-forwards received signals to the *stronger* BS, hence to the BS that can achieve a better UE sum rate even without BS cooperation, than vice versa². More precisely, we assume that it is better to let BS A forward signals to BS B if and only if $|h_B^e|^2 / \sigma_B^2 > |h_A^e|^2 / \sigma_A^2$.

Proof. Initially, let us consider a simplified setup with $M = 2$ BSs with only $N_{\text{bs}} = 1$ receive antenna each, and only $K = 1$ UE. In this case, we denote the two involved (effective) channel coefficients as h_A^e and h_B^e , and denote the sum of channel estimation related noise and thermal noise at the BSs as σ_A^2 and σ_B^2 , respectively. We assume the UE transmits one message at unit power, such that no power terms are required in the following derivations. Let us first consider the case where the inter-BS correlation is *not* exploited, hence where quantization is performed on the unconditional receive signal variance at the DAS-forwarding BS. Here, we can state the sum rate as

$$r_{\text{sum}}^{A \rightarrow B} = \log_2 \left(1 + \frac{|h_B^e|^2}{\sigma_B^2} + \frac{|h_A^e|^2}{\sigma_A^2 + \zeta (|h_A^e|^2 + \sigma_A^2)} \right), \quad (\text{F.19})$$

where $\zeta = (2^\beta - 1)^{-1}$ in the case where BS A forwards to BS B , or

$$r_{\text{sum}}^{B \rightarrow A} = \log_2 \left(1 + \frac{|h_A^e|^2}{\sigma_A^2} + \frac{|h_B^e|^2}{\sigma_B^2 + \zeta (|h_B^e|^2 + \sigma_B^2)} \right) \quad (\text{F.20})$$

²Note that in cases of very low backhaul and low interference, it can be beneficial to let both BSs simultaneously forward signals to the other BS for separate decoding, as we observe in Section 3.3.2.

in the opposite case. Clearly, under an infinite sum backhaul $\beta \rightarrow \infty$ (i.e. $\zeta = 0$), Equations (F.19) and (F.20) yield the same result, as we then simply obtain MAC-performance. Also, it is clear that without BS cooperation ($\beta = 0$ or $\zeta \rightarrow \infty$), it is best for BS B to decode both UEs if and only if $|h_B^e|^2/\sigma_B^2 > |h_A^e|^2/\sigma_A^2$, hence if and only if it has the better link to the UE. For any finite $\beta > 0$, we can derive from (F.19) and (F.20) that the cooperation direction $A \rightarrow B$ is superior if and only if

$$r_{\text{sum}}^{A \rightarrow B} - r_{\text{sum}}^{B \rightarrow A} > 0 \quad (\text{F.21})$$

$$\frac{|h_B^e|^2}{\sigma_B^2} + \frac{|h_A^e|^2}{\sigma_A^2 + \zeta (|h_A^e|^2 + \sigma_A^2)} - \frac{|h_A^e|^2}{\sigma_A^2} - \frac{|h_B^e|^2}{\sigma_B^2 + \zeta (|h_B^e|^2 + \sigma_B^2)} > 0 \quad (\text{F.22})$$

$$\Leftrightarrow \left(\zeta^2 (|h_A^e|^2 + \sigma_A^2) (|h_B^e|^2 + \sigma_B^2) + \zeta \sigma_A^2 \sigma_B^2 \right) \left(\frac{|h_B^e|^2}{\sigma_B^2} - \frac{|h_A^e|^2}{\sigma_A^2} \right) + \dots$$

$$\dots + \zeta \sigma_A^2 \sigma_B^2 \left(\frac{(|h_B^e|^2)^2}{(\sigma_B^2)^2} - \frac{(|h_A^e|^2)^2}{(\sigma_A^2)^2} \right) > 0 \quad (\text{F.23})$$

$$\Leftrightarrow \frac{|h_B^e|^2}{\sigma_B^2} - \frac{|h_A^e|^2}{\sigma_A^2} > 0, \quad (\text{F.24})$$

as $|h_A^e|^2, |h_B^e|^2, \sigma_A^2, \sigma_B^2 > 0$. Hence, it is best to let the BS with the weaker non-cooperative performance DAS-forward to the other one. We now want to observe the case where Wyner-Ziv source coding is applied, hence where we can restate (F.19) and (F.20) as

$$r_{\text{sum}}^{A \rightarrow B} = \log_2 \left(1 + \frac{|h_B^e|^2}{\sigma_B^2} + \frac{|h_A^e|^2}{\sigma_A^2 + \zeta \left(|h_A^e|^2 \frac{\sigma_B^2}{|h_B^e|^2 + \sigma_B^2} + \sigma_A^2 \right)} \right) \quad (\text{F.25})$$

and

$$r_{\text{sum}}^{B \rightarrow A} = \log_2 \left(1 + \frac{|h_A^e|^2}{\sigma_A^2} + \frac{|h_B^e|^2}{\sigma_B^2 + \zeta \left(|h_B^e|^2 \frac{\sigma_A^2}{|h_A^e|^2 + \sigma_A^2} + \sigma_B^2 \right)} \right), \quad (\text{F.26})$$

with ζ as defined before, given that the variance of the signals received at BS A , conditioned on those received by BS B , or vice versa, is derived from (D.18) in Appendix D.2 as

$$\sigma_{A|B}^2 = |h_A^e|^2 \left(1 + \frac{|h_B^e|^2}{\sigma_B^2} \right)^{-1} + \sigma_A^2 \quad \text{and} \quad \sigma_{B|A}^2 = |h_B^e|^2 \left(1 + \frac{|h_A^e|^2}{\sigma_A^2} \right)^{-1} + \sigma_B^2. \quad (\text{F.27})$$

The observations for the case with no or infinite BS cooperation obviously remain the same as in (F.19) and (F.20), and for cases of finite backhaul, we can state that it is better

to let BS A forward received signals to BS B if and only if

$$\frac{|h_A^e|^2}{\sigma_A^2} + \frac{|h_B^e|^2}{\sigma_B^2 + \zeta \left(|h_B^e|^2 \frac{\sigma_A^2}{|h_A^e|^2 + \sigma_A^2} + \sigma_B^2 \right)} - \frac{|h_B^e|^2}{\sigma_B^2} - \frac{|h_A^e|^2}{\sigma_A^2 + \zeta \left(|h_A^e|^2 \frac{\sigma_B^2}{|h_B^e|^2 + \sigma_B^2} + \sigma_A^2 \right)} > 0 \quad (\text{F.28})$$

$$\Leftrightarrow \underbrace{\left(\zeta^2 \left(\frac{|h_B^e|^2 \sigma_A^2}{|h_A^e|^2 + \sigma_A^2} + \sigma_B^2 \right) \left(\frac{|h_A^e|^2 \sigma_B^2}{|h_B^e|^2 + \sigma_B^2} + \sigma_A^2 \right) + \zeta \sigma_A^2 \sigma_B^2 \right) \left(\frac{|h_B^e|^2}{\sigma_B^2} - \frac{|h_A^e|^2}{\sigma_A^2} \right)}_{\text{Positive if } |h_B^e|^2/\sigma_B^2 > |h_A^e|^2/\sigma_A^2} + \dots$$

$$\dots + \zeta \sigma_A^2 \sigma_B^2 \left(\frac{\sigma_A^2}{|h_A^e|^2 + \sigma_A^2} \frac{(|h_B^e|^2)^2}{(\sigma_B^2)^2} - \frac{\sigma_B^2}{|h_B^e|^2 + \sigma_B^2} \frac{(|h_A^e|^2)^2}{(\sigma_A^2)^2} \right) > 0. \quad (\text{F.29})$$

The last line in (F.28) is not as easy to interpret as in the case without source coding in (F.21). The emphasized term is clearly positive under the same condition as before, namely that $|h_B^e|^2/\sigma_B^2 > |h_A^e|^2/\sigma_A^2$. The remaining term, however, shows that under source coding it is even more important (hence the performance gap even larger) for the weaker BS to forward to the stronger. If we assume that BS B has the dominant link to the terminal, then $(|h_B^e|^2)^2/(\sigma_B^2)^2$ will be large, and at the same time, $\sigma_B^2/(|h_B^e|^2 + \sigma_B^2)$ will be (comparatively) small. Hence, it is in this case better to forward quantized signals from BS A to BS B as on one hand, the non-cooperative performance at BS B is already better, and on the other hand, the signal variance at BS A conditioned on the signals at BS B is lower, leading to a lower quantization noise for a given β .

Without explicit derivation, we conclude that the aspects shown above also hold for an arbitrary number of UEs (as this can simply be expressed through a modification of terms $|h_A^e|^2$, $|h_B^e|^2$, σ_A^2 , σ_B^2 , and the same proof applies as above) and for an arbitrary number of BS antennas N_{bs} . It becomes difficult, however, to state the proof directly for arbitrary N_{bs} , as there is then no closed-form expression for the quantization covariance Φ^{qq} [dCS08]. \square

F.5 Superiority of DIS over CIF

In this section, we state and prove the following theorem:

Theorem F.5.1. *DIS in conjunction with superposition coding is always superior or equal to CIF, for any channel realization and any extent of backhaul. This is the case if both compared schemes make use of source coding concepts, or if both schemes don't.*

Proof. Let us first consider the case where source coding is not applied, hence where side-information at the BS benefiting from cooperation is not exploited. We observe a simplified scenario with $M = K = 2$ and $N_{\text{bs}} = 1$, where we denote the corresponding effective channel coefficients between the four entities as h_a^{eA} , h_b^{eA} , h_a^{eB} , h_b^{eB} , and the overall channel estimation and thermal noise related noise variances at the two BSs as σ_A^2 and σ_B^2 , respectively. We assume that UE a transmits a superposition of messages \hat{F}_a^A and $\hat{F}_a^{A \rightarrow B}$, where the latter is forwarded to BS B directly (in the case of DIS), or in form of a quantized version $q(\hat{X}_a^{A \rightarrow B})$ of the corresponding transmit sequence (in the case of CIF). BS B can then decode the message \hat{F}_b^B transmitted by UE b under a reduced level of interference. Note that in both cases, the

rate that UE a can achieve is the same, as the two messages \hat{F}_a^A and $\hat{F}_a^{A \rightarrow B}$ are simply decoded conventionally by BS A and do not profit from the cooperation. Hence, it is sufficient in this proof to observe the rate that UE b can achieve. In the case of CIF, we can derive this as

$$r_b^{\text{CIF}} = \log_2 \left(1 + \left(|h_a^{eB}|^2 \left(\rho_{\hat{F}_a^A} + \xi^2 \right) + \sigma_B^2 \right)^{-1} |h_b^{eB}|^2 \rho_{\hat{F}_b^B} \right) \quad (\text{F.30})$$

$$\text{s.t. } \log_2 \left(\frac{\rho_{\hat{F}_a^{A \rightarrow B}}}{\xi^2} \right) \leq \beta, \quad (\text{F.31})$$

where ξ^2 is the quantization noise that remains as interference to BS B . We can then solve the backhaul constraint in (F.30) for ξ^2 to obtain

$$r_b^{\text{CIF}} = \log_2 \left(1 + \left(|h_a^{eB}|^2 \left(\rho_{\hat{F}_a^A} + \frac{\rho_{\hat{F}_a^{A \rightarrow B}}}{2\beta} \right) + \sigma_B^2 \right)^{-1} |h_b^{eB}|^2 \rho_{\hat{F}_b^B} \right). \quad (\text{F.32})$$

From (F.32), it becomes clear that there is no gain of superposition coding for CIF schemes, i.e. it is best to invest the complete transmit power p_a of UE a into message $\hat{F}_a^{A \rightarrow B}$, yielding

$$r_b^{\text{CIF}} = \log_2 \left(1 + \left(|h_a^{eB}|^2 \frac{p_a}{2\beta} + \sigma_B^2 \right)^{-1} |h_b^{eB}|^2 \rho_{\hat{F}_b^B} \right). \quad (\text{F.33})$$

In the case of DIS, we have

$$r_b^{\text{DIS}} = \log_2 \left(1 + \left(|h_a^{eB}|^2 \rho_{\hat{F}_a^A} + \sigma_B^2 \right)^{-1} |h_b^{eB}|^2 \rho_{\hat{F}_b^B} \right)$$

where $\log_2 \left(1 + \left(|h_a^{eA}|^2 \rho_{\hat{F}_a^A} + |h_b^{eA}|^2 \rho_{\hat{F}_b^B} + \sigma_A^2 \right)^{-1} |h_a^{eA}|^2 \rho_{\hat{F}_a^{A \rightarrow B}} \right) \leq \beta. \quad (\text{F.34})$

We can then derive the power $\rho_{\hat{F}_a^A}$ of the message which is not made available to BS B from the backhaul constraint in (F.34) as

$$\rho_{\hat{F}_a^A} = \frac{p_a}{2\beta} - \left(1 - \frac{1}{2\beta} \right) \frac{|h_b^{eA}|^2 \rho_{\hat{F}_b^B} + \sigma_A^2}{|h_a^{eA}|^2}, \quad (\text{F.35})$$

leading with (F.34) to

$$r_b^{\text{DIS}} = \log_2 \left(1 + \left(|h_a^{eB}|^2 \left(\frac{p_a}{2\beta} - \underbrace{\left(1 - \frac{1}{2\beta} \right) \frac{|h_b^{eA}|^2 \rho_{\hat{F}_b^B} + \sigma_A^2}{|h_a^{eA}|^2}}_{\text{Difference in interference power to CIF}} \right) + \sigma_B^2 \right)^{-1} |h_b^{eB}|^2 \rho_{\hat{F}_b^B} \right). \quad (\text{F.36})$$

If we now compare (F.36) to (F.33), we can see that the rate achievable with DIS is always larger than for CIF, due to fact that the effective interference power is less. In conjunction with Slepian-Wolf source coding, the gap between DIS and CIF becomes even larger. In this case, the required backhaul is reduced by the extent to which BS B can already decode message $\hat{F}_a^{A \rightarrow B}$ (in the case of DIS), or the quantization $q(\hat{X}_a^{A \rightarrow B})$ of the corresponding transmit sequence without cooperation. We can see from (F.33) and (F.36), that the power ratio of

message $\hat{F}_a^{A \rightarrow B}$ over \hat{F}_a^A is larger than the power ratio of the quantized sequence over its quantization noise (i.e. $p_a(1 - 2^{-\beta})$ over $p_a \cdot 2^{-\beta}$), hence the gain of source coding will be less in the case of CIF.

Without explicit derivation, we conjecture that the superiority of DIS in conjunction with superposition coding over CIF also holds for an arbitrary number N_{bs} of BS antennas, which is also reflected in our simulation results. \square

The results (e.g. in Figure 3.8) also show, however, that the performance gap between DIS and CIF can be rather small, and hence CIF schemes are interesting from a practical point of view, as these do not require modifications at the UE side. Further, they allow to easily adjust the rate/backhaul trade-off through changing the quantization function, which is not possible when using DIS schemes.

Bibliography

- [3GP09] 3GPP. Spatial channel model for Multiple Input Multiple Output (MIMO) simulations. *TR 25.996 V6.1.0 (2003-09)*, 2009.
- [AEH06] E. Aktas, J. Evans, and S. Hanly. Distributed base station processing in the uplink of cellular networks. In *Proc. of the IEEE International Conference on Communications (ICC'06)*, volume 4, 2006.
- [AEH08] E. Aktas, J. Evans, and S. Hanly. Distributed Decoding in a Cellular Multiple-Access Channel. *IEEE Trans. on Wireless Comms.*, 7(1):241–250, Jan. 2008.
- [Ahl71] R. Ahlswede. Multi-way communication channels. In *Proc. of the 2nd IEEE International Symposium on Information Theory (ISIT'71)*, pages 103–135, 1971.
- [Ahl74] R. Ahlswede. The capacity region of a channel with two senders and two receivers. *The Annals of Probability*, 2(5):805–814, 1974.
- [And05] J.G. Andrews. Interference cancellation for cellular systems: A contemporary overview. *IEEE Transactions on Wireless Communications*, 12(2):19–29, 2005.
- [Ass93] Telecommunication Industry Association. TIA/EIA/IS-95 Interim Standard, Mobile Station-Base Station Compatibility Standard for Dual-Mode Wideband Spread Spectrum Cellular System, July 1993.
- [Ass09] M. Assaad. Reduction of the feedback delay impact on the performance of Scheduling in OFDMA systems. In *Proc. of the 70th IEEE Vehicular Technology Conference (VTC'09 Fall)*, Sept. 2009.
- [BC07a] S. Bavarian and J.K. Cavers. Reduced Complexity Belief Propagation Algorithm Based on Iterative Groupwise Multiuser Detection. In *Proc. of the Canadian Conference on Electrical and Computer Engineering (CCECE'07)*, pages 466–468, April 2007.
- [BC07b] S. Bavarian and J.K. Cavers. Reduced Complexity Distributed Base Station Processing in the Uplink of Cellular Networks. In *IEEE Global Telecommunications Conference (GLOBECOM'07)*, pages 4500–4504, 2007.
- [Ber74] P. Bergmans. A simple converse for broadcast channels with additive white Gaussian noise. *IEEE Transactions on Information Theory*, 20(2):279–280, 1974.
- [Ber78] T. Berger. Multiterminal source coding. *The Information Theory Approach to Communications*, 229:171–231, 1978.

- [BH07] F. Boccardi and H. Huang. Limited downlink network coordination in cellular networks. In *Proc. of the 18th Annual IEEE International Symposium on Personal Indoor and Mobile Radio Communications (PIMRC07)*, 2007.
- [BHO⁺79] T. Berger, K. Housewright, J. Omura, S. Yung, and J. Wolfowitz. An upper bound on the rate distortion function for source coding with partial side information at the decoder. *IEEE Trans. on Inf. Theory*, 25(6):664–666, Nov. 1979.
- [BLM03] I. Barhumi, G. Leus, and M. Moonen. Optimal training design for MIMO OFDM systems in mobile wireless channels. *IEEE Transactions on Signal Processing*, 51(6):1615–1624, June 2003.
- [BMTT00] P.W. Baier, M. Meurer, T. Weber, and H. Troeger. Joint Transmission (JT), an alternative rationale for the downlink of Time Division CDMA using multi-element transmit antennas. In *Proc. of the IEEE Int. Symposium on Spread Spectrum Techniques and Applications (ISSSTA'00)*, pages 1–5, Sept. 2000.
- [BS02a] H. Boche and M. Schubert. A general duality theory for uplink and downlink beamforming. In *Proc. of the IEEE Vehicular Technology Conference (VTC'02 Fall)*, Sept. 2002.
- [BS02b] H. Boche and M. Schubert. Solution of the SINR downlink beamforming problem. In *Proc. of the Conference on Information Sciences and Systems (CISS'02)*, March 2002.
- [Buc08] S. Buckley. Breaking the backhaul bottleneck. *Telecommunications Global*, March 2008.
- [Bus52] J.J. Bussgang. Crosscorrelation functions of amplitude-distorted Gaussian signals. 1952.
- [BV04] S. Boyd and L. Vandenberghe. *Convex Optimization*. Cambridge University Press, 2004.
- [BZV96] T. Berger, Z. Zhang, and H. Viswanathan. The CEO problem [multiterminal source coding]. *IEEE Trans. on Information Theory*, 42(3):887–902, May 1996.
- [CA07a] W. Choi and J.G. Andrews. Downlink performance and capacity of distributed antenna systems in a multicell environment. *IEEE Transactions on Wireless Communications*, 6(1):69–73, 2007.
- [CA07b] I. Cosovic and G. Auer. Capacity of MIMO-OFDM with Pilot-Aided Channel Estimation. *EURASIP Journal on Wireless Comms. and Networking*, 2007.
- [Car75] A. Carleial. A case where interference does not reduce capacity. *IEEE Transactions on Information Theory*, 21(5):569–570, Sept. 1975.
- [Car78] A. Carleial. Interference channels. *IEEE Transactions on Information Theory*, 24(1):60–70, Jan. 1978.
- [Car83] A. Carleial. Outer bounds on the capacity of interference channels. *IEEE Transactions on Information Theory*, 29(4):602–606, July 1983.

- [CCC00] W.-J. Choi, K.-W. Cheong, and J.M. Cioffi. Iterative soft interference cancellation for multiple antenna systems. In *Proc. of the IEEE Wireless Communications and Networking Conference (WCNC'00)*, volume 1, pages 304–309, 2000.
- [CG79] T. Cover and A.E. Gamal. Capacity theorems for the relay channel. *IEEE Transactions on Information Theory*, 25(5):572–584, 1979.
- [Chu08] R. Chundury. Mobile broadband backhaul: Addressing the challenge. *Ericsson Review*, 3:49, 2008.
- [CJCU07] P.M. Castro, M. Joham, L. Castedo, and W. Utschick. Optimized CSI Feedback for Robust THP Design. In *Proc. of the 41st Asilomar Conference on Signals, Systems and Computers (ASILOMAR'07)*, 2007.
- [CMGE06] H.F. Chong, M. Motani, H.K. Garg, and H. El Gamal. On The Han-Kobayashi Region For The Interference Channel. *IEEE Transactions on Information Theory*, 2006.
- [Com09] Paul Budde Communication. Global Mobile Communications - Statistics, Trends and Forecasts. March 2009.
- [Cos83] M. Costa. Writing on dirty paper. *IEEE Transactions on Information Theory*, 29:439–441, May 1983.
- [Cov72] T. Cover. Broadcast channels. *IEEE Transactions on Information Theory*, 18(1):2–14, 1972.
- [CS03] G. Caire and S. Shamai (Shitz). On the achievable throughput of a multi-antenna Gaussian broadcast channel. *IEEE Transactions on Information Theory*, 49(7):802–811, June 2003.
- [CT06] T.M. Cover and J.A. Thomas. *Elements of Information Theory*. Wiley-Interscience New York, 2006.
- [CY97] K.L. Chung and W.M. Yan. The complex Householder transform. 1997.
- [DBC93] P. Dent, G.E. Bottomley, and T. Croft. Jakes fading model revisited. *Electronics Letters*, 29(13):1162–1163, 1993.
- [dCS08] A. del Coso and S. Simoens. Distributed compression for the uplink channel of a coordinated cellular network with a backhaul constraint. In *Proc. of the 9th IEEE Workshop on Signal Processing Advances in Wireless Communications (SPAWC'08)*, pages 301–305, 2008.
- [Die09] F. Diehm. *On the Impact of Scheduling on the Performance of multi-cell cooperative Detection in a Cellular Network with a Constrained Backhaul*. Vodafone Chair Mobile Communications Systems, TU Dresden, Germany, 2009. Diploma thesis.
- [DLS05] R. Doostnejad, T.J. Lim, and E. Sousa. Precoding for the MIMO broadcast channels with multiple antennas at each receiver. In *Proc. of the 39th Annual Conference on Information Sciences and Systems (CISS05)*, 2005.

- [DLZ05] P. Ding, D.J. Love, and M.D. Zoltowski. On the sum rate of multi-antenna broadcast channels with channel estimation error. *Proc. of the 39th Asilomar Conference on Signals, Systems and Computers (ASILOMAR'05)*, pages 1524–1528, Nov. 2005.
- [DLZ07] P. Ding, D.J. Love, and M.D. Zoltowski. Multiple antenna broadcast channels with shape feedback and limited feedback. *IEEE Transactions on Signal Processing*, 55(7):3417–3428, July 2007.
- [DMFR09] F. Diehm, P. Marsch, G. Fettweis, and B. Ramamurthi. A Low-Complexity Algorithm for Uplink Scheduling in Cooperative Cellular Networks with a Capacity-Constrained Backhaul Infrastructure. In *Proc. of the IEEE Global Conference on Communications (GLOBECOM'09)*, Nov. 2009.
- [Dro05] B. Dropping. Changes in base station backhaul drive new sync solutions. Nov. 2005.
- [DS06] R. Dabora and S.D. Servetto. A multi-step conference for cooperative broadcast. In *Proc. of the IEEE International Symposium on Information Theory (ISIT'06)*, pages 2190–2194, 2006.
- [dS08] A. del Coso and S. Simoens. Uplink rate region of a coordinated cellular network with distributed compression. In *Proc. of the IEEE International Symposium on Information Theory (ISIT'08)*, pages 2091–2095, July 2008.
- [DSH06] A.F. Dana, M. Sharif, and B. Hassibi. On the capacity region of multi-antenna gaussian broadcast channels with estimation error. *Proc. of the IEEE Int. Symposium on Information Theory (ISIT'06)*, pages 1851–1855, July 2006.
- [ECS⁺98] R.B. Ertel, P. Cardieri, K.W. Sowerby, T.S. Rappaport, and J.H. Reed. Overview of spatial channel models for antenna array communication systems. *IEEE Personal Communications*, 5(1):10–22, 1998.
- [ER97] M. Escartin and P. A. Ranta. Interference rejection combining with a small antenna array at the mobile scattering environment. In *Proc. of the IEEE Signal Proc. and Wireless Comms. Conference (SPAWC'97)*, pages 165–168, 1997.
- [Erg09] M. Ergen. Long-Term Evolution of 3GPP. 2009.
- [Et05] U. Erez and S. ten Brink. A close-to-capacity dirty paper coding scheme. *IEEE Transactions on Information Theory*, 51(10):3417–3432, 2005.
- [ETW08] R.H. Etkin, D.N.C. Tse, and H. Wang. Gaussian interference channel capacity to within one bit. *IEEE Trans. on Information Theory*, 54(12):5534–5562, 2008.
- [FF62] L.R. Ford and D.R. Fulkerson. *Flows in Networs*. Princeton University Press, 1962.
- [FG98] G.J. Foschini and M.J. Gans. On Limits of Wireless Communications in a Fading Environment when Using Multiple Antennas. *Wireless Personal Communications*, 6(3):311335, March 1998.

- [FKV06] G.J. Foschini, K. Karakayali, and R.A. Valenzuela. Coordinating multiple antenna cellular networks to achieve enormous spectral efficiency. *IEEE Proceedings - Communications*, 153(4):548–555, Aug. 2006.
- [For09] Cisco VNI Forecast. Cisco Visual Networking Index (VNI) Global Mobile Data Traffic Forecast Update. August 2009.
- [FU98] G.D. Forney and G. Ungerboeck. Modulation and coding for linear Gaussian channels. *IEEE Transactions on Information Theory*, 44(6):2384–2415, 1998.
- [FWLH02] R.F.H. Fischer, C. Windpassinger, A. Lampe, and J.B. Huber. MIMO Precoding for Decentralized Receivers. In *Proc. of the IEEE International Symposium on Information Theory (ISIT'02)*, June 2002.
- [Gal63] R.G. Gallager. L.D.P.C. Codes, 1963.
- [Gas03] M. Gastpar. On Wyner-Ziv networks. *Proc. of the 39th Asilomar Conference on Signals, Systems and Computers (ASILOMAR'03)*, 1:855–859, Nov. 2003.
- [Gas04] M. Gastpar. The wyner-ziv problem with multiple sources. *IEEE Transactions on Information Theory*, 50(11):2762–2768, Nov. 2004.
- [GDV02] M. Gastpar, P.L. Dragotti, and M. Vetterli. The distributed Karhunen-Loeve transform. In *Proc. of the IEEE Workshop on Multimedia Signal Processing*, pages 57–60, 2002.
- [GHEM04] A. Grant, S. Hanly, J. Evans, and R. Muller. Distributed decoding for Wyner cellular systems. In *Proc. of the 5th Australian Communication Theory Workshop*, pages 77–81, 2004.
- [GK00] P. Gupta and P.R. Kumar. The capacity of wireless networks. *IEEE Transactions on Information Theory*, 46(2):388–404, 2000.
- [GMF09] M. Grieger, P. Marsch, and G. Fettweis. Uplink Base Station Cooperation by Iterative Distributed Interference Subtraction. In *Proc. of the 20th IEEE International Symposium On Personal, Indoor and Mobile Radio Communications (PIMRC'09)*, Sept. 2009.
- [GMF10a] M. Grieger, P. Marsch, and G. Fettweis. Ad Hoc Cooperation for the Cellular Uplink with Capacity Constrained Backhaul. In *Proc. of the IEEE International Conference on Communications (ICC'10)*, May 2010.
- [GMF10b] M. Grieger, P. Marsch, and G. Fettweis. Progressive Uplink Base Station Cooperation for Backhaul Constrained Cellular Systems. In *11th IEEE International Workshop on Signal Processing Advances in Wireless Communications (SPAWC'10)*, June 2010.
- [GMFC09] M. Grieger, P. Marsch, G. Fettweis, and J.M. Cioffi. On the Performance of Compressed Interference Forwarding for Uplink Base Station Cooperation. In *Proc. of the IEEE Global Telecomms. Conf. (GLOBECOM'09)*, Nov. 2009.

- [GMRF10] M. Grieger, P. Marsch, Z. Rong, and G. Fettweis. Field Trial Results for a Coordinated Multi-Point (CoMP) Uplink in Cellular Systems. In *Proc. of the ITG/IEEE Workshop on Smart Antennas (WSA '09)*, February 2010.
- [GP80] S.I. Gelfand and M.S. Pinsker. Coding for a channel with random parameters. *Problems of Control and Information Theory*, 9:19–31, 1980.
- [Gri09] M. Grieger. *Information Theoretic Examination of Multi-Cell Signal Processing in Mobile Communication Networks*. Vodafone Chair Mobile Communications Systems, TU Dresden, Germany, 2009. Master thesis.
- [HJ08] R. Hunger and M. Joham. A General Rate Duality of the MIMO Multiple Access Channel and the MIMO Broadcast Channel. In *Proc. of the IEEE Global Telecommunications Conference (GLOBECOM'08)*, pages 1–5, 2008.
- [HJU09] R. Hunger, M. Joham, and W. Utschick. On the MSE-Duality of the Broadcast Channel and the Multiple Access Channel. *IEEE Transactions on Signal Processing*, 57(2):698–713, Feb. 2009.
- [HK81] T. Han and K. Kobayashi. A new achievable rate region for the interference channel. *IEEE Transactions on Information Theory*, 27(1):49–60, Jan. 1981.
- [HKF10] J. Holfeld, V. Kotzsch, and G. Fettweis. Order-recursive precoding for cooperative multi-point transmission. In *Proc. of the ITG/IEEE Workshop on Smart Antennas (WSA '09)*, February 2010.
- [HKR97a] P. Hoeher, S. Kaiser, and P. Robertson. Pilot-symbol-aided channel estimation in time and frequency. *Multi-carrier spread-spectrum (A 98-43106 12-32)*, pages 169–178, 1997.
- [HKR⁺97b] P. Hoeher, S. Kaiser, P. Robertson, et al. Two-dimensional pilot-symbol-aided channel estimation by Wiener filtering. In *Proc. of the IEEE International Conference on Acoustics and Speech and Signal Processing (ICASSP'97)*, volume 3, pages 1845–1848, 1997.
- [HM72] H. Harashima and H. Miyakawa. Matched-Transmission Technique for Channels With Intersymbol Interference. *IEEE Transactions on Communications*, 20(4):774780, Aug. 1972.
- [HM06] A. Host-Madsen. Capacity bounds for cooperative diversity. *IEEE Transactions on Information Theory*, 52(4):1522–1544, 2006.
- [HPS05] B.M. Hochwald, C.B. Peel, and A.L. Swindlehurst. A vector-perturbation technique for near-capacity multiantenna multiuser communication-part II: perturbation. *IEEE Transactions on Communications*, 53(3):537–544, 2005.
- [HS07] J. He and M. Salehi. Low-complexity coordinated interference-aware beamforming for MIMO broadcast channels. pages 685–689, Sept. 2007.
- [HSU09] C. Hellings, D.A. Schmidt, and W. Utschick. Optimized Beamforming for the Two Stream MIMO Interference Channel at High SNR. In *Proc. of the IEEE/ITG Workshop on Smart Antennas (WSA '09)*, 2009.

- [HT08] H. Huang and M. Trivellato. Performance of multiuser MIMO and network coordination in downlink cellular networks. In *Proc. of the 6th International Symposium on Modeling and Optimization in Mobile, Ad Hoc, and Wireless Networks and Workshops (WiOPT'08)*, pages 85–90, 2008.
- [HVKS03] H. Huang, S. Venkatesan, A. Kogiantis, and N. Sharma. Increasing the peak data rate of 3G downlink packet data systems using multiple antennas. In *Proc. of the 57th IEEE Semiannual Vehicular Technology Conference (VTC'03 Spring)*, volume 1, pages 311–315, April 2003.
- [HWS09] R.W. Heath Jr, T. Wu, and A.C.K. Soong. Progressive Refinement of Beamforming Vectors for High Resolution Limited Feedback. *EURASIP Journal on Wireless Communications and Networks*, 2009.
- [I⁺09] R. Irmer et al. Multisite Field Trial for LTE and Advanced Concepts. *IEEE Communications Magazine*, 47(2):92–98, 2009.
- [JB03] E. Jorswieck and H. Boche. Transmission strategies for the MIMO MAC with MMSE receiver: Average MSE optimization and achievable individual MSE region. *IEEE Transactions on Signal Processing*, 51(11):2872–2881, Nov. 2003.
- [JCCU08] M. Joham, P.M. Castro, L. Castedo, and W. Utschick. MMSE Optimal Feedback of Correlated CSI for Multi-User Precoding. In *Proc. of the IEEE International Conference on Acoustics, Speech, and Signal Processing (ICASSP'08)*, pages 3129–3132, 2008.
- [JF07] S.A. Jafar and M.J. Fakhreddin. Degrees of freedom for the MIMO interference channel. *IEEE Transactions on Information Theory*, 53(7):2637–2642, 2007.
- [Jin06a] N. Jindal. A feedback reduction technique for MIMO broadcast channels. In *Proc. of the IEEE International Symposium on Information Theory (ISIT'06)*, pages 2699–2703, 2006.
- [Jin06b] N. Jindal. MIMO broadcast channels with finite-rate feedback. *IEEE Transactions on Information Theory*, 52(11):5045, 2006.
- [JJT⁺09] V. Jungnickel, S. Jäckel, L. Thiele, J. Lei, U. Kruger, A. Brylka, and C. von Helmlolt. Capacity Measurements in a Cooperative MIMO Network. *IEEE Transactions on Vehicular Technology*, 58(5):2392–2405, 2009.
- [JJVG02] N. Jindal, S. Jafar, S. Vishwanath, and A. Goldsmith. Sum power iterative water-filling for multi-antenna Gaussian broadcast channels. In *Proc. of the 37th Asilomar Conference (ASILOMAR'02)*, 2002.
- [JRV⁺05] N. Jindal, W. Rhee, S. Vishwanath, S.A. Jafar, and A. Goldsmith. Sum power iterative waterfilling for multiple-antenna Gaussian broadcast channels. *IEEE Transactions on Information Theory*, 51(4):1570–1580, April 2005.
- [JST⁺09] V. Jungnickel, M. Schellmann, L. Thiele, T. Wirth, T. Haustein, O. Koch, W. Zirwas, and E. Schulz. Interference-aware scheduling in the multiuser MIMO-OFDM downlink. *IEEE Communications Magazine*, 47(6):56–66, 2009.

- [JTH⁺07] S. Jing, D.N.C. Tse, J. Hou, J.B. Soriaga, J.E. Smee, and R. Padovani. Multi-cell downlink capacity with coordinated processing. In *Proc. of the Information Theory and Applications Workshop (ITA'07)*, 2007.
- [JTW⁺09] V. Jungnickel, L. Thiele, T. Wirth, T. Haustein, S. Schiffermller, A. Forck, S. Wahls, S. Jaeckel, S. Schubert, C. Juchems, F. Luhn, R. Zavrtak, H. Droste, G. Kadel, W. Kreher, J. Mueller, W. Stoermer, and G. Wannemacher. Coordinated Multipoint Trials in the Downlink. In *Proc. of the 5th IEEE Broadband Wireless Access Workshop (BWAWS'09), co-located with IEEE GLOBECOM 2009*, Nov. 2009.
- [JVG04] N. Jindal, S. Vishwanath, and A. Goldsmith. On the duality of Gaussian multiple-access and broadcast channels. *IEEE Transactions on Information Theory*, 50(5):768–783, 2004.
- [Kay93] S.M. Kay. *Fundamentals of statistical signal processing: estimation theory*, volume 1. 1993.
- [KdFG⁺07] M. Kountouris, R. de Francisco, D. Gesbert, D.T.M. Slock, and T. Salzer. Efficient Metrics for Scheduling in MIMO Broadcast Channels with Limited Feedback. In *Proc. of the IEEE International Conference on Acoustics, Speech and Signal Processing (ICASSP'07)*, volume 3, pages III–109 – III–112, April 2007.
- [KF07] S. Khattak and G. Fettweis. Distributed iterative detection in an interference limited cellular network. In *Proc. of the 65th IEEE Vehicular Technology Conference (VTC'07 Spring)*, pages 2349–2353, 2007.
- [KF08] S. Khattak and G. Fettweis. Low Backhaul Distributed Detection Strategies for an Interference Limited Uplink Cellular System. In *Proc. of the 67th IEEE Vehicular Technology Conference (VTC'08 Spring)*, May 2008.
- [KF10] V. Kotzsch and G. Fettweis. Interference Analysis in Time and Frequency Asynchronous Network MIMO OFDM Systems. In *IEEE Wireless Communications and Networking Conference (WCNC'10)*, April 2010.
- [KFV06] M.K. Karakayali, G.J. Foschini, and R.A. Valenzuela. Network coordination for spectrally efficient communications in cellular systems. *IEEE Transactions on Wireless Communications*, 13(4):56–61, Aug. 2006.
- [KFVY06] M.K. Karakayali, G.J. Foschini, R.A. Valenzuela, and R.D. Yates. On the maximum common rate achievable in a coordinated network. In *Proc. of IEEE International Conference on Communications (ICC'06)*, June 2006.
- [KHF09] V. Kotzsch, J. Holfeld, and G. Fettweis. Joint Detection and CFO Compensation in Asynchronous Multi-User MIMO OFDM Systems. In *Proc. of the 69th IEEE Vehicular Technology Conference (VTC'09 Spring)*, April 2009.
- [KJUB05] K. Kusume, M. Joham, W. Utschick, and G. Bauch. Efficient Tomlinson-Harashima precoding for spatial multiplexing on flat MIMO channel. In *Proc. of the IEEE Int. Conference on Communications (ICC'05)*, volume 3, 2005.

- [KM98] N. Kong and L. B. Milstein. Combined average SNR of a generalized diversity selection combining scheme. In *Proc. of the IEEE International Conference on Communications (ICC'98)*, volume 3, pages 1556–1560, June 1998.
- [KPK⁺07] I.Z. Kovács, K.I. Pedersen, T.E. Kolding, A. Pokhariyal, and M. Kuusela. Effects of non-ideal channel feedback on dual-stream MIMO-OFDMA system performance. In *Proc. of the 66th IEEE Vehicular Technology Conference (VTC'07 Fall)*, 2007.
- [KPKG05] M. Kountouris, A. Pandharipande, Hojin Kim, and D. Gesbert. QoS-based user scheduling for multiuser MIMO systems. In *Proc. of the 61st IEEE Vehicular Technology Conference (VTC'05 Spring)*, volume 1, pages 211–215, May 2005.
- [Kra04] G. Kramer. Outer bounds on the capacity of Gaussian interference channels. *IEEE Transactions on Information Theory*, 50(3):581–586, March 2004.
- [KRF07] S. Khattak, W. Rave, and G. Fettweis. On the Impact of User Positions on Multiuser Detection in Distributive Antenna Systems. In *Proc. of the 13th European Wireless Conference (EW'07)*, April 2007.
- [KRF08] S. Khattak, W. Rave, and G. Fettweis. Distributed iterative multiuser detection through base station cooperation. *EURASIP Journal on Wireless Communications and Networking*, 2008:13, 2008.
- [LBG80] Y. Linde, A. Buzo, and R. Gray. An Algorithm for Vector Quantizer Design. *IEEE Transactions on Communications*, 28(1):84–95, 1980.
- [Lia72] H.H.J. Liao. Multiple Access Channels. *Ph.D. thesis*, 1972.
- [Lim08] Horsebridge Network Systems Limited. Network Synchronization Overview - Synchronizing Cellular Networks, 2008.
- [LJ06] L. Liu and H. Jafarkhani. Novel Transmit Beamforming Schemes for Time-Selective Fading Multiantenna Systems. *IEEE Transactions on Signal Processing*, 54(12):4767, 2006.
- [LJ07] L. Liu and H. Jafarkhani. Successive transmit beamforming algorithms for multiple-antenna OFDM systems. *IEEE Transactions on Wireless Communications*, 6(4):1512–1522, 2007.
- [LS02] A. Lapidoth and S. Shamai. Fading channels: how perfect need "perfect side information" be? *IEEE Transactions on Information Theory*, 48(5):1118–1134, May 2002.
- [LSW05] A. Lapidoth, S. Shamai, and M. Wigger. On the capacity of fading MIMO broadcast channels with imperfect transmitter side-information. In *Proc. of the 43rd Allerton Conference on Communication, Control and Computing*, 2005.
- [LYG06] Y. Liang, T. Yoo, and A. Goldsmith. Coverage spectral efficiency of cellular systems with cooperative base stations. In *Proc. of the 40th Asilomar Conference on Signals, Systems and Computers (ASILOMAR'06)*, pages 349–353, 2006.

- [MAMK08] M.A. Maddah-Ali, A.S. Motahari, and A.K. Khandani. Communication over MIMO X channels: Interference alignment, decomposition, and performance analysis. *IEEE Transactions on Information Theory*, 54(8):3457–3470, 2008.
- [Mar79] K. Marton. A coding theorem for the discrete memoryless broadcast channel. *IEEE Transactions on Information Theory*, 25(3):306–311, 1979.
- [MB05] N. Mysore and J. Bajcsy. The Impact of Channel Estimation Errors and Co-antenna Interference on the Performance of a Coded MIMO System. *EURASIP Journal on Applied Signal Processing*, 2005(11):1680–1697, 2005.
- [MBW⁺00] M. Meurer, P.W. Baier, T. Weber, Y. Lu, and A. Papathanassiou. Joint transmission: advantageous downlink concept for CDMA mobile radio systems using time division duplexing. *Electronics Letters*, 36:900, 2000.
- [McC07] W. McCoy. Overview of 3GPP LTE Physical Layer: White Paper by Dr. Wes McCoy. *White Paper*, 2007.
- [Med00] M. Medard. The effect upon channel capacity in wireless communications of perfect and imperfect knowledge of the channel. *IEEE Transactions on Information Theory*, 46(3):933–946, May 2000.
- [MF07a] P. Marsch and G. Fettweis. A Decentralized Optimization Approach to Backhaul-Constrained Distributed Antenna Systems. In *Proc. of the 16th IST Mobile and Wireless Communications Summit (IST'07)*, pages 1–5, July 2007.
- [MF07b] P. Marsch and G. Fettweis. A Framework for Optimizing the Uplink Performance of Distributed Antenna Systems under a Constrained Backhaul. In *Proc. of the IEEE Int. Conference on Communications (ICC'07)*, pages 975–979, June 2007.
- [MF07c] P. Marsch and G. Fettweis. A framework for optimizing the downlink of distributed antenna systems under a constrained backhaul. In *Proc. of the 13th European Wireless Conference (EW'07)*, April 2007.
- [MF08a] P. Marsch and G. Fettweis. A direct solution for multi-user beamforming under per-antenna power constraints. In *Proc. of the 7th International ITG Conference on Source and Channel Coding (SCC'08)*, January 2008.
- [MF08b] P. Marsch and G. Fettweis. On Backhaul-Constrained Multi-Cell Cooperative Detection based on Superposition Coding. In *Proc. of the IEEE International Symposium On Personal, Indoor And Mobile Radio Communications (PIMRC'08)*, Sept. 2008.
- [MF08c] P. Marsch and G. Fettweis. On Base Station Cooperation Schemes for Downlink Network MIMO under a Constrained Backhaul. In *Proc. of the IEEE Global Telecommunications Conference (GLOBECOM'08)*, Nov. 2008.
- [MF08d] P. Marsch and G. Fettweis. On Base Station Cooperation Schemes for Uplink Network MIMO under a Constrained Backhaul. In *Proc. of the 11th Int. Symposium on Wireless Personal Multimedia Comms. (WPMC'08)*, Sept. 2008.

- [MF08e] P. Marsch and G. Fettweis. Rate Region of the Multi-Cell Multiple Access Channel under Backhaul and Latency Constraints. In *Proc. of the Wireless Communications and Networking Conference (WCNC'08)*, pages 830–834, 2008.
- [MF09a] P. Marsch and G. Fettweis. On Downlink Network MIMO under a Constrained Backhaul and Imperfect Channel Knowledge. In *Proc. of the IEEE Global Telecommunications Conference (GLOBECOM'09)*, Nov. 2009.
- [MF09b] P. Marsch and G. Fettweis. On Uplink Network MIMO under a Constrained Backhaul and Imperfect Channel Knowledge. In *Proc. of the IEEE International Conference on Communications (ICC'09)*, June 2009.
- [MG02] D. Micciancio and S. Goldwasser. *Complexity of Lattice Problems*. Kluwer Academic Publishers, 2002.
- [MH99] T.L. Marzetta and B.M. Hochwald. Capacity of a mobile multiple-antenna communication link in Rayleigh flat fading. *IEEE Transactions on Information Theory*, 45(1):139–157, Jan. 1999.
- [MJH06] T. Mayer, H. Jenkac, and J. Hagenauer. Turbo base-station cooperation for intercell interference cancellation. In *IEEE International Conference on Communications (ICC'06)*, volume 11, 2006.
- [MK06] T.F. Maciel and A. Klein. A Low-Complexity SDMA Grouping Strategy for the Downlink of Multi-User MIMO Systems. In *Proc. of the 17th IEEE International Symposium on Personal, Indoor and Mobile Radio Communications (PIMRC'06)*, pages 1–5, Sept. 2006.
- [MK07] T.F. Maciel and A. Klein. A Convex Quadratic SDMA Grouping Algorithm Based on Spatial Correlation. In *Proc. of the IEEE International Conference on Communications (ICC'07)*, pages 5342–5347, June 2007.
- [MKF06] P. Marsch, S. Khattak, and G. Fettweis. A framework for determining realistic capacity bounds for distributed antenna systems. In *Proc. of the IEEE Information Theory Workshop (ITW'06)*, Oct. 2006.
- [MKP07] M. Morelli, C.C.J. Kuo, and M.O. Pun. Synchronization techniques for orthogonal frequency division multiple access (OFDMA): A tutorial review. *Proceedings of the IEEE*, 95(7):1394–1427, 2007.
- [MLG99] C. Mihailescu, X. Lagrange, and P. Godlewski. Soft handover analysis in downlink UMTS WCDMA system. In *Proc. of the IEEE International Workshop on Mobile Multimedia Communications (MoMuC'99)*, pages 279–285, 1999.
- [Mot07] Motorola. Overview of LTE Air-Interface, Technical White Paper. 2007.
- [MRF10] P. Marsch, P. Rost, and G. Fettweis. Application Driven Joint Uplink-Downlink Optimization in Wireless Communications. In *Proc. of the ITG/IEEE Workshop on Smart Antennas (WSA'09)*, February 2010.
- [MW04a] I. Maniatis and T. Weber. Joint Channel Estimation with Array Antennas in OFDM based Mobile Radio Systems. *COST 273 TD (04)*, 9, 2004.

- [MW04b] M. Meurer and T. Weber. Imperfect channel knowledge: An insurmountable barrier in Rx oriented multi-user MIMO transmission? In *Proc. of the 5th International ITG Conference on Source and Channel Coding (SCC'04)*, 2004.
- [MWSL02] L. Maniatis, T. Weber, A. Sklavos, and Y. Liu. Pilots for joint channel estimation in multi-user OFDM mobile radio systems. In *Proc. of the IEEE 7th International Symposium on Spread Spectrum Techniques and Applications (ISSSTA'02)*, volume 1, 2002.
- [NEBP02] R.U. Nabar, V. Erceg, H. Bölcskei, and A.J. Paulraj. Performance of multi-antenna signaling strategies using dual-polarized antennas: Measurement results and analysis. *Wireless Personal Communications*, 23(1):31–44, 2002.
- [NEH07] B.L. Ng, J. Evans, and S. Hanly. Distributed downlink beamforming in cellular networks. In *Proc. of the IEEE International Symposium on Information Theory (ISIT'07)*, pages 6–10, 2007.
- [NEHA08] B.L. Ng, J.S. Evans, S.V. Hanly, and D. Aktas. Distributed Downlink Beamforming With Cooperative Base Stations. *IEEE Transactions on Information Theory*, 54(12):5491–5499, Dec. 2008.
- [Ooh97] Y. Oohama. Gaussian multiterminal source coding. *IEEE Transactions on Information Theory*, 43(6):1912–1923, Nov. 1997.
- [Ooh98] Y. Oohama. The rate-distortion function for the quadratic Gaussian CEO problem. *IEEE Transactions on Information Theory*, 44(3):1057–1070, May 1998.
- [PA09] S. Parkvall and D. Astely. The Evolution of LTE towards IMT-Advanced. *Journal of Communications*, 4(3), 2009.
- [PDF⁺08] S. Parkvall, E. Dahlman, A. Furuskar, Y. Jading, M. Olsson, S. Wanstedt, and K. Zangi. LTE-Advanced - Evolving LTE towards IMT-advanced. In *Proc. of the 68th IEEE Vehicular Technology Conference (VTC'08 Fall)*, pages 1–5, 2008.
- [PGH08] A. Papadogiannis, D. Gesbert, and E. Hardouin. A Dynamic Clustering Approach in Wireless Networks with Multi-Cell Cooperative Processing. In *Proc. of the IEEE International Conference on Communications (ICC'08)*, pages 4033–4037, May 2008.
- [PHG08] A. Papadogiannis, E. Hardouin, and D. Gesbert. A Framework for Decentralising Multi-Cell Cooperative Processing on the Downlink. In *Proc. of the IEEE Global Telecommunications Conference (GLOBECOM'08)*, pages 1–5, Nov. 2008.
- [PHG09] A. Papadogiannis, E. Hardouin, and D. Gesbert. Decentralising Multicell Cooperative Processing: A Novel Robust Framework. *EURASIP Journal on Wireless Communications and Networking*, 2009.
- [PHS05] C.B. Peel, B.M. Hochwald, and A.L. Swindlehurst. A vector-perturbation technique for near-capacity multiantenna multiuser communication-part I: channel inversion and regularization. *IEEE Trans. on Comms.*, 53(1):195–202, 2005.
- [PS95] J.G. Proakis and M. Salehi. *Digital communications*. McGraw-Hill Boston, 1995.

- [PSS04] G. Primolevo, O. Simeone, and U. Spagnolini. Effects of imperfect channel state information on the capacity of broadcast OSDMA-MIMO systems. In *Proc. of the 5th IEEE Workshop on Signal Processing Advances in Wireless Communications (SPAWC'04)*, pages 546–550, 2004.
- [PTR04] V. Prabhakaran, D. Tse, and K. Ramachandran. Rate region of the quadratic Gaussian CEO problem. *Proc. of the IEEE International Symposium on Information Theory (ISIT'04)*, June 2004.
- [PV09] V.M. Prabhakaran and P. Viswanath. Interference channels with destination cooperation. *CoRR*, July 2009.
- [Rap96] T.S. Rappaport. *Wireless Communications: Principles and Practice*. IEEE Press Piscataway, NJ, USA, 1996.
- [Rav09] W. Rave. Quantization of Log-Likelihood Ratios to Maximize Mutual Information. *IEEE Signal Processing Letters*, 16, April 2009.
- [RBL⁺91] J.P. Rossi, J.C. Bic, A.J. Levy, Y. Gabillett, and M. Rosen. A ray launching method for radio-mobile propagation in urban area. In *Antennas and Propagation Society International Symposium*, pages 1540–1543, 1991.
- [Res09] Infonetics Research. Mobile Backhaul Equipment and Services Biannual Worldwide and Regional Market Size and Forecasts. May 2009.
- [RFL09] P. Rost, G. Fettweis, and J. N. Laneman. Broadcast and Interference in Relay-Assisted Next-Generation Cellular Systems. In *Proc. of the IEEE Communications Theory Workshop (CTW'09)*, May 2009.
- [RHZF08] I. Riedel, R. Habendorf, E. Zimmermann, and G. Fettweis. Multiuser Transmission in Cellular Systems With Different Sector Configurations. In *Proc. of the 68th IEEE Vehicular Technology Conference (VTC'08)*, Sept. 2008.
- [Sat78] H. Sato. An outer bound to the capacity region of broadcast channels. *IEEE Transactions on Information Theory*, 24(3):374–377, 1978.
- [SB04] M. Schubert and H. Boche. Solution of the multiuser downlink beamforming problem with individual SINR constraints. *IEEE Transactions on Vehicular Technology*, 53(1):18–28, Jan. 2004.
- [Sch09] B.T. Scheme. LTE: The Evolution of Mobile Broadband. *IEEE Communications Magazine*, page 45, 2009.
- [SCJ07] S. Shamai, G. Caire, and N. Jindal. On the Required Accuracy of Transmitter Channel State Information in Multiple-Antenna Broadcast Channels. In *Proc. of the Asilomar Conf. on Signals, Systems and Computers (ASILOMAR'07)*, 2007.
- [SDS⁺05] J. Salo, G. Del Galdo, J. Salmi, P. Kysti, M. Milojevic, D. Laselva, and C. Schneider. MATLAB implementation of the 3GPP Spatial Channel Model (3GPP TR 25.996). Jan. 2005.

- [SGP⁺09] O. Simeone, D. Gündüz, H.V. Poor, A. Goldsmith, and S. Shamai. Compound multiple access channels with partial cooperation. *IEEE Transactions on Information Theory*, 55:2425–2441, 2009.
- [SH05] M. Sharif and B. Hassibi. On the capacity of MIMO broadcast channels with partial side information. *IEEE Transactions on Information Theory*, 51(2):506–522, 2005.
- [SJ09] M. Schellmann and V. Jungnickel. Multiple CFOs in OFDM-SDMA Uplink: Interference Analysis and Compensation. *EURASIP Journal on Wireless Communications and Networking*, 2009.
- [SKC07] X. Shang, G. Kramer, and B. Chen. A New Outer Bound and the Noisy-Interference Sum-Rate Capacity for Gaussian Interference Channels. *IEEE Transactions on Information Theory*, 712, 2007.
- [SMW⁺01] A. Sklavos, I. Maniatis, T. Weber, P.W. Baier, E. Costa, H. Haas, and E. Schulz. Joint Channel Estimation in Multi-User OFDM Systems. In *Proc. of the 6th International OFDM Workshop (InOWo01)*, page III1–III4, Sept. 2001.
- [SSB⁺09] C. Shi, D.A. Schmidt, R.A. Berry, M.L. Honig, and W. Utschick. Distributed interference pricing for the MIMO interference channel. In *Proc. of the IEEE International Conference on Communications (ICC'09)*, June 2009.
- [SSH04] Q.H. Spencer, A.L. Swindlehurst, and M. Haardt. Zero-forcing methods for downlink spatial multiplexing in multiuser MIMO channels. *IEEE Transactions on Signal Processing*, 52(2):461–471, 2004.
- [SSPS07] O. Simeone, O. Somekh, H.V. Poor, and S. Shamai. Downlink macro-diversity with limited backhaul capacity. In *CCIT Report 671*, 2007.
- [SSPS08a] O. Simeone, O. Somekh, H.V. Poor, and S. Shamai. Distributed MIMO in multi-cell wireless systems via finite-capacity links. In *Proc. of the 3rd International Symposium on Communications, Control and Signal Processing (ISCCSP'08)*, pages 203–206, March 2008.
- [SSPS08b] O. Simeone, O. Somekh, H.V. Poor, and S. Shamai. Enhancing uplink throughput via local base station cooperation. In *Proc. of the Asilomar Conference on Signals, Systems and Computers (ASILOMAR'08)*, 2008.
- [SSPS09a] O. Simeone, O. Somekh, H.V. Poor, and S. Shamai. Downlink Multicell Processing with Limited-Backhaul Capacity. *EURASIP Journal on Advances in Signal Processing*, 2009.
- [SSPS09b] O. Simeone, O. Somekh, H.V. Poor, and S. Shamai. Local base station cooperation via finite-capacity links for the uplink of simple cellular networks. *IEEE Transactions on Information Theory*, 55(1):190–204, 2009.
- [SSS07a] A. Sanderovich, O. Somekh, and S. Shamai. Uplink macro diversity with limited backhaul capacity. In *Proc. of the IEEE International Symposium on Information Theory (ISIT'07)*, June 2007.

- [SSS⁺07b] S. Shamai, O. Somekh, O. Simeone, A. Sanderovich, B.M. Zaidel, and V. Poor. Cooperative Multi-Cell Networks: Impact of Limited-Capacity Backhaul and Inter-Users Links. In *Proc. of the Joint Workshop on Communications and Coding (JWCC'07)*, Oct. 2007.
- [SSS⁺08a] S. Shamai, O. Simeone, O. Somekh, A. Sanderovich, B.M. Zaidel, and H.V. Poor. Information-Theoretic Implications of Constrained Cooperation in Simple Cellular Models. In *Proc. of the 19th IEEE International Symposium on Personal, Indoor and Mobile Radio Communications (PIMRC'08)*, pages 1–5, 2008.
- [SSS⁺08b] O. Somekh, O. Simeone, A. Sanderovich, B.M. Zaidel, and S. Shamai. On the impact of limited-capacity backhaul and inter-users links in cooperative multicell networks. In *Proc. of the 42nd Annual Conference on Information Sciences and Systems (CISS'08)*, pages 776–780, 2008.
- [SSS09] A. Sanderovich, S. Shamai, and Y. Steinberg. Distributed MIMO receiver-achievable rates and upper bounds. *IEEE Transactions on Information Theory*, 55(10):4419–4438, 2009.
- [SSSK05] A. Sanderovich, S. Shamai, Y. Steinberg, and G. Kramer. Communication via decentralized processing. *Proc. of the IEEE International Symposium on Information Theory (ISIT'05)*, pages 1201–1205, Sept 2005.
- [SSSP06] A. Sanderovich, Shamai S, Y. Steinberg, and M. Peleg. Decentralized receiver in a MIMO system. *Proc. of the IEEE International Symposium on Information Theory (ISIT'06)*, pages 6–10, July 2006.
- [SSSP08] S. Shamai, O. Simeone, O. Somekh, and H.V. Poor. Joint Multi-Cell Processing for Downlink Channels with Limited-Capacity Backhaul. In *Proc. of the Information Theory and Applications Workshop (ITA'08)*, 2008.
- [SSZ04] S. Shamai, O. Somekh, and B.M. Zaidel. Multi-cell communications: An information theoretic perspective. In *Proc. of the Joint Workshop on Communications and Coding (JWCC'04)*, Oct. 2004.
- [SW73] D. Slepian and J. Wolf. Noiseless coding of correlated information sources. *IEEE Transactions on Information Theory*, 19(4):471–480, July 1973.
- [SWC⁺02] A. Sklavos, T. Weber, E. Costa, H. Haas, and E. Schulz. Joint Detection in multi-antenna and multi-user OFDM systems. *Multi-Carrier Spread Spectrum and Related Topics*, pages 191–198, 2002.
- [SZ01] S. Shamai and B. Zaidel. Enhancing the cellular downlink capacity via co-processing at the transmitter end. *Proc. of the IEEE Semiannual Vehicular Technology Conference (VTC'01 Spring)*, pages 1745–1749, 2001.
- [Tan89] A.S. Tanenbaum. *Computer Networks*. Englewood Cliffs, Prentice-Hall, 1989.
- [Tay04] R.M. Taylor Jr. Overview of Space-Time Wireless Communications in Quasi-static Rayleigh Flat Fading Channels. 2004.

- [Tel99] E. Telatar. Capacity of multi-antenna Gaussian channels. *European Transactions on Telecommunications*, 10(6):585–595, 1999.
- [TM08] Informa Telecoms and Media. Global Mobile Forecasts to 2013, Worldwide Market Analysis, Strategic Outlook and Forecasts to 2013. Dec. 2008.
- [Tom71] M. Tomlinson. New automatic equaliser employing modulo arithmetic. *Electronics Letters*, 7(5/6):138139, March 1971.
- [TSS⁺08] L. Thiele, M. Schellmann, S. Schiffermuller, V. Jungnickel, and W. Zirwas. Multi-Cell Channel Estimation using Virtual Pilots. In *Proc. of the IEEE Vehicular Technology Conference (VTC'08 Spring)*, pages 1211–1215, May 2008.
- [Tun78] S. Tung. *Multiterminal source coding*. PhD thesis, Univ. microfilms int., 1978.
- [VAG05] D. Varodayan, A. Aaron, and B. Girod. Rate-adaptive distributed source coding using low-density parity-check codes. In *Proc. of the 39th Asilomar Conference on Signals, Systems and Computers (ASILOMAR'05)*, pages 1203–1207, 2005.
- [VB97] H. Viswanathan and T. Berger. The quadratic Gaussian CEO problem. *IEEE Transactions on Information Theory*, 43(5):1549–1559, Sept. 1997.
- [VBW98] L. Vandenberghe, S. Boyd, and S.P. Wu. Determinant Maximization with Linear Matrix Inequality Constraints. *SIAM Journal on Matrix Analysis and Applications*, 19(2):499–533, April 1998.
- [VJG03] S. Vishwanath, N. Jindal, and A. Goldsmith. Duality, achievable rates and sum-rate capacity of Gaussian MIMO broadcast channels. *IEEE Transactions on Information Theory*, 49:2658–2668, Oct. 2003.
- [VRJG03] S. Vishwanath, W. Rheet, S. Jafar, and A. Goldsmith. Sum Power Iterative Waterfilling for Gaussian Vector Broadcast Channels. In *Proc. of the International Symposium on Information Theory (ISIT'03)*, June 2003.
- [VT03] P. Viswanath and D.N.C. Tse. Sum capacity of the vector Gaussian broadcast channel and uplink-downlink duality. *IEEE Transactions on Information Theory*, 49(8):1912–1921, 2003.
- [VTA01] P. Viswanath, D.N.C. Tse, and V. Anantharam. Asymptotically optimal waterfilling in vector multiple-access channels. *IEEE Transactions on Information Theory*, 47(1):241–267, Jan. 2001.
- [VTL02] P. Viswanath, D.N.C. Tse, and R. Laroia. Opportunistic beamforming using dumb antennas. *IEEE Transactions on Information Theory*, 48(6):1277–1294, June 2002.
- [VVGZ94] A.J. Viterbi, A.M. Viterbi, K.S. Gilhousen, and E. Zehavi. Soft handoff extends CDMA cell coverage and increases reverse link capacity. *IEEE Journal on Selected Areas in Communications*, 12(8):1281–1288, 1994.
- [VVH03] H. Viswanathan, S. Venkatesan, and H. Huang. Downlink capacity evaluation of cellular networks with known-interference cancellation. *IEEE Journal on Selected Areas in Communications*, 21(5):802–811, June 2003.

- [WBOW00] T. Weber, P.W. Baier, J. Oster, and M. Weckerle. Performance enhancement of time division CDMA (TD-CDMA) by multistep joint detection. In *Proc. of the 7th International Conference on Telecommunications (ICT'00)*, volume 2, pages 1038–1044, 2000.
- [WES06] A. Wiesel, Y.C. Eldar, and S. Shamai (Shitz). Linear precoding via conic optimization for fixed MIMO receivers. *IEEE Transactions on Signal Processing*, 54(1):161–176, Jan. 2006.
- [WIN03] WINNER. Ist-2003-507581 winner d5.4 final report on link level and system level channel models v1.4. <https://www.ist-winner.org>, 2003.
- [WL97] D. Wong and T.J. Lim. Soft Handoffs in CDMA Mobile Systems. *IEEE Personal Communications*, page 7, 1997.
- [WMSL02] T. Weber, I. Maniatis, A. Sklavos, and Y. Liu. Joint transmission and detection integrated network (JOINT), a generic proposal for beyond 3G systems. In *Proc. of the 9th International Conference on Telecommunications (ICT'02)*, volume 3, pages 479–483, June 2002.
- [WSM06] T. Weber, A. Sklavos, and M. Meurer. Imperfect channel-state information in MIMO transmission. *IEEE Transactions on Communications*, 54(3):543–552, March 2006.
- [WSS04] H. Weingarten, Y. Steinberg, and S. Shamai. The capacity region of the Gaussian MIMO broadcast channel. *Proc. of the IEEE International Symposium on Information Theory (ISIT'04)*, June 2004.
- [WSS06] H. Weingarten, Y. Steinberg, and S. Shamai. The Capacity Region of the Gaussian Multiple-Input Multiple-Output Broadcast Channel. *IEEE Transactions on Information Theory*, 52(9):3936–3964, 2006.
- [WT08] I.-H. Wang and D.N.C. Tse. Gaussian interference channels with multiple receive antennas: Capacity and generalized degrees of freedom. In *Proc. of the 46th Annual Allerton Conference on Communication, Control, and Computing*, pages 715–722, 2008.
- [WT09] I.-H. Wang and D.N.C. Tse. Interference Mitigation Through Limited Receiver Cooperation: Symmetric Case. *Imprint*, 2009.
- [WTI08] ITU World Telecommunication/ICT Indicators WTI. Worldwide mobile cellular subscribers to reach 4 billion mark late 2008. *Press Release*, 2008.
- [Wyn78] A.D. Wyner. The Rate-Distortion Function for Source Coding with Side Information at the Decoder-II: General Sources. *Inform. and Control*, 38:60–80, 1978.
- [Wyn94] A.D. Wyner. Shannon-theoretic approach to a Gaussian cellular multiple-access channel. *IEEE Transactions on Information Theory*, 40(6):1713–1727, 1994.

- [WZ76] A. Wyner and J. Ziv. The rate-distortion function for source coding with side information at the decoder. *IEEE Transactions on Information Theory*, 22(1):1–10, Jan. 1976.
- [XLC04] Z. Xiong, A.D. Liveris, and S. Cheng. Distributed source coding for sensor networks. *IEEE Signal Processing Magazine*, 21(5):80–94, 2004.
- [YC04] W. Yu and J.M. Cioffi. Sum capacity of Gaussian vector broadcast channels. *IEEE Transactions on Information Theory*, 50(9):1875–1892, 2004.
- [YG06] T. Yoo and A. Goldsmith. Capacity and power allocation for fading MIMO channels with channel estimation error. *IEEE Transactions on Information Theory*, 52(5):2203–2214, 2006.
- [YL07] W. Yu and T. Lan. Transmitter optimization for the multi-antenna downlink with per-antenna power constraints. *IEEE Transactions on Signal Processing*, 55:2646–2660, June 2007.
- [YRBC04] W. Yu, W. Rhee, S. Boyd, and J.M. Cioffi. Iterative water-filling for Gaussian vector multiple-access channels. *IEEE Transactions on Information Theory*, 50(1):145–152, Jan. 2004.
- [Yu03] W. Yu. A dual decomposition approach to the sum power Gaussian vector multiple access channel sum capacity problem. In *Proc. of the 37th Annual Conference on Information Sciences and Systems (CISS'03)*, volume 14, pages 16–18, 2003.
- [Zam96] R. Zamir. The rate loss in the wyner-ziv problem. *IEEE Transactions on Information Theory*, 42(6):2073–2084, Nov. 1996.
- [ZCA⁺08] J. Zhang, R. Chen, J.G. Andrews, A. Ghosh, and R.W. Heath. Networked MIMO with clustered linear precoding. *Imprint*, 29:27, 2008.
- [ZD04] H. Zhang and H. Dai. Cochannel interference mitigation and cooperative processing in downlink multicell multiuser MIMO networks. *EURASIP Journal on Wireless Communications and Networking*, 2004(2):222–235, 2004.
- [ZM09] M. Zivkovic and R. Mathar. Preamble-based SNR estimation algorithm for wireless MIMO OFDM systems. In *Proc. of the 6th IEEE International Symposium on Wireless Communication Systems (ISWCS'09)*, Sept. 2009.
- [ZN04] Y. Zeng and T.S. Ng. A semi-blind channel estimation method for multiuser multi-antenna OFDM systems. *IEEE Transactions on Signal Processing*, 52(5):1419–1429, 2004.
- [ZY08] L. Zhou and W. Yu. Gaussian Z-interference channel with a relay link: Achievable rate region and asymptotic sum capacity. In *Proc. of the International Symposium on Information Theory and Its Applications (ISITA'08)*, Dec. 2008.

Publication List

Journal Publications and Book Chapters

- [1] P. Marsch and G. Fettweis. Uplink CoMP under a Constrained Backhaul and Imperfect Channel Knowledge. Submitted to *IEEE Transactions on Wireless Communications*, Feb. 2010. Available at <http://arxiv.org/abs/1002.3356>.
- [2] P. Marsch and G. Fettweis. On Multi-Cell Cooperative Transmission in Backhaul-Constrained Cellular Systems. In *Annales des Télécommunications*, 63(5-6), May 2008.
- [3] P. Marsch and G. Fettweis. On Multi-Cell Cooperative Signal Processing in Backhaul-Constrained Cellular Systems. In *Advances in Mobile and Wireless Communications - Views of the 16th IST Mobile and Wireless Communications Summit*, 2008.

Conference Publications

- [1] M. Grieger, P. Marsch, and G. Fettweis. Progressive Uplink Base Station Cooperation for Backhaul Constrained Cellular Systems. In *Proc. of the 11th IEEE International Workshop on Signal Processing Advances in Wireless Comm. (SPAWC'10)*, June 2010.
- [2] M. Grieger, P. Marsch, and G. Fettweis. Ad Hoc Cooperation for the Cellular Uplink with Capacity Constrained Backhaul. In *Proc. of the IEEE International Conference on Communications (ICC'10)*, May 2010.
- [3] F. Diehm, P. Marsch, and G. Fettweis. The FUTON Prototype: Proof of Concept for Coordinated Multi-Point in Conjunction with a Novel Integrated Wireless/Optical Architecture. In *Proc. of the IEEE Wireless Communications and Networking Conference (WCNC'10)*, April 2010.
- [4] G. Fettweis, J. Holfeld, V. Kotzsch, P. Marsch, E. Ohlmer, Z. Rong, and P. Rost. Field Trial Results for LTE-Advanced Concepts. In *Proc. of the IEEE International Conference on Acoustics, Speech, and Signal Processing (ICASSP'10)*, March 2010.
- [5] P. Marsch, P. Rost, and G. Fettweis. Application Driven Joint Uplink-Downlink Optimization in Wireless Communications. In *Proc. of the ITG/IEEE Workshop on Smart Antennas (WSA'09)*, Feb. 2010.

- [6] M. Grieger, P. Marsch, Z. Rong, and G. Fettweis. Field Trial Results for a Coordinated Multi-Point (CoMP) Uplink in Cellular Systems. In *Proc. of the ITG/IEEE Workshop on Smart Antennas (WSA '10)*, Feb. 2010.
- [7] P. Marsch and G. Fettweis. On Downlink Network MIMO under a Constrained Backhaul and Imperfect Channel Knowledge. In *Proc. of the IEEE Global Telecommunications Conference (GLOBECOM'09)*, Nov. 2009.
- [8] M. Grieger, P. Marsch, J. Cioffi, and G. Fettweis. On the Performance of Compressed Interference Forwarding for Uplink Base Station Cooperation. In *Proc. of the IEEE Global Communications Conference (GLOBECOM'09)* Nov. 2009.
- [9] F. Diehm, P. Marsch, G. Fettweis, and B. Ramamurthi. A Low-Complexity Algorithm for Uplink Scheduling in Cooperative Cellular Networks with a Capacity-Constrained Backhaul Infrastructure. In *Proc. of the IEEE Global Conference on Communications (GLOBECOM'09)*, Nov. 2009.
- [10] M. Grieger, P. Marsch, and G. Fettweis. Uplink Base Station Cooperation by Iterative Distributed Interference Subtraction. In *Proc. of the 20th IEEE International Symposium On Personal, Indoor and Mobile Radio Comm. (PIMRC'09)*, Sept. 2009.
- [11] P. Marsch and G. Fettweis. On Uplink Network MIMO under a Constrained Backhaul and Imperfect Channel Knowledge. In *Proc. of the IEEE International Conference on Communications (ICC'09)*, June 2009.
- [12] P. Marsch and G. Fettweis. On Base Station Cooperation Schemes for Downlink Network MIMO under a Constrained Backhaul. In *Proc. of the IEEE Global Telecommunications Conference (GLOBECOM'08)*, Nov. 2008.
- [13] P. Marsch and G. Fettweis. On Backhaul-Constrained Multi-Cell Cooperative Detection based on Superposition Coding. In *Proc. of the IEEE International Symposium On Personal, Indoor And Mobile Radio Communications (PIMRC'08)*, Sept. 2008.
- [14] P. Marsch and G. Fettweis. On Base Station Cooperation Schemes for Uplink Network MIMO under a Constrained Backhaul. In *Proc. of the 11th International Symposium on Wireless Personal Multimedia Communications (WPMC'08)*, Sept. 2008.
- [15] P. Marsch and G. Fettweis. Rate Region of the Multi-Cell Multiple Access Channel under Backhaul and Latency Constraints. In *Proc. of the Wireless Communications and Networking Conference (WCNC'08)*, March 2008.
- [16] C. Jandura, P. Marsch, A. Zoch, and G. Fettweis. A Testbed for Cooperative Multi Cell Algorithms. In *Proc. of the 4th International Conference on Testbeds and Research Infrastr. for the Development of Networks and Communities (TRIDENTCOM'08)*, March 2008.

- [17] P. Marsch and G. Fettweis. A Direct Solution for Multi-user Beamforming under per-antenna Power Constraints. In *Proc. of the 7th International ITG Conference on Source and Channel Coding (SCC'08)*, Jan. 2008.
- [18] P. Marsch and G. Fettweis. A Decentralized Optimization Approach to Backhaul-Constrained Distributed Antenna Systems. In *Proc. of the 16th IST Mobile and Wireless Communications Summit (IST'07)*, pages 1–5, July 2007.
- [19] P. Marsch and G. Fettweis. A Framework for Optimizing the Uplink Performance of Distributed Antenna Systems under a Constrained Backhaul. In *Proc. of the IEEE International Conference on Communications (ICC'07)*, pages 975–979, June 2007.
- [20] P. Marsch and G. Fettweis. A Framework for Optimizing the Downlink Performance of Distributed Antenna Systems under a Constrained Backhaul. In *Proc. of the 13th European Wireless Conference (EW'07)*, April 2007.
- [21] P. Marsch, W. Rave, and G. Fettweis. Quasi-Orthogonal STBC using Stretched Constellations for Low Detection Complexity. In *Proc. of the IEEE Wireless Communications and Networking Conference (WCNC'07)*, March 2007.
- [22] A. Fehske, P. Marsch, and G. Fettweis. On the Complexity of Feedback Generation in MISO Beamforming and Diversity Schemes. In *Proc. of the International Symposium on Information Theory and its Applications (ISITA'06)*, Oct. 2006.
- [23] P. Marsch, S. Khattak, and G. Fettweis. A Framework for Determining Realistic Capacity Bounds for Distributed Antenna Systems. In *Proc. of the IEEE Information Theory Workshop (ITW'06)*, Oct. 2006.
- [24] P. Marsch, E. Zimmermann, and G. Fettweis. Smart Candidate Adding: A new Low-Complexity Approach towards Near-Capacity MIMO Detection. In *Proc. of the 13th European Signal Processing Conference (EUSIPCO'05)*, Sept. 2005.
- [25] P. Marsch, E. Zimmermann, and G. Fettweis. Improved Methods for Search Radius Estimation in Sphere Detection Based MIMO Receivers. In *Proc. of the 14th IST Mobile and Wireless Communications Summit (IST Summit'05)*, June 2005.

Patents

- [1] P. Marsch, S. Khattak, and P. Rost. Selection of a Base Station for the Cell-Overlapping Signal Decoding. *WO/2009/033475*.

Curriculum Vitae

Patrick Marsch

born on October 13th 1976 in Erlangen, Germany

Email: pmarsch@pmarsch.de

- 04/2009 - now **Vodafone Chair Mobile Comm. Systems**, Dresden, Germany
Senior research associate, heading a group of 8 Ph.D. students in the field of system level analysis and optimization of heterogeneous cellular systems w.r.t. spectral efficiency, energy efficiency, or cost.
- 09/2005 - 03/2009 **Vodafone Chair Mobile Comm. Systems**, Dresden, Germany
Research associate. Technical project leader of the research project EASY-C, in which the world-wide first large-scale research test beds for LTE-Advanced have been established.
- 02/2005 - 08/2005 **Philips Research East Asia**, Shanghai, P.R. China
Internship in the wireless communications research department, focusing on fixed-mobile convergence and wireless sensor networks.
- 10/1999 - 12/2004 **Technische Universität Dresden**, Dresden, Germany
Studies of *Information System Technology*, leading to a German diploma equivalent to a Master of Science. During the studies:
- Internship at **Infineon Technologies**, Munich, Germany, concerned with the evaluation of staff efficiency in production plants.
 - Visiting student at **McGill University**, Montréal, Canada, partially funded by a scholarship from the **Kulturstiftung Dresden der Dresdner Bank**, Dresden, Germany.
 - Vice president marketing, student organization **AIESEC** Dresden.
- 06/1999 - 10/1999 **Siemens Business Services**, Munich, Germany
Full-time job position as an Intranet developer.
- 08/1996 - 06/1999 **Siemens AG**, Paderborn, Germany
Apprenticeship as an *Integrated Services Consultant*.